Understanding the role of glia and oligomeric tau in the early synapse loss of Alzheimer disease dementia

by

Raquel N. Taddei

A thesis submitted for the degree of Doctor of Philosophy in Neuroscience

University College London

April 2024

Declaration

I, Raquel N. Taddei, confirm that the work presented in this thesis is my own. Where information has been derived from other sources, I confirm that this has been indicated in the thesis.

Table of Contents

Acknowledgements

First and foremost, I would like to thank my two supervisors, Karen Duff and Teresa Gomez-Isla, for their unwavering support and guidance throughout my thesis. I am deeply grateful to Karen for her continuous and honest feedback, for the exciting discussions that enabled me to deepen my knowledge of science, for her patience during my process of learning the scientific mindset, and for being a supporting and caring mentor whose excellent advice has been fundamental to the work of this thesis and beyond. I want to thank Teresa for providing me with every possible means to enable my growth and progress, and for setting the ground for my development into a mature and independent neuroscientist. Without her, this work and important step of my career would not have happened.

I want to thank my thesis committee, Henrik Zetterberg, for his very insightful comments and advice, and Soyon Hong, for her significant contribution and expertise, both of which have substantially contributed to this thesis. I also wish to thank the outstanding scientists and people in Karen's team, Steph, Martha, Mathieu, Emir, Sumi, and Saisha, for their insightful advice, for exchanging ideas and sharing protocols, and for giving critical and constructive feedback in our weekly lab meetings, all of which have been fundamental to deepening and solidifying my scientific knowledge and expertise. I also wish to greatly thank Brad Hyman for his time and advice, for listening and helping me with science and career-related matters throughout this work, and for being a great mentor and helping me set the ground and form vital connections for my next career steps.

I wish to greatly thank my collaborators and friends Romain, Anastasie, Mari, Orla, Joanna, Adel, Moustafa, Florian, Rosie, Lindsey, Leon, Yael, and Clara, who are remarkable scientists and, most importantly, wonderful people, for serving as a source of strong support and encouragement, for always being willing to listen and provide valuable feedback on countless presentations, for sitting in the first row at conferences to give me moral support during my talks, for taking the time to discuss and brainstorm on scientific questions and uncertainties, and for sharing so many amazing days, weekends, and holidays together, which have made my PhD experience a truly unique one, that I will always think back with pleasure.

Last but not least, thank you from the bottom of my heart to my loving family, Monica, Sergio, Bettina, Nina, Sandro, Monika, Gabriel, and Andrea, and my dearest friends Lynsey, Marta, Alex, Alfonso, and Ellen, for being such supporting and inspirational people, whose presence and connection, even in the distance and across countries and continents, will always be here.

I dedicate this thesis to my dad, a truehearted and free-spirited soul who sadly left us way too early and whom I dearly miss. You are and will remain a profound source of inspiration and a unique example of unboundary and freedom, and I am grateful for every moment we spent together.

Abstract

Synapse loss is the strongest correlate of dementia in AD. Yet, the underlying causes of synaptic derangement remain largely unknown. Emerging evidence suggests that glial cells play a central role in synapse elimination and recent studies have shown that microglia internalize more synapses in demented than in control brains. Additionally, amyloid-β and tau oligomers are significantly higher in the synapses of demented brains. The present study included 60 human brains of demented and resilient individuals at intermediate stages of tau pathology (Braak III-IV) and cognitively unimpaired controls (Braak 0-II). The temporal cortex, a Braak III-IV region with incipient neurofibrillary tangles (NFTs), and the visual cortex, a Braak VI region without NFTs were evaluated. Glial cell phenotypic changes were quantified with immunohistochemistry and artificial intelligence-supported analyses, and synaptic elements with expansion microscopy and Imaris analyses, complemented with western blotting. Demented brains showed higher inflammatory and lower homeostatic but no change in total glial cell numbers compared with resilient and controls. Notably, these glial cell changes occurred irrespectively of amyloid-β and NFTs (temporal cortex) and ahead of NFT development (visual cortex). Moreover, a significant synapse loss was present in the NFT-free visual cortex of demented brains and showed a strong association with cognitive scores, especially with visual memory tasks. Synapses extracted from the visual cortex of demented brains contained more oligomeric and hyperphosphorylated tau compared with resilient but no change in tau truncation or detectable seeding activity. Importantly, microglia and astrocytes of demented brains harboured significantly more internalized synaptic elements and particularly high tau oligomer-positive synapses. A primary glial cell dysfunction may determine the early synapse loss driving AD dementia irrespectively of AD-typical lesions, and this may be promoted and perpetuated by oligomeric tau contained in synapses, leading to chronic synapse elimination and the development and progression of AD dementia.

Impact statement

The present work evaluated the role of early glial changes in AD, and how glial cells may relate to synapse loss and dementia development in a cohort of human brains with similar amyloid-β and tau burdens but opposite cognitive outcomes prior to death (demented vs. `resilient'). The novel technique of expansion microscopy was applied to allow an unprecedented in situ evaluation of the interactions between glia, synapses, and oligomers in these brains. The in-depth characterization of the studied brains showed that demented but not resilient subjects had early glial cell changes and loss of synapses despite both having equal amyloid-β and tau burdens. In addition, glial cells of demented brains engulfed a significantly higher number of synapses compared with resilient brains, and glia-internalized synapses of demented brains contained substantially more tau oligomers. Importantly, the present study shows, for the first time in early dementia AD brains, that astrocytes and not only microglia internalize higher amounts of synapses, and that accumulation of tau oligomers in synapses could be driving the dysfunctional glial cell responses on synapse engulfment.

These findings are novel and suggest a primary role of microglia- and astrocyte-driven synapse elimination in the early phases of dementia and they propose a potential key contribution of tau oligomers in mediating these dysfunctional effects. This would support a novel pathogenic model of AD where an early dysfunction in glial cells together with oligomeric tau mislocalized to synapses, rather than the only presence of amyloid-β and tau deposits, would determine the fate of an individual to develop dementia or to remain cognitively unimpaired (`resilient') in the presence of amyloid-β and tau pathologies.

These results could have important implications with impact on clinical practice, public health, economy, and quality of life. First, these findings apply to the early phases of the clinical and

neuropathologic AD process, and this is important for the potential development of novel biomarkers and effective treatments targeting the most preventable phases of the disease. Future synapse-protecting therapies derived from the study of early dementia stages hold the greatest promise to be most effective in halting the inexorable progression of synapse loss and the development and progression of cognitive dysfunction. Secondly, potential future treatment avenues derived from the present study could possibly be applied to other neurodegenerative and/or neurodevelopmental disorders beyond AD, where synapse loss and inflammatory glial cell changes are common hallmarks and key neuropathologic features. Thirdly, our proposed alternative `AD model' involving early synapse loss associated with glial cell changes and synaptic oligomeric tau could aid in the development of more precise and clinically relevant neuropathological definitions of AD using synaptic biomarkers in combination with glial cell phenotypic changes and soluble tau species as potential proximity markers, and this could help to better detect, classify, and study demented individuals, both in vivo and at post-mortem, in the future. Lastly, the development of effective future treatment targets for AD dementia could have a substantial impact on public health and the economic burden associated with dementia care, and most importantly, this could substantially improve the quality of life of affected patients and their families.

Paper declaration forms

UCL Research Paper Declaration Form

referencing the doctoral candidate's own published work(s)

1. **For a research manuscript that has already been published** (if not yet published, please skip to section 2)

   a) **What is the title of the manuscript?**

   Changes in glial cell phenotypes precede overt neurofibrillary tangle formation, correlate with markers of cortical cell damage, and predict cognitive status of individuals at Braak III-IV stages

   b) **Where was the work published?**

   Acta Neuropathologica Communications

   c) **Who published the work?** (e.g., OUP)

   Springer Nature

   d) **When was the work published?**

   09 May 2022

   e) **List the manuscript's authors in the order they appear on the publication**

   Raquel N. Taddei, Maria V. Sanchez-Mico, Orla Bonnar, Theresa Connors, Angelica Gaona, Dominique Denbow, Matthew P. Frosch & Teresa Gómez-Isla.

   f) **Was the work peer reviewed?**

   Yes

   g) **Have you retained the copyright?**

   Yes

   h) **Was an earlier form of the manuscript uploaded to a preprint server?** (e.g., medRxiv). If 'Yes', please give a link or doi)

   No

   If 'No', please seek permission from the relevant publisher and check the box next to the below statement:

☐

*I acknowledge permission of the publisher named under **1d** to include in this thesis portions of the publication named as included in **1c**.*

2. **For a research manuscript prepared for publication but that has not yet been published** (if already published, please skip to section 3)

   a) **What is the current title of the manuscript?**

   Click or tap here to enter text.

   b) **Has the manuscript been uploaded to a preprint server?** (e.g., medRxiv; if 'Yes', please give a link or doi)

   Click or tap here to enter text.

   c) **Where is the work intended to be published?** (e.g., journal names)

   Click or tap here to enter text.

   d) **List the manuscript's authors in the intended authorship order**

   Click or tap here to enter text.

   e) **Stage of publication** (e.g., in submission)

   Click or tap here to enter text.

3. **For multi-authored work, please give a statement of contribution covering all authors** (if single-author, please skip to section 4)

   RNT participated in study design, carried out immunostaining and image analysis, contributed to data analysis and interpretation, and drafted the manuscript. MSVM and OB participated in data acquisition. DD, TC and AG prepared the tissue blocks and sections from cases. MPF carried out the neuropathologic examination of cases, and participated in the study design, analysis and interpretation of data. TGI conceived the study and participated in its design and coordination, analysis and interpretation of data and drafted the manuscript. All authors read and approved the final manuscript.

4. **In which chapter(s) of your thesis can this material be found?**

   2.1-2.3, 2.11, 3.1-3.5, 4.2, 5

5. **e-Signatures confirming that the information above is accurate** (this form should be co-signed by the supervisor/ senior author unless this is not appropriate, e.g., if the paper was a single-author work)

   Candidate:

   Raquel N. Taddei
   Date:
   24/08/2023

   Supervisor/ Senior Author (where appropriate)

   Karen Duff
   Date:
   01/04/2024

UCL Research Paper Declaration Form
referencing the doctoral candidate's own published work(s)

6. For a research manuscript that has already been published (if not yet published, please skip to section 2)

i) **What is the title of the manuscript?**

Tau oligomer-containing synapses are engulfed by microglia and astrocytes and correlate with cognition in Alzheimer disease

j) **Where was the work published?**

JAMA Neurology

k) **Who published the work?** (e.g., OUP)

American Medical Association

l) **When was the work published?**

09/10/2023

m) **List the manuscript's authors in the order they appear on the publication**

Raquel N. Taddei, Romain Perbet, Anastasie Mate de Gerando, Anne E. Wiedmer, Maria V. Sanchez-Mico, Theresa Connors, Angelica Gaona, Alexandra Melloni, Ana C. Amaral, Karen Duff, Matthew P. Frosch & Teresa Gómez-Isla.

n) **Was the work peer reviewed?**

Yes

o) **Have you retained the copyright?**

No

p) **Was an earlier form of the manuscript uploaded to a preprint server?** (e.g., medRxiv). If 'Yes', please give a link or doi)

No

If 'No', please seek permission from the relevant publisher and check the box next to the below statement:

☒

*I acknowledge permission of the publisher named under **1d** to include in this thesis portions of the publication named as included in **1c**.*

7. For a research manuscript prepared for publication but that has not yet been published (if already published, please skip to section 3)

f) **What is the current title of the manuscript?**

Click or tap here to enter text.

g) **Has the manuscript been uploaded to a preprint server?** (e.g., medRxiv; if 'Yes', please give a link or doi)

Click or tap here to enter text.

h) **Where is the work intended to be published?** (e.g., journal names)

Click or tap here to enter text.

i) **List the manuscript's authors in the intended authorship order**

Click or tap here to enter text.

j) **Stage of publication** (e.g., in submission)

Click or tap here to enter text.

8. **For multi-authored work, please give a statement of contribution covering all authors** (if single-author, please skip to section 4)

   RNT participated in study design, carried out expansion microscopy, immunostaining and image analysis, contributed to data analysis and interpretation, and drafted the manuscript. RP, AMG, and AEW participated in data acquisition. TC, AG and AM prepared the tissue blocks and sections from cases. AA provided insightful input on expansion microscopy. MPF carried out the neuropathologic examination of cases. KD and MPF participated in the study design, analysis and interpretation of data. TGI conceived the study and participated in its design and coordination, analysis and interpretation of data and drafted the manuscript. All authors read and approved the final manuscript.

9. **In which chapter(s) of your thesis can this material be found?**

   2.1, 2.4-2.9, 2.11, 3.6-3.9, 13.11-3.12, 4.2, 5

10. **e-Signatures confirming that the information above is accurate** (this form should be co-signed by the supervisor/ senior author unless this is not appropriate, e.g., if the paper was a single-author work)

Candidate:

Raquel N. Taddei
Date:
24/08/2023

Supervisor/ Senior Author (where appropriate)

Karen Duff
Date:
01/04/2024

Aims

This project aims to evaluate the involvement of glia as a potential driver of the excessive synapse elimination and a contributor to dementia development in the early stages of AD dementia and to assess the role of synaptotoxic oligomeric tau species in potentially driving the early elimination of synapses by glial cells in these brains.

The unique study setup with a well-matched cohort of brains that harbour similar amyloid-β and tau deposits enables the assessment of other neuropathologic signatures, including glial cell changes and oligomeric tau species, that could instead be more meaningfully driving the development and severity of cognitive dysfunction. While other variables associated with amyloid-β and tau themselves (e.g., morphologic features of plaques and tangles, temporospatial associations with other co-pathologies) may be playing a role in anatomical and functional brain changes, the matching for burdens of these two proteins excludes an important proportion of possible variability and allows to interpret changes in other neuropathologic features largely excluding the effects of amyloid-β and tau deposits in these brains. Thus, in view of a virtually `negligible' impact of amyloid-β and tau deposits across the studied groups, the results derived from the study of these brains could unravel truly meaningful contributors to dementia development and severity, in the presence of classical AD neuropathologies.

By studying a select cohort of human brains with intermediate (Braak III-IV) stages of tau pathology but differing antemortem cognitive statuses (resilient vs demented), the present study enables the unprecedented possibility to address early neuropathologic changes in human AD brains that could be meaningful to the presence or absence of cognitive dysfunction in an individual. The inclusion of a healthy control group (Braak stages 0-II) enables to distinguish neuropathologic features of normal healthy ageing from specific signatures of resilient brains intended to better cope with ADNC. The study of brain regions that lie ahead of NFT development in these brains (e.g., visual cortex) offers a unique temporal window to evaluate other early neuropathologic features and assess their clinical significance in the absence and ahead of NFTs. In addition, the inclusion of a subset of cases without cortical amyloid-β deposits (primary age-related tauopathy (PART) cases) enables to evaluate those early neuropathologic changes in the absence of both, amyloid-β and tau deposits in the visual cortices of these brains. The study results will ultimately enable to propose a primary role of other elements distinct from typical AD lesions in the pathogenesis of AD largely excluding their alternatively secondary or reactive role to the presence of amyloid-β/tau deposits in these brains.

Most individuals included in the present study were in the early stages of dementia at the time of death and the study of prodromal (mild cognitive impairment or MCI) and mild dementia stages at post-mortem is rare and allows the unique possibility to address the earliest neuropathologic hallmarks that are associated with incipient clinical changes in AD. The brain cohort included here is quite unique since most individuals who die and donate their brains for research studies are at more advanced dementia stages. Thus, the findings and conclusions derived from the present work could be relevant to understanding the early neuropathologic mechanisms initiating and driving the consecutive decline in memory function and be relevant for the development of novel therapeutic interventions aimed at targeting those early and potentially still reversible phases of neuropathologic changes in AD.

The present work assessed the following key points:

- Are microglia and/or astrocytes phenotypically and morphologically distinct in the brains of ADNC-matched early demented and resilient cases?

- Is there a key glial cell signature (e.g., inflammatory, homeostatic) that allows to differentiate early demented from resilient brains?

- Does that glial cell signature associate with early cognitive dysfunction and with neuronal damage in these brains, irrespectively and ahead of amyloid-β and/or tau deposits?

- Is synapse loss, the strongest neuropathologic signature of memory dysfunction, already present in brain regions that lie ahead of tau tangle development?

- Does synapse loss associate with cognition and with neuronal damage in these brains?

- Are microglia and/or astrocytes possibly involved in the early synapse loss by engulfing higher amounts of synaptic elements in demented brains?

- Do tau oligomers target and mislocalize to synapses in brains at early dementia stages and in the absence of NFTs?

- Are the synapses that contain tau oligomers the ones that are preferentially internalized and eliminated by glia?

- Lastly, is the presence or absence of this tissue injury response what determines whether an individual who harbours amyloid-β and tau deposits in the brain will manifest or not clinical symptoms of disease?

Hypotheses

1. Synaptic loss and cognitive impairment in early AD are due to a primary dysfunction in glia, and not to the effects of amyloid-β and tau deposits in these brains.

2. The elimination of synapses by dysfunctional glia that results in synapse loss and cognitive impairment, is driven by a mis-localization of oligomeric tau to synapses.

1. Introduction

1.1 Resilience to AD neuropathologic change (ADNC)

1.1.1 Histopathologic diagnosis of AD

Alzheimer disease (AD) is a neuropathologic diagnosis defined by the presence of amyloid-β and tau in the brain, and not by the clinical syndrome of dementia. AD is viewed as a continuum that initiates with the appearance of brain pathologic changes in asymptomatic individuals and progresses to increasing pathologic burdens, eventually leading to the appearance of clinical symptoms. AD is diagnosed at post-mortem with the use of the NIA-AA Reagan guidelines revised in 2012 (1), and *in vivo* by abnormalities in core biomarkers following the ATN framework published in 2018 (currently under revision) (2).

AD neuropathologic diagnosis requires a histopathologic evaluation of multiple brain regions using staining methods that detect extracellular amyloid-β plaques and intracellular neurofibrillary tangles (NFTs). This detailed microscopic assessment ultimately allows to estimate the topographic distribution and burden of AD neuropathologic change (ADNC) (3) and to evaluate the likelihood of ADNC being the cause of antemortem dementia using a scoring system proposed in the NIA-AA Reagan criteria (1). The scores obtained from amyloid-β plaque (A), NFT stage (B), and neuritic plaque (C) assessments are combined into an `ABC' score which is transformed into the likelihood of ADNC at an individual level into `not', `low', `intermediate', or `high' (1).

Amyloid-β plaques are composed of the extracellular accumulation of predominantly Aβ40 and Aβ42 amyloid peptides that result from the abnormal processing of amyloid precursor protein (APP) by β- and γ-secretases (3). They can be found in the form of senile plaques, that stain weakly for amyloid-β antibodies and show an absence of tau positive staining, and neuritic plaques, that are intensely positive for amyloid-β staining and additionally contain phospho-tau positive dystrophic neurites. Neuritic plaques are more closely associated with neuroinflammatory changes and with neuronal loss than senile plaques (4,5).

The currently used staging scheme to assess the distribution of amyloid-β plaques in AD brains was proposed by Thal and Braak (6,7) and it comprises the use of highly sensitive amyloid-β antibodies to determine the topographic distribution and stereotypical progression pattern of these deposits in the brain. Importantly, these antibodies detect all amyloid-β plaque subtypes. Amyloid-β plaque deposits start to form in the neocortex, in particular in the temporal lobe (Thal phase 1), then progress to allocortex (Thal phase 2), subsequently affecting diencephalon, striatum, and basal forebrain (Thal stage 3), next involve the brainstem nuclei (Thal stage 4), and lastly affect the cerebellum (Thal stage 5) (6,7). In the neuropathologic evaluation of amyloid-β plaques following the Thal stages only the distribution but not the burden of amyloid-β plaque deposits is taken into account.

To detect neuritic plaques, which are composed of amyloid-β deposits that contain phospho-tau positive dystrophic neurites, thioflavin S or Bielschowsky silver staining methods are used which detect axons, neurofibrils, and amyloid-β plaques. The staging scheme used for neuritic plaques comprises a semiquantitative assessment of neuritic plaque burden using the Consortium to Establish a Registry for Alzheimer disease (CERAD) standardized criteria (1,8). The CERAD score assesses the density of neuritic plaques in the most severely affected region of the isocortex (frontal, temporal, or parietal) and it takes into account the patient's age at death to obtain an age-related plaque score (9). Neuritic plaques are staged into no (C0), sparse (C1), moderate (C2), and frequent (C3) neuritic plaque burden. Of note, amyloid-β peptides not only deposit in the form of amyloid-β plaques in the brain parenchyma but also in cerebral blood vessels in the form of cerebral amyloid, angiopathy (CAA). In fact, it is estimated that 85-95% of AD brains have at least some degree of CAA and the severity of CAA pathology in vessels is commonly assessed with the Vonsattel staging system (10), however and despite CAA being very common in AD brains, the CAA burden does not form part of the current neuropathologic criteria to diagnose ADNC.

Tau in the form of neurofibrillary tangles (NFTs) is the second defining neuropathologic feature of AD. In the AD brain, tau proteins are hyperphosphorylated and abnormally folded, and they form tau aggregates such as NFTs. Detection of NFTs is usually assessed with tau-specific antibodies that label phospho-epitopes of tau protein, most commonly with the use of AT8 antibody. The currently used staging scheme for tau distribution was proposed by Braak&Braak and it follows a sequential deposition pattern in the human brain (11) with NFTs initially affecting the transentorhinal region (Braak stage I), entorhinal region (Braak stage II), fusiform/occipitotemporal gyrus (Braak stage III), medial temporal gyrus (Braak stage IV), occipital lobe/peristriate areas (Braak V), and lastly involving

the occipital lobe/striate regions (Braak VI) (11). The frontal, parietal, and occipital neocortices remain largely unaffected by NFTs up to a Braak stage IV, NFTs develop in the frontal and parietal neocortices in the stage V, and in the occipital and striate cortices at the very last stages V-VI (12). Similarly to the amyloid-β plaque scoring system, the Braak NFT staging only assesses the distribution but not the burden of NFT deposits in the brain.

The three subscores A (Thal amyloid-β plaque score), B (Braak NFT stage), and C (CERAD neuritic plaque score) are ultimately combined into an ABC score that allows to estimate the degree of likelihood that AD was the cause of antemortem dementia in a particular brain (1,8). The `ABC' scoring system is shown in **Table 1**.

		Likelihood of ADNC as the cause of dementia		
A: Thal phase	**C**: CERAD score	**B**: Braak stage (None or I/II)	**B**: Braak stage (III/IV)	**B**: Braak stage (V/VI)
A0 (0)	C0	Not	Not	Not
A1 (1/2)	C0 or C1	Low	Low	Low
	C2 or C3	Low	Intermediate	Intermediate
A2 (3)	Any C	Low	Intermediate	Intermediate
A3 (4/5)	C0 or C1	Low	Intermediate	Intermediate
	C2 or C3	Low	Intermediate	High

Table 1: Likelihood of ADNC as the cause of dementia using the `ABC' scoring system
Likelihood of ADNC as the cause of dementia (not, low, intermediate, high) as a combination of Thal phase score (A), Braak stage (B), neuritic plaque burden (C). Thal phase: No amyloid deposition (A0), amyloid in neocortex (A1), amyloid in allocortex/limbic region (A2), amyloid in diencephalon/basal ganglia (A3), amyloid in brainstem/midbrain (A4), amyloid in cerebellum (A5); Braak stage: NFTs in transentorhinal region (Braak stage I), entorhinal region (Braak stage II), fusiform/occipitotemporal gyrus (Braak stage III), medial temporal gyrus (Braak stage IV), occipital lobe/peristriate areas (Braak V), occipital lobe/striate region (Braak VI). CERAD score: No neuritic plaques (C0), sparse plaques (C1), moderate plaques (C2), frequent plaques (C3). ADNC: Alzheimer disease neuropathologic change.

1.1.2 Definition and concept of human brain resilience to ADNC

Alzheimer disease (AD) is defined histopathologically by the accumulation of amyloid-β plaques and neurofibrillary tangles (NFTs) in the brain. Yet, these two neuropathologic hallmarks are not sufficient to explain the full extent of synaptic and neuronal loss observed in a demented AD brain. Moreover, these two proteins do not inevitably lead to cognitive impairment when present (13,14), nor to an amelioration of dementia when removed from the brain (15). In fact, human brains of cognitively unimpaired subjects who harbour amyloid-β and NFT deposits at post-mortem have been found in up to 1/3 of unselected autopsies in longitudinal ageing studies (16–18), and recent post-mortem evaluations of the first amyloid-β immunotherapy-treated individuals dating back to 2003, have shown that despite sustained removal of amyloid-β (and concomitant reduction of tau pathology) in some of these brains at autopsy after 14 years (15), a considerable subset of individuals still progressed to severe dementia stages prior to death (15). Growing evidence has suggested that NFTs are a better correlate of cognitive impairment (19,20) and neuronal loss (21,22) in AD, and this has recently shifted the drug discovery field in AD to tau. However, tau-immunotherapies, which are in clinical trials since 2013 (23), have also been disappointing and have, so far, shown no clinical improvement in subjects treated in the prodromal and early stages of AD dementia despite evidence of target engagement and reduction of tau CSF levels in these subjects (24). In line with these observations, biomarker studies have found that up to 50% of healthy elderly display biomarker evidence of AD neuropathology but absence of dementia (25), and unselected

autopsies of `most' healthy individuals aged >85 years show `some degree' of ADNC, which by large exceeds the expected ante-mortem prevalence of dementia in individuals aged >85 years which is estimated at around 50% (26–28). This important disconnect between `presence of classic AD neuropathology at post-mortem' but `absence of dementia during lifetime' has been termed `resilience' (28,29), and some research groups have also referred to this phenomenon with the terms of `cognitive reserve', `brain reserve', `brain maintenance', and `compensation' (30). Overall, human brain resilience to `high-pathology' (Braak V-VI) stages is rare and is found in 5-7% of post-mortem human brains, while resilience to `intermediate-pathology' (Braak III-IV) stages is more common and is estimated at 45% of autopsies (9), overall suggesting an estimated prevalence of resilience to ADNC of around 1/3 in unselected autopsies from aged individuals (16,17).

Resilience is an abstract concept with no consensus definition as of today (31). While the definition of resilience has historically been based on the combination of a detailed post-mortem neuropathologic examination, most commonly using the NIA-AA Reagan `ABC-scoring' system (1), together with a detailed antemortem memory evaluation, several operational definitions have been developed (32–34) and various algorithms have been created to aid in the systematic definition of resilience (29,31). Importantly, recent advances in the measurement of *in vivo* pathologic changes using imaging (e.g., amyloid-/tau-PET) as well as brain-derived biofluids (cerebrospinal/plasma) have enabled the use of the term `resilience' for living individuals, although this term was originally limited to a post-mortem definition only (35).

In an effort to standardize the term of `resilience', studies have used proxy variables of demographic and/or clinical features to define it, but many of these variables have shown high correlation with other measures known to be associated with AD risk, and they do not as such specifically define resilience. Several other groups have used *in vivo* proxy measures and their change over time to better define resilience (e.g., cerebrospinal fluid, MRI, and/or PET measures) but they have been criticized for their heavy reliability on parametric models that may underestimate the single effects of those measures, and for the fact that they are in discrepancy with the basic idea that resilience is a `post-mortem' diagnosis and that these antemortem measures do not always correlate with the later post-mortem findings (31,36). Recently, a novel approach using models that evaluate variables accounting for cognitive resilience after adjusting for AD-related post-mortem pathology have been proposed, and they have generated an `AD cognitive resilience' (AD-CR) score. This score represents the difference between the `observed' and the `expected' level of cognition, and it is based on a global measure of antemortem cognition (assessed with a battery of 19 cognitive tests obtaining global z-scores for the subdomains episodic memory, semantic memory, working memory, perceptual speed, and visuospatial ability) and a `gold standard' post-mortem AD neuropathologic examination (using the NIA-AA Reagan criteria (1)). This score is fully non-parametric, and it allows to independently assess individual variables including clinical/demographic ones. AD-CR score has been recently validated using two longitudinal ageing studies for its potential future use in research settings (31).

Nonetheless, and despite efforts aimed at creating a consensus definition of `resilience', to date there is no such operational definition, which may be partly due to the ongoing and important lack of understanding of its underlying causes.

1.1.3 First description of human brain resilience to ADNC and initial reports on contributing factors

Human brain `resilience' to AD neuropathology was first described in the late 1980s when two longitudinal ageing studies surprisingly found that a small subset of post-mortem human brains of healthy human elderly showed typical neuropathological changes that would essentially have met

the neuropathological criteria of `high-pathology AD' (Braak V-VI), but were present in individuals who had not suffered from cognitive impairment during lifetime (37,38). However, the first descriptions of isolated cases of human brain autopsies where presence of NFTs and senile plaques were found in the brains of `cognitively well preserved elderly', had already been described by the Swedish pathologist Gellerstedt in 1933 (39). The concept and interest in the phenomenon of `resilience' was however not further explored until the later published studies in the 1980's. Although the concept of resilience to AD neuropathology classically refers to a post-mortem brain feature of cognitively unimpaired elderly, a similar concept can be studied *in vivo* with the use of AD biomarkers. In this context, the findings of discrepancies between positive AD biomarkers and absence of dementia receive different names including `cognitively healthy with AD', `clinically unimpaired elderly with AD', and/or `preclinical AD', among others (40,41). Thus, the concept of resilience is commonly reserved for the post-mortem findings of ADNC in cognitively unimpaired elderly, while the *in vivo* definition of this same concept exists but is termed differently from resilience. In the present study the term of resilience is used to refer to the neuropathologically confirmed presence of ADNC in subjects without antemortem evidence of dementia.

The first of these two studies assessed 28 subjects who were followed up longitudinally with yearly clinical evaluations and who had been seen within <28 months prior to death. Their post-mortem exam showed presence of senile plaques and NFTs in the hippocampus and frontal cortices in the demented subjects using thioflavin S staining, but these ADNCs were also found in a subset of 5 cases where formal clinical criteria for dementia had not been met at antemortem. Interestingly, while senile plaques did not distinguish well between demented and non-demented subjects, highest burdens of NFTs were found only in the demented but not in the non-demented brains (37). In the second study, 137 subjects were followed up longitudinally with annual clinical evaluations, and at post-mortem, 10 of the non-demented individuals showed amyloid-β plaque and NFT pathology in the hippocampus, frontal, parietal, and temporal cortices using thioflavin S staining. Interestingly, these non-demented subjects scored higher in memory tests compared with healthy controls, and they showed the highest brain weights of all studied individuals, as well as a higher counts of large neuronal cell bodies. These two studies thus suggested that a subset of `resilient' individuals existed, and they proposed that resilient subjects may be able to escape the development of AD dementia through a better preservation of neuronal structures and/or by starting off with higher brain weights and neuronal numbers.

Two subsequent key populations that have added substantial knowledge to the study of ageing and resilience are the Honolulu and the Nun studies, both large-scale longitudinal studies of healthy US-Japanese men and US-born Caucasian sisters, respectively (28). These two studies included a total of 852 and 605 subjects, of whom 392 and 355 subjects had had a clinical antemortem evaluation within 2 years prior to death and a neuropathologic examination at post-mortem, respectively. These two studies estimated, for the first time, an overall prevalence of resilience between 5% and 7% for `high-pathology' ADNC (Braak V-VI stages) using the NIA-AA Reagan criteria (1), and they began to unravel potential early lifestyle factors including social engagement, intellectual enrichment, as well as neuropathologic changes including the cumulative effect of >1 neuropathologic change in the brain, as potential contributors to dementia development and/or absence of cognitive dysfunction in resilient subjects with similar ADNCs as demented individuals (42,43).

These early descriptions of resilient human brains gave rise to two novel and interesting concepts named `brain reserve' and `cognitive reserve' (44). The brain reserve model proposes that some people have larger brains with more neurons and synapses at baseline (37,38), which may place them in a better position to sustain the potentially deleterious effects of amyloid-β and tau aggregates on brain function, and to be therefore better suited to not developing cognitive

impairment until a substantial burden of neuronal and synapse loss is surpassed in more advanced disease stages, which these individuals may never experience during lifetime (38). However, this idea has shown discrepancies in recent studies, with some resilient brain cohorts showing a comparable (or even mildly lower) average brain weight compared with age-matched healthy control brains (18). Some groups have also found that even in the face of multiple cumulative neuropathologic changes in resilient brains, they still do not show substantially higher brain weights compared with controls (45). In addition to the neuroanatomical model of `brain reserve' which may partly explain resilience, there is also a more functional model of resilience called `cognitive reserve' which proposes that sustained and enriched lifetime exposure to cognitively stimulating environments may confer the brain with increased and more robust cognitive networks that would allow an individual to better cope and compensate for brain dysfunction in the event of amyloid-β and tau pathologies. This model encompasses an `active' potential of brain circuitry which can theoretically be altered throughout life and which could create resilience by enhancing the functional abilities of the brain to cope with the detrimental effects of neuropathologic changes (46). In line with this encouraging idea, some studies have observed that lower levels of education likely increase the risk for dementia development (47,48) and that resilient individuals show higher levels of education compared with demented subjects (49).

Resilience to AD pathology is a neuropathological concept that characterizes a select subset of individuals with a favourable, but yet unknown, set of traits that enable them to sustain the detrimental effects of ADNC on cognition. The interest of studying resilience traits is nicely exemplified by other medical discoveries including the slower progression of HIV-1 in a subset of `resilient' cases to HIV infection in which a mutation in CCR5delta32 was later found to underlie those interesting outliers. This discovery eventually led to the development of now widely used CCR5-inhibitors for treatment of HIV-1 (50). Similarly, but with less therapeutic significance, a subset of `resilient' individuals against classical malaria caused by *Plasmodium falciparum* infection were described and these individuals were later found to harbour the trait of sickle cell anaemia, which leads to lower oxygen levels in the infected red blood cells triggering their rapid and more efficient elimination by macrophages, thus conveying those subjects with lower burdens of *Plasmodium falciparum* in blood. Since sickle cell anaemia can also have detrimental effects its potential use as a therapeutic avenue is not warranted (51). These two examples reflect the importance of studying outliers across diseases which could hold the potential to unravel protective pathways and aid in the discovery of treatment targets that could lessen the effects of a disease in the general population. Although the present work was focused on the study of resilience to AD, resilient cases to alpha-synuclein and to TDP43 neuropathologies have also been described, and their combined study could be of great interest.

1.1.4 Difference between `resilience' and `resistance' to ADNC

As of today, resilience is defined as the brain's ability to cope with neuropathologic changes to preserve brain integrity/function in the face of significant burdens of AD pathology, while another interesting concept, that of resistance, refers to the brain's ability to avoid the accumulation of neuropathologic changes where those would have been expected to occur given the age of the individual and/or the presence of other risk factors (e.g., genetic predisposition) (52,53). While preserving function despite amyloid-β and tau pathologies would indicate resilience, remaining relatively free of these pathologies would refer to resistance, and both these concepts could ultimately be closely linked and enable normal cognitive functioning in healthy ageing. Although these two ideas may seem different in nature, they could share underlying mechanisms and act in combination. Both these concepts are highly intriguing and important to better understand the cognitive effects of neuropathological change(s) in AD brains, but it is the resilient individuals who could be key to better understand the elements and processes that, in addition to amyloid-β and

NFT deposits in a brain, would be needed for dementia to develop, and help determine which additional elements would be leading to dementia occurrence on top of the presence of amyloid-β and NFT pathologies. Ultimately, factors promoting resilience could, in a second step, be assessed in resistant brains, to evaluate whether the mechanisms involved in resilience are a hallmark of these brains irrespectively of ADNC, or whether they rather represent a specific feature present in close temporal association with AD neuropathology development to overcome the potentially deleterious effects of amyloid-β and NFT deposits in those brains. Ultimately, resiliency and resistance factors could both be assessed as a proof of concept in a subset of recently described human brains who show no apparent accumulation of neuropathologies (e.g., ADNC, Lewy body pathology, and/or vascular changes) but who had antemortem presence of dementia, a phenomenon that has been described to occur in around 5% of autopsies and has been called `frailty' or `frail brains' by some groups (54,55). This would allow to assess whether the absence of resiliency/resistance factors alone in these brains could potentially explain the presence of dementia in the absence of amyloid-β and tau deposits (and presumably other concomitant lesions) in these subjects and help find the common mechanisms between demented and frail brains that could be central to the development of dementia.

Interestingly, recent longitudinal studies of resilient subjects have found that while resiliency is highly effective to avoid cognitive decline when an individual remains asymptomatic, if progression to dementia occurs in a resilient subject, the clinical course is much more aggressive than the one observed in a typical demented individual (56). This could suggest that the mechanisms linked to resilience are closely associated with amyloid-β and/or tau pathologies in these brains, and that if resilience mechanisms are overcome and `eliminated' from these brains, the high level of pathologic changes that were present but functionally `suppressed' before are now released and exert a full blown pathologic and clinical effect within a relatively short period of time. Thus, the importance of evaluating the intricate associations between amyloid-β, tau, and other determinants of cognitive function in combination could possibly unravel some of the protective mechanisms linked to brain resilience and/or expose the determinants of dementia development in a brain with ADNC and enable development of novel biomarkers and/or effective treatment targets.

1.1.5 Neuropathologic, demographic, and genetic features of resilience to AD

Resilient brains show robustly preserved neuronal numbers, synaptic markers, and axonal morphologies compared with demented brains (57). In addition, `high-pathology' resilient brains harbour substantially less inflammatory glial cell responses, complement activation, and proinflammatory cytokines compared with demented brains (57,58). Resilient brains also display significantly lower amyloid-β and tau oligomers as well as hyperphosphorylated tau in the synapses, lower burdens of cortical tau deposits in some studies (27,57,58), and lower burdens of microvascular lesions. Evaluation of presynaptic and postsynaptic densities in resilient brains has shown preservation of synaptic elements when compared with demented, and similar synaptic densities between resilient and control brains (59,60). While `intermediate-pathology' resilient and demented AD brains have not been widely evaluated, one recent study has suggested that early morphologic changes in glial cells already occur in these intermediate stages of tau neuropathologic changes and ahead of NFT development, although no significant changes in total numbers of glial cells between resilient and demented brains were observed in this study, which may be partly due to the small number of cases of N=8 demented and N=5 resilient brains included (61). Of note, brains of Parkinson's disease patients in the early disease stages with Lewy body pathology restricted to the olfactory bulb (Braak stage I for Lewy body pathology), have shown significantly higher numbers of T-cell macrophages in the neocortex in the absence of evident Lewy body pathology (62), supporting that early inflammatory changes may be a common phenomenon of neurodegenerative conditions and involve not only brain-derived but also peripheral immune cell responses.

Clinical and demographic features of resilience include higher level of education, a younger age, a lower BMI, and female gender, while interestingly, the presence of ApoE4 allele and cardiovascular risk factors show no clear differences in resilient compared with demented individuals in some studies (35,49,63). Unexpectedly, recent smoking history and use of anticoagulant/antiplatelet agents (presumably indicated for concomitant cardiovascular/cerebrovascular disease), were recently shown to be more common in resilient compared with demented subjects (63).

Genome-wide association studies of resilient individuals have identified a series of genetic variants and pathways that are associated with protection from the downstream consequences of AD neuropathology, including vascular, metabolic, and neuropsychiatric genetic risk factors while also providing novel resilience gene pathways such as the recent finding of a gene related to the bile acid metabolism (64,65) and the novel description of a rare variant in Reelin that protects against autosomal dominant (AD) AD presenilin 1 (PSEN1) mutations (66). Previously, the same group described another genetic variant called ApoE3 Christchurch mutation which was found to confer partial protection to the development of dementia in an individual carrying the PSEN1 mutation. This individual carried two copies of this rare ApoE3 variant, and the onset of MCI did not occur until he reached the age of 70. Autopsy showed high amyloid-β burden but only limited tau and neurodegenerative measures, suggesting that this mutation may alter the neuropathologic processes leading to dementia development in ADAD carriers, in spite of high burdens of amyloid-β pathology (67). Interestingly, the resilience-linked genes are distinct from the typical genetic risk factors characterizing AD and this thus suggests that distinct pathways unique to resilient individuals could exist and offer novel insights into alternative therapeutic targets that by enhancing resilience could treat dementia (68).

A recent proteomic study on synaptic fractions derived from the parietal association cortex (angular gyrus) of late-stage AD demented, non-demented with high AD neuropathologic burden (resilient), non-demented with low or negligible neuropathologic burden (termed here `frail'), and healthy controls, identified significant changes in >100 protein categories between demented and resilient synapse proteins including reduced serotonin release, depletion of proteasome components, reduced glucose metabolism, and increased oxidative phosphorylation (55), and it identified three proteins that were significantly lower in resilient compared with demented, including LAP3, MACROD1, and SEMA7A. The first two proteins have been associated with the pathogenesis of various cancers, and SEMA7A plays a role in atherosclerosis-associated endothelial dysfunction. Importantly, resilient brains also showed significantly lower enrichment in adaptive and innate immunity proteins compared with demented and frail brains. Interestingly, there was a significant overlap between resilient and healthy control clusters suggesting common pathways associated with synaptic and cognitive preservation regardless of ADNC presence of absence. Although frail subjects showed overlap with some of the protein clusters of demented brains, they also showed some distinctive features such as enrichment in DNA repair and in translation machinery proteins, suggesting that the development of dementia in brains with high and with low/negligible ADNC may involve some common, but also a subset of unique and distinct pathways.

Another recent study using single-cell transcriptomic analyses in demented and resilient brains assessing the prefrontal cortex identified a subset of inhibitory neurons comprised of RELN/LAMP5 and somatostatin neurons that were significantly increased in resilient compared with demented brains at high burdens of ADNC suggesting a potential link between inhibitory neuron preservation and resilience to ADNC. Moreover, this study also evaluated several genes associated with phenotypic variability in cognitive performance and found a set of synaptic genes that were associated with increased global cognitive function (69). This suggests that resilience to AD may be due to a better preservation of inhibitory neurons, and it reinforces the idea that a selective

vulnerability of synaptic elements may be closely associated with the development of cognitive dysfunction in AD.

From a neuropathologic perspective, resilient cases to ADNC show substantially lower comorbid alpha-synuclein and TDP-43 co-pathologies when compared with demented individuals (70). However, a recent case report has shown that, in some rare instances, an individual can develop resilience to high burdens of these three neuropathologies combined (71). Interestingly, a recent biomarker study in cognitively unimpaired elderly has found that CSF changes in alpha-synuclein occurred in around 8% of cases and that all Lewy body positive subjects progressed to dementia over a time span of 10 years, while this was not the case for the asymptomatic amyloid-β and/or tau positive individuals. While resilience to TDP43 and alpha-synuclein pathologies has been described in post-mortem studies with estimated prevalences of up to 24% for TDP-43 (72) and 21% for alpha-synuclein (73,74), little is known about the resilience factors conveying protection against dementia development in the presence of these other neuropathologic changes, and this could be an interesting future study avenue to understand the individual and combined effects of different neuropathologic changes on cognitive function in individuals with and without cognitive impairment.

Overall, these data suggest that inflammatory glial cell responses, vascular injury, oligomeric forms of amyloid-β and tau, and comorbid neuropathologies could be relevant to determining dementia development in the presence of concomitant AD neuropathology, and that some of these elements, such as inflammatory glial changes, may precede the respective neuropathology in a demented AD brain, and be intimately linked with incipient development of dementia in AD.

1.1.6 Clinical relevance of neuropathologic changes observed in demented AD brains

NFT deposits are a key hallmark in the brains of demented AD individuals, but they are also found in other conditions termed `tauopathies' which include corticobasal syndrome, frontotemporal dementia, and chronic traumatic encephalopathy, among others (75). Tau deposits follow a sequential and highly predictive spatiotemporal deposition pattern in the human brain following the Braak stages (11) which begin with NFT deposits in the transentorhinal region (Braak stage I), entorhinal region (Braak stage II), fusiform/occipitotemporal gyrus (Braak stage III), medial temporal gyrus (Braak stage IV), occipital lobe/peristriate areas (Braak V), and lastly affect the occipital lobe/striate areas (Braak VI) (11). The frontal, parietal, and occipital neocortices remain largely unaffected by NFTs up to a Braak stage IV. While NFTs develop in the frontal and parietal neocortices in the stage V, they do so in the occipital and striate cortex only at the very last stages V-VI (12). Several studies have shown that dementia conversion and severity increases in parallel with increasing Braak stages, and that dementia severity goes in parallel with higher burdens of NFT deposits in the brain (76). However, in some instances which are described at around 5-7% for high-pathology and 45% for intermediate-pathology stages, NFTs can be present in the brains of healthy elderly without causing dementia (9,57,58).

Amyloid-β deposits are classically described as the pathognomonic signature of AD brains (77). Amyloid-β deposits spread in a stereotyped deposition pattern in the human brain following the Thal stages (6), which start in the neocortex, particularly in the temporal lobe (Thal phase 1), and progress to allocortex (Thal phase 2), diencephalon, striatum, and basal forebrain (Thal stage 3), brainstem nuclei (Thal stage 4), and cerebellum (Thal stage 5) (6,7). Despite their AD defining signature, amyloid-β deposits show little association with dementia presence and progression (78), and amyloid-β deposits do not predict or correlate well with brain atrophy measures (79), overall suggesting that amyloid-β deposits may be more `neutral' with respect to clinically detectable cognitive and/or structural neuropathologic changes (80). In fact, between 25% and 40% of cognitively unimpaired elderly show evidence of amyloid-β neuropathology at autopsy (16,81–83).

Brain atrophy is a reliable proxy measure of synaptic and neuronal loss, and it relates to structural and functional changes in demented AD subjects. Brain atrophy can be reliably measured *in vivo* with brain MRI, and it has been recently proposed that brain atrophy follows a predictive spatiotemporal progression in AD, likewise to tau and amyloid-β deposits (84). Interestingly, a brain atrophy staging system has been recently proposed by combining longitudinal MRI atrophy measures of healthy controls and demented AD subjects, which were followed up from preclinical to advanced dementia stages. The results of these large-scale analyses showed that brain atrophy progresses similarly but not exactly in parallel to the tau progression patterns described by Braak, albeit differently to the deposition patterns of amyloid-β plaques (84). The newly proposed staging system for brain atrophy starts in hippocampus and amygdala (stage I), middle temporal gyrus (stage II), entorhinal cortex, parahippocampal cortex, and other temporal areas (stage III), striatum and thalamus (stage IV), lastly affecting middle frontal, cingular, parietal, insular cortices and pallidum (stage V). Although tau progression and brain atrophy show an overall close overlap, there is an inverse order in the atrophy observed in the entorhinal and mesiotemporal lobe structures compared with the tau accrual in these regions following the Braak staging system, which could indicate that the later atrophy observed in the entorhinal cortex may underlie a lower vulnerability of this brain region to the effects of NFT deposits, and/or that a particularly detrimental early tau-driven damage to axonal tracts targeting the mesiotemporal cortex could be accounting for the earlier atrophy observed in this region instead. Importantly, the degree of atrophy has been closely associated with cognitive dysfunction and severity irrespectively of dementia etiology (85), and it is found to be a strong predictor of future cognitive change in asymptomatic ADAD mutation carriers (86).

Advances in the development of PET radiotracers in recent years has enabled to image presynapses in the living human brain with the use of SV2A, a synaptic vesicle protein radioligand (87). Validation of SV2A-binding in post-mortem brain and in animal models has shown a good correlation between SV2A signal in PET imaging and synaptic density assessed with synaptophysin in western blot and in quantitative immunohistochemical analyses, making SV2A-PET a potentially useful tool for the assessment of synapse densities in the human brain. In the first SV2A-PET study in AD demented individuals published in 2018, a substantial loss of SV2A-PET signal of 41% was observed in the hippocampus of AD demented compared with healthy controls, which was larger than the volume loss of 21% measured by brain MRI in these same brains (88). In addition, the hippocampal signal of SV2A-PET tracer has been correlated with memory scores and with the severity of cognitive decline in subjects with MCI and AD dementia (88). When assessing the association of SV2A-PET with amyloid-PET and tau-PET signal, inverse associations between synapse densities and amyloid-β/tau burdens have been observed (89). While the use of this novel tracer needs further validation, in particular evaluating post-mortem human brain binding to assess specificity and off-target binding, the initial *in vivo* experiences suggest that SV2A-PET could be a promising and reliable measure of synaptic and cognitive change in early AD with the potential to accurately detect early changes in synapse densities and determine the onset and severity of cognitive decline.

While novel PET radiotracers targeting TSPO to measure neuroinflammation in the brain have been recently developed, they are not widely used in clinical practice due to concerns of unspecific binding, concomitant expression of TSPO in endothelial cells and neurons, issues with passage of the radiotracer through the blood-brain barrier, and sensitivity of TSPO-binding patterns to some genetic polymorphisms that alter its signal and lead to higher variability, among others (90,91). A recent study assessing TSPO binding in post-mortem human brain tissue reported a predominant binding of TSPO to microglial cells with minimal binding to endothelial cells, supporting the specificity of this potential novel PET tracer (92), however further validation is needed for its potential application in research and/or clinical settings in the future.

Overall, the propagation and burden of tau pathology is more closely associated with brain atrophy, synapse dysfunction, and cognitive decline in AD, while amyloid-β pathology in the human brain remains less clear as to its pathogenic role and its direct cognitive effects. In contrast, the cognitive change observed in AD is more closely associated with atrophy and synapse loss, followed by tau deposits and, to a lower extent, amyloid-β pathology, proposing that the effect of ADNC on cognitive dysfunction may be overall limited and partly explain our currently still deficient understanding of AD pathogenesis.

1.1.7 Biomarker definition of AD using the ATN classification system

AD is diagnosed at post-mortem with the NIA-AA Reagan criteria (1), and during lifetime following the ATN classification, which includes biomarker evaluation of amyloid-β (A), tau (T), and neurodegeneration (N)(2). Recent advances in the field have led to an amendment of the present biomarker definition of AD with the addition of new CSF measures and novel plasma-biomarkers some of which have been clinically validated (NIA-AA revised clinical criteria 2023, AAIC). Oftentimes, imaging and fluid biomarker changes in AD are not equivalent, as they measure distinct states of one same protein target (93). While imaging techniques measure the aggregated and deposited forms of proteins and show patterns of accumulation in the brain enabling assessment of topographic distribution and change over time, biofluids detect dysregulation in the production/degradation of the same target proteins and may assess a broader range of protein species that are not detectable by imaging tracers, such as soluble proteins (94,95). Thus, biofluid biomarkers often become abnormal before imaging abnormalities do, and they show discordances mostly in the early-mid phases of the disease. However, the individual values of imaging and fluid biomarkers clearly complement each other, and they may offer important insights into the anatomical and biological changes along the disease spectrum when assessed together.

The newly proposed biomarker definition of AD proposes that A and T are specific for AD while N is important to AD pathogenesis but may also be a common hallmark of other neurological conditions (NIA-AA revised clinical criteria, AAIC, 2023). Within A category, Aβ42/40 in CSF or plasma, and amyloid-PET have been validated for clinical use, and the recent addition of Aβ37 and Aβ38 and Aβ oligomers are being explored in research settings for their potential future clinical use. Within T category, ptau181 and ptau217 in CSF or plasma, and tau-PET are used in clinical settings, and ptau231, ptauT205, and MTBR-243 are proposed for research use. For the N category, NfL in CSF or plasma, and brain MRI or FDG-PET are validated for clinical use, and addition of presynaptic SNAP25 and GAP43, of postsynaptic neurogranin, and pan-synaptic NPTX2 all in CSF together with diffusion MRI and SV2A-PET have been proposed for their use in research settings. Of note, total-tau has been eliminated from the N category, since this measure parallels increasing tau pathology making it more suitable for the T category, but it also dramatically increases in other neurological conditions, overall making it unclear where to best include this biomarker. In addition to ATN measures, current consensus definition of biologically defined AD has proposed addition of inflammatory biomarkers (I) including glial fibrillary acidic protein (GFAP) in CSF and plasma which is validated for clinical use, and the addition of YKL-40 for astrocytes and sTREM2 for microglia in CSF for research use, in addition to vascular injury (V) using brain MRI measures of white matter hyperintensities (WMH) and dilated perivascular spaces, and alpha-synuclein (S) measured in CSF with the use of seed amplification assays. The rationale behind the addition of alpha-synuclein as a very common co-neuropathologic proteinopathy observed in AD brains is to provide a better understanding of underlying contributors to cognitive decline at an individual level. If a patient presents with classical signs and symptoms of a common non-AD disease such as Parkinsonism, quantitative assessment of alpha-synuclein is warranted to realistically attribute some of the cognitive dysfunction to AD and/or LBD. Although TDP-43 also commonly co-occurs in brains with AD, there are currently no available biomarkers to

assess TDP-43 *in vivo*. Importantly, alternative underlying etiologies of dementia other than AD can be derived from certain combinations of ATN components, including limbic-predominant age-related TDP-43 encephalopathy (LATE) when N is present but T absent, and PART when N is present but A absent, both in individuals with cognitive decline.

Novel fluid and imaging biomarkers in AD are rapidly advancing and they offer promising avenues to help better define the underlying pathological substrates of AD dementia and other dementing disorders during lifetime and propose novel treatment targets for better therapeutic interventions.

1.1.8 Biomarker evidence of association between clinical scores and ADNC

Clinical staging of AD dementia severity is usually assessed with the use of common cognitive testing scales (e.g., MMSE, MoCA, CDR) and studies have shown that the degree of cognitive decline closely correlates with brain atrophy measures in brain MRI and with the amount of synapse loss in post-mortem histopathologic and biochemical analyses (96). However, the association between cognitive decline and biomarkers of amyloid-β and/or tau pathologies is not always close. In a recent study including 5500 subjects with dementia diagnosis and biomarker availability, the magnitude of association between MMSE score and CSF amyloid, and between MMSE score CSF p-tau in demented cases reached only weak to moderate associations (97). This is in line with previous studies where correlation analyses between CSF AD biomarkers and MCI or AD dementia stages showed only weak-moderate associations, overall proposing a limited reliability of CSF AD biomarkers for assessment of disease onset and progression (98). In line with data derived from fluid biomarkers, amyloid-PET and tau-PET studies have found that the association of amyloid-PET signal and cognitive decline is weak (and in some cases only present in female) (99), and that tau-PET signal shows an overall stronger association with cognitive scores when signal is assessed in entorhinal cortex, but that this correlation is again weak (100). In fact, even when assessing combined measures of amyloid-β and tau in CSF together with amyloid-PET imaging in demented AD individuals, the prevalence of consistently positive AD biomarkers was reported in only 1/3 of clinically diagnosed subjects with AD dementia (101).

Alternatively, recent studies have proposed that oligomeric amyloid-β, phosphorylated tau, and other post-translational modifications of tau can be measured in biofluids and that they may be more closely associated with cognitive measures, and better distinguish subjects along the dementia spectrum spanning from MCI to advanced dementia stages (102). Some of these AD biomarkers can be assessed in plasma, which adds the potential of a less invasive assessment method with more accessible use. In fact, plasma measures of phospho-tau, including ptau181, ptau217, and more recently also ptau231, have shown strong correlation with their measurement in CSF, which is not the case for total tau that has shown poor correlation between its plasma and CSF values (103,104). In addition, amyloid-β oligomers have been recently proposed as a reliable early measure of cognitive change, and these oligomers can be obtained from CSF and also from plasma through amplification assays, serving as a better measure to discriminate demented from healthy control and SCD subjects (103). This is further reinforced by the recent discovery of the Osaka mutation which induces amyloid-β oligomerization with very little amyloid-β plaque formation and which is clinically characterized by typical AD dementia syndrome in the sole presence of amyloid-β oligomers (105). Similarly, another APP mutation found in families of Swedish ancestry known as the Arctic mutation induces the formation of amyloid-β oligomers and protofibrils over monomeric or fibrillar amyloid-β leading to early onset cognitive decline, further supporting the idea that the intermediate amyloid-β species exert the most neurotoxic effects in AD (106,107). In fact, plasma amyloid-β oligomers have shown moderate-strong correlations with measures of cognition, overperforming the association of monomeric and/or fibrillar amyloid-β forms with cognitive scores (108). Tau oligomers have also been recently measured in CSF and they have shown good discriminatory potential between control,

mildly demented, and moderate-severely demented individuals (102). Comparative analyses of the performance of tau oligomers and phospho-/total-tau in biofluids are however lacking. While the use of combined AD biomarkers in CSF shows an overall good diagnostic accuracy for the detection of AD vs other forms of dementia and a predictive value of around 80% to determine progression of MCI to AD dementia (109,110), the addition of oligomeric amyloid-β and/or other forms of tau to the current AD biomarker scheme could substantially improve diagnostic accuracy of AD dementia from the preclinical and prodromal stages of AD.

Overall, amyloid-PET is somewhat less sensitive to cognitive dysfunction than tau-PET and it can be positive in cognitively unimpaired individuals in around 10-30% of cases (111), while tau-PET has shown lower rates of false positivity in cognitively unimpaired individuals of around 5-10% (112). Importantly, recent tau-PET validation studies across Braak stages have suggested that tau-PET accurately detects tau deposition at Braak stages IV and above, but that its detection threshold is low for tau burdens at or below Braak IV stages including PART cases (113). Of note, the first and only currently available tau-PET radiotracer flortaucipir was just recently approved in 2020 by the FDA for its use in clinical settings. Interestingly, studies comparing the performance of biochemical and imaging biomarkers assessing the more commonly used amyloid-PET have found a concordance of >80% between CSF AD biomarkers and amyloid-PET (114) and, in clinical practice, both can be used interchangeably to identify early stages of AD with similar diagnostic accuracy, and without an additional improvement when assessing them in combination (115). However, the more recently approved tau-PET radiotracer flortaucipir has not yet been widely used in clinical practice and may show lower accuracy in detecting early-stage AD compared with tau fluid biomarkers due to its low detection burden for tau Braak stages IV and below. When predicting progression, studies have shown that measures of neurodegeneration, including MRI measures of hippocampal atrophy, achieve the highest predictive value, and that for MCI to dementia conversion the best predictor is set by patterns of hypometabolism using FDG-PET followed by amyloid-PET and tau-PET measures (116,117).

In vivo biomarker data suggest that, in general, tau overperforms amyloid serving as a better proxy measure of presence and progression of cognitive decline in AD, but that the association between AD biomarkers and dementia is by far insufficient to accurately predict the cognitive trajectory of an individual. Instead, to date the strongest determinant of dementia onset and progression is set by biomarker evidence of cellular and synaptic dysfunction.

1.1.9 Rationale for the study of AD brains/regions at intermediate stages of tau pathology (Braak III-IV)

The here called `intermediate stages' of tau pathology (Braak III-IV stages) are brains that contain NFT deposits restricted to hippocampal, mesiolimbic, and neocortical temporal lobe structures, while most of the neocortex of these brains remains unaffected by NFTs. Importantly, the temporal pole (Brodmann area 38) represents a region of the anterior temporal lobe that becomes affected in the late Braak III stages, as such representing a region of transition between Braak III and Braak IV stages. In contrast, the primary and secondary visual cortices (Brodmann areas 17 and 18) belong to the neocortical regions that get affected at the very end of the tau deposition cascade (Braak V-VI stages). Although the hippocampus represents the clinically and pathologically most affected brain region in AD and it belongs to the so-called allocortex, it is phylogenetically distinct from the two neocortical structures studied here. Yet, recent work has suggested the presence of highly preserved anatomic and functional brain networks that allow to cluster some of these distinct brain structures, including mesiotemporal and neocortical structures, proposing that processes occurring in the hippocampus in early AD may be echoed in the associated neocortical brain regions in the disease process (118). From a neuropathologic standpoint, brains at intermediate Braak III/IV stages of tau

deposition allow the assessment of tau-containing and of tau-free brain regions in one same brain. The study of neuropathologic changes in NFT+ and NFT- areas enables to study the association of neuroinflammatory and other brain changes along the continuum of AD neuropathology development and it helps address the important question of whether neuroinflammation is a primary or a secondary/reactive phenomenon to AD neuropathology, by evaluating the presence of neuroinflammatory changes that occur ahead of amyloid-β plaques and/or NFT development, potentially suggesting a primary role of glia in early synapse and neuronal loss in these brains.

The choice of the two studied brain regions was primarily motivated by their neuropathological relevance along the ADNC continuum. While some of the cognitive deficits observed in AD dementia may derive from dysfunctions in these neocortical structures, the earliest clinical symptoms of AD are typically mediated by other brain regions, such as the hippocampus, and the possibility of remote effects via synaptic projections to these and other (non-examined) areas should be considered. The temporal pole has been involved in several higher-order cognitive functions including mnestic (semantic, autobiographical memory, general knowledge), language (naming, reading, comprehension), visual (complex object recognition, face recognition, visual memory), and socio-emotional functions (emotion recognition/`theory of mind', empathy) as demonstrated by lesion studies and functional imaging studies (119). The temporal pole is clinically impaired from the MCI stages of AD and recent neuroimaging studies in MCI subjects have found that atrophy in the temporal pole is associated with loss of autobiographical memory (120). The visual cortex is the integrating brain region for visual perception and processing, and it has been recently involved in working memory tasks (121,122). Visual acuity assessment in individuals with cognitive decline are not consistent and both, decreased and increased visual acuity have been reported in the early phases of AD dementia, making this parameter unreliable to track development or progression of cognitive decline (123,124). In contrast, visuo-spatial navigation difficulties, reduced visual learning, and altered occipital evoked potentials have been proposed as parameters with functional relevance in the early phases of AD dementia (125), supporting the involvement of occipital-frontal pathway dysfunctions in AD. Yet, in some instances, visual deficits represent the main and earliest clinical feature in what later becomes a typical AD dementia syndrome, and when visual features predominate over memory dysfunction early on, an AD variant called posterior cortical atrophy (PCA) or Benson's syndrome is diagnosed. PCA is characterized by ADNC with predominance in the visual cortex and by an earlier age of symptom onset, typically between 50 and 65 years of age (126,127). Of note, none of the included demented subjects were diagnosed with PCA syndrome prior to death, which is important to ensure optimal comparability of the visual cortical neuropathologic changes assessed here. The temporal cortex which precedes the visual cortex in the acquisition of NFTs following the Braak continuum, shows anatomical and functional connections with the visual cortex through the inferior longitudinal fasciculus (ILF) (128). The ILF represents a bidirectional tract that connects the anterior portions of the temporal cortex with the occipital cortex, and its disruption has been associated with visual cognitive dysfunction signs, including visual agnosia, prosopagnosia, and alexia, as well as semantic memory difficulties (128). These observations are interesting since some of the early features of AD dementia overlap with the functional changes of lesions to the ILF, proposing that some of the early clinical signs and symptoms of AD may derive from changes to temporal and visual brain areas.

From a clinical perspective, demented individuals with Braak III-IV stages at autopsy were mostly in the early stages of dementia prior to death, including MCI and mild AD dementia. Given that AD-typical signs and symptoms usually start to manifest in the 70s and they progress over a period of 8-10 years (129–131), the post-mortem study of MCI and mild AD dementia cases is for obvious reasons limited. However, the early clinical phases of AD are particularly informative as they could inform on other neuropathologic changes beyond amyloid-β and NFTs that could be driving the early dementia development in brains with relatively low burdens of amyloid-β and tau lesions, and

relatively preserved brain structure. These brains could also be key to address early neuropathologic changes in brain areas not yet impacted by NFTs and assess the association of those elements with cognitive decline in the absence of NFTs. Lastly, studying altered mechanisms and pathways that could contribute to dementia development in the early disease stages holds greatest potential to find promising treatment targets that would result in best clinical outcomes in the early and most preventable phases of dementia.

In sum, the study of intermediate stage (Braak III-IV) AD brains could be key to understanding earliest neuropathologic hallmarks driving dementia development in AD and enable the study of early neuropathologic changes in brain areas with and without tau deposits in one same brain.

1.1.10 Contribution of other neuropathologies to dementia

The presence of a pure AD neuropathology at autopsy is rare and is found only in 21-24% of AD brains (132). In contrast, vascular co-pathology in the form of cortical or white matter (WM) lesions is very common in aged brains, presenting in up to 85% of unselected autopsies, and 75% of demented AD brains (133–135). Comorbid alpha-synuclein pathology presents in up to 60% of AD brains and in up to 90% of autosomal dominant PSEN1 gene mutation carriers (136,137), and TDP-43 pathology is found in 50% of AD brains (138). In fact, when assessing the attributable risk of these additional pathologies to cognitive decline in post-mortem studies, TDP-43 accounts for around 15-20% and alpha-synuclein for around 10-15% of premortem Alzheimer's clinical syndrome suggesting an important contribution of these other neuropathologies to the cognitive dysfunction in AD (139). Interestingly, a recent study has described synergistic effects of TDP-43 pathology on tau with increased burdens of phospho-tau and higher tau seeding activity in human brains affected by both pathologies (140). Overall, combined neuropathologies are much more frequent in demented than in healthy elderly brains (overall 45% vs 12%) (141), and alpha-synuclein and vascular co-pathologies are the most common (142). Interestingly, studies have shown that the effects of harbouring one additional co-pathology increases the risk of MCI to AD conversion by up to 20x, and that it doubles the severity of cognitive impairment in readily demented subjects (143). This is in line with *in vitro* and *in vivo* evidence of a synergistic effect of TDP-43 and alpha-synuclein pathologies on amyloid-β and tau toxicity (144,145,136,146–149). Interestingly, combined oligomeric forms of amyloid-β, tau, and the synaptic protein alpha-synuclein have been observed in other tauopathies, and their interaction enhances toxicity and aggregation propensity in *in vitro* models (150). Of note, in the currently under-revision ATN biomarker criteria (NIA-AA, AAIC, 2023), the addition of alpha-synuclein has been proposed to biologically mimic the likely close and very frequent association of ADNC with this proteinopathy at post-mortem. Although almost equally frequent, TDP-43 pathology is not presently included in this revised guideline since there are no currently available biomarkers for TDP-43 proteinopathy, and this could be an important future addition.

Altogether, amyloid-β and tau deposits alone likely do not represent the full neurobiological spectrum of ADNC, and the contribution of other common co-pathologies, in particular alpha-synuclein and TDP-43, may unravel additional neuropathologic processes which may more closely associate with cognitive outcomes in AD. This could help redefine the current biological signatures of AD and aid in the development of future treatments, which could target multiple co-pathologies at the same time and be individualized for each patient.

1.1.11 Vascular pathology

Vascular disease is a very common finding in the brains of healthy elderly (85%) and demented AD subjects (75%) (133–135). The main risk factors for the development and progression of vascular disease are age and vascular risk factors, especially hypertension in middle age (151–153). Vascular

disease in AD brains very commonly presents as subcortical vascular lesions in WM in around 2/3 of cases and as larger infarcts in more severely affected subjects in around 1/3 of cases (153). While some reports have suggested that small infarcts in the setting of full-blown AD neuropathology may not significantly impact cognitive decline given that the detrimental effects on cognition are overcome by ADNC, cerebrovascular lesions in the early dementia phases may very well be influencing and contributing to cognitive impairment (153). Although some of the prototypical vascular lesions of AD brains, such as CAA, show a close association with cortical amyloid-β deposits and typically start to form in neocortical vessels, vascular disease in AD typically affects small penetrating arteries that branch off of large cerebral arteries and course through the parenchyma regulating cerebral blood flow in capillary beds (154). Hence vascular disease in AD predominates in subcortical WM rather than the cortex, manifesting in brain MRI as WMH (155). WM is also particularly vulnerable to vascular injury in normal ageing, partly due to the tortuosity of vessels and to the lower tissue oxygen tension in this brain location (156,157). In fact, WM vascular pathology at autopsy is reported in around 85% of non-demented healthy elderly and in 75% of demented subjects (158). While this suggests that more commonly than not vascular lesions do not seem to cause detrimental cognitive effects when present in the human brain, it has been shown that in the setting of a similar burden of WM lesions in non-demented and early-stage demented individuals, subjects with dementia are more vulnerable to sustain more pronounced cognitive effects of WM injury (159). This suggests that the detrimental effects of vascular pathology may be intimately linked to early ADNC in demented brains and that they may possibly interact and promote structural and functional changes in these brains. Interestingly, WM vascular lesions can be caused by cerebrovascular disease (hypoperfusion) but also by AD pathology (retrograde degeneration) (160) and their detrimental effect on cognition can be influenced by the location of WM lesions, with reports suggesting that anatomical distribution of WM lesions may have differential effects on cognition (161). WM lesions in brain MRI show significant correlation with cortical and medial temporal lobe atrophy (162) and with functional network disruption and frontal dysfunction independently of their location, being commonly associated with the presence of episodic memory loss and executive dysfunction (163).

Hence, microvascular lesions, especially in subcortical WM, are very common in AD brains and they may negatively impact cortical structure and function, particularly in the early dementia phases. While vascular and ADNC are commonly co-existent, the interactions and effects of one on another are not well understood, and they could influence each other to induce cognitive dysfunction. It remains possible that vascular disease and increased vascular leakage may enable the influx of peripheral substances into the brain microenvironment, which may induce or perpetuate the neurodegenerative process of AD.

1.2 Clinical characterization of brains with intermediate stages of tau pathology

1.2.1 Definition of major neurocognitive disorder (dementia)

Dementia derives from Latin and means `without a mind/soul' (`de-mentia'). Dementia was first used to describe people `with mental illness' in the 13$^{th}$ century, although it was only adopted by the medical community in the 18$^{th}$ century to refer to subjects with `psychiatric and/or neurological conditions leading to psychosocial consequences' (164). Despite the stigma associated with its name and meaning, the term `dementia' has been and is still widely used. The term dementia was also still formally accepted by the medical community in the `Diagnostic and Statistical Manual of Mental Disorders' (DSM) IV manual until 2013, when the updated DSM V manual eventually changed the name `dementia' to `major neurocognitive disorder'. Still, most of the publications, medical books, and clinical assessments contain the word `dementia'.

The present definition of `major neurocognitive disorder' (or former `dementia') requires: 1) a substantial impairment in at least one of the six main cognitive domains, and 2) a loss of independence in basic and/or instrumental activities of daily life. In addition, exclusion of 3) other acute medical illnesses and/or 4) additional mental disorders that could explain the cognitive change is required.

The six cognitive domains include: 1) Learning and memory, 2) Language, 3) Executive function, 4) Complex attention, 5) Perceptual-motor, and 6) Social cognition. While the prior DSM IV criteria required impairment in `memory' and at least one other additional domain, the new DSM V criteria only require cognitive decline in one cognitive domain, not restricting the requirement to `memory' only. This is due to the fact that cognitive dysfunction is a hallmark of various different dementia syndromes, in which memory loss is sometimes minimal or not present initially, such as in frontotemporal dementia, PCA variant of AD, and/or cerebrovascular disease (127,165). The diagnosis of cognitive decline additionally requires a subjective change in cognitive performance compared with previous level (informed by the patient, or an informant/clinician), and evidence of decline in a standardized and/or quantifiable clinical test. The cognitive test performance normally falls at least 2 standard deviations below the normative mean. The DSM V manual does not give specific recommendations as to which and how many tests should be applied to assess and diagnose major neurocognitive disorder.

The second defining criterion of major neurocognitive disorder is the presence of functional decline. In the new DSM V guidelines, this is defined by a `loss of independence in daily living', which refers to a series of daily activities needed to accomplish various tasks/requirements and get around in society, and they are commonly subdivided into basic and complex/instrumental activities of daily living. The requirement here is that, at minimum, there is a need of support in `some of the complex/instrumental activities'. This functional loss of independence can be assessed in the anamnesis and/or be complemented by formal testing scales given to the patient and/or the close family members. Again, there are no consensus requirements as to the type of scale or exact cut-off of points to be qualified as functionally impaired.

1.2.2 Causes of dementia and epidemiology of AD dementia

Within the dementia spectrum there are different underlying etiological conditions, and AD represents the most frequent cause of dementia (50-70%), followed by vascular dementia (20-30%), frontotemporal dementia (5-10%), and Lewy body dementia (5%) (166). It is also common for AD to co-occur with vascular dementia and estimates suggest that they coexist in around 30-40% of AD cases (132). Overall, AD is 1.9x more frequent in females than in males, while vascular dementia is 1.8x more frequent in males than in females.

AD has been classically divided into early-onset (EOAD) and late-onset AD (LOAD) based on the age of onset of clinical symptoms. The cut-off is typically set at 65 years of age, although this threshold is arbitrary and cut-offs of 60 years of age have also been used to distinguish EOAD from LOAD (167). Of all AD cases, around 5-10% fall into the EOAD category and 90-95% are classified as LOAD. Previous studies have proposed that EOAD is primarily driven by genetic mutations, but recent evidence has suggested that only a small proportion of EOAD is actually caused by known mutations and that both, EOAD and LOAD may have common neuropathologic substrates (168). Nonetheless, EOAD and LOAD show differences in clinical presentation, disease severity and progression, and in the degree of brain atrophy and hypometabolism with an overall higher severity of dementia syndrome in EOAD compared with LOAD (168).

Recent large scale meta-analyses of US-based study populations have estimated that around 2/3 of Americans experience some level of cognitive impairment at the age of 70, which represents the most commonly reported age of onset of MCI (169). For established dementia, the mean age of onset in the USA is estimated at 83.7 years of age (170). Women have an overall higher risk of developing dementia during lifetime compared with men, which is mainly attributed to the higher life expectancy of female and to age being one of the principal risk factors for sporadic dementia (171). In fact, the risk of developing dementia does not significantly differ between females and males until the age of 80, above which the risk of developing dementia is higher in females (172). In line with this, mean age of onset of dementia is by around 4 years higher in female than male (173).

The prodromal stage of MCI has an estimated prevalence of 10-15% in individuals aged 65 years (174) and it increases to 60% in individuals aged 85 years and above (175). The risk of conversion from prodromal to dementia stage (MCI to AD dementia) is estimated at 10-15% per year (176). Factors that can influence the conversion from MCI to dementia are older age, female gender, lower level of education, ApoE4 status, and positive AD biomarkers in CSF, among others (177).

The prevalence of AD dementia in the USA has been recently estimated at around 10% in individuals aged 65 years and above, and 33% in individuals aged 85 years and above, as shown in data derived from the Alzheimer Association. AD prevalence is known to increase with age and when substratifying for age groups, the estimated prevalence increases from around 4% in individuals aged 65-74 years, to 14% among those aged 75-84 years, and 33% among those aged ≥85 years (178). Previous estimates of AD prevalence in the USA have suggested even higher prevalences of around 50% in individuals aged ≥85 years (26,179). Overall, the prevalence of AD is higher in female (13.3%) compared with male (9.2%) (178). The large variabilities observed in the overall prevalence of AD across studies has been attributed to the substantial underdiagnosis of AD dementia, which is estimated at 39.5% in US-based populations (180) and at over 50% in a primary care setting of a Europe-based community cohort (181). Potential factors that may contribute to the striking underdiagnosis of AD in high income countries despite advanced universal healthcare systems in most of them, may be complex and involve lack of awareness, stigma associated with dementia, the belief that treatment and support may be unavailable, and/or denial from side of the patients and family (181).

AD shows important racial and ethnic disparities with highest incidence of AD in Black and Hispanic populations (182,183). Black individuals have the highest prevalence of AD (14.7%), followed by Hispanics (12.9%), non-Hispanic Whites (11.3%), American-Indian and Alaska Natives (10.5%), and Asian and Pacific Islanders (10.1%) in age-corrected analyses (178). These differences have been attributed to potential medical decision-making bias, with higher diagnosis rates of dementia in Black or Hispanic participants due to conscious or unconscious bias of the clinician, and to overall worse cognitive test performances among non-White compared with White participants due to language barrier and/or lower educational attainment (183). In addition, discrepancies in other risk factors commonly associated with AD such as cardiovascular disease, level of education, and psychiatric comorbidity have been found more frequently in non-White compared with White individuals and may account for some of the differences observed in AD prevalence (184).

Level of education has been suggested to be a protective factor for the development and severity of dementia. Higher education may promote cognitive reserve and improved compensatory mechanisms in the presence of ADNC in the brain. While significant effects between lesser years of education and increased risk of dementia have been reported in several studies, this association is not always present and it seems particularly strong in developed compared with developing countries (185). Interestingly, most `cognitively' advantaged groups (e.g., highly educated White populations) show a delay and a compressed trajectory of cognitive impairment towards the very

end of life, while less advantaged subgroups show an earlier age of onset and more total years of life lived with cognitive impairment. For example, White women have an average duration of cognitive impairment of 6 years, while Black and Hispanic women have 12-13 years of cognitively-impaired life expectancy (173). Recent evidence has estimated that completing >10 years of education seems to be an important threshold to reduce dementia risk while lower duration of education does not substantially alter dementia risk (186). This could explain the overall low effect of education on dementia observed in developing countries. In line with the cognitive reserve model, duration of mental activities plays an important role in building brain networks that may lower dementia risk. Although increased childhood mental ability (e.g., higher grades) are associated with reduced dementia risk in later life, the number of acquired years of education and continuous mental stimulation throughout adulthood may additionally contribute to lowering dementia development (187).

1.2.3 Definition of mild neurocognitive disorder or mild cognitive impairment (MCI)

Recognition of a prodromal stage of neurocognitive decline such as `mild neurocognitive disorder', also referred to as `mild cognitive impairment' (MCI), was first described in 1988 (188). The addition of the MCI stage was incited by the recognition of the importance of an earlier diagnosis of AD dementia and by emerging evidence suggesting that the AD process may have started several years prior to the emergence of clinical symptoms. However, the formal addition of MCI as a clinical diagnosis to the DSM V criteria was also criticized for medicalizing `normality' and for causing potential distress in individuals without a dementia diagnosis and who may never have experienced progression to formal dementia stages. On the other hand, the study of novel biomarkers and the performance of therapeutic trials have shifted to preferentially targeting the earlier dementia phases encompassing MCI, and the obliteration of this newly recognized and very informative disease stage may preclude from future advances in the field.

In the new DSM V diagnostic criteria, MCI is defined as: 1) a `modest' decline in cognitive function in at least one of the six abovementioned cognitive domains and 2) no interference with independence in everyday activities. Again, exclusion of 3) other acute medical illnesses and/or 4) additional mental disorders that could explain the cognitive change is required.

Although no standardized test types or test numbers are specified to establish an MCI diagnosis, it is recommended that a formal broad neuropsychologic testing be performed using different subtests since MCI stages need to be accurately differentiated from both, normal cognitive ageing and major neurocognitive disorder. The performance in cognitive testing normally falls between 1 and 2 standard deviations (SD) below the normative mean.

The second defining criterion of MCI is the absence of functional decline, although greater effort, compensatory strategies, and accommodation may be required. Preserved independence in everyday activities represents the key distinction between mild and major neurocognitive disorder and it needs to be insightfully assessed through report of the patient and/or close family members.

MCI is considered a prodromal transition stage between normal cognition and major neurocognitive disorder (174). MCI forms a continuum in which pathologic changes and clinical symptoms are already objectively present, suggesting a dysfunctional state that clearly differs from healthy cognitive ageing. Although MCI is a heterogeneous syndrome that may coexist with systemic and/or neuropsychiatric disorders, it commonly underlies an incipient neurodegenerative process (189). Overall, MCI affects 10-15% of the population over the age of 65 (174). There are two main subtypes of MCI, one called amnestic MCI, which is slightly more prevalent and presents with early memory loss and a higher risk of dementia conversion, and non-amnestic MCI which is slightly less prevalent

and primarily impairs domains other than memory, and it more commonly converts to other forms of dementia such as dementia with Lewy bodies (DLB) (190,191). MCI is not always a precursor of major neurocognitive disorder, and while the course of MCI can be that of a continuing neurodegenerative process in around 10-40% of individuals (192), it can also remain static and never progress beyond the mild stage of cognitive decline. On average, the yearly rate of conversion from mild to major neurocognitive disorder is estimated at 10-15% (193–195), which is much higher than the yearly incidence of dementia of 1-2% in the general population (196). Interestingly, an important subset of 20-30% of MCI cases have also been found to `revert to normal' cognitive function at 1-year follow up evaluations (197–199). This highlights the need to diagnose MCI stages better and more systematically at baseline to avoid potential under- and overdiagnoses that could lead to changes in cognitive status in subsequent clinical evaluations.

Overall, the average duration of the MCI stage in otherwise healthy subjects is estimated at 7 years although there is high reported variability in literature. Depending on the age of onset of cognitive manifestations total life expectancy can significantly vary ranging from around 21 years for MCI cases with age of onset at age 60 to around 3 years with MCI age of onset at age 95 (200). The average duration of the mild dementia stage is estimated at 2 years, the intermediate or moderate dementia stage is the longest in duration and lasts for 2-4 years, and the late or severe stage is the shortest with an average disease duration of 1-2 years (Alzheimer's society UK*, Dementia life expectancy: Duration and stages (medicalnewstoday.com)*). The most frequent cause of death in AD dementia is due to infection, where aspiration pneumonia is the most common (201).

1.2.4 Definition of subjective cognitive decline (SCD)

Subjective cognitive decline (SCD) refers to a self-reported decline in cognitive function which cannot be determined by neuropsychological testing scales (202,203). Increasing life expectancy and improved awareness of brain health are leading to growing concerns about cognitive function in ageing, and for elderly individuals to seek more and earlier medical advice. In fact, between 50-80% of cognitively normal older individuals report some decline in cognitive function when specifically asked (202).

SCD was formally defined in 2014 to create a framework and consensus definition for the surge in individuals with subjective cognitive complaints but absence of observable deficits in memory testing (203,204). To date, the biological significance and clinical trajectory of SCD remains largely unknown, and SCD has been considered an unspecific symptom that may be part of normal ageing or be associated with other medical conditions, such as psychiatric disorders, sleep problems, and medication/substance abuse (205). Others have termed SCD an at-risk stage for the future development of MCI and dementia. Although most of SCD subjects (~90%) will not develop progressive cognitive decline, in some cases SCD may be the first sign of an underlying neurodegenerative process. A recent meta-analysis found that progression of SCD to MCI and dementia stages occurred in 6.6% and 2.3% of subjects at 1 year, respectively, suggesting that the majority of individuals with SCD (around 90%) remained cognitively stable (206). Factors negatively affecting the risk of progression in SCD were the presence of typical AD biomarkers in CSF and ApoE4 allele status (207). Importantly, AD biomarker abnormalities in SCD are overall low and recent studies have estimated that AD biomarker positivity in CSF of SCD individuals is of 46% for amyloid-β, of 26% for total-tau, and of 40% for p-tau. Presence of typical AD biomarkers in CSF (abnormal CSF-amyloid-β and CSF-p-tau values) in SCD subjects is low and presents in only 18% of cases (208). This is comparable to the prevalence of abnormal AD biomarkers in CSF in cognitively healthy subjects which is estimated at around 16% (209). In contrast, MCI subjects show AD typical biomarkers in CSF in around 54% of cases (210).

Overall, SCD biologically more closely resembles healthy controls than MCI, and it may represent a subform of healthy cognitive ageing which is essentially indistinguishable from cognitively healthy elderly. However, future studies may find biological cues that could better characterize SCD neuropathologically, and which could reveal distinct cognitive trajectories in SCD compared with control subjects, possibly including SCD into the preclinical stages of AD continuum in the future.

1.2.5 Cognitive testing scales – MMSE, MoCA, CDR, WAIS scores

Cognitive impairment is frequently missed by clinicians in the early disease stages, and the prevalence of missed diagnoses considering all stages of dementia is estimated at between 25-90% (211). Dementia is clinically defined as a loss of cognitive function together with functional decline. Cognitive tests are thus essential for the early detection and the quantitative and qualitative characterization of dementia, and >40 clinical testing tools are currently available (211). Yet, the currently used DSM-V guidelines for dementia diagnosis establish no standardized recommendation as to which cognitive test to use, nor do they suggest a minimum number and/or forms of cognitive battery testings required for an accurate diagnosis.

Mini-mental state exam (MMSE) is the most widely used cognitive assessment tool (212). This test assesses six areas of cognitive function, it can be administered within 5-10 minutes, and it is scored up to 30 points (30 points being normal cognition) (213). Its overall sensitivity is moderate (80%) and its specificity slightly higher (87%) to discriminate demented from non-demented subjects using cut-off scores of <26, while its sensitivity drops to 63% but specificity increases to 96% when using cut-off scores of <24 points (211,214). The ability of MMSE to detect early stages of MCI is limited and drops to a sensitivity of 75% and specificity of 71% for cut-offs of <26, and to a sensitivity of 62% but specificity of 87% for cut-offs of <24, which makes this test overall less useful for the detection of early cognitive changes in an individual (211,215). In clinical settings the standard cut-off score of <24 is used, with scores between 24-30 points indicating normal cognition. However, recent efforts to increase the ability of MMSE to identify early cognitive decline stages have proposed using a more stringent cut-off score of 26 to define normal cognition (216). The reduced ability of the test to detect MCI stages has been attributed to the rather limited assessment of executive and visuospatial functions that typically affect the early disease phases and may also be due to the `ceiling effect' of the test which enables more individuals to reach the maximum scores and, as such, limits the detection of mild dementia stages.

Montreal Cognitive Assessment (MoCA) test is another very commonly used cognitive screening test for dementia. It assesses six cognitive domains, and it puts higher weight on executive and visuospatial functions compared with MMSE. MoCA is therefore particularly useful to detect mild cognitive changes, including individuals who score above the normal cut-off of MMSE, and for highly educated individuals who complain about memory loss (217). Like the MMSE, the MoCA test is administered in 5-10 minutes, and it is scored up to 30 points (30 points being normal cognition). The sensitivity of this test is 95% and specificity is 87% when using cut-offs of <26 to detect memory loss in MCI and AD subjects compared with healthy controls (218). In clinical settings, the standard cut-off score of 26 is used, with scores between 26-30 indicating normal cognition. Overall, the detection of MCI stages using MoCA test is superior to that of MMSE. In fact, community-based studies evaluating both testing tools in the same cohort showed a better performance of MoCA over MMSE for detection of early dementia, with prevalence of MCI estimated at 36% when using MoCA and at 29% when using MMSE (195). It is therefore recommended to use MoCA for the assessment of cognitive dysfunction in the early phases of dementia.

MoCA has largely substituted MMSE testing due to its better sensitivity for detecting MCI and mild dementia stages, however MMSE scale was developed in 1975 and MoCA only 30 years later in

2005. Therefore, many studies evaluating the longitudinal trajectory of cognitive change may initially have used MMSE instead of MoCA, which potentially limits the comparability between cohorts and within one same individual when cognition was assessed with both scales (212,219). However, MMSE and MoCA can be converted into one another using conversion tables. While MMSE assesses orientation in greater detail (10/30 points), MoCA is more heavily comprised of visuospatial (4/30 points) and executive tasks (6/30 points). MoCA scores are overall lower than MMSE scores at an individual level, because visuospatial and executive domains are more difficult than tests of orientation. Thus, the conversion between these two scales is not linear. Recent evaluations of the predictive value of MoCA to MMSE and of MMSE to MoCA conversion, concluded that MoCA to MMSE conversion is more accurate than MMSE to MoCA conversion. The use of these conversion tables can thus enable to standardize cognitive screening tools to evaluate and compare individuals or populations assessed with these two different cognitive scales at baseline (220).

Clinical Dementia Rating scale (CDR) was developed in 1988 as a scoring system intended to rate dementia severity. It assesses cognition and daily functioning in six domains comprising memory, orientation, judgement/problem solving, community affairs, home/hobbies, and personal care on a scale that ranges from 0-3 (total of 18 points, indicating a higher burden of functional/cognitive impairment) (221). The score contains two measures, one representing the sum of each of these subdomains into a CDR-sum of boxes score (CDR-SoB) that ranges between 0-18 (18 indicating more severe cognitive changes) and another score generated by an algorithm called CDR-global score (CDR-G) which goes from 0-3 (3 indicating more severe cognitive changes) (221). Both scores are reliable for dementia staging, although CDR-SoB is superior to CDR-G for tracking changes in dementia severity over time (222). MCI stages are not detected well using CDR which may be due to its partial reliability on measures of functional change (that by definition are not present in MCI stages), however its ability to track dementia progression over time is high (223).

Wechsler Adult Intelligence Scale (WAIS) was developed in 1955 and revised in the WAIS-R version in 1981 (224). The most commonly used WAIS-IV scale assesses four cognitive subdomains including working memory, verbal memory, perceptual memory, and processing speed. The final score can be represented as a numeric value ranging from 0-140 or as a percentile (higher scores indicating better cognitive function). In the present study cohort, the Digit Symbol Substitution Test (DSST), a specific subscore of the WAIS-IV scale, was used (225,226). This subtest requires the subject to draw a series of symbols matched to specific numbers following a pregiven key code within a maximum time of 90 seconds, and it measures visuospatial processing, visual memory, and attentional skills. Its score ranges from 0 to 93, and the DSST has been found to be particularly sensitive to age and level of education. There is another test version of the DSST which assesses the same task but in 120 seconds, and its score ranges from 0 to 100 (227). The sensitivity of DSST to discern SCD and MCI subjects from AD dementia is estimated at 90-100% and its specificity at 70-80% when using cut-off scores between 24 and 34 (scores ranging from 0 to 100) with adaption for age and level of education (228).

Although there are no standardized recommendations on the type or quantity of tests that should be administered to an individual with cognitive decline for optimal evaluation of dementia, MoCA is superior to MMSE for detection of early dementia stages, CDR can be used in the more advanced disease stages for measuring the trajectory of cognitive change, and WAIS-DSSN subscore is useful for early cognitive change and, in particular, for visual-perceptual memory assessment.

To stage the severity of dementia, the scores of MMSE, MoCA, and/or CDR-global tests can be combined to characterize healthy controls, MCI, and mild, moderate, and severe dementia. Testing scale cut-offs are not standardized, and they may slightly differ across studies. Dementia stages can be staged using the following cut-off scores (215):

- **Healthy control** MMSE ≥24/26, MoCA ≥26, CDR-G 0-0.5.
- **MCI** MMSE 24-26, MoCA 17-26, CDR-G 0.5.
- **Mild dementia** MMSE 19-23, MoCA 12-16, CDR-G 1.
- **Moderate dementia** MMSE 10-18, MoCA 4-15, CDR-G 2.
- **Severe dementia** MMSE <10, MoCA <4, CDR-G 3.

1.2.6 Operational definition of control, resilient, and demented subjects

In the present study, 60 human brains of healthy controls, resilient, and demented subjects were included. The resilient and demented brains were in the intermediate stages of tau pathology (Braak III-IV), and most of the demented subjects were mildly demented (MCI or mild AD dementia). Of the total of 29 demented cases, 2 cases fulfilled criteria of MCI, 25 cases fulfilled criteria of mild dementia, and 2 cases fulfilled criteria of moderate dementia. Of the total of 21 resilient cases, 1 fulfilled criteria of SCD and 20 were classified as normal cognition. Of the total of 10 control cases, 2 fulfilled criteria of SCD, and the remaining 8 were classified as healthy controls.

To create uniformity in the categorization of the N=60 subjects into control, resilient, and demented groups, an operational definition assessing cognitive status, clinical impression, and functional status was created (see **Table 2**). Cognitive characterization was ultimately combined with the neuropathologic diagnosis to categorize the cases. Importantly, the last clinical assessments prior to death took place within 2 years for most of the included subjects (except for one control case) and this relatively short time interval is important to ensure that resilient and control subjects did not progress and convert to dementia just prior to death, as this could have led to a change in group category (57,49,58). The 2-year rule between the last clinical assessment and the time of death has been set arbitrarily and it is recommended to ensure the quality of clinical data when studying human brains with dementia. In addition, the shorter the time interval between last cognitive assessment and time of death, the stronger the association between premortem clinical and post-mortem neuropathologic changes. In fact, proximal (1 year) as well as more distant (4.5 years) cognitive assessments in demented subjects both closely correlate with the extent and severity of neuropathologic burden, but more proximal clinical assessments prior to death (1 year) show stronger association with NFT burden, and a lack of difference with neuritic plaque burden (229).

Category	Cognitive scores						Clinical impression		Functional status	Group
CTRL	MMSE ≥ 26		CDR-G 0-0.5		CDR-SoB ≤ 2.5		no decline from previous cognitive level		no functional impairment	**C**
SCD	MMSE ≥ 26		CDR-G 0-0.5		CDR-SoB ≤ 2.5		no decline from previous cognitive level		no functional impairment	**C or R**
RES	MMSE ≥ 26	OR	CDR-G 0-0.5	OR	CDR-SoB ≤ 2.5	AND	no decline from previous cognitive level	AND	no functional impairment	**R**
MCI	MMSE 24-26		CDR-G 0.5-1		CDR-SoB 3-4		with decline from previous cognitive level		no functional impairment	**D**
DEM	MMSE < 24		CDR-G ≥ 1		CDR-SoB ≥ 2.5		with decline from previous cognitive level		with functional impairment	**D**

Table 2: Operational definition of control, resilient, and demented groups
Cognitive scores, clinical impression, and functional status defining each of the categories (control, subjective cognitive decline, resilient, mild cognitive impairment, demented) and the respective group assigned in the present study (C, R, D). Of note, the subdivision of SCD into C or R is defined by the presence or absence of ADNC. C/CTRL: control; SCD: subjective cognitive decline; R/RES: resilient; MCI: mild cognitive impairment; D/DEM: demented. MMSE: Mini-Mental State Examination; CDR-G: Clinical Dementia Rating Scale Global score; CDR-SoB: Clinical Dementia Rating Scale Sum of Boxes.

1.3 Synapse loss in AD

1.3.1 Definition of a synapse

Chemical synapses are the means of communication between neurons, and they enable a neuron to rapidly and effectively excite or inhibit the activity of a neighbouring neuron. The synapse is comprised of a presynaptic element (such as an axonal terminal), a synaptic cleft, and a postsynaptic element (such as a dendritic spine). The presynapse contains synaptic vesicles filled with neurotransmitters and they accumulate around a protein-rich area in the axonal terminal called the active zone. When presynaptic axonal depolarization occurs, calcium channels open and the influx of calcium allows the fusion of neurotransmitter-containing vesicles with the presynaptic membrane at the active zone. This induces the release of neurotransmitters to the synaptic cleft which is a small space of around 30-60 nm width that separates the presynapse from the postsynapse of another neuron. At the postsynaptic spine the neurotransmitters bind to neurotransmitter-specific channels, allowing selective ions to enter the postsynaptic terminal. Depending on whether the influx of ions is positive or negative, this creates a hyperpolarization or a depolarization, leading to an inhibitory or excitatory effect on neuronal activity (230).

In the human brain there are two types of chemical synapses, inhibitory ones which represent around 10-20% of all synapses, and excitatory ones which comprise around 80-90% of all synapses (231,232). These two subtypes of synapses are determined either by the respective neurotransmitter that is released by the presynaptic neuron, e.g., glutamate for excitatory and GABA for inhibitory synapses, or by the receptors present at the postsynaptic spine. For example, the postsynaptic protein PSD95 is only expressed in glutamatergic synapses and is strongly associated with excitatory synapses, while the postsynaptic protein gephryn interacts with GABA and glycine receptors and is strongly associated with inhibitory neurons (233). Importantly, recent studies have shown that spines are highly dynamic and that they assemble and disassemble into functional synapses continuously with turnover rates estimated at 40% every 5 days, meaning that at any given time only a proportion of synapses are stably connected and functional in the human brain (234). Moreover, recent evidence has found that new spines can be formed upon task-specific stimulation, and that the extent of new spine formation is associated with the quality of the respective skill acquisition (235,236). Maintenance of new spines correlates with ongoing stimulation and persistence of the learned skill. The preservation of learning-induced spines as opposed to the maintenance of readily present spines, is particularly stable an can persist for several months and up to years after training, representing the anatomical basis of long-term memory (237). Spines in the hippocampus of mice tracked with *in vivo* imaging at different time points show an average lifetime of 1-2 weeks, resulting in a complete turnover of the entire synaptic population in 3x that time, that is in 4-6 weeks, which corresponds with the temporary nature of memory storage in the hippocampus (238). In addition, in the visual cortex of these mice around 75% of spines remain stable at 2 weeks suggesting a much lower turnover rate in this brain region that may be responsible for the long-term memory function ascribed to neocortical synapse circuitry (239). This is in line with other mouse model studies where around 30% of synapses are described as `silent' synapses (240). It is important to note that these animal experiments were done without specific visual stimulation and under experimental conditions, and that the higher average neocortical turnover rates estimated in humans (around 40% every 5 days in humans, as opposed to 25% at 2 weeks in mice) (234) may be due to a more enriched environment and/or to the fact that there are intrinsic biological differences in a human and a mouse brain.

1.3.2 Limitations of synapse imaging

The high density of synapses in the human neocortex (estimated at up to 1 trillion synapses/cm^3) and the small size of synaptic elements (presynapses are estimated to measure 200-400 nm, the synaptic cleft 30-60 nm, and the postsynaptic densities 200-800 nm (241,242)), have posed major challenges in the study of synapses in the healthy and diseased human brain.

Initial studies assessing synapse densities used electron microscopy (EM) to reconstruct synaptic elements in the 2-dimensions and estimate the density of synapses in the respective brain region. However, the limited tissue volume with very thin sectioning needed for EM imaging (around 60-100 nm), the tissue preparation which largely eliminates the preservation of molecular entities, and the lack of possibility to assess different synapse subtypes (e.g., excitatory and inhibitory) limit the use of EM for optimal synapse assessment (233). Alternatively, array tomography (AT) can overcome some of these limitations (243). AT involves serial thin tissue sectioning (50-100nm) followed by resin-embedding to preserve tissue structure, and imaging of adjacent sections generating 3-dimensional (3D) reconstructions. Imaging can be performed using fluorescence or EM, and it generates 3-D ultrastructures at high-resolution (244). However, AT is labour-/time-intensive and costly, and the immunolabeling efficiency can be significantly reduced by resin-embedding of the epitopes of interest limiting the optimal assessment of highly dense nanostructures such as synapses (243). On the other hand, optical microscopy is ideally suited to image large tissue samples, it can reveal different molecular entities of synapses, it allows to assess pre- and postsynapses individually, and it is compatible with multiplexed imaging and allows reconstruction of thicker tissue sections in the 3-dimensions (87). However, an important limitation is the low resolution of optical microscopy due to the limits of light diffraction (~200 nm), which make this technique less able to visualize synapses and their connections. Alternatively, super-resolution microscopy can break the diffraction limit of light, but it requires thin sample slicing and is limited by a reduced throughput which can substantially reduce data acquisition. Alternatively, to overcome the important setbacks of current imaging methods, the novel technique of expansion microscopy (ExM) was recently developed which physically magnifies tissue samples at the nanoscale by separating biomolecules isotropically to increase resolution above the threshold of currently used conventional imaging techniques (245,246).

1.3.3 Benefits of added expansion microscopy for synapse evaluation

ExM is a newly developed technique that allows a physical magnification of tissue specimens through embedding in a polymer gel and immersing the hydrophilic gel in water (245,246). ExM has advantages over EM and AT and it may be particularly well suited for synapse assessment. The time, labor, equipment, and skill demands for ExM are substantially lower when compared with EM and AT (244,247). ExM also allows conventional molecular immunolabelling and imaging in a multiplexed fashion with the use of optical microscopes, which enables the study of synapses in association with other elements. ExM is compatible with different tissue types, including FFPE and frozen tissue samples (248). Antibody staining in ExM can be performed before or after the ExM process. In the earlier versions of ExM fixed tissue was stained with antibodies before it was gelled and expanded, and some synaptic antibody markers seemed to be particularly well suited when using this approach (e.g., Bassoon and Homer1). However, the immunostaining of densely packed synaptic elements has low efficiency due to the limited accessibility of antibodies to densely packed areas with small inter-protein distances that can be smaller than the size of the used antibodies (249). To overcome this potential limitation and improve optimal synapse assessment, methods were developed to allow antibody staining after the tissue digestion and homogenization steps of ExM. This was achieved by

using milder chemical digestions with detergent-containing buffers (instead of enzymatic digestions with proteinase-K) to preserve more antigens for immunostaining after tissue homogenization (250).

Recent studies have shown that ExM increases the accessibility of antibodies to synaptic proteins which may be masked in the dense synaptic mesh prior to expansion, a phenomenon that has been called `decrowding' (249). Molecular decrowding refers to the enhanced unfolding and exposing of epitope binding sites that occurs in the expansion process, and it significantly increases the efficiency of immunostaining compared with non-expanded immunolabelled tissue. This phenomenon poses a substantial benefit of ExM over other 3-D nanoscale imaging techniques such as AT, improving the accessibility of antibodies and immunolabelling efficiency of synaptic and other nanoscale structures. Synapses have been effectively visualized in expanded mouse and *Drosophila* brain using light-sheet microscopy (an imaging technique with faster image acquisition but lower resolution than confocal microscopy (248,251)), and confocal microscopy in mouse brain (252). While the combination of ExM with super-resolution techniques, such as STED, STORM, and SOFI, can substantially add to image resolution, to date only STED combined with ExM has been used to image synapses in the mouse brain (253).

Studies have shown that ExM can be repeated by re-embedding the expanded tissue into a new gel matrix achieving an expansion factor of 16-22x after one round and 53x after two rounds of re-expansion (254). This variant has been called iterative expansion microscopy (iExM) (254) and it has allowed to study synaptic elements and neurotransmitter receptors in the synaptic cleft, such as GLUR1 and GABA-A, providing relevant information on the distribution and interactions of synaptic channels. However, the use of iExM requires the application of nanoantibodies since the highly expanded proteins are not retained in their initial state anymore and they are not detected by commercially available antibodies. While the resolution of ExM with expansion factors between 4-5x is of at least at 70-80 nm in lateral resolution, depending on the resolution capacity of the imaging technique used (246), iExM allows an average resolution of around 25nm (233).

Altogether, conventional ExM enables an expansion of 4-5x and it also benefits from a decrowding phenomenon driven by the physical expansion of densely packed nanostructures. Validation studies of conventional ExM protocols (245,246) have demonstrated the preservation of isotropy and tissue structure across various tissue types, including human samples, without significant rearrangement of synapses and a relative preservation of position of synaptic proteins after expansion (248,249). This enables an unprecedented assessment of synaptic elements in brain tissue with the use of ExM combined with conventional optical microscopy.

1.3.4 Synapse densities in normal ageing, preclinical, prodromal, and dementia stages

Synapses are the biological substrate of cognitive function and synapse loss represents an early neuropathologic hallmark of neurodegenerative disorders and the strongest determinant of dementia severity in AD (255–259). Synapse densities are a better predictor of cognition than amyloid-β plaque burden, NFT deposition, neuronal loss, and brain atrophy (9,257). Healthy elderly display largely preserved synapse densities during normal ageing, exhibiting only minor synaptic losses of at most 15% (260,261) which do not cause a relevant functional cognitive change. However, demented individuals lose 15-25% of synapses in mild dementia stages and 20-50% in advanced dementia stages, and these changes correlate with the onset and progression of cognitive decline across various memory tasks (259,262–265). Although large-scale synaptosome mappings of healthy and demented human brains are currently lacking, synapse density loss in AD initiates in the hippocampus and temporal neocortex (266) and then progresses to parietal regions, overall affecting the cortical brain structures whose function is typically affected in AD dementia (267). Interestingly, some research groups have found that in the very early dementia stages and ahead of

any functional impairment, some synaptic proteins in the brain and in the CSF of demented individuals are increased, possibly in an effort to create novel synaptic connections through increased turnover rates that would compensate for the incipient synapse dysfunction and help maintain cognitive function (255,268,269). However, once these mechanisms subside or fail, total synapse loss surpasses the functionally relevant threshold leading to dementia development and its inexorable progression (270,271). Contrary to the presumed compensatory increase in synapses in the MCI stage, recent studies including MCI and mild dementia subjects have found that synapse density strongly correlates with cognition from the prodromal AD stages, reinforcing that cognitive change is closely paralleled by synapse loss along the full spectrum of AD (255,272,273). Of note, whilst synapse loss is a universal phenomenon present in every demented AD brain, not every synapse subpopulation is equally affected in the disease process. While studies have proposed that excitatory synapses are the main synaptic subtype that gets preferentially targeted in AD, recent evidence has also pointed to a loss of inhibitory synapses as a potential early and crucial step in AD pathogenesis, with findings of selective downregulation of GABA in the brains of demented individuals at post-mortem (274). This reinforces the need to better define biological and anatomical underpinnings of synapse loss in AD, and to evaluate changes in different synapse subpopulations along the AD continuum that could be relevant for future preventative treatments targeting specific synapse subtypes at the right time in AD and in other neurodegenerative disorders characterized by an early synapse loss.

1.3.5 Neuropathological assessments of synapse densities in human AD brains

The first study that reported a loss of synapses in the human AD brain was published in 1987 (275) after a previous attempt in 1983 (276) to quantify synapses in demented AD brains using EM had failed to detect any difference in demented compared with healthy control brains in frontal (average synapse density $1.2x10e^8/mm^3$) and temporal cortices (average synapse density $1.4x10e^8/mm^3$). This was likely due to not considering the brain volume loss caused by brain atrophy in demented individuals that led to an overestimation of synapse densities in those brains. Subsequently, the first study that detected a significant loss of synapses in demented compared with healthy control brains employed stereological morphometry analyses of synapses using EM together with neuronal counts using light microscopy, and created a synapse-neuron ratio to overcome the previous potential bias introduced by brain atrophy (275). By doing so, significant differences in synapse densities were reported in demented ($1.7x10e^8/mm^3$) compared with healthy control brains ($7.3x10e^8/mm^3$) in cortical layers II-III, and a decreased synapse-neuron ratio was reported in demented compared with healthy controls. Importantly, a significant reduction of synapses in layers II-III and layer V of the temporal cortex (25% and 36% respectively) was also present in a subset of 5 AD cases that were in the early stages of the disease (mean age 58.5 years and mean disease duration 2.3 years), and an excess of synapse loss compared with neuronal loss (of 38% in layers II-III of the temporal pole) was described in these subjects, suggesting, for the first time, that the AD disease process may target synapses in the early disease stages.

Subsequent neuropathologic studies of synapses in human AD brains using western blotting replicated the above findings, and additionally found that not only the colocalized synapses but also specific components thereof were reduced in AD brains. Specifically, they showed that the presynaptic proteins synaptophysin, synaptotagmin, and GAP-43, as well as the postsynaptic protein neurogranin were significantly lower in the brains of AD demented compared with healthy controls (277). Moreover, synapse densities were found to be strongly associated with MMSE scores ($R= -0.83$, $p <0.0001$) and with Blessed memory scores ($R= -0.74$, $p < 0.001$) (278). Importantly, while the association of memory loss and synapse densities showed a strong correlation, only weak associations were observed between amyloid-β plaque and/or NFT burden and cognitive loss (257),

proposing, for the first time, that synapses may be better and stronger correlates of the degree of cognitive dysfunction and that they may serve as an early measure of cognitive decline in AD.

Among more recent studies on synapse densities in post-mortem human brains, EM remains the goldstandard method although immunofluorescent histological assessments have emerged as a comparable and more commonly used technique for synapse evaluation owe to its wide accessibility, ease of use, and lower cost. EM requires very thin sectioning (around 60-100 nm thickness) and images obtained with EM are only 2-dimensional, potentially underestimating the true densities of synapses in the brain (279,280). Alternatively, a more recently emerged EM technique called Focused Ion Beam Scanning Electron Microscopy (FIB-SEM) can automatically generate 3-D images with superior z-axis resolution (281). Using FIB-SEM a recent study estimated an average synapse density across the six layers of the entorhinal cortex in healthy human brains at around 6.7±0.21 $x10^8$ synapses/mm^3 (270). A recent comparative study of 10 human brains by the same group showed that demented AD brains (N=5) had lower synapse densities compared with healthy controls (N=5) in the hippocampus, with estimated synapse densities of 9.9±0.18 $x10^8$ synapses/mm^3 in controls, and 6.4±0.35 $x10^8$ synapses/mm^3 in demented brains (270). Another recent study assessing synapse densities in human temporal and visual cortices using optical microscopy combined with 100x oil objective estimated the average synapse density in temporal cortex at 3.6 $x10^8$ synapses/mm^3 and in visual cortex at 3.4 $x10^8$ synapses/mm^3 (232). In another recent study assessing excitatory synapses with synaptophysin and PSD95 antibodies in the inferior temporal cortex of controls (N=12) and demented individuals at tau Braak V-VI stages (N=20) using AT, synapse densities were estimated at 4.29 $x10^8$ ± 7.49 $x10^7$ in controls and 3.45 $x10^8$ ± 9.99 $x10^7$ in demented subjects (282). Comparative studies assessing different synapse densities across different brain regions in the same cases are however lacking, and they could be interesting to create synaptic maps and evaluate subtype specific synaptic density gradients and distributions in healthy and diseased human brains to better understand synaptic changes in normal ageing and in dementia.

1.3.6 Biomarkers of synapse loss in AD

Early synapse loss in AD can be measured in biofluids, brain imaging, and in electrophysiological studies. In fact, synaptic proteins have been first-ever measured in cerebrospinal fluid in 1996 (283) and in plasma in 2015 (284). Recent evidence has proposed that synapse dysfunction and loss is a fundamental process that underlies several neurodegenerative disorders from the preclinical stages, and that signatures of synapse derangement may be specific to each neurological condition (285,286). The diversity in synapse pathology across neurodegenerative diseases is further reflected by the presence (and/or absence) of associations between some synaptic proteins and markers of cellular damage (e.g., NfL) and cognitive status across different neurological conditions (285,286).

Patients with AD dementia show increased synaptic proteins in cerebrospinal fluid (CSF) (287) and plasma (288–292), both reflecting the presumable extracellular release of whole synaptic elements from degenerating functional synapses (293–295). They also show reduced SV2A-PET signal (89), and altered resting-state electroencephalography, which reflects cortical electrical activity and serves as a proxy measure for synaptic activity (296–298). Interestingly, earliest changes in synaptic biomarkers start around 10 years prior to the clinical onset of dementia, they predict conversion from preclinical to prodromal (MCI) stages and dementia, and they closely parallel increasing dementia severity thereafter (288,299).

Measurement of synaptic proteins in CSF has substantially improved with advances in mass spectrometry and immunoassays allowing accurate quantifications of synaptic proteins in biofluids. As of today, there are four main presynaptic proteins (GAP43, SNAP-25, synaptotagmin-1, and alpha-synuclein), and one main postsynaptic protein (neurogranin) that can be reliably obtained and

measured in CSF (262), and they have been shown to be increased in (amnestic) MCI and AD subjects compared with healthy controls making them particularly valuable for the early detection of dementia of likely AD etiology (300). Moreover, recent proteomic studies in CSF of demented individuals have detected 97 additional proteins related to synaptic function that are associated with AD (262). Of note, the currently revised guidelines for the biomarker-based *in vivo* diagnosis of AD (NIA-AA, AAIC 2023) included, for the first time, synaptic biomarkers measured in CSF and SV2A-imaging for the evaluation of AD in research settings, with their potential future use in clinical settings. Although quantitative synaptic protein changes have been widely reported in biofluids of demented compared with healthy controls (285,289,291,293,300–303), no synaptic biomarker has yet been validated for its clinical use which is partly due to variability in protein measurements and peripheral co-expression of some synaptic proteins.

Evidence from studies assessing different synaptic markers in CSF longitudinally have found that in the preclinical disease stages there is already an increase in a subset of synaptic markers in CSF including GluR4, neurogranin, SNAP-25, GAP-43, and synaptotagmin-1 (288). Interestingly, this increase in synaptic markers persists into the prodromal (MCI) stages and MCI subjects show, on average, higher synapse proteins in CSF compared with healthy controls and demented individuals which may reflect the compensatory increase in synapse turnover of the prodromal disease phases. In addition, MCI subjects with higher CSF synaptic protein levels show higher rates of progression to dementia (269). The selective synaptic upregulation in the MCI stage could possibly serve to compensate for synapse loss and keep cognitive function maintained, and it could be used as a surrogate marker of imminent cognitive decline (17,302,304). In subsequent disease stages, synapse loss reflected in CSF continues to progress along with AD, with most synaptic markers, including GAP-43, synaptophysin, PSD95, and neurogranin, further increasing with increasing dementia severity (293,300,305,306), while a few synaptic markers, such as neuronal pentraxins (NPTX), paradoxically decrease with increasing dementia severity (299). This paradoxical effect has been attributed to the dysfunction of a very discrete and specific subpopulation of synaptic proteins assessed by NPTX in the brain that may get lost and eliminated prior to them reaching the CSF, in contrast to the broader loss of synapse populations measured by the other synaptic markers which may be reflected in the CSF by an overall increase of those synaptic proteins (307). The mechanisms of release of proteins from synapses remain unknown and while the disease-associated changes in CSF likely reflect synaptic dysfunction, it is unknown if they also reflect synapse degeneration and/or loss. This remains an area of important ongoing and future research.

PET imaging radioligands that target the synaptic vesicle glycoprotein 2A (SV2A) and bind to presynaptic vesicle transmembrane proteins in the brain have been developed in 2013 as a novel imaging tool for the *in vivo* assessment of synaptic densities in the human brain (308). SV2A is virtually expressed in all synapses and it is located at the presynaptic terminal (309). Of note, SV2A is the binding site of the antiepileptic drug levetiracetam, whose mechanism of action involves the modulation of synaptic neurotransmitter release in the brain (310). Recent studies have found that significant synapse density loss measured with SV2A-PET is present in medial temporal lobe and frontal/parietal neocortical structures in individuals with mild AD dementia compared with healthy controls (89), and that SV2A signal closely correlates with memory dysfunction in early AD (273). Interestingly, the signal of SV2A-PET overlaps with measures of brain atrophy (MRI) and hypometabolism (FDG-PET), but it is more confined to hippocampal lobe structures in the early disease stages, which may more accurately reflect the early loss of synapses in entorhinal synaptic projections to the hippocampus. SV2A-PET is however not specific for AD-related synapse loss, as it has been found to show signal reductions in PD, progressive supranuclear palsy (PSP), corticobasal syndrome (CBS), and epilepsy as well (88). In addition, the tracer has not yet been validated for its use in clinical practice and studies are ongoing to increase the understanding of target engagement, off-target binding, and other biological influences on SV2A-PET signal *in vivo* and at post-mortem

(311). While fluid synaptic biomarkers are thought to represent synapse dysfunction in a demented individual, SV2A-PET may more accurately reflect the synapse density loss in the brain, although the reduced SV2A expression could also represent synapses that are still alive but dysfunctional.

Plasma biomarkers for AD have recently emerged as a less invasive and more widely available tool for the early diagnosis and longitudinal assessment of AD, however the measurement of synaptic proteins in blood is limited by high variability, existence of peripheral expression of some synaptic proteins, and lack of formally validated plasma biomarkers for synapse pathology in AD (291). Recent studies have found that presynaptic neuregulin 1 (NRG1) plasma levels correlate with NRG1 CSF levels and that plasma NRG1 is also independently correlated with memory loss (291). Interestingly, extracellular vesicles (EVs) including exosomes, are small membrane-bound circulating compartments secreted by virtually all brain cells (312), and they are increasingly recognized as central to communication between cells (313). EVs carry proteins that allow to identify from which cell they were secreted, and they can cross the blood-brain barrier bidirectionally into the circulation (314), providing a population of brain-derived molecules that can be measured in blood. Moreover, their cargo remains undiluted and largely protected from the peripheral influence of enzymes through their lipid bilayer (315). Recent studies comparing demented and healthy control-derived exosomes have found decreased synaptic proteins in neuron-derived exosomes (292,316) and increased complement proteins in astrocyte-derived exosomes (317,318). Moreover, astrocyte-derived exosomes have been recently found to carry synaptic proteins in *in vitro* and *in vivo* neurodegenerative disease models (319,320) suggesting an key role of astrocytes in regulating neuronal homeostasis. Moreover, studies have found that the levels of postsynaptic neurogranin are increased in the plasma of demented compared with healthy controls, and that neurogranin levels in brain-derived exosomes in plasma are reduced in demented compared with healthy controls, likely reflecting the overall loss of this synaptic protein in neurons and in the brain (321). Likewise, a recent study evaluating brain-derived EVs in the plasma of demented individuals identified a significant reduction in NMDA-R2A in AD plasma-derived EVs compared with healthy control plasma-derived EVs (322). NMDA-R2A is a receptor for the neurotransmitter glutamate, and it is involved in facilitating synapse transmission, serving as a proxy measure of synapse function. Changes in NMDA receptors occur early in the AD process and one of the currently used treatment strategies for treatment of dementia include blocking postsynaptic NMDA receptors with the drug memantine to prevent over-activation of the glutamatergic system. Still, this study identified reductions in NMDA receptor as a potential proxy measure of early synapse loss in AD subjects, which may reflect a reactive effect paralleling the over-activation of this system in the disease process. Other studies have proposed to measure the presynaptic protein alpha-synuclein in plasma which has previously shown increases in AD brains and in the CSF of MCI and AD demented individuals. Interestingly, alpha-synuclein levels in the blood were found to accurately identify cognitive impairment in patients with amnestic MCI but not in established AD dementia stages compared with healthy control subjects, suggesting that this marker may contribute to the dementia disorder in the early disease process (321).

The only non-invasive tool to assess synaptic activity *in vivo* is with the use of electroencephalography (EEG), which measures the summated post-synaptic potentials generated by cortical pyramidal neurons. Resting state EEG is considered a proxy measure of cortical synaptic activity when assessed under task-absent resting state conditions. In MCI and AD dementia, EEG resting state patterns are altered, and they show generalized slowing and decreased measures of global synchronization. Interestingly, EEG alterations have shown association with cognitive measures, CSF biomarkers of AD neuropathology, CSF synaptic proteins (296,323), and FDG-PET measures of hypometabolism (324). However, the lack of large-scale studies assessing these associations and recent inconsistencies found between EEG changes and measures of ADNC using e.g. amyloid-PET imaging, have hindered the further validation and use of this unique technique in

clinical practice (324). Future studies may provide a better understanding of the underlying substrates of EEG measures and enable the use of this non-invasive tool in clinical settings.

In sum, surrogate *in vivo* measures of synapse loss can be obtained from brain PET imaging, CSF and plasma measurements, and functional EEG, however, to date these measures have not been widely validated for *in vivo* synapse assessment and use in clinical practice. Recent inclusion of some synaptic biomarkers measured in CSF and SV2A-PET imaging for their use in research settings (NIA-AA, AAIC, 2023), may enable the validation and formal use of synaptic biomarkers in clinical settings in the near future, to help more accurately diagnose and track progression of AD dementia.

1.3.7 Effect of ADNC on synapse loss in AD

Synapse loss is known to precede neuronal cell death in AD (325), however the ultimate cause(s) of synapse loss in AD remain largely unknown. Recent evidence has proposed that synapses are vulnerable to some forms of amyloid-β and to oligomeric and hyperphosphorylated species of tau (282,326) and that glial cells excessively engulf synapses in demented brains (272,327). Little is understood about the type of synapse that is preferentially targeted (excitatory vs inhibitory) (328), the initial site of synaptic dysfunction (pre- vs post-synaptic), and the ultimate pathways involved (329,330). Recent evidence has suggested that excitatory and inhibitory synapses may be equally affected, and that presynapses may precede the loss of postsynapses in the human AD brain (289,296,328,331,332).

Synapse loss is most prominent in the immediate vicinity of amyloid-β plaques, within a distance of around 50 µm (333,334). Synaptic densities are especially low in the penumbra of amyloid-β plaques which are areas that contain high amounts of oligomeric amyloid-β (335), and they normalize with increasing distance from the plaque core (336). In fact, *in vitro* and *in vivo* studies have shown that amyloid-β oligomers, but not monomers or fibrils, disrupt synaptic structure and function (337), and that they preferentially target excitatory presynapses (338–340) before they diffuse trans-synaptically to affect postsynaptic receptors in more advanced disease stages (341–344). The selective vulnerability of excitatory synapses in AD is thought to be due to a higher activity of excitatory neurons which induces amyloid-precursor protein (APP) processing (345–347) and enhances oligomeric amyloid-β production in the excitatory pre-synapses (348,349). Interestingly, recent studies have found that resilient brains harbour significantly lower amounts of oligomeric amyloid-β in synaptic terminals compared with demented brains despite both having similar amounts of aggregated amyloid-β in the brain, suggesting that amyloid-β oligomers but not plaques may be an important biological substrate for the development of dementia (350,351). Studies combining synaptic radiotracer SV2A-PET with amyloid-PET imaging have found that SV2A-signal inversely correlates with amyloid-PET signal in the MCI stages, but not in the subsequent AD dementia phases (352). This suggests that amyloid-β deposits may be contributing to synapse dysfunction in the early phases of likely still ongoing amyloid-β accumulation, but that the later more mature amyloid-β deposits may uncouple from the neurodegenerative process (352). It is likely that those more mature amyloid-β plaques would be sequestering higher amounts of amyloid-β oligomers which may hereby lose their synaptotoxic effects (353). This is in line with the classical `amyloid cascade' hypothesis where (oligomeric) amyloid-β is most relevant in the early disease phases while it partly loses neuropathologic and clinical significance in the more advanced stages with deposited aggregates of amyloid-β.

NFT deposits are overall better correlates of cognitive impairment than amyloid-β plaques (354). However, animal and human studies have shown that neurodegeneration and dementia can occur in the absence of NFT deposits (27,57,58,355), that presence of NFTs does not necessarily result in dementia (57,58), and that NFTs may even be protective, scavenging toxic tau moieties (356) and

repairing free-radical damage (357). Moreover, post-mortem human brain studies have found that the burden of neuronal loss largely exceeds the amount of NFTs and ghost tangles in a given brain region (326,358). Additionally, there is no evidence to suggest a loss of synapse densities in the vicinity of neurons affected by NFTs (13,282,359). This is thought to be due to the intracellular sequestration of fibrillar and (synaptotoxic) oligomeric tau within NFTs, which may hereby protect the surrounding synapses from the deleterious effects of oligomeric tau contained inside the neuronal cell body. Growing evidence proposes that oligomeric, rather than monomeric or fibrillar tau, is the most neurotoxic tau moiety (360). Oligomeric tau comprises dimers, trimers, small oligomers and granular oligomers, and it derives from hyperphosphorylated or truncated tau subunits (361). Tau oligomers are potent synaptotoxic proteins that alter synaptic vesicle release and synaptic receptor expression, and they can lead to neuronal death in cell culture (13,362–366).

Tau is found under physiological conditions in its native form in the synapses of healthy neurons (367) and it translocates from pre- to postsynapses upon synaptic stimulation acting as a modulator of synaptic signal transmission (368,369). When tau suffers post-translational modifications such as hyperphosphorylation or conformational changes, it can detach from microtubules and excessively accumulate in synaptic terminals (329,370). This translocation and accumulation of non-native tau alters synapse activity and leads to synapse loss (371). Although the mechanisms of translocation of non-native tau to synapses remain unknown, transport through exosomes, lysosomal release, and passage from extracellular space through plasma membrane have been recently proposed (369). In line with this, hyperphosphorylated tau is higher in the pre- and post-synapses of demented compared with healthy control brains (57,282,372), and oligomeric tau is higher in the pre- and post-synapses of demented compared with resilient and control brains (57,282,331,372). Importantly, tau oligomers are observed in synapses from prodromal stages of dementia and they show a closer association with neuronal loss than NFT burden (373). Conversely, resilient brains may escape the detrimental effects of these toxic tau species by harbouring protective mechanisms (57,58) to avoid oligomeric tau accumulation in synapses.

Hyperphosphorylated tau binds to APP and induces the amyloidogenic processing of amyloid protein into oligomeric amyloid-β (374), and amyloid-β induces the hyperphosphorylation and mis-sorting of tau (375,376) promoting its conversion into toxic tau. When evaluating both proteins combined, the concomitant administration of low subtoxic doses of oligomeric amyloid-β and oligomeric tau leads to immediate disruption of synaptic plasticity and loss of cognitive function in animal models of AD (377). In addition, *in vivo* and *in vitro* studies have shown that in the presence of previously accumulated synaptic amyloid-β oligomers, tau oligomers are more toxic to synapses and overcome the toxic effects of amyloid-β oligomers (378). Overall, these findings support that synaptotoxicity in AD is driven by oligomeric and not by fibrillar forms of amyloid and tau proteins, and that an interaction between oligomeric proteins at the synapse may ultimately promote their individual toxicity and lead to synapse derangement and loss in AD.

1.3.8 Synaptotoxic modifications of tau – hyperphosphorylation, truncation, seeding activity

Tau protein can sustain different posttranslational modifications including hyperphosphorylation, truncation, and ubiquitination, which alter the physiological functions of tau and may lead to synapse and neuronal dysfunction (259).

Hyperphosphorylation of tau can occur at over 85 phosphorylation sites represented by either serine, threonine, or tyrosine residues (379). Tau hyperphosphorylation is present during some physiological processes including brain development, hibernation, and hypothermia (380) where a temporary increase in tau phosphorylation is mediated by an increase in kinases or by decreased activity of phosphatases (381). In brains of demented individuals with AD, excessive tau

hyperphosphorylation is commonly observed, and studies have found that aggregated tau isolated from AD brains contains 3-4x higher phosphorylation levels (8 mol per protein) compared with tau derived from healthy control brains (2-3 mol per protein) (382). Hyperphosphorylation of tau occurs prior to its pathological assembly into NFTs (383,384) and it follows a sequential order along the tau hyperphosphorylation sites that are associated with different stages of tau tangle maturity and with disease stage (385). Earliest tau hyperphosphorylation sites in AD brains include AT8+ (pSer 202, pThr 205, pSer 208) and CP13+ (pSer 202) pretangles, followed by PHF1+ and TauC3+ mature tangles, and GT38+ and MN423+ ghost tangles, overall reaching a cumulative burden of 55 hyperphosphorylated tau sites in advanced stages of the disease (386). The higher the burden of hyperphosphorylated `hotspots', especially in mid- and C-terminal tau domains, the higher the neurotoxicity and propagation propensity of tau (387). While some tau phosphorylation sites such as Ser199, Ser202/Thr205, Thr231, Ser262, Ser396 and Ser422 closely parallel the increasing dementia severity, some of these sites (e.g., Ser199, Ser202, Ser262, Ser396) and other hyperphosphorylated tau epitopes (e.g., Thr181, Thr217) have also been found in healthy control brains (380). The overlap in tau hyperphosphorylation patterns between demented and control brains reinforces the still incompletely understood biological significance of tau post-translational modifications, which further underpins the incomplete association between NFTs and cognitive loss observed in AD (326). In fact, while the extent and burden of NFTs show correlation with increasing dementia severity (388), NFT-bearing neurons do not always show imminent cell death (389) and neuronal loss in an AD brain exceeds by around 7x the burden of NFT-bearing neurons and ghost tangles (358,390). In addition, ghost tangles which are the ultimate reflection of neuronal cell death of NFT-bearing neurons, are exceedingly rare in animal models of AD and in human AD brains, and they are estimated at only around 1% of the total NFT population (391) suggesting that NFTs most commonly do not lead to imminent neuronal cell death in the brain.

Tau truncation is another posttranslational modification of tau that has been associated with synapse dysfunction (387,392–394) and that also confers tau with pathogenic properties including self-aggregation and propagation (392,393). In particular, C-terminal truncated tau has been associated with increased hyper-phosphorylation and seeding activity (392,395,396). Interestingly, recent *in vitro* studies have shown that C-terminal tau truncation is higher in the synapses of both, demented and age-matched control brains, but that upon axonal depolarization and subsequent presynaptic vesicle release, only tau derived from demented brains is substantially released when compared with tau derived from healthy controls (397) suggesting that the toxicity of truncated tau may be partly attributed to its pathogenic spread across the brain. Whether tau truncation precedes or follows hyperphosphorylation and NFT formation remains unknown (387). However, recent studies have suggested that tau truncation is independently and directly associated with neurotoxicity (398), and that it is correlated with dementia severity (387). Ultimately, the mechanisms driving the toxic effects of truncated tau proteins and/or cleaved fragments in the brain remain unclear, but truncated tau may be associated with the toxic property of tau to spread, contributing to the progression of neuropathologic and cognitive changes in AD.

Tau pathology is known to spread in a predictive spatiotemporal pattern along the well-defined Braak stages following anatomical connections in the human brain (399) and the accumulation of tau pathology in subsequent brain regions has been associated with the progression of cognitive decline. Evidence suggests that the prion-like ability of tau to propagate is particularly enriched at the synapse where toxic forms of tau may accumulate (400–402). Tau seeding assays measure the ability of tau to induce tau conformational changes in native tau proteins serving as a proxy measure of toxic tau bioactivity. Tau seeding is measured with the use of fluorescence resonance energy transfer (FRET)-based biosensor cell lines (403,404). These cell lines are HEK293 cells that express aggregation-prone repeat domains of tau fused to either cyan fluorescent protein (CFP) or yellow fluorescent protein (YFP) at an approximately equal concentration level in each cell (405). Under

nascent conditions, diffuse fluorescence can be measured in cells expressing these proteins, however upon introduction of appropriate seeds the two fluorescent proteins aggregate bringing the fluorescent proteins into close proximity (<10nm) which allows FRET signal to occur. FRET signal is measured and quantified using flow cytometry (405,406). Although it remains unclear which forms of tau are more prone to seed, recent studies have proposed that seeding activity is closely linked to the presence of high molecular weight tau (>2,000 kDa), oligomeric and small fibrillar tau (>10 mer), and hyperphosphorylated AT8+ and AT100+ tau (407–410). In particular tau oligomers harbour increased propensity to propagate trans-cellularly (411) and to induce auto-aggregation of native tau in the invaded cells (412–414). Human studies have found that seed-competent tau is significantly higher in the synapses of demented compared with control brains (402) and that tau seeding activity is present from the early disease stages in brain regions that lie up to one Braak stage ahead of tau deposition (402). This has proposed that seeding activity is closely linked to the synaptic compartment, and that the spread of toxic tau may preferentially occur trans-synaptically, leading to the early synapse and cognitive dysfunction of AD. However, other studies have raised questions on the trans-synaptic spread of tau, highlighting that there is no evidence in support of an anterograde propagation of tau seeds when inoculated into mouse brains (415), and by recent post-mortem human evidence showing an inverse order in the dendritic tau acquisition in the temporal cortex compared with tau presence in the hippocampal formation (416).

Overall, tau posttranslational modifications may be crucial for the development of early synapse derangement and cognitive loss in AD, and the role of oligomeric, hyperphosphorylated, and truncated tau at the synapse could harbour essential processes with biological significance contributing to the early synapse derangement and cognitive dysfunction in AD (401,404,417–419).

1.4 Neuroinflammation in AD

1.4.1 Neuroinflammatory changes in AD

Neuroinflammation has recently gained considerable interest in AD (258) supported by genome-wide association studies and by novel insights into glial-mediated synapse elimination (420). A crucial discovery in the field has been that complement, an element of the innate immune system, increases on synaptic membranes upon presence of oligomeric amyloid-β in synapses (421) and tags synapses for elimination by microglia (422). This has been further supported by *in vitro* and *in vivo* evidence of a complement-mediated engulfment of synapses by microglia and astrocytes, which is additionally stimulated by synaptic accumulation of amyloid-β and tau (421,423–428). Although several animal models have shown compelling evidence of an increased elimination of synapses by microglia and astrocytes in AD, human evidence on glial-mediated synapse elimination remains scarce (429). First human data showing an increased engulfment of synapses by microglia have been recently suggested by two studies where higher amounts of synapsin1+ presynapses were found colocalizing with CD68+ microglia in demented compared with healthy control brains in the first study (430), and an increase in synaptophysin+ presynapses were shown to colocalize with IBA1+ microglia in the brains of demented compared with neuropathology-matched resilient and healthy controls in the second study (327). These relevant findings strongly support that microglia ingest synapses in the adult human brain, and that higher synaptic uptake occurs in AD, proposing, for the first time, that altered innate immunity and associated neuroinflammatory pathways could be a pivotal contributor to early synapse loss in AD. Although astrocyte-driven engulfment of synapses has been shown in animal models of AD, the potential role of astrocytes in the excessive elimination of synapses in human brains remains unknown.

Recent evidence from tauopathy mouse models has suggested that altered microglial cell responses and increased T-cells are present in close vicinity to tau deposits and that this association is less

common in amyloid-β mouse models (431). Moreover, the depletion of microglia or T-cells in these mice was found to ameliorate neurodegeneration suggesting that tauopathy and neurodegeneration may be linked through the effects of microglial and T-cell responses (431). Studies evaluating earliest neuropathologic changes in animal models of AD have found that increased inflammatory microglial and astrocytic cell responses occur early and that they precede the development of amyloid-β and tau pathologies in these brains (432). In addition, human studies have shown that in brain regions yet unaffected by AD pathology there are significant increases in microglial cell markers before any tau deposits develop (61), and that in brains of Parkinson's disease patients there are increased T-cell accumulations in brain regions not yet impacted by Lewy bodies comprised of alpha-synuclein pathology (62). Interestingly, when using TSPO-PET to assess neuroinflammatory changes *in vivo*, longitudinal PET-imaging studies in humans have found that an increase in TSPO-PET signal is independently associated with the severity and progression of dementia (433), and that TSPO-PET signal is predictive of longitudinal decline in memory tests (434).

Overall, innate (e.g microglia) and adaptive immune responses (e.g., peripheral T-lymphocytes) may be altered in the early stages of neurodegenerative diseases and ahead of the respective histopathologic signature characterizing these disorders, and these early immune cell responses may be initiating and driving the early neuropathologic and clinical changes of AD dementia.

1.4.2 Phenotypic, morphologic, and functional hallmarks of microglia

Glial cells comprise macroglia (astrocytes and oligodendrocytes) and microglia. The most abundant glial cells in the human brain are oligodendrocytes (45-60%), followed by astrocytes (20-40%), and microglia (5-20%) (435,436). Microglia account for 5-20% of total glial cells in the brain, and their main role is to support and sustain neuronal functions (435). Microglia are considered long-lived cells with small renewal rates of around 0.5-2% and average lifespans of 4.2 years with some microglial cells even persisting for over two decades (437). Microglial cells are also involved in synaptic pruning and axonal guidance in postnatal development, and in phagocytosis of apoptotic debris. They are the key regulators of proinflammatory cytokine release and neuroinflammatory responses, and they can result in potential damage if excessively activated (438). Microglia also own the unique intrinsic ability to migrate (439). This function confers them with an important role in response to tissue injury and it has resulted in microglia being considered the primary phagocytic cell of the brain. The functions of microglia are thus broad and diverse, and their functional state is closely determined by the expression of specific receptor signatures and changes in glial cell morphology. While the number of antigenic receptors expressed by glia are large and novel antigens are still being discovered, the morphologic characterization of microglia is more succinct and currently includes five main subtypes, namely resting or `surveying', activated, ameboid, and dystrophic microglia, and the more recently described rod-shaped subtype (440–442). Morphologic subtypes of microglia are shown in **Figure 1**.

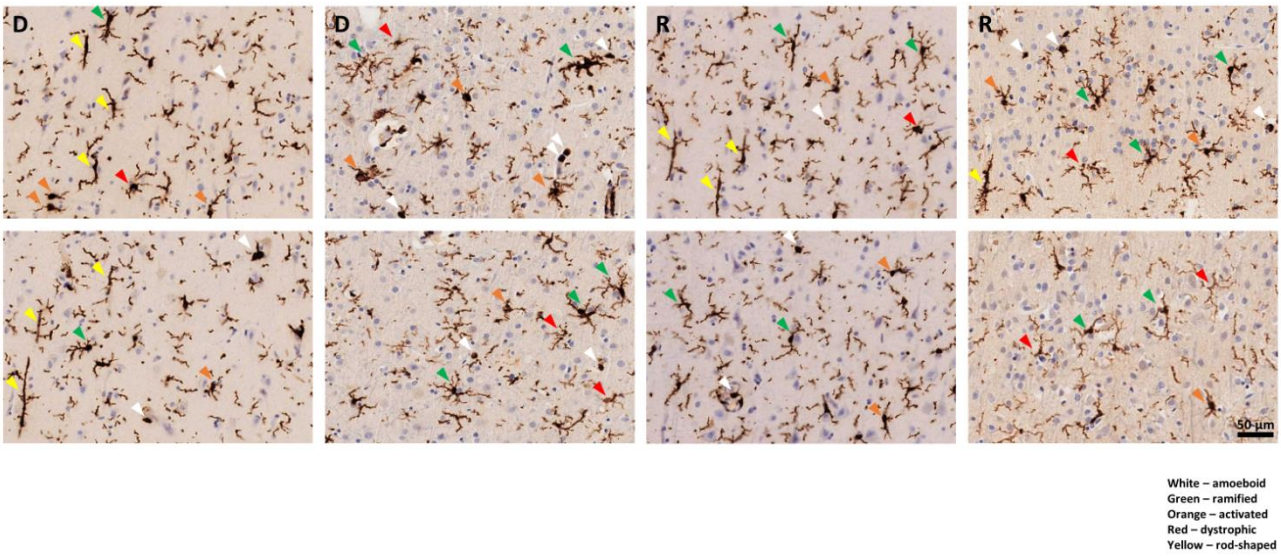

Figure 1: Example of different microglial morphologies in the human visual cortex using pan-microglial antibody IBA1
Microphotographs of microglial IBA1 staining of the visual cortex of two representative demented (D) and two resilient (R) cases showing morphological subtypes of microglia including ameboid (white), ramified (green), activated (orange), dystrophic (red), and rod-shaped (yellow). Each case is shown as two representative microphotographs taken from two distinct regions of the visual cortex. D: demented; R: resilient. Scale bar 50 µm.

Microglia-specific gene signature and antigenic targets include TMEM119, P2RY12, CD81, Sall1, and Hexb among others, and they are uniquely expressed by microglia and are absent in other infiltrating immune cells (e.g., macrophages and lymphocytes). P2RY12 is considered an excellent marker for homeostatic microglia, it is a marker of motility and chemotaxis, and it is rapidly lost in the pathological state. TMEM119 is also specific to microglia although its function remains largely unknown, and it becomes downregulated upon microglial activation in response to injury, but this process is often incomplete and slow (438). IBA1 is the most widely used pan-microglial marker that labels every microglial cell irrespectively of its functional state, binding to the calcium-ionised binding adapter molecule 1 in the cytoplasm. IBA1 is routinely assessed given the reliable visualization of the full microglial cell body and its processes due to its binding to a cytoplasmic target. However, this marker is not specific for microglia as it also labels perivascular and meningeal macrophages which are typically found near vessels and meninges, respectively. Immunoreactivity against the lysosomal marker macrosialin CD68 antibody reveals the degree of lysosomal activity of microglia and is a marker of pro-inflammatory phagocytic glia. Antibodies against human leukocyte antigen DR (HLA-DR) are also commonly used and serve as a marker of pro-inflammatory glia characterized by increased antigen presentation (438).

Microglia are highly dynamic cells that can change their morphology within minutes in response to changes in the microenvironment (438). `Resting' or `surveying' microglia show a small cell body and very fine and highly ramified processes which allow the cell to screen the local microenvironment for signs of injury or pathogens. The change into an `activated' form of microglia occurs in response to the release or secretion of molecules by injured cells or pathogens, which triggers a microglial morphologic change with process retraction and increase in cell soma size. When this activation is

sustained and at its fullest expression, microglia turns into an `ameboid' morphology, where processes are completely retracted and soma is typically roundish and foamy in appearance (438). This morphologic signature of microglia is associated with highly phagocytic and motile microglia an it can occur under physiological conditions such as during prenatal brain development and normal ageing but also under pathological conditions (440,443). Importantly, the phagocytic efficiency of microglia is further enhanced by their ability to increase acidification of their lysosomes upon microglial activation and by their ability to rapidly migrate to the target object within minutes of sustained injury (444) at an average speed of ~5 µm/min and peak speeds >10 µm/min in *in vitro* studies (445). Between the spectrum ranging from resting/`surveying' to ameboid microglia there is a variety of morphological transition states which may reflect disease specific functional states, but their precise roles remain less well defined (442). With ageing, microglia become `dystrophic' and this morphological signature is characterized by cytoplasmic fragmentation, reduction of fine ramifications, and spheroidal swellings. Dystrophic microglia have been suggested to contribute to neuronal impairment and synaptic dysfunction. Recent studies have described a fifth subtype of microglia called `rod-shaped', which was already observed in 1899 by Franz Nissl but did not receive much attention due to the relatively infrequent observation of this morphologic subtype (446). Rod-shaped microglia show narrowing of the cell soma and decreased number of secondary branches, and they have been associated with ageing and neurodegenerative diseases including AD and Lewy body dementia, although their role remains unknown (446). Several studies have shown that total numbers of microglial cells do not change in normal ageing or in a demented human AD brain (447), and that the distribution of microglia in the brain is fairly uniform under healthy conditions. Finding `spots' with two or more microglial cells accumulating is rare and may be a sign of an underlying pathological process (438), such as microglia clustering around amyloid-β plaques or tau aggregates (448). This suggests that not only the morphologic signature of a microglial cell at an individual level, but also the morphologic distribution of microglial cells as a whole may be indicative of functional or dysfunctional properties of this glial cell subtype. Representative images highlighting examples of the five main morphological microglial subtypes are shown in **Figure 1.**

While disentangling the antigenic vs. morphologic characteristics and order of acquisition of antigenic-morphologic signatures of microglia upon pro-phagocytic conversion in AD remains challenging, recent *in vitro* studies have suggested that both, pro-phagocytic receptor expression upregulation and morphologic changes occur, and that they are temporally proximate to one another. Recent studies have found that microglial cells rapidly change their morphology within minutes (438), while the expression of an antigenic signature occurs somewhat slower and can be detected within hours, further increasing over a period of days to weeks (449). In fact, *in vivo* studies have found that the acquisition of an inflammatory microglial antigen signature occurs after around 6 hours of brain injury and that it further increases at 24-48 hours continuing to do so at 7 days for some of the inflammatory markers such as CD68 (450). This suggests that morphological phenotypes may precede the antigenic expression of microglia and be among the first glial cell changes that occur in response to a change in the microglial microenvironment, and that both may ultimately be reflective and contribute to the particular functional state of the microglial cell. While the phenotypic characteristics of glial cells at a given timepoint may reflect their functional effects, it is likely that this process is dynamic and that glial cells continuously adapt their phenotype and adopt varying functions along the spectrum of glial phenotypic signatures.

Overall, microglia are highly dynamic and multifunctional, and they are responsible for the maintenance of brain homeostasis. They act as the principal surveyors of tissue injury in the brain and rapidly elicit inflammatory responses and prophagocytic behaviour upon respective stimulation. Microglia can be defined by the expression of various microglial antigens which are indicative of

different functional states. In addition, more recent evidence has suggested that morphologic changes of microglia may convey the cell with specific functional properties inherent to the adoption of a range of morphological signatures. Morphologic hallmarks of microglia may be of particular interest as they temporally precede the respective change in molecular signatures, and they may therefore represent the first microglial adaption to tissue damage signals (440). Ultimately, a combined antigenic-morphologic approach may be the best way to characterize microglia and to help understand the biological effects of each microglial sub-phenotype in health and disease.

1.4.3 Phenotypic, morphologic, and functional hallmarks of astrocytes

Astrocytes account for 20-40% of total glial cells in the human brain (436) and their functions comprise providing structural support, maintaining cerebral homeostasis, controlling the blood-brain-barrier, and supplying energy to neurons (451). Importantly, astrocytes are the only central nervous system (CNS) cell with glycogen storages and this makes astrocytes essential for energy supply (452). Given that the brain is the organ that proportionally consumes most energy, using around 20% of total body energy despite its proportionally relatively small size which accounts for only ~2% of total body weight, the function of astrocytes is crucial for brain function. Astrocytes are also key for adequate synapse activity as they closely interact with synaptic elements in a functional entity called `tripartite synapse' composed of an astrocytic end-foot and two neurons (a presynaptic and a postsynaptic, respectively) (453), or the more recently proposed `tetrapartite synapse' which additionally involves presence of microglial cell processes in the above interaction (454). One astrocyte can interact with up to 100'000 synapses in the mouse brain and with up to 2'000'000 synapses in the human brain (455), suggesting that the close and continuous interaction between astrocytes and synapses may be crucial for healthy synapse function but may also be associated with earliest synapse dysfunction in disease. Astrocytes establish close interactions with CNS vasculature, and they are an essential element of the newly described `glymphatic system' which is involved in the elimination of toxic soluble proteins from the brain into the blood vessels and peripheral lymphatic system. This function of astrocytes is essential since the brain has no primary lymphatic system as lymphatic vessels are essentially absent in brain parenchyma. The elimination of waste products from the brain is thus highly dependent on the adequate functioning of astrocyte-vascular interactions. Intriguingly, the glymphatic system functions mainly during sleep and is disengaged during the waking hours, serving as a possible biological substrate of the need and benefits associated with sleep across species (456). Recent evidence from animal models has suggested that astrocytes can be pro-phagocytic in the adult brain, and that they can engulf amyloid-β, alpha-synuclein, and tau, and also synapses and cell debris (457,458). Interestingly, astrocytes have also been involved in the potential spread of tau pathology across the brain, contributing to the propagation of toxic tau and disease progression (457). Astrocytes are viewed as the second main phagocytic cell of the brain after microglia and, interestingly, the phagocytic targets of astrocytes and microglia are very similar suggesting that these glial cells either compete for the same targets or that they may act in combination cooperating to effectively remove debris from the brain (458). Of note, although astrocytes are considered non-migratory cells under physiological conditions, they can acquire migratory ability under pathological activation (459).

Astrocyte-specific antigenic signatures comprise the ubiquitous and pan-astrocytic markers ALDH1L1, glutamine-synthetase, and aldolase-C which label cytosolic targets and enable to visualize the cell body and proximal processes with a slightly lower binding affinity to distal astrocytic processes. Moreover, astrocytes upregulate and rearrange their intermediate filaments composed of GFAP, vimentin, nestin, and synemin upon tissue injury responses including trauma, ischemia, or neurodegeneration. The most commonly used marker to label reactive astrocytes is GFAP which binds to astrocytic intermediate filaments and is implicated in cell migration and motility (460). Its upregulation occurs in early response to injury and it increases in parallel to the severity of injury in

mouse models (461). However, this marker is not specific for astrocytes as it can be expressed by ependymal cells and neural stem cells and be increased in degenerating neurons (462). Moreover, GFAP can be lost in quiescent astrocytes (463). GFAP upregulation goes along with changes in astrocyte morphology, mostly comprising an hypertrophy and extension of astrocytic processes towards the injury site (464) and a migration of the astrocytic cell body. Astrocytes in the adult brain are, in contrast to microglial cells, considered non-migratory cells under physiological conditions, however under pathological conditions such as tissue injury or neurodegeneration astrocytes can become motile and migrate (465). Studies have found that reactive but not resting astrocytes show ability to migrate through upregulation of proteins that participate in motility such as integrins and pannexin-1 (466). Moreover, *in vivo* and *in vitro* studies have found that cultured astrocytes transplanted into the mouse brain migrate to multiple brain regions for redistribution under normal physiologic conditions, and that a subset of astrocytes migrates to sites of cortical injury in mouse models (467). The average speed of astrocyte migration has been estimated at 10 µm/hour in *in vitro* studies (468), which is substantially lower than the migration speed of microglial cells, which is estimated at 5-10 µm/min (445). However, some studies have also reported a lack of migration of astrocytes after stab wounds and after traumatic brain injury in *in vivo* imaging studies (469) suggesting that not all but only a subpopulation of reactive astrocytes may migrate upon tissue injury.

Astrocytes can acquire different morphological signatures. The main morphologic subtypes of astrocytes are protoplasmic, fibrous, layer-I astrocytes (specific to mouse brain), interlaminar astrocytes (unique to human brains), and varicose-projection astrocytes (unique to human brains). Protoplasmic astrocytes are predominantly found in the grey matter, and they are highly branched with end-feet enwrapping blood vessels, creating the outer wall of the blood-brain barrier. They are involved in regulating synapse homeostasis due to their close association with a large number of synapses. One single astrocyte can interact with around 100’000 synapses in the mouse brain and with up to 2’000’000 synapses in the human brain (470). On the other hand, fibrous astrocytes are mainly found in the WM, and they are characterized by straight and long processes. The expression of GFAP is overall higher in fibrous astrocytes than in protoplasmic astrocytes, where expression of GFAP is oftentimes limited to the end-feet. While the function of protoplasmic astrocytes remains less clear, they have been associated with vasculature and are likely involved in maintaining blood-brain barrier function. Interestingly, the morphologic changes observed in these two astrocytic subtypes upon injury responses differ in that protoplasmic astrocytes exhibit an increase in length and complexity of processes while fibrous astrocytes show condensation and retraction of processes (463). Layer I astrocytes (specific to mouse brain) show similar morphological hallmarks to protoplasmic astrocytes, but they strongly express GFAP, like fibrous astrocytes do (470). The counterpart of this astrocytic subtype in human brains are the interlaminar astrocytes which are similar to layer-I astrocytes and show preference for upper cortical layers and are composed of astrocytes with short processes, and the varicose-projection astrocytes which are commonly found in deeper layers V-VI, are frequently GFAP+, and often show very long processes that can extend for up to 1 mm and typically terminate in the neuropil or vasculature.

1.4.4 Microglia and astrocyte receptors involved in synapse phagocytosis

Microglia, and to a lesser extent also astrocytes, are the two main cells involved in phagocytosis in the human brain. Both can engulf a broad range of target elements upon expression of specific antigen receptors. For example, synapses are eliminated by C1q, C3, and phosphatidyl-serine (PS) (also called osteopontin) receptor upregulation on synaptic membranes which are detected by MEGF10, CD11b, CD18, C1q-R and CR3 on glial cell surface, apoptotic cell debris is detected through MERTK, AXL, and BAI1 receptors on glial cell membrane, and dystrophic axons and myelin sheets are associated with LRP1 and CR3 on glial cell membrane (458,471–473). One of the most recently

described receptors involved in phagocytosis in AD is TREM2, and this receptor is uniquely expressed by microglia but not astrocytes. TREM2 is found on microglial membranes and it has been shown to be a phagocytic receptor for amyloid-β oligomers (474) and apoptotic cell debris (475). Its pathologic mutation with hypoactivation is associated with increased dementia risk (476). Microglia as opposed to astrocytes also specifically express CR3, CD11b, and CD18, which are phagocytic receptors that specifically detect opsonized synapses (458). A key receptor expressed only by astrocytes but not microglia and which is involved in apoptotic cell debris and synapse elimination is MEGF10. This receptor has been associated with the engulfment of excitatory synapses by astrocytes (477) which responds to presence of PS and C1q opsonized synapses. Microglia do not express MEGF10 but they express Mertk, which is one of the main phagocytic receptors of microglia for synapse engulfment, and this receptor is also expressed by astrocytes.

1.4.5 Phagocytic ability of microglia and astrocytes and mechanisms involved

In the human brain, microglia are the primary phagocytic cell responsible for the elimination of cellular debris and apoptotic cells, however in a breakthrough discovery in 2013 it was found that astrocytes are also able to phagocytose synapses in the developing brain (425), which was followed by evidence of astrocytic ability to engulf cellular debris (425,478,479). It is known that the rapid and efficient removal of apoptotic cells and cellular debris is needed for unimpaired brain function, and that defective clearance of dying cells can lead to neurodevelopmental, autoimmune, neuroinflammatory, and neurodegenerative conditions (480). There are several receptors expressed by brain phagocytes that are essential for effective removal of apoptotic cells, including Axl and Mertk, and many of them are commonly expressed by both, microglia and astrocytes (458,481). Interestingly, recent evidence has suggested that microglia and astrocytes closely interact to engulf specific components of apoptotic cells, rather than acting independently or outcompeting each other for the target object (482). Upon injury signal, microglia and astrocytes are simultaneously polarized to the lesion site. Subsequently, microglia effectively target and remove dendrites, cell bodies, and nuclei, which is further facilitated by their ability to migrate to the injury site (482), while astrocytes engulf dendritic and synaptic elements through extension of their distal processes which requires less cell body migration. Importantly, there is a territorial difference in the phagocytosis accomplished by glial cells, in that microglia show predilection for engulfment of ischemic core while astrocytes predominate in the penumbra of ischemic lesions, respectively (482). This territorial polarization is also maintained microenvironmentally where microglia preferentially engulf cell bodies and astrocytes engulf neurites. Overall, cultured microglia engulf and digest significantly more cellular debris than astrocytes, and the size of engulfed material by microglia is much larger than the one engulfed by astrocytes, overall proposing that microglial efficiency to engulf target objects is superior than that of astrocytes (426,458). However, *in vivo* studies have recently shown that under certain circumstances astrocytes can take over the principal role of engulfment of dying or dead cells (458). In fact, upon reducing the number of microglial cells *in vitro*, astrocytes are able to compensate for functions typically accomplished by microglia such as cell body engulfment, though in a less efficient manner. Moreover, animal models have shown that upon ablation of microglia or induction of highly dysfunctional microglia, cell debris are engulfed by astrocytes and not by non-microglial mononuclear phagocytes such as CNS-associated or peripheral circulating macrophages suggesting that even in the event of a primary microglial cell dysfunction, peripheral immune system does not take over the phagocytic function of CNS-specific glial cells (483), and that this is rather accomplished by astrocytes. Interestingly, recent evidence has shown that the depletion of astrocytic expression of ApoE4, which is the main genetic risk factor known to date for sporadic AD that is predominantly produced and expressed by astrocytes and conveys them with increased phagocytic ability (484), leads to an alteration of synapse phagocytosis by microglia, proposing that a close interaction between microglia and astrocytes may be necessary for the effective removal of target objects (485). However, the effects of astrocyte depletion on microglial

phagocytic efficiency have so far not been explored and this could be interesting to understand the biological significance of glial cell interactions and evaluate pathways that may differ in the physiological vs. pathological elimination of target elements by glia.

Astrocytes are in a privileged anatomical location when it comes to interactions with synaptic elements, which may also enable them to cause deleterious effects including synapse elimination and loss under pathological conditions. However, not all synapses are covered by astrocytic processes and the majority of interactions with astrocytes are physiological. Astrocytes establish contacts with synapses in an activity dependent manner, with preference for excitatory synapses. While microglia are the main cell type involved in synaptic pruning, some synapse subtypes including a subset of excitatory synapses in the hippocampus are exclusively targeted and eliminated by astrocytes and not by microglia (477). In contrast to astrocytes which are continuously interacting with synapses, microglial cells extend their processes to touch synapses and survey the synaptic state, and these contacts occur in an activity dependent manner. Studies have shown that the intermittent interactions of microglia with synapses are physiological but that, when prolonged in time, some synapses disappear (486) suggesting that the continuous recruitment of microglia to synapses may lead to synapse elimination. Astrocytes and microglia crosstalk to effectively accomplish phagocytosis of target elements, and astrocytes release chemo-attractants such as ATP and IL33 to enhance microglial recruitment to sites of phagocytosis (487). In contrast, microglial secretion of proinflammatory molecules such as IL1α and C1q can suppress phagocytic activity of astrocytes for synapses, myelin, and cells debris (488) and recent *in vitro* studies have proposed that co-incubation of astrocytes with microglia-conditioned media inhibits the uptake of synaptosomes by astrocytes (458). This suggests that, collectively, microglia may have advantages over astrocytic phagocytic ability of synapses and other elements, and that microglia may protect from an uncontrolled and excessive phagocytic activity through inhibition of a subset of astrocytes. It is likely that the phagocytic targets of microglia and astrocytes and the crosstalk between glial cells in healthy brains may differ from the ones found in demented individuals, and that microglia may not only become excessively pro-phagocytic and mis-target physiologic elements, but also potentially lose inhibitory capacity over astrocytic phagocytosis leading to an overall excessive elimination of healthy synapses and other physiologic elements.

Phagocytosed elements undergo different degradation fates once they are engulfed by microglia or astrocytes. Recent studies have shown that the degradation capacity of microglia is substantially higher than the one of astrocytes, and that it takes microglia approximately 20 hours to eliminate a single apoptotic neuron, while astrocytes would need more than 50 hours to effectively degrade a similar apoptotic cell (482). In line with this, studies using cultures of macrophages and primary astrocytes co-incubated with cell debris, have shown that macrophages remove cell debris in 3 days, while it takes astrocytes up to 12 days to do so (489). In trying to understand the less efficient degradation ability of astrocytes in contrast to macrophages and microglia, studies have found that lysosomal pH significantly differs between macrophages and astrocytes. Changes in lysosomal pH measured after the addition of cellular debris to cultures of macrophages and astrocytes have found that while macrophages acidify their lysosomes within 5 hours, the lysosomal acidification of astrocytes is hardly observed even after 12 days, suggesting that the slower degradation of engulfed material by astrocytes may partly be due to their overall higher lysosomal pH (490). Interestingly, in AD brains an early lysosomal dysfunction in microglia and astrocytes has been proposed, which may contribute to the defective elimination of toxic cellular and protein debris by glial cells in these brains (491,492) leading to a toxic accumulation of those elements. In addition, recent studies have shown that one potential mechanism of lysosomal dysfunction in microglial and astrocytic cells may involve the internalization of oligomeric amyloid-β and tau proteins by glia (493–496), which could prime those glial cells into an inflammatory state and lead to their dysfunctional mis-targeting of synapses alongside an impaired degradation of toxic proteins (497).

Overall, dysfunctional glial cells may mistarget and excessively eliminate synapses while also show impaired elimination of toxic products in AD brains, and this effect could be further perpetuated by soluble oligomeric amyloid-β and tau. Whether the primary pathogenic process initiates at the synapse with increased oligomeric protein species, or it involves a primary dysfunction in glial cells, and what triggers these effects remains largely unclear. Future studies evaluating the temporal association between these pathogenic elements could unravel the underlying mechanisms involved in the vicious cycle that may ultimately lead to the slowly progressive synapse loss in AD. Also, the potential effect on microglia and astrocytes of oligodendrocytes, the most frequent glial cell subtype in the brain, and the possible influence of peripheral immune system components that may infiltrate the brain through the leaky blood-brain-barrier of demented AD brains, remain to be explored.

1.4.6 Glia in the interaction with amyloid-β pathology

Microglia accumulate around amyloid-β plaques and they become reactive when associated with amyloid-β (498). In fact, the number of peri-plaque microglia increases with increasing amyloid-β plaque size (498) and peri-plaque microglia show higher expression of inflammatory markers such as CD68 (499). Studies have proposed that microglia contribute to amyloid-β plaque growth through amyloid-β phagocytosis which induces microglial cell dysfunction and subsequent amyloid-β release (500). Interestingly, animal models have proposed that microglia take up and convert amyloid-β into toxic forms of the protein which they subsequently spread to brain regions not yet impacted by amyloid-β deposits (498,501). Reactive astrocytes are also found in close proximity to amyloid-β plaques (496) where they show higher expression of inflammatory markers including GFAP (499). Peri-plaque astrocytes engulf large amounts of amyloid-β, convert it into toxic amyloid-β species, and release it to neighbouring cells via microvesicles causing neuronal apoptosis in cell culture (494). *In vivo* studies have recently proposed that soluble forms of amyloid-β induce calcium dysregulation in astrocytes (428) and lysosomal dysfunction (494), leading to astrocytic dysfunction.

Reactive astrocytes can be induced by activated microglia through the release of inflammatory cytokines including IL1, IL6, and C1q. These cytokines also increase β- and γ-secretase activity in astrocytes stimulating APP processing into pathogenic forms of amyloid-β in astrocytes (451). Although APP is also highly expressed in microglia, only astrocytes have been found to be able to process APP to generate amyloid-β (502). This is possibly due to the higher expression levels of BACE1 by astrocytes, which is a key enzyme involved in the pathogenic processing of APP (503). Microglia have not been found to produce amyloid-β through cleavage of APP although microglia theoretically possess the needed machinery to do so. Interestingly, mouse models of AD show that inhibition of BACE1 in microglia reduces amyloid-β load through its more efficient uptake and degradation of amyloid-β, rather than through a reduced production of amyloid-β (504). It has been postulated that the levels of BACE1 in microglia may not suffice for amyloid-β generation, and that the acidic cytoplasm of microglia may hinder generation of amyloid-β species. Importantly, recent evidence has suggested that amyloid-β in astrocytes induces an NFKB-mediated enhanced production and release of C3 by astrocytes, and that astrocytic C3 interacts with C3R on microglial cells altering phagocytosis of amyloid-β by microglia and leading to cognitive dysfunction in animal models which can be effectively treated with C3R-inhibitors (505).

Overall, amyloid-β and glial cells show intricate associations and potential common mechanisms that could elicit a primary glial cell dysfunction together with toxic conversion of amyloid-β species, which could lead to the propagation of neuropathologic changes across the brain.

1.4.7 Glia in the interaction with tau pathology

Studies have shown that reactive microgliosis and astrogliosis linearly increase along with dementia severity and that glial cell responses positively correlate with NFT burden while this association is less consistent with amyloid-β plaques, suggesting that astroglial responses and tau deposits may be more closely linked (506). Microglia are in physical proximity with NFTs in AD brains and they show inflammatory immunophenotypes when associated with tau deposits (507). Microglia engulf tau to eliminate potentially neurotoxic tau species and protect the brain from its pathogenic effects (508). However, as the disease progresses, microglia containing tau become dysfunctional (509) and they release tau to extracellular space hereby likely contributing to the progressive accumulation of NFTs that increase in parallel with dementia severity. Studies have suggested that the switch of microglia from retaining and sequestering potentially toxic tau to later becoming unable to remove toxic tau releasing it to extracellular space, may set the turning point for the initiation of neurodegeneration and cognitive dysfunction in AD (508). Interestingly, despite the fact that microglial cells have not been found to produce tau, and the main primary source of tau in the brain is neuronal, microglia have been involved in the toxic conversion of tau by generating and releasing seed-competent tau after engulfment of live neurons containing tau aggregates (509), and microglia can induce propagation of toxic tau through release of tau oligomers inside exosomes (259).

Astrocytes express very low levels of endogenous tau under normal conditions (457), however substantially higher burdens of tau have been observed inside astrocytes of AD brains (510). Astrocytes engulf tau *in vitro* and *in vivo* and they can engulf tau monomers, oligomers, or fibrils from extracellular space. In fact, they have been found to potentially invade ghost tangles and take up tau from those dead neuronal cell remnants (400). Importantly, not only tau released by neurons but also tau contained in synapses can be taken up by astrocytes, and this is particularly relevant given their intimate association with synapses (457). Astrocyte-internalized tau alters astrocytic function and viability in *in vitro* studies (511) and oligomeric tau can induce calcium dyshomeostasis in astrocytes (512) promoting their dysfunction upon tau ingestion. Cultured human astrocytes have also been shown to convert tau into seed-competent species and release it in exosomes even without stimulation (513,514). While astrocytes can internalize tau from different external sources and spread it across brain regions, evidence of an increased primary production of tau by astrocytes in AD has so far not been found (512).

Overall, *in vitro* and *in vivo* models support that toxic tau ingestion, conversion and propagation in AD may be intimately linked with the interactions between tau and glial cells, and that these bi-directional effects may contribute to tau-driven neurodegeneration in AD.

1.4.8 Intersection of amyloid-β, tau, and glia in AD

The most widely accepted neuropathologic explanation of AD is described by the amyloid cascade hypothesis, which begins with amyloid-β plaque pathology accumulating around 15-20 years prior to cognitive change, followed by tau deposits that increase around 5-7 years prior to clinical symptoms, and synapse loss which occurs in the prodromal disease stages and shows close temporal association with neuroinflammatory changes (299). While astrocytic dysfunction has been identified in the presymptomatic/preclinical disease phases, microglial activation typically occurs in the prodromal/MCI stages and shows close temporal association with hypometabolism and brain atrophy (515). The sequential change in these neuropathologic substrates along the AD continuum has been replicated in animal models of AD (343) and in human biomarker studies giving rise to the Jack hypothesis of biomarker progression (516–518). Despite the primarily sequential nature of the neuropathologic events described by this disease model, it is likely that the ultimately truly significant neurodegenerative determinants may arise once several or all the above elements are

present and interacting in the brain. This would ultimately set off the inexorable neurodegenerative process alongside the cognitive changes of AD.

Recent evidence has shown that amyloid-β and tau oligomers are synaptotoxic by themselves but that their toxic effects are enhanced upon the presence of both (378). In fact, human AD brains show higher frequency of multiple oligomeric species in their synapses compared with neuropathology-matched resilient and healthy control brains (519–521), and amyloid-β and tau oligomers are closely associated with the onset of dementia (343). Recent evaluation of the microenvironment of NFTs in demented brains using transcriptomic and in situ proteomic analyses have found that demented brains show more abundant interactions involving NFT, APP, and synaptic proteins compared with neuropathology-matched resilient brains (522,523). This suggests that amyloid-β, tau, and synaptic integrity are likely spatially and mechanistically linked. Indeed, recent *in vivo* studies have found that oligomeric amyloid-β alters physiological functions of tau on synaptic transmission (368,369), and that amyloid-β can induce hyperphosphorylation and propagation of tau (372,524). In turn, hyperphosphorylated tau increases APP processing and enhances amyloid-β production (525). Interestingly, the removal of amyloid-β or tau from the brain with the use of immunotherapies has been shown to reduce the levels of the other protein, respectively, suggesting that amyloid-β and tau pathologies may be intimately linked (15,526,527). Importantly, amyloid-β and tau oligomers in synapses can induce the release of cytokines and induce aberrant astroglial activation. It is known that microglia and astrocytes take up tau via endocytosis and secrete it contributing to tau spread (514). Similarly, astrocytes are a major contributor to amyloid-β plaque formation (503) and recent evidence has suggested that microglia are able to carry and release amyloid-β from affected to unaffected brain regions in *in vivo* studies (498), pointing to the likely pivotal effects of glia on amyloid-β and tau conversion to toxic and seed-competent species.

These data suggest that oligomeric amyloid-β, tau, and glia likely interact at the synapse of AD brains resulting in synaptotoxic effects (519,528). This interaction is likely bidirectional, with glia contributing to amyloid-β and tau toxicity, and AD pathology leading to chronic glial dysfunction and enhanced synapse elimination, which may overall explain the slowly progressive neuropathologic and clinical disorder characterizing AD (259,427).

1.4.9 Neuroinflammatory changes in white matter in AD

WM abnormalities are very commonly found in healthy elderly and in AD brains when assessed with neuroimaging, and the burden of WM hyperintensities has been associated with incidence of AD and rate of cognitive decline (83). Interestingly, in autosomal dominant gene mutation carriers, WM abnormalities are observed around 20 years prior to the onset of symptoms, and they show close temporal association with changes in amyloid-β and tau measured in CSF. While the underlying etiology of WM abnormalities remains unclear, a primary vascular etiology given most prominent WM lesions in areas of low perfusion, and/or a secondary etiology caused by the retrograde effects of AD neuropathology on WM vasculature have been proposed. Interestingly, many of the WM changes are observed in association with the presence and burden of overlying cortical ADNC.

WM imaging abnormalities are neuropathologically defined by a loss of axons and reduced myelin densities, and they have been described as one of the earliest neuropathologic changes of AD brains (83,529) that can present even before amyloid-β and NFT deposition and ahead of neuronal cell loss (530,531). However, WM abnormalities are also exceedingly frequent in normal ageing (~85%) without causing any change in brain function, and they may therefore represent a concomitant phenomenon of normal ageing with little effect on cognitive function. WM lesions at autopsy (532) have been associated with the burden of overlying neocortical AD neuropathology (356), and they have shown independent and significant correlation with incipient memory loss and subsequent

dementia severity (533,534). WM is known to harbour particularly high densities of glial cells compared with neocortical brain regions, while the proportions of glial cell subtypes in WM and neocortex remain largely preserved. Oligodendrocytes are the most frequent glial cell subtype (45-60% of total glial cells), followed by astrocytes (20-40%) and microglia (5-20%). In addition, there is a small percentage of interstitial neurons in the WM which comprise around 3-5% of total neurons of the brain (535) and whose function remains largely unknown. The glia-neuron ratio in the human neocortex has been estimated at 1.5, while this ratio increases to 3 when including cortex and WM (536), overall suggesting that the vascular changes in WM could be associated and affect the densely packed population of glial cells in this brain location.

Oligodendrocytes are the most common glial cell subtype of the WM, and they are involved in producing myelin, stabilizing neuronal connectivity, and secreting neurotrophic factors (83). Oligodendrocytes are closely associated with neurons and with postsynaptic elements, and they show early morphologic changes in the brains of demented individuals, including changes in their nuclear diameter and morphology (537). Studies have found that soluble amyloid-β species, which are increased in the WM of demented AD brains, are toxic to oligodendrocytes (538). In addition, oligodendrocytes together with astrocytes are the two main non-neuronal cell subtypes that can express tau protein (539). Tau inclusions in AD are mostly neuronal, but in some primary tauopathies tau accumulates inside glial cells, likely involving glial cells in the disease process. Interestingly, recent *in vivo* studies have shown that inoculation of tau into the WM of wild-type mice induces an uptake of tau by oligodendrocytes and a subsequent release and spread of seed-competent tau to adjacent brain regions (539). Thus, it is possible that oligodendrocytes may be involved in the pathogenic processing of AD, and that some of these detrimental effects may be closely associated with WM, where glia is most dense, vascular damage is most prominent, and the potential influx of peripheral elements through damaged vessels in AD brains may be driving some of these dysfunctional effects. The close anatomical interaction of oligodendrocytes with postsynaptic elements is intriguing, and the effects of oligodendroglia on synapse health in AD remain largely unexplored.

In sum, subcortical WM is an understudied brain region in AD that could harbour key neuropathologic processes that may be associated with the early development and progression of AD dementia. The study of glial cell changes in this anatomical location, where close interactions with vulnerable blood vessels are highest, could enable to understand the potential effect of peripheral-central crosstalks that may be contributing to the primary glial cell dysfunction in AD.

Based on previous literature, the present work aims to address a series of important and not yet studied questions in the field of AD research. First, it aims to address whether phenotypic glial cell changes occur as a primary vs secondary effect to AD neuropathologic brain changes, and if they are associated with the presence or absence of dementia in an individual. To this end, a select cohort of human brains from subjects who died at intermediate stages of ADNC (defined as Braak III-IV stages of tau pathology) will be used. Within this group, a subset of cases will have mild dementia and a subset will be cognitively unimpaired ('resilient'). This will enable to explore the relevance of glial cell changes as the potential determinant of cognitive function/dysfunction in two groups of individuals who display comparable ADNC in the brain but differing cognitive statuses (demented vs. resilient). To consider the potential effects of ageing on glial cell signatures, a third group of cognitively healthy age-matched controls will be included. Two brain regions, one affected by NFTs (temporal pole) and one unaffected by NFTs (visual cortex) will be assessed. Glial cells will be evaluated with immunohistochemistry to label ADNC and different glial cell markers in these two brain regions. This will offer the unprecedented possibility to study glial cell changes before (visual cortex) and after (temporal pole) the development of NFTs in one same brain, and evaluate the temporality between the acquisition of selective glial cell signatures and NFT development, to address the primary vs

secondary role of glial cell changes in AD. Secondly, this work aims to evaluate if synapse loss is associated with the presence of early glial cell changes, and whether oligomeric tau may be interacting and/or associated with the early elimination of synapses by glial cells. To this end, ExM will be used to resolve synaptic structures and oligomeric tau species in the visual cortex of the studied brains, and quantitative analyses of synapse densities and of the interactions between synapses, tau oligomers, and microglia/astrocytes will be performed. The use of a brain region with particularly low ADNC and absence of NFTs (visual cortex) will be crucial to address the possibility of an early involvement and pivotal role of glial cells in the early synapse loss of AD dementia. In addition, this work intends to evaluate the early tau modifications that may be particularly enriched in the synapses of early-stage demented individuals and which could be relevant to the early synapse loss in these individuals. This will be addressed with biochemical analyses of synaptosome-enriched fractions extracted from the visual cortex of these subjects and assessed using western blot analyses and tau seeding assays. Overall, the results of this work will enable to provide a better understanding of the role of glial cells in the early AD neuropathologic process, and propose potential mechanisms associated with the early synapse loss in demented AD, and/or synapse preservation in resilient AD brains. This will provide a solid ground for the development of synapse-protective therapies targeting the early and most preventable phases of the disease.

2. Methods

2.1 Human brain cohort

A total of 60 human brains from the Massachusetts General Hospital Brain Bank were included in the present work. Cases were scored by Thal phase for amyloid-β deposition (0-5) (540), Braak stage for NFTs (0–VI) (11), and the Consortium to Establish a Registry for Alzheimer's Disease (CERAD) scale for neuritic plaques (A-C) (541), and divided into three groups: 1) non-demented individuals whose post-mortem examination demonstrated a Braak stage 0-II (controls); 2) non-demented individuals whose post-mortem examination demonstrated a Braak stage III-IV (resilient); and 3) demented individuals whose post-mortem examination demonstrated a Braak stage III-IV (demented) (11). All autopsies were performed according to standardized protocols (542). Cases with evidence of cortical Lewy body pathology, phospho-TDP-43 aggregates, or other lesions different to classic AD pathology were excluded. Braak III/IV stages were pooled into `intermediate stages' of NFT pathology, and the temporal pole (Brodmann area 38) was chosen as a representative brain region affected by NFT deposits. To ensure that all brains were at least in the late Braak III stages and contained NFT deposits in this region, the temporal poles of all cases were stained with AT8 antibody and only cases with presence of NFT deposits in this region were included (**Figure 2**). In addition, and to study an NFT-free brain region in these brains, the primary and secondary visual cortices (Brodmann areas 17 and 18) were selected, where NFTs are known to reach the neocortex only at the very last stages of NFT deposition (Braak V-VI) following the Braak deposition pathways. All visual cortices were stained for AT8 to ensure that there were no NFTs in this region, however a minimal amount of AT8+ neuropil threads were present across brains, and the burden of AT8+ neuropil was similar in resilient and demented brains (**Figure 2** and **Figure 3**). NTs are presumably dendritic and axonal elements (`neurites') containing filamentous tau and they are thought to originate from tau derived from NFTs. Given the abundance of tau pathology in the neuritic compartment, NTs may show a higher cumulative tau burden than NFTs and they could exert an important influence on cognition (3,543). Importantly, recent evaluation of NT progression in the human brain has shown that NTs follow a similar 6-stage deposition scheme as the NFT deposition pattern suggested by Braak&Braak, and that there is a subset of brains, estimated at around 6%, that can harbour NTs at post-mortem without displaying cognitive dysfunction at antemortem (543).

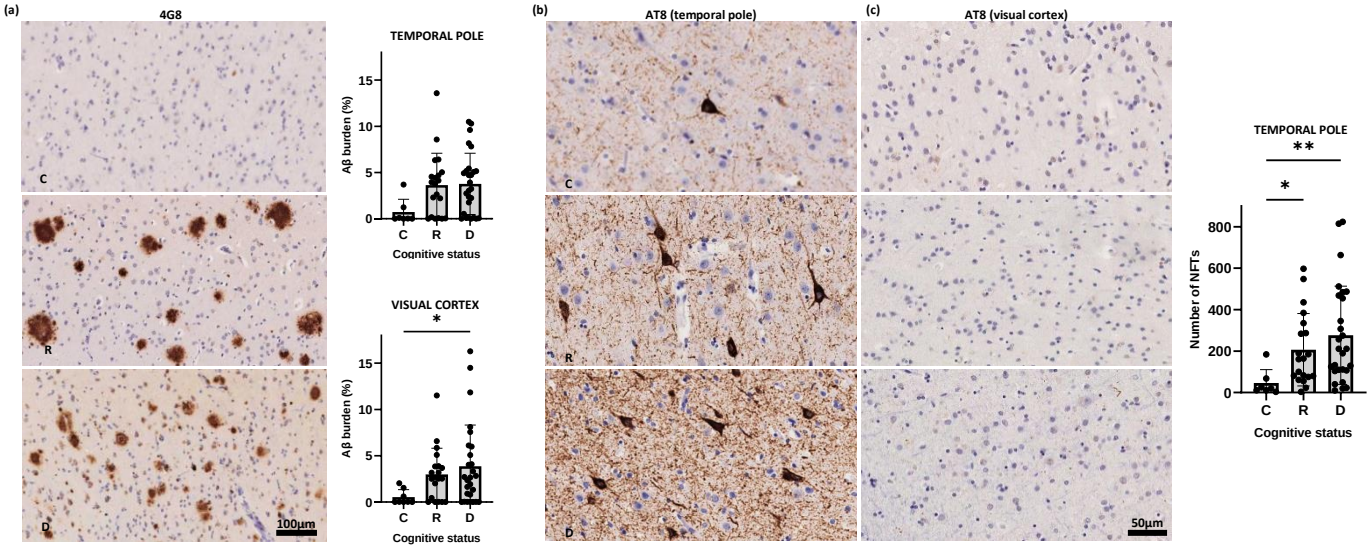

Figure 2: 4G8+ amyloid-β plaque and AT8+ tau neurofibrillary tangle burden in the temporal pole and visual cortices of the N=60 studied cases

Regional 4G8+ amyloid-β plaque burden in the temporal and visual cortices (**a**) and AT8+ neurofibrillary tangle counts in the temporal cortex (**b**) did not significantly differ in demented compared with resilient cases. AT8+ neurofibrillary tangles were absent in the visual cortex of the studied cases (**c**). Representative images (**a-c**) and semiquantitative analyses of 4G8+ amyloid-β plaque burden and AT8+ neurofibrillary (**a-c**) in the temporal and visual cortices of demented, resilient, and control brains. C: Control (Braak 0-II); R: Resilient (Braak III/IV); D: Demented (Braak III/IV). ***p** < 0.05; ****p** < 0.01. Scale bars 50 µm and 100 µm. Data is presented as mean ± standard deviation.

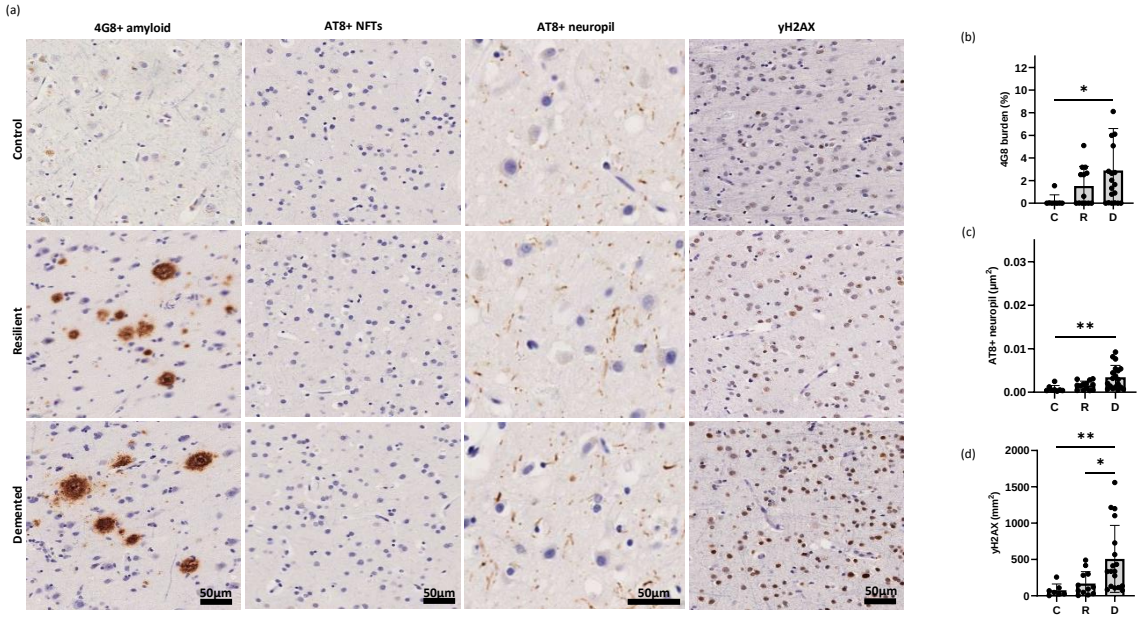

Figure 3: 4G8+ amyloid-β plaque burden, AT8+ tau neuropil burden, and cellular damage marker (γH2AX) in the visual cortex of a subset of N=40 of the studied cases

Regional 4G8+ amyloid-β plaque burden (**a, b**) and AT8+ neuropil thread burden (**b**, **c**) did not significantly differ in demented compared with resilient cases. Early cellular damage marker (γH2AX) was significantly higher in demented compared with resilient and controls (**d**). Representative photomicrographs of amyloid-β plaques, neuropil threads, and γH2AX (**a**) in the visual cortex of control, resilient and demented cases. C Control (Braak 0-II); R Resilient (Braak III/IV); D Demented (Braak III/IV); ***p** < 0.05; ****p** < 0.01. Scale bars 50 μm. Data is presented as mean ± standard deviation.

Amyloid-β neuropathologic changes begin to accumulate in the neocortex according to the Thal stages and they form around 15-20 years prior to cognitive symptoms and about 10 years ahead of tau tangle development (544). Thus, most of the studied AD brains had amyloid-β plaques in the temporal pole and visual cortex. In fact, the majority of demented and resilient brains harboured intermediate loads of neuritic plaques (moderate CERAD scores) and Thal stages 2 or 3 of amyloid-β deposition, meeting criteria of an `intermediate probability of AD' at autopsy according to NIA-AA guidelines (545). However, and to evaluate the possible changes in inflammatory glial responses in the presence, but also in the absence of amyloid-β deposits, a subset of AD cases without amyloid-β in the neocortex was selected (5/21 or 23.8% of the resilient cohort, and 7/29 or 24.1% of the demented cohort), fulfilling neuropathologic criteria of PART. PART is an independent tauopathy observed in the elderly, that is distinct from AD pathology and lacks the presence of amyloid-β deposits or neuritic plaques. NFT pathology in PART is indistinguishable from that of AD as it is composed of 3R and 4R tau, it evolves in a similar fashion from pretangles to ghost tangles, and it propagates along the same pathways described by Braak for classical AD neuropathology, albeit only up to a Braak stage IV (3). In the higher-stage PART cases (Braak III-IV), cognitive complaints are commonly observed and they do not differ in their clinical presentation and/or prevalence of around 50% from those presenting in individuals with classical AD neuropathology and dementia (546). Of all PART cases, 6 demented and 1 resilient case fulfilled criteria for `definite' PART (CERAD score of 0 and Thal stage of 0), and the remaining demented and 4 resilient PART cases were categorized as `possible' PART (CERAD score of 0 and 1, and Thal stage of 1 and 0, respectively) (547).

Of all cases, 26 (including 4 controls, 6 resilient and 16 demented) had undergone formal cognitive evaluation and they had been last seen within 2 years of death (except for one control case who had been seen 4.2 years prior to death) (548). The rest were individuals with either no reported dementia or dementia according to their clinical records and death certificates. Cognitive tests performed in the detailed cognitive assessments included measures of attention, executive function, episodic memory, visuospatial processing, and language using MMSE, CDR-global and CDR-SoB, WAIS-R subscore (digit symbol substitution test), Boston naming test, Trail-making-Test A, and two tests of verbal fluency.

The three groups were matched for age, gender, apoE allele status, brain weight, and post-mortem interval (PMI). Resilient and demented groups were also matched for Thal phase, Braak stage, and CERAD neuritic plaque scores. A composite vascular score was calculated using sub-scores for hypertensive cerebrovascular, atherosclerosis, cerebral atherosclerosis, occlusive atherosclerosis, and cerebral amyloid angiopathy assessed with the Vonsattel scoring system (10), as evaluated by neuropathologists on a rating scale from 0-3 (none, mild, moderate, severe) in tissue blocks derived from the cortex, WM, and basal ganglia. Cases were not matched for composite vascular score, where the demented showed a significantly higher total vascular lesion burden compared with resilient and controls. All the subjects included came from highly educated backgrounds with, on average, >14 years of education, however the demented group showed a significantly higher number of years of education compared with the resilient subjects. The average disease duration in the demented cohort was of 14.7 years (mean age of onset 73.3 years), which is above the average disease duration of AD dementia that is estimated at 8-10 years (130). The particularly high cognitive reserve of the highly educated cohort of demented individuals may explain the relatively mild

dementia syndrome despite an overalll relatively long disease duration. Lastly, the race of the subjects included in the study was biased towards an overrepresentation of White individuals, while only one demented subject was Asian, and one control subject was African-American.

The inclusion and exclusion criteria for the N=60 cases and subselection criteria for individual analyses are shown below:

Inclusion criteria: Braak stage III-IV for R/D and Braak 0-II stage for C; amyloid-β plaque score 0-5 (a subset of PART cases was included in the R/D group); neuritic plaque CERAD score 0-3 for R/D and 0 for C; cognitive status assessed with chart review or detailed neurologic examination; D/R/C cases were matched for age, gender, and PMI; vascular score (microvascular lesion burden) was unrestricted; tissue availability either as FFPE and/or frozen tissue.

Exclusion criteria: Braak stages >IV; presence of cortical TDP43 and/or alpha-synuclein inclusions; unavailability of cognitive status; evidence of macrovascular lesions (ischemic or hemorrhagic stroke) except for acute brain hemorrhage as the imminent cause of death; unavailable tissue (some tissue blocks became depleted/unavailable).

Of the N=60 cases, N=55 cases were available for FFPE quantitative assessments of glial phenotypes at the time of the study. Of the N=60 cases, N=40 cases were selected for detailed synaptic evaluations. Criteria for the subselection of the N=40 cases were tissue availability for FFPE (thick sections for ExM) and/or frozen tissue (synaptosome extractions and WB analyses); where possible cases with detailed neurocognitive assessments were included (N=26) and the remaining N=14 cases showed chart review verification of respective cognitive status. Of the N=60 cases, N=10 cases were used for oligomeric tau in synapses and TOC1-glial cell interactions; these N=10 cases were selected based on matched vascular scores excluding any PART cases and on availability of FFPE tissue for ExM. All the set of groups were matched for ADNC burden, age, gender, and PMI. The demographics and neuropathological data of the N=60 cases are summarized in **Table 3**.

Cognitive status	Control	Resilient	Demented
Number of subjects, total N=60	10	21	29
Cognitive scores			
MMSE (mean, SD)	29 (0.5)	29.5 (1.2)	24 (5.8)*
CDR-global (mean, SD)	0.3 (0.3)	0.1 (0.2)	1.5 (0.9)****
CDR-SoB (mean, SD)	0.8 (0.9)	0.1 (0.2)	8.6 (5.6)****
WAIS-R subscore (mean, SD)	41.3 (5.3)	47.5 (7)	30.3 (9.1)**
Boston naming test (mean, SD)	29 (0.8)	26.8 (1.2)	22.4 (5.6)**
Trail making Test A (mean, SD)	35 (3.5)	31.7 (6.9)	57 (27.8)*
Verbal fluency (animals) (mean, SD)	19.5 (4.8)	18.3 (3)	11.2 (5.5)*
Verbal fluency (vegetables) (mean, SD)	15.8 (5.4)	15 (2.9)	6.9 (3.3)**
Age (years)			
Mean (SD)	84.8 (9.3)	87.9 (9.5)	88 (6)
Gender			
Female N (%)	4 (44%)	12 (55%)	15 (52%)
Male N (%)	5 (56%)	10 (45%)	14 (48%)
Years of education			
Mean (SD)	17.5 (1.7)	14.4 (1.7)	17.4 (1.9)*
ApoE allele status			
ApoE2 allele (%)	1 (8%)	1 (7%)	3 (14%)
ApoE3 allele (%)	11 (92%)	12 (86%)	18 (82%)
ApoE4 allele (%)	0 (0%)	1 (7%)	1 (4%)
Neuropathology ('ABC' score)			
A-Thal phase, range (mean)	A0-4 (0.7)	A0-4 (2.2)	A0-5 (2.1)
B-Braak stage, range (mean)	B0-II (1.2)	BIII-IV (3.4)	BIII-IV (3.5)
C-CERAD score, range (mean)	C0-1 (0.2)	C0-2 (1.4)	C0-3 (1.1)
Brain weight (grams)			
Mean (SD)	1289 (204)	1222 (153)	1197 (146)
Vascular score			
Composite score, mean (SD)	3.7 (2.1)	2.9 (1.9)	5.3 (2.7)**
PMI (hours)			
Mean (SD)	24.1 (12.5)	18.2 (12.2)	18 (9.3)
Last clincial visit prior to death (years)			
Mean (SD)	1.5 (2.2)	0.6 (0.4)	0.5 (0.4)
Disease duration (years)			
Mean (SD)	NA	NA	14.7 (6.5)

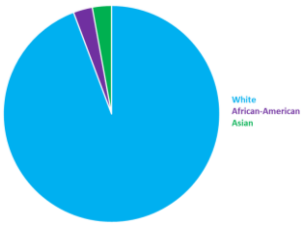

Table 3: Demographic, clinical, and neuropathologic features of the N=60 studied cases
Demographic, clinical, and neuropathologic features of the N=60 subjects. All antemortem cognitive measures were significantly worse in demented compared with resilient. Cognitive measures in resilient were not significantly different than in controls. Years of education were significantly higher in demented compared with resilient. Vascular composite score was significantly higher in demented compared with resilient. Thal phase: No amyloid-β deposition (A0), amyloid-β in neocortex (A1), amyloid-β in allocortex/limbic regions (A2), amyloid-β in diencephalon/basal ganglia (A3), amyloid-β in brainstem/midbrain (A4), amyloid-β in cerebellum (A5); CERAD score: No neuritic plaques (C0), sparse plaques (C1), moderate plaques (C2), frequent plaques (C3); Cerebrovascular composite score includes subscores for: hypertensive cerebrovascular, atherosclerosis, cerebral atherosclerosis, occlusive atherosclerosis, and cerebral amyloid angiopathy score; MMSE: Mini-Mental State Examination score; CDR-global: Clinical Dementia Rating global score; CDR-SoB: Clinical Dementia Rating Sum of Boxes score; PMI: Post-mortem interval; SD: Standard deviation. Pie chart showing the distribution of subjects by race (96.2% White, 1.9% Asian, 1.9% African-American). Significance levels (*) indicate differences between demented and resilient brains with their respective p-value. *$p < 0.05$; **$p < 0.01$; ****$p < 0.0001$.

2.2 Immunohistochemistry for amyloid-β, tau, and glial cell characterization

Quantitative neuropathological assessments were performed in brain tissue sections containing the temporal pole (Brodmann area 38) and visual cortex (Brodmann areas 17/18), representative of brain regions known to be affected by NFT pathology at Braak III-IV and at Braak V-VI stages, respectively. For immunohistochemical assessments, brain tissue derived from formalin-fixed paraffin-embedded tissue blocks were cut at a thickness of 7 µm. Immunohistochemical staining was conducted using a Bond RX autostainer from Leica Biosystems. Briefly, slides were `baked' (30 min at 60° C) and dewaxed using Bond Dewax Solution (Leica Biosystems, 72° C). For the epitope retrieval, a heat-induced epitope retrieval step (citrate-based solution, pH 6.0, 30 min at 100 °C for AT8, ALDH1L1, γH2AX, CD68, HLA-DR, and TMEM119, or EDTA-based solution, pH 9.0, 30 min at 100 °C for 4G8, IBA1, P2RY12, and Olig2) was used. GFAP was applied with heat-induced epitope retrieval only. Of note, although the use of formic acid (pH 2-3) for amyloid-β immunostaining is commonly used to unfold the densely packed and highly pleated amyloid-β sheets, studies comparing the labelling patterns and efficiency of extracellular amyloid-β plaques with heat-induced vs FA (549) and/or with FA vs no FA pre-treatments, have shown identical results (550). Of note, the Leica autostainer does not permit the use of FA, and the staining protocol used for 4G8 immunostaining was performed without FA pre-treatment. Primary antibodies to label amyloid-β deposits (4G8, Bio Legend, 1:8000), phospho-tau (AT8, Thermo Fisher, 1:500), phospho-TDP43 (Fisher Scientific, 1:3000), alpha-synuclein (Fisher Scientific, 1:200), cellular DNA damage (γH2AX, Abcam, 1:1000), constitutive and inflammatory astrocytic markers (ALDH1L1, Abcam, 1:200; GFAP, Sigma Aldrich, 1:20,000), constitutive oligodendrocyte markers (Olig2, Abcam, 1:100), and constitutive, inflammatory and homeostatic microglial markers (IBA1, Abcam, 1:500; CD68, Dako, 1:500; HLA-DR, Abcam, 1:50; TMEM119, Sigma Aldrich, 1:50; P2RY12, Fisher Scientific, 1:100) were used, followed by secondary anti-mouse and anti-rabbit horseradish peroxidase (HRP) antibody conjugation (BOND Polymer Refine Detection, catalogue number DS9800, Leica Biosystems Newcastle, UK) following the Leica autostainer protocol. Immunolabeling was visualized using 3,3'-diaminobenzidine (DAB) and slides were counterstained with the nuclear marker haematoxylin using the Leica Biosystems autostainer protocol. Slides were manually dehydrated, cover-slipped using Permount mounting medium and scanned with a Nanozoomer XR (NDP.scan 3.3.3, Hamamatsu Photonics, Hertfordhsire, UK) using a 20X objective.

Amyloid-β plaque burden (defined as the percentage of cortex occupied by amyloid-β plaques), AT8+ NFT counts, density of AT8+ neuropil threads/mm^2, and number of different glial cell markers and γH2AX+ cells were calculated. To quantify lesion burdens, a semiautomated deep-learning algorithm

was created using the software provided by the company Aiforia. For quantification of AT8+ tau neuropil burden slides were analysed using the QuPath software (551) with the use of the pixel classifier module.

2.3 Quantitative 2D analyses for immunohistochemical cell counts and lesion burdens (Aiforia)

Artificial intelligence (AI) with deep-learning algorithm was used for semiautomated quantification of positively labelled cells and lesions (Aiforia version 5.2, Aiforia Inc, Cambridge, MA). 2-D AI models were trained for each of the 11 antibodies of interest (4G8, AT8, γH2AX, IBA1, Olig2, ALDH1L1, CD68, HLA-DR, P2RY12, TMEM119, GFAP), human-based validation(s) were performed, and individual AI models were applied to quantify cell and lesion burden(s) in predetermined regions of interest (ROI). To this end, scanned slides were uploaded to the Aiforia cloud-based platform and stored in folders. Each deep-learning model was trained based on annotations of positive `objects' and negative `background', on a subset of sections that comprised around 10% of the total amount of sections used for each model. Training sections were chosen based on representative cases considering the variability of image and staining quality in the dataset. The models consisted of different `layers' where the first layer comprised detection of the tissue (including grey and WM), and the second layer only detected pixels within the previous `tissue' layer and was trained to detect objects specific to the immunostaining used. The two layers were combined to generate one single model for the accurate detection of objects of interest for each of the staining protocols. Models were trained using an increasing number of annotations and iterations (training rounds) until the model performed satisfactorily and the rates of false positive and false negative object detection was below 5%. Validation of the trained AI models was performed on an independent set of images comprising around 10% of the total dataset by marking five validation regions per section. Within these validation regions, three independent human validators were asked to annotate the respective objects of interest. The percentage of false positive, false negative, and sensitivities were calculated for each validator and AI model, and the model passed the validation test when the human validators individually and combined were outperformed by the annotations generated by the AI model.

For the quantitative analyses of the studied brains, two ROIs were selected for each brain slide in cortical and adjacent subcortical areas, respectively. Cortical ROIs were determined based on well-preserved and representative brain regions containing the six cortical layers and measuring a total of 6 mm in length along the pial surface (**Figure 4**). Importantly, the average brain weight and cortical thicknesses of the temporal and visual cortices of the studied cases were similar, enabling a reliable comparison of cell counts and/or cell and lesion densities contained in the ROIs between groups, and eliminating the potential error in cell count or density assessment potentially introduced by the tissue contraction in more advanced dementia stages (**Figure 5**). Subcortical ROIs were selected in the juxtacortical WM immediately adjacent to the cortical ROI and were drawn as circular or oval sections, avoiding inclusion of major vessels or gross artifacts. Two ROIs were selected for each case in cortical and adjacent subcortical brain regions, respectively. Total number of cells and lesions, average density (cells or lesions/mm^2), and lesion burdens (% of cortex and WM occupied by lesions) were quantified within the two cortical and subcortical ROIs and averaged for each case.

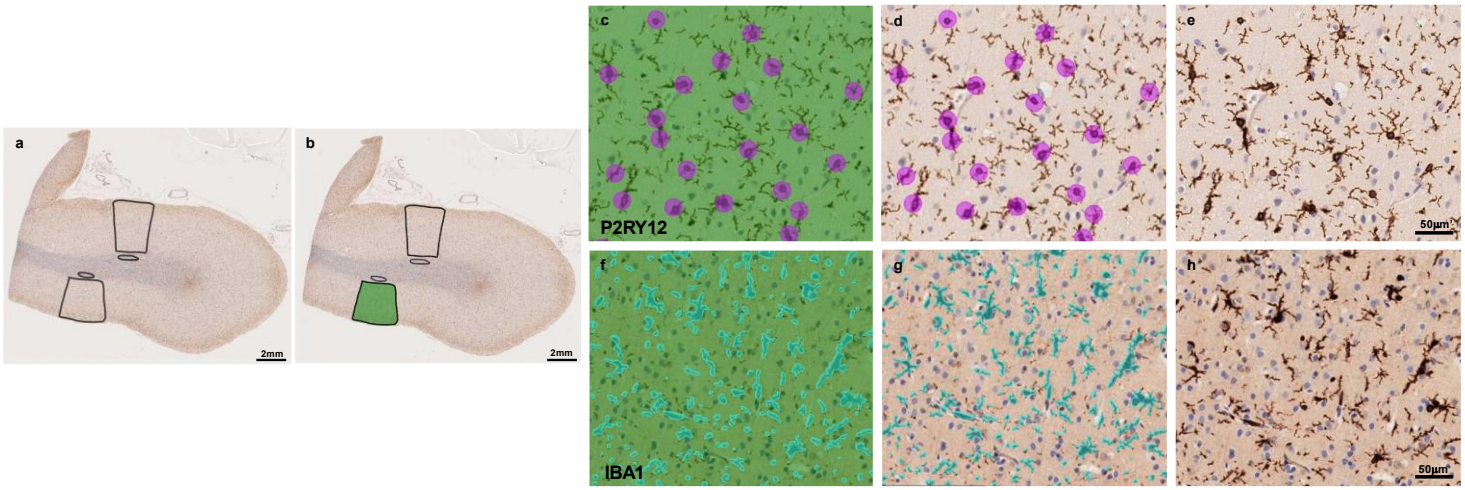

Figure 4: Example of two (P2RY12 and IBA1) of the eleven artificial intelligence-based deep-learning algorithm models created for the semiquantitative analyses of IHC stained temporal and visual cortices
Example temporal cortex section showing the selection of cortical and subcortical white matter (WM) regions of interest (**a**, **b**). Tissue layer is shown in green (**b**, **c**, **f**), P2RY12 count detector is shown in purple (**c**, **d**), IBA1 area detector is shown in blue (**f**, **g**), and unannotated slides stained with P2RY12 (**e**) and IBA1 (**h**). Scale bars 2mm (**a, b**) and 50 µm (**c**-**h**).

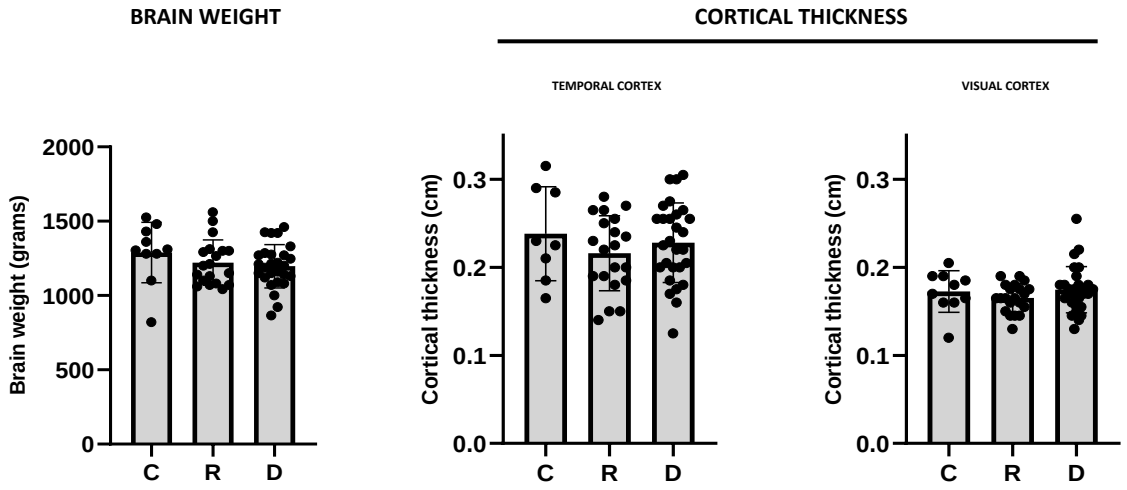

Figure 5: Brain weight and cortical thicknesses of the N=60 studied cases in the temporal and visual cortices
Brain weight (grams) and cortical thicknesses of the temporal and visual cortices of control, resilient, and demented brains showed no significant differences across groups. Cortical thicknesses were calculated by averaging two representative tissue thicknesses obtained for each section. The regions were chosen in similar regions to the ones used for selection of previously used ROIs. cm: centimetre; C: Control; R: Resilient; D: Demented. Data are presented as mean ± standard deviation.

Aiforia-based AI models and quantifications were performed in the cortex for the antibodies 4G8, AT8, γH2AX, ALDH1L1, IBA1, CD68, HLA-DR, P2RY12, TMEM119, and GFAP, and in subcortical WM for Olig2, IBA1, CD68, HLA-DR, P2RY12, and TMEM119. Models were created to quantify `objects' (positively labelled cells) for AT8, γH2AX, ALDH1L1, CD68, HLA-DR, GFAP, P2RY12, and TMEM119 antibodies, and `burdens' (% of cortex/juxtacortical WM labelled by the antibody of interest) for 4G8

and IBA1. No AI model for the formal quantification of alpha-synuclein or TDP43 was performed since absence of those comorbidities was a prerequisite when selecting the brains included in the present study, and accordingly, the stainings with these two antibodies showed no signal.

To better assess colocalization of γH2AX with glial markers (IBA1 and GFAP) at increased resolution, brain sections were expanded following the previously published ExM protocol (245,246). Primary antibodies to label IBA1 (Synaptic Systems, 1:100), GFAP (G3893, 1:100) and γH2AX (Abcam, 1:100), followed by the appropriate secondary antibodies (Alexa Fluor 488, 555, 647, 1:100) were applied.

2.4 Quantitative 2-D analyses for immunohistochemical signal intensity assessment (Q-path)

To quantify tau neuropil burden, brain slides stained with AT8 antibody were analysed using the QuPath software (551) with the pixel classifier module. A control brain and an AD brain were used to train the classifier to distinguish AT8-positive from AT8-negative signal. The classifier was applied to two representative and well-preserved ROIs in the cortex of each case and the results were averaged and represented as density of neuropil burden (per μm^2 given the very low burden of neuropil in the studied cases).

2.5 Expansion microscopy

Physical magnification of tissue specimens by separating biomolecules at the nanoscale level overcomes the diffraction limit of optical microscopes to visualize nanostructures in tissue (248). The first physical expansion of a mouse brain was reported in 2011 in a study where a novel clearing protocol was developed to reduce light scattering and improve subcellular imaging of neurons, and the unintentional effect of brain tissue expansion was reported (552). However, tissue expansion was not identified as a means to potentially improve spatial resolution of tissue imaging until Boyden's laboratory introduced the concept of ExM in 2015 (245).

ExM is a technique that was developed by Boyden's laboratory and which enables the physical expansion of tissue specimens isotropically in three dimensions to around 4-5x their original size (245,246). ExM combines the physical property of swellable hydrophilic polyelectrolyte gels that increase in size when immersed in water or low salt buffers (233,553), with the biochemical discovery of embedding tissue specimens into polyelectrolyte gels. The spacings within the densely cross-linked polymer gels are between 1-2 nm (554) which largely preserve the spatial resolution to a high level of detail introducing minimal errors in the expansion process (245). The protocol of ExM involves a series of steps which can be accomplished within 3-4 days. Most of the previously published protocols have used mouse brain sections of 30-100 µm thickness (245,246,555).

The first step of ExM requires treatment of the sample with the reagent Acryolyl-X (AcX) which reacts will all amines (556) and modifies amino acid side chains by covalently attaching a chemical anchor to them that later participates in the radical polymerization and allows the AcX-tagged proteins to be mechanically coupled to a dense polymer mesh. Of note, aldehyde-fixed samples result in fewer free amines available to react with AcX and may require higher concentrations of AcX (555). Secondly, a hydrogel matrix is formed in situ surrounding the AcX-labelled proteins with the addition of a gelling solution composed of a monomer solution (acrylamide, sodium acrylate, and N-N- methylenebisacrylamide) and the sequential addition of tetramethyl-ethylenediamine (TEMED), 4-Hydroxy-TEMPO (4-HT), and ammonium persulfate (APS). The accelerator TEMED and initiator APS induce the crosslinking of N-N-Mb to form a dense polyelectrolyte hydrogel. TEMED accelerates radical generation by APS, and APS generates free radicals to initiate polymerization. The inhibitor 4-HT inhibits premature gel polymerization allowing a complete tissue embedding in the gelling matrix.

The sodium acrylate increases permeability of the polyelectrolyte gel, and the presence of both, acrylamide and sodium acrylate increase the expansion of the gel (249,555). Thirdly, a digestion step is performed enzymatically or with a milder heat-detergent treatment which has been shown to better preserve epitopes in post-expanded tissue specimens (233).

The expansion factor of ExM can be further optimized to the target object of interest by adjusting the crosslinker (e.g., Acryloyl-X) and/or monomer concentrations. Recently, a X10 ExM protocol was developed, where the use of a modified monomer solution enabled an expansion factor of 10-11x (557). Higher expansion factors can be achieved by decreasing the cross-linker (AcX, N-N-Mb) concentration and by reducing the monomer density, and/or by increasing acrylamide and/or sodium acrylate concentrations. However, the higher gel expansion factors also increase the linkage error (= the distortion between target protein and fluorophore when fluorophores are added pre-expansion due to the larger physical separation in the expansion process) and lead to greater gel instability. Moreover, it is possible to expand tissue samples in series in the so-called iterative expansion microscopy (iExM) variation of the protocol (254), enabling expansion factors of up to 53x when repeating the ExM protocol twice on a readily expanded gel. Here, the staining and imaging of such enlarged samples is further complicated by the dilution of labelling intensity and by the linkage error introduced by the pre-expansion labelling of proteins and the physical separation between fluorophore and target proteins (254,558).

Staining of expanded tissue with immunofluorescent-labelled antibodies can be done before or after the expansion process. The pre-expansion staining comes with some relevant potential drawbacks: The step of tissue homogenization through either protease digestion or heat-detergent protein denaturation is crucial for isotropic expansion without structural distortion. However, this step also washes out incompletely anchored primary and secondary antibodies in the tissue sample. In addition, the gel polymerization step produces free radicals that destroy some of the fluorophores. Altogether, these two factors combined lead to a >50% loss of target fluorophore molecules when labelled pre-expansion (246,558). Moreover, the higher the aimed expansion factor, the higher the need of using stronger digestion reagents, and the more labelled antibodies are lost. Some of the dyes are particularly vulnerable to ExM, such as Alexa Fluor 647 or Cy5, which suffer >90% washout after the digestion and polymerization steps (246). Moreover, the bulky labels of primary and secondary antibodies can introduce a localization displacement when applied pre-expansion (250). Alternatively, post-expansion immunolabeling can be performed to overcome some of these drawbacks. Using labels post-expansion can avoid dye loss during digestion and polymerization steps and improve labelling efficiency with reduced linkage error. However, it can also be problematic for certain protein targets because proteins can be altered by the denaturation step and may not be recognizable by some antibodies after the expansion process anymore, thus leading to under-labelling (250). The alternative use of smaller antibodies or antibody fragments such as Fab fragment antibodies to label selected regions of the post-expanded epitopes has been found to increase antibody binding and signal intensity in ExM sections (559). However, the use of these nanoantibodies is limited by their recent discovery and reduced overall availability, and their use has been limited to ExM protocols with higher magnification factors such as X10. Recent studies have shown that ExM improves accessibility of antibodies to epitopes on the tissue samples which may be masked prior to expansion, a phenomenon that has been called `decrowding' (249). Molecular decrowding thus enables to significantly enhance efficiency of immunostaining when performed post-expansion, and it may allow to more accurately reflect the true number of synaptic and/or oligomeric elements in an expanded brain section.

In the present study, ExM protocol was applied following the previously published protocols of Chen 2015 (245), Asano 2018 (560), Klimas 2019 (555), and Sarkar 2020 (249) with minor modifications. Briefly, the monomer solution containing 2.5% acrylamide, 8.6% sodium acrylate, and 0.1% N-N-

methylenebisacrylamide (N-N-Mb) was used, as these proportions have been shown in previous publications to attain a linear expansion factor in the range of 4-5x (555). In addition, a heat-detergent digestion and homogenization step was applied to eliminate biomolecules other than proteins, and to allow optimal staining of target epitopes in the post-expanded tissue. Of note, because polymerization and gelling steps are temperature-dependent, the preparation and application of the gelling solution was performed on ice and the solution was applied while it was cold to avoid premature gelation and possibility of incomplete retention of target molecules (555). For the digestion step, and given that human samples are heavily formalin-fixed which can lead to an uneven tissue expansion, a higher concentration of 25 mM ethylenediaminetetraacetic acid (EDTA) (instead of 1 mM as used in the original ExM protocol) was used following previously published validation studies using human tissue samples with the so-called ExPath protocol (248). Antibody staining was applied at post-expansion to obtain optimal signal intensity and to additionally benefit from the decrowding principle of this technique.

ExM has been previously validated in several publications for its use across various tissue types (FFPE, frozen) and tissue specimens (mouse, human) and it has been shown to have low tissue distortion rates (in the scale of a few percent over length scales of tens to hundreds of microns, or 1-2 nm on average) in a variety of species and tissue types (88,245,246,248,248). Moreover, recent validation of ExM in human derived tissue specimens using the ExPath protocol in differently fixed tissue samples including FFPE sections, has shown that the distortion introduced by expansion is minimal when comparing pre-expansion superresolution microscopy images with post-expansion confocal images using various human tissue samples (248).

Of note, discontinuous and punctate appearance of cytoplasmic IBA1+ microglial staining has been previously described in microglia of demented and age-matched control brains (447) and punctate microglial staining patterns have also been observed when using other microglial antibodies, including microglia-specific ones such as TMEM119 in post-mortem brain tissue (561). When using ExM, post-expansion immunolabeling of some cytoplasmic protein targets show increased punctate appearance, suggesting that the physical magnification of tissue may separate target molecules rendering them less continuous in post-expanded tissue material (562). In line with this, the presently used IBA1 immunostaining in post-expanded tissue showed a punctate appearance. This could be due to previously described increased punctate staining patterns of IBA1 in aged human brains, and to the effects of ExM on microglial staining, which could partially reduce IBA1 epitope binding sites in the homogenization step and separate target elements in the expansion process (562).

The presently used ExM comprised the following steps:

Preparation of glass-slide mounted FFPE sections: 25 µm thick formalin-fixed paraffin embedded human brain sections from the visual cortex (Brodmann area 17 and 18) were deparaffinized in Xylene (2x 5 mins) and rehydrated in decreasing ethanol concentrations 100%-95%-90%-80%-50%-ddH2O (2x 5 mins each). Slides were dried at room temperature. A 0.5 mm thick silicon isolator (Grace Bio Labs, catalogue number NC1652199) was cut into a round shape and placed on top of the slide to fully surround the tissue for subsequent anchoring and gelling steps.

Anchoring step: AcX solution was prepared diluting the AcX stock to 1:100 in Triton-PBS (0.5%). 500 µl of freshly prepared AcX solution was placed on top of the slide covering the full tissue until reaching the borders of the silicon isolator. The anchoring solution was left incubating overnight in a humidified environment at room temperature. The next day the slide was washed in PBS (3x 5 mins) and left to dry at room temperature before the gelling step.

Gelling step: Gelling solution was freshly prepared on the same day. For 500 µl gelling solution 467.5 µl of monomer solution (2.5% acrylamide, 8.6% sodium acrylate, and 0.1% N-N-methylenebisacrylamide, diluted in distilled water), 10 µl of 4HT, 10 µl of TEMED, and 12.5 µl of APS were added in this sequential order to an Eppendorf tube on ice. The gelling solution was immediately placed on top of the slide and a gel chamber was created by placing a glass coverslip (24x40mm, Thermo Fisher, catalogue number 102440) on the tissue resting on the silicon isolator. This ensured a homogenous distribution and thickness of the gelling solution on every slide and allowed to create an enclosed space on top of the tissue, necessary for the optimal gelling process. The gelling solution was left incubating overnight in a humidified environment at room temperature.

Digestion step: The glass coverslip and silicon isolator were carefully detached and removed. The now well-formed gel was trimmed with a razor blade up to the edges of the tissue. Gel not covering the tissue was removed. The trimmed gels, still mounted on the glass slide, were placed in 50ml Falcon tubes. Digestion buffer was prepared adding beta-mercaptoethanol (0.7%) to the digestion stock solution stock (5% 1M Tris, 5% 500mM EDTA, 0.5% Triton-X, 20% SDS, diluted in distilled water). The buffer was added to the Falcon tubes until it covered the full tissue/gel. A heat-detergent digestion was performed placing the Falcon tubes in an autoclave and running it at 121°C for 60 mins. The samples were left to cool down inside the autoclave for at least 6 hs.

Gel processing: Falcon tubes were taken out of the autoclave. Gels now detached from the glass slides were carefully removed from the Falcon tubes and washed in PBS (3x 5 mins). Gels were measured to obtain the `expansion factor 1' (**Figure 6**). The now still transparent gels were incubated in Trueblack Plus (Biotium, catalogue number 23014) diluted in PBS (1:140) for 48 hs in a humidified environment at room temperature; this step was performed to quench auto-fluorescent background signal and to visualize grey and WM boundaries. Gels with visually evident cortical/WM structures were cut into ~0.5x0.5 cm small sections labelled as `cortex' and/or `WM' and placed into wells in a 24-well plate (Greiner BioOne, Fisher Scientific, catalogue number 07000680). Gel sections were numbered and placed in an ordered manner with adjacent cortical and WM sections placed sequentially and labelled as such.

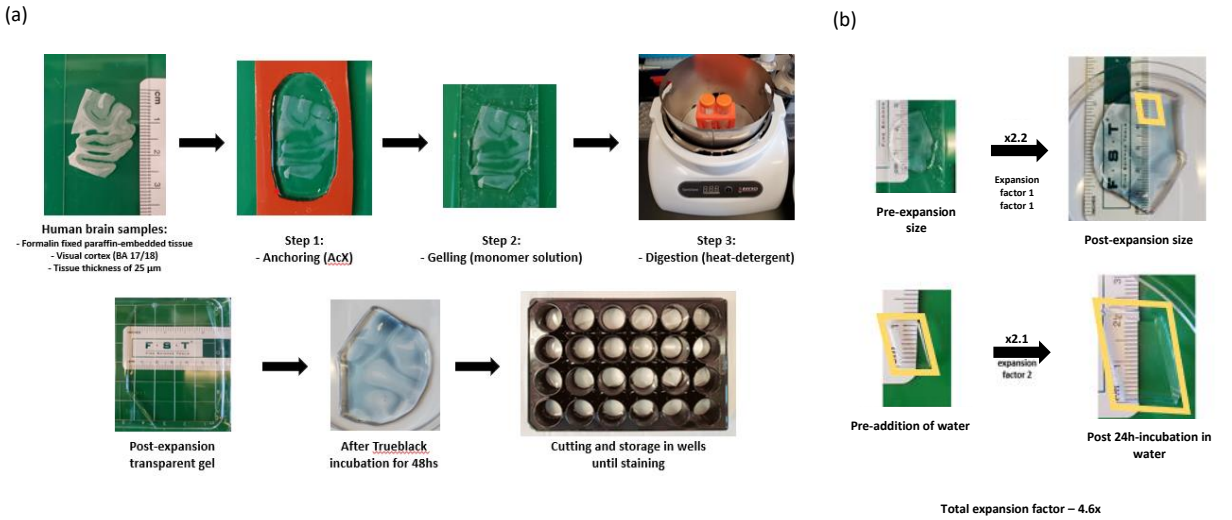

Figure 6: Example of the expansion microscopy (ExM) protocol method
Slides and steps of the ExM protocol exemplified using a brain section derived from the visual cortex (**a, b**). ExM steps including anchoring, gelling, digestion, and Trueblack incubation are shown in images **a**. The average expansion factor obtained after steps 1-3 (`expansion factor 1') and after 24 h incubation in double distilled H2O prior to imaging (`expansion factor 2') is shown in images **b**. AcX: Acryloyl-X; BA: Brodmann Area.

Staining: Primary and secondary antibody stainings were performed inside the wells. Briefly, gel sections were blocked (MaxBlock, Active Motif) overnight at room temperature and washed in washing buffer (MaxWash, Active Motif) 3x 10 mins the next day. Primary antibodies were diluted at 1:100 in staining solution (MaxStain, Active Motif) and incubated at room temperature for 24 hs (all antibodies except for IBA1) or 48 hs (IBA1 antibody) (**Table 4**). Gel sections were washed in washing buffer (MaxWash, Active Motif) 3x 10 mins, incubated with secondary antibodies (Alexa 405, Alexa 488, Alexa 555, Alexa 647) diluted at 1:100 in staining solution (MaxStain, Active Motif), and incubated overnight at room temperature. Of note, the dilutions used for the primary (1:100) and secondary (1:100) antibodies corresponded to the optimal dilutions published in previous work using ExM in human brain tissue (248). Stainings were done sequentially to limit the possibility of unspecific co-labelling of primary and/or secondary antibodies to other targets. Gel sections were washed in washing buffer (MaxWash, Active Motif) 3x 10 mins and incubated in ddH20 for 24hs to allow for maximal expansion of the tissue section(s) prior to imaging. Gel pieces were measured to obtain the `expansion factor 2' shown in **Figure 6**. After imaging and for long-term storage, gels were placed in PBS and stored at 4°C.

Antibody	Host, clonality	ExM	WB	IHC/IF	Distributor	Cat. Number
4G8	Mouse, monoclonal	1:100		1:8000	Bio Legend	800709
ALDH1L1	Rabbit, monoclonal			1:200	Abcam	ab177463
ALDH1L1	Mouse, monoclonal	1:100			EMD	MABN495
AT180	Mouse, monoclonal		1:200		Thermo Fisher	MN1040
AT270	Mouse, monoclonal		1:200		Thermo Fisher	MN1050
AT8	Mouse, monoclonal	1:100	1:1000	1:500	Thermo Fisher	MN1020
Bassoon	Mouse, monoclonal	1:100			Abcam	ab82958
CD68	Mouse, monoclonal			1:500	Dako	M0814
GAPDH	Rabbit, monoclonal		1:1000		Cell Signaling	14C10
GFAP	Mouse, monoclonal	1:100		1:20000	Sigma Aldrich	SAB4300647
GFAP	Rat, monoclonal	1:100			Abcam	ab279291
HLA-DR	Mouse, monoclonal			1:50	Abcam	ab7856
IBA1	Chicken, monoclonal	1:100			Synaptic Systems	140009
IBA1	Rabbit, monoclonal			1:500	Abcam	ab178847
LAMP2	Rabbit, monoclonal	1:100			Abcam	ab199946
MAP2	Chicken, polyclonal	1:100			Abcam	ab5392
Olig2	Rabbit, monoclonal			1:100	Abcam	ab109186
P2RY12	Rabbit, polyclonal			1:100	Thermo Fisher Scientific	NBP2 33870
PSD95	Rabbit, monoclonal	1:100	1:1000		Cell Signaling	D74D3-3409S
PSD95	Mouse, monoclonal	1:100			Abcam	ab192757
Synaptophysin	Mouse, monoclonal		1:1000		Abcam	ab8049
Synapsin1	Rabbit, monoclonal	1:100			Abcam	ab254349
Tau p217	Rabbit, polyclonal		1:500		Thermo Fisher	44-744
Tau12 biotin	Mouse, monoclonal		1:500		BioLegend	806505
Tau46 biotin	Mouse, monoclonal		1:1000		Cell Signaling	96767
Tau5	Mouse, monoclonal		1:500		Abcam	ab80579
TMEM119	Rabbit, polyclonal			1:50	Sigma Aldrich	HPA051870
TOC1	Rabbit, monoclonal	1:100	1:500		Absolute Antibodies	Ab02650-23.0
Trueblack Plus	NA	1:140			Biotium	23014
yH2AX	Mouse, monoclonal			1:1000	Abcam	ab26350
Alexa Fluor 405	Donkey/Goat	1:100	1:5000		Invitrogen	A5760
Alexa Fluor 488	Donkey/Goat	1:100	1:5000		Invitrogen	A10436
Alexa Fluor 555	Donkey/Goat	1:100	1:5000		Invitrogen	A30677
Alexa Fluor 647	Donkey/Goat	1:100	1:5000		Invitrogen	A30107
HRP Streptavidin	NA		1:5000		Thermo Fisher	31030

Table 4: Detailed list of antibodies used
List of antibodies, host, clonality, distributor, catalogue number, and their respective dilutions used for ExM, western blot (WB), and immunohistochemistry or immunofluorescence stainings (IHC/IF).

Expansion factor: Total expansion factor was calculated by multiplying the `expansion factor 1' obtained after the digestion step times the `expansion factor 2' obtained after 24h incubation of gels in ddH2O. With the presently used ExM protocol an average expansion factor across all brains (N=28) of 4.6x was obtained, which is in line with previous publications (245,249,560).

Validation of ExM protocol: To ensure that the presently used ExM protocol was aligned with previously published validation studies in human samples and did not introduce a distortion of targets of interest, a validation using pre-expanded frozen tissue sections and post-expanded FFPE tissue sections on a subset of cases was performed and it showed that target objects (astrocytes and synapses) did not show significant distortions and displayed similar quantitative analyses when considering the additional decrowding phenomenon of ExM technique (**Figure 7 and 8**). A subset of astrocytes was co-stained for two distinct targets within the same glial cell, using GFAP (intermediate filament) and ALDH1L1 (cytoplasm) to assess overlap of GFAP signal with ALDH1L1. This assessment showed an accurate overlap of GFAP with ALDH1L1 which as such indicated that the boundaries labelled by GFAP did not exceed the ALDH1L1 staining signal, suggesting that the GFAP labelling was specific to astrocytic intermediate filament processes and that the expansion process did not lead to a significant distortion of target proteins (**Figure 8**). Moreover, assessment of internalized material by glial cells with the use of lysosomal marker LAMP2 showed colocalization of synaptic elements with lysosomes inside the glial cell body of microglia and astrocytes (**Figure 9**).

A table of the primary and secondary antibodies used for ExM are shown in **Table 4.**

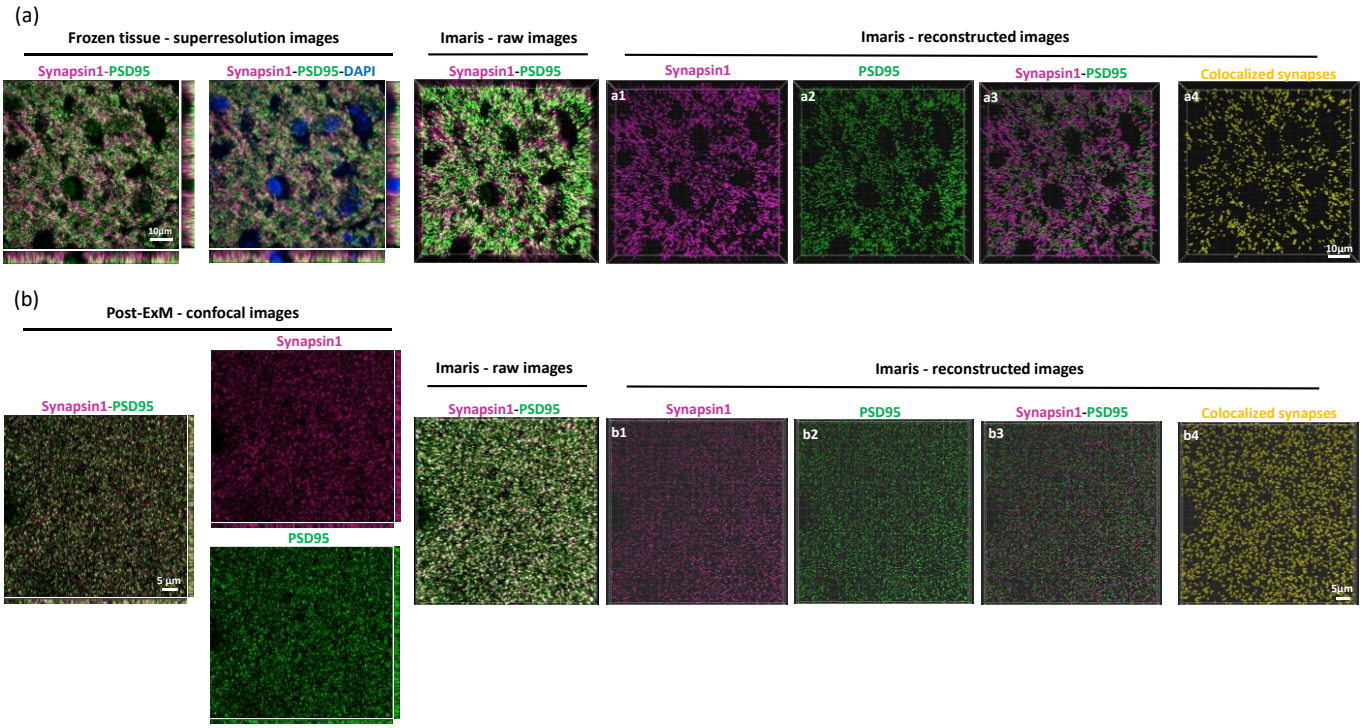

Figure 7: Validation of expansion microscopy (ExM) technique – synaptic elements
Validation of ExM technique using nonexpanded frozen tissue sections imaged with superresolution microscopy (**a**) and expanded FFPE tissue sections imaged with confocal microscopy (**b**) showing synapsin1+ presynapses in magenta and PSD95+ postsynapses in green. Reconstructed 3-D Imaris images showing synapsin1+ presynapses in magenta (**a1, b1**), PSD95+ postsynapses in green (**a2, b2**), synapsin1+ and PSD95+ synapses in magenta and green (**a3, b3**) and colocalized synapsin1-PSD95+ synapses in yellow (**a4, b4**). ExM: expansion microscopy; FFPE: formalin-fixed paraffin-embedded. Scale bars 5 µm.

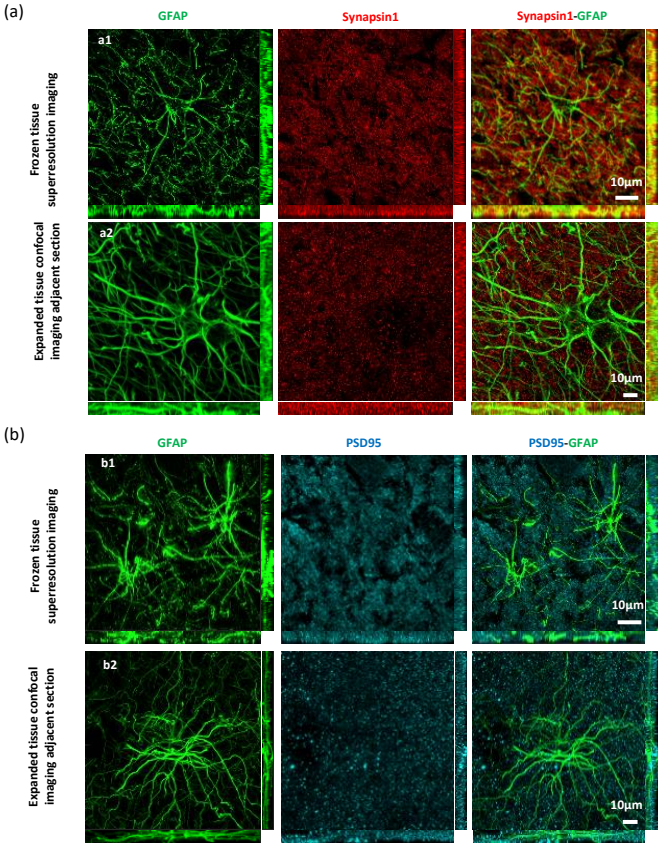

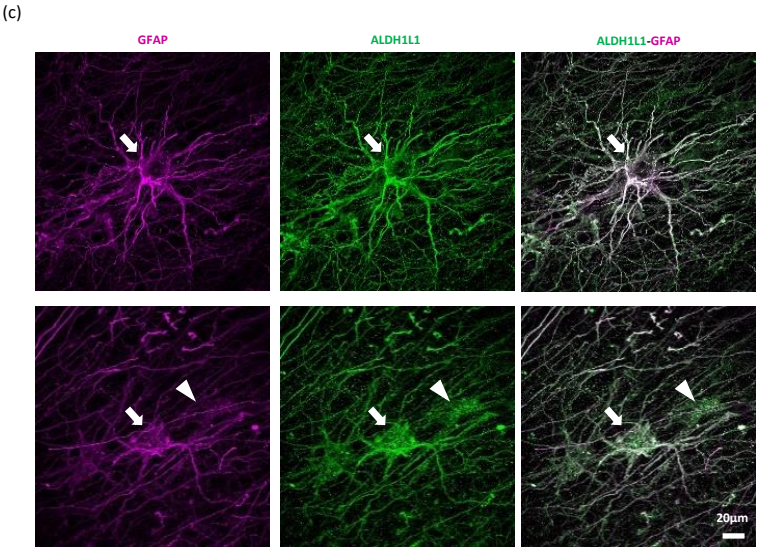

Figure 8: Validation of expansion microscopy (ExM) technique – synaptic elements and glial cells
Validation of ExM technique showing similar proportions of engulfed synaptic elements by glial cells when assessing internalized synapsin1+ presynapses by GFAP+ astrocytes in non-expanded frozen tissue sample (10 µm thickness) imaged with superresolution microscopy (**a1**) compared with expanded FFPE tissue sample (25 µm thickness) imaged with confocal microscopy (**a2**). Similar results were obtained when assessing internalized PSD95+ postsynapses by GFAP+ astrocytes in non-expanded frozen tissue sample (10 µm thickness) imaged with superresolution microscopy (**b1**) compared with expanded FFPE tissue sample (25 µm thickness) imaged with confocal microscopy (**b2**). Representative images showing colocalization of astrocytic intermediate-filament antibody GFAP (magenta) with cytoplasmic astrocytic antibody ALDH1L1 (green) in expanded tissue sections (**c**), as a proof of the maintenance of isotropy after the expansion process. GFAP antibody labels astrocyte-specific cell body and processes and GFAP+ intermediate filament marker does not exceed the limits of ALDH1L1+ cytoplasmic marker in expanded tissue material (**c**). Arrows indicate GFAP+/ALDH1L1+ astrocytes and arrowheads indicate GFAP-/ALDH1L1+ astrocytes. ExM: expansion microscopy. FFPE: formalin-fixed paraffin-embedded. Scale bars 10 µm (**a, b**) and 20 µm (**c**).

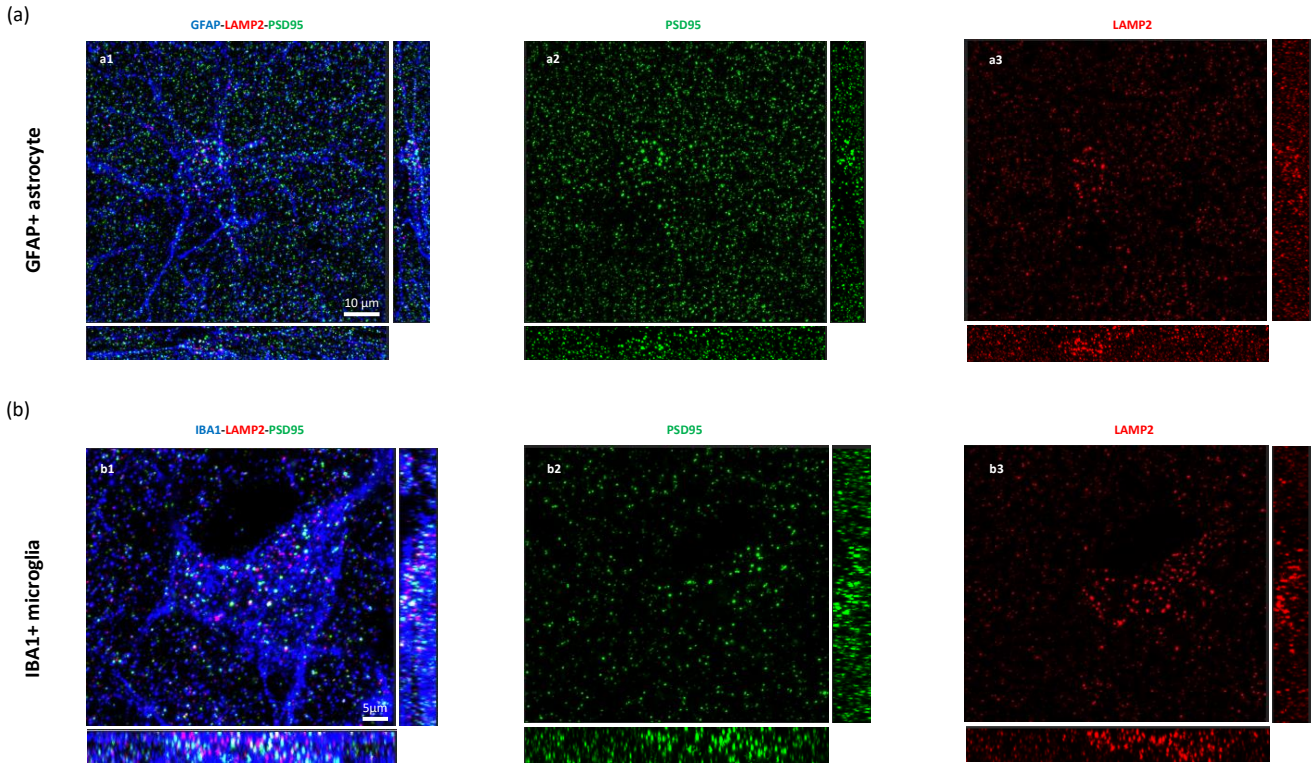

Figure 9: Validation of expansion microscopy (ExM) technique – glia-mediated synapse internalization GFAP+ astrocyte (**a1**) and IBA1+ microglia (**b1**) in blue colabelled with PSD95+ postsynapses in green (**a1/a2, b1/b2**) and LAMP2+ lysosomes in red (**a1/3, b1/3**) showing glia-internalized PSD95+ elements colocalized with LAMP2+ lysosomes inside the astrocyte and microglial cell, respectively. ExM: expansion microscopy. Scale bars 5 µm and 10 µm.

2.6 Imaging

2.6.1 Imaging of expanded tissue sections using confocal microscopy

Gel sections were imaged using an Olympus FV3000 confocal microscope equipped with lasers of 405nm, 488nm, 561nm, and 640nm emissions. A 63x (NA 1.3) oil objective was used and images were sampled at a resolution of 1024 x 1024 pixels. A z-stack of 0.46 µm was selected, which was optimized to the size of the target objects with a post-expansion diameter of 1.4 µm on average (range 0.8-1.8 µm); the z-stack size was set at <50% of the target object size to discriminate true signal (puncta that would be present in a minimum of two consecutive z-stack images) from unspecific background and/or artifacts (563). A 2x software zoom was used for synaptic and oligomeric imaging to capture a representative visual field and optimally assess synaptic/oligomeric densities without including major artifacts. For glial cell imaging, a 2x software zoom was used for astrocytes, and a 2.5x software zoom for microglia.

ROI selection for synapse quantification and glial cell sampling: For synapse density measurements, 3-4 ROIs were randomly selected in layer II of the visual cortex in two non-adjacent gel sections in each brain tissue sample (generating 6-8 ROIs per case). The layers were identified using the neuronal marker MAP2 and identifying the cortical layer II through orientation and size of neuronal cell bodies, and distance from the tissue edge and/or underlying WM. Layer II is part of the `supergranular' layers together with layer III, and it contains abundant excitatory projection neurons that send axons to nearby cortical areas such as V3-V5 and is thereby involved in higher-order visual integration and processing (564). In contrast, layer I is the `molecular layer' which contains very few neuronal cell bodies but a high abundance of axons and dendrites of which around 80% transmit the inhibitory neurotransmitter GABA. Layer IV is the `granular' layer and the main receptor layer of the neocortex that receives information from the lateral geniculate nucleus, and layers V and VI are called the `infragranular layers' and they send axonal projections back to the lateral geniculate nucleus to provide feedback to this output nucleus (564). Glial cells were randomly sampled within

the six cortical layers. For GFAP+ astrocytes, interlaminar astrocytes of layer I were excluded, and GFAP+ cells with well-preserved full cell bodies and representative astrocytic processes were selected. For microglial cells, IBA1+ microglial cells were randomly sampled in the six cortical layers, and ameboid-shaped microglial cells were included. A total of 3-4 GFAP+ astrocytes and 2-3 IBA1+ ameboid microglial cells were imaged for each brain section.

2.6.2 Imaging of nonexpanded frozen tissue sections using superresolution microscopy

For super-resolution imaging, 10 µm thick cryosections were prepared from fresh frozen blocks and fixed in 4% paraformaldehyde for 10 mins. The slides were stained with primary antibodies for presynapses (synapsin1, Abcam, 1:100), postsynapses (PSD95, Abcam, 1:100), and astrocytes (GFAP, Abcam, 1:100) and with immunofluorescent secondary antibodies using Alexa Fluor 488 (1:500), Alexa Fluor 555 (1:500), and Alexa Fluor 647 (1:500). Imaging was performed using an Elyra Zeiss 7 superresolution microscope with Lattice SIM² and setting the z-stack size at 0.126 µm. To improve resolution, SIM² reconstruction using ZenBlack software were performed.

2.7 Quantitative 3-D image analyses for synaptic densities and colocalizations (Imaris)

Quantitative synapse/oligomer density and synapse/oligomer-glia colocalization analyses were done with Imaris software (BitPlane, South Windsor, CT, USA). Individual `layers' were created for each synaptic element selecting a `diameter of largest sphere' of 0.8 µm and a `seed point diameter' of 0.5 µm which yielded the best results. In the settings of `filter surfaces' the option `area' was selected, and the minimum and maximum values were adapted to include as many spots as possible excluding artifacts. These steps were repeated for pre- and postsynaptic elements. To assess colocalizing pre-/postsynaptic puncta, pre- and postsynaptic layers were `masked' and the setting `voxels outside the surface' distance was set to 0 µm. A third layer was created selecting a `diameter of largest sphere' of 0.8 µm and a `seed point diameter' of 0.5 µm, that only detected colocalized spots of the two previously masked layers. The option `filter surfaces' was selected and the `shortest distance to surfaces=surfaces 2' was set to a maximum distance of 1 µm. These steps were repeated for oligomeric puncta using a `diameter of largest sphere' of 0.8 µm and a `seed point diameter' of 1 µm. A third layer was created selecting a `diameter of largest sphere' of 0.8 µm and `seed point diameter' of 0.8 µm, that only detected colocalized spots of the two previously masked layers. The option `filter surfaces' was selected and the `shortest distance to surfaces=surfaces 2' was set to a maximum distance at 1 µm.

For colocalization analyses between glial cells, and synapses and/or oligomeric puncta, `create surface' was selected to generate a layer for the glial cells. For GFAP+ astrocytes, the `smoothing tool' was disabled due to a very good noise-background ratio and a full reconstruction of the cell body and its processes. For IBA1+ microglia, the `smoothing tool' was activated and adapted to a maximum of 0.3. This enabled to fully reconstruct the microglial cell body and to close cell boundaries in areas of low staining intensity. Each of the previously created object layers (for synaptic and oligomeric puncta, respectively) were analysed as to their `distance to surface' to the astrocyte and/or microglial cell. The data on the distance between each individual synaptic/oligomeric spot and the glial cell were calculated and exported, and only negative values were included as synapses/oligomers contained `inside a glial cell'. Values of 0 or higher were not considered as `internalized' to avoid including physiologic contacts between synapses and astrocytes. The total amount of puncta internalized by each glial cell was divided by the total number of puncta in the image and a proportion (`% of internalized elements') was calculated. Data were normalized for glial cell volume.

2.8 Synaptosome and cytosolic preparations

Synaptosome (SYN) and cytosolic (CYT) fractions were prepared following the DeVos 2018 (404), Perez-Nievas 2013 (57), and Tai 2012 (363) protocols with minor modifications: 300 mg of frozen human brain tissue from the visual association cortex (Brodmann area 18) was gently homogenized with 25 strokes in a 2 ml Potter-Elvehjem tissue grinder in chilled 750 µL of Buffer A1 (25 mM HEPES pH 7.5, 120 mM NaCl, 5 mM KCl, 1 mM $MgCl_2$, 2 mM $CaCl_2$ in distilled water (dH_2O), supplemented with 1 mM DTT and 1:100 phosphatase-/protease-inhibitor). Of note, the synaptosome extraction protocol used here involved a series of centrifugation and filtration steps to ultimately obtain a synaptic fraction enriched in presynaptic and postsynaptic proteins as validated by western blotting. Given conflicting and not standardized terminologies referring to different synaptic protein isolation methods (454), in the present study the term `synaptosome' is used to describe the abovementioned synaptic components isolated from total brain homogenates.

The homogenate plus 900 µL of Buffer A2 (25 mM HEPES pH 7.5, 120 mM NaCl, 5 mM KCl, 1 mM $MgCl_2$, 2 mM $CaCl_2$ in dH_2O) was passed through 2 layers of Nylon 80 µm filters using 25 mm Filter Holders to remove tissue debris. The crude filtered homogenate was passed through 5 µm Supor membrane filters, along with 450 µL of Buffer A2 to filter out large organelles and nuclei. The filtered homogenate was centrifuged at 1,000 × g for 10min at 4°C. The supernatant was transferred into pre-CYT tubes, and the pellet was chilled in ice in pre-SYN tubes.

The pre-CYT tubes were centrifuged at 10,000 × g for 15min at 4°C to remove any remaining debris. The supernatant was transferred to CYT tubes to obtain the final CYT samples. The pre-SYN tubes were washed with 500 µL of Buffer A2, then equally divided into two tubes (pre-SYN-DTT and pre-SYN-PBS) and centrifuged at 1,000 × g for 10min at 4°C to remove any remaining debris. The pre-SYN pellets were resuspended in either 100 µL of Buffer B1 (PBS, 1.5% SDS, 2 mM DTT, 1:100 phosphatase-/protease-inhibitor) to obtain the final SYN-DTT samples, or in 100 µL of Buffer B2 (PBS, 1.5% SDS, 1:100 protease-inhibitor) to obtain the final SYN-PBS samples.

A bicinchoninic acid (BCA) assay (Thermo Scientific Pierce) was performed to determine total protein concentration. SYN-DTT samples were used for conventional reducing/denaturing western blot analyses, and SYN-PBS samples for tau seeding assays and non-reducing/non-denaturing native western blot analyses.

2.9 Western blot analyses

Reducing and denaturing WBs: Twenty to fifty micrograms of total protein were loaded per well on 4–12% Bis-Tris SDS-PAGE gels (Invitrogen) and run in MOPS buffer (Invitrogen) at 160 V for 1 hour. Samples were prepared diluted in PBS together with loading and reducing agents and heated at 95°C for 5 mins. Proteins were transferred to nitrocellulose membrane (Invitrogen) with an iBlot2 transfer device using a protocol of 25 V for 7 min. Membranes were incubated in blocking solution (Intercept Blocking buffer) for 1 hour at room temperature. Primary antibodies were diluted in antibody diluent (Intercept Antibody diluent) and incubated overnight at 4°C on a rotating plate. Blots were washed in Tris buffered saline + 0.25% Tween (TBS-T) 3x 10min and incubated with infrared and/or horseradish peroxidase (HRP) secondary antibodies at 1:5000 dilution in antibody diluent (Intercept Antibody diluent) for 1 h at room temperature. Blots were washed in TBS-T 3x 10 min and imaged on an Odyssey CLx Infrared Imaging System for infrared secondary antibodies and/or on a chemiluminescent BioRad ChemiDoc Imaging System for HRP secondary antibodies, respectively. Blots were converted to grayscale and densitometric analysis was performed with ImageJ (64-bit Java 8).

Native WBs: Samples were prepared diluted in PBS with NativePage loading buffer and NativePAGE™ 5% G-250 Sample additive without reducing agent and/or sample heating. Sixty micrograms of total protein were loaded per well on NativePage 3–12% Bis-Tris gels (Invitrogen). Gels were run in NativePage anode and cathode running buffers at 150 V for 20 mins followed by 170 V for 50 mins after changing the cathode buffer. Proteins were transferred to PVDF membrane (Invitrogen) with an iBlot2 transfer device and a protocol of 20 V for 7 min. Membranes were quickly washed with methanol to remove the excess of blue and placed in acetic acid (8%) for 5 mins followed by double-distilled water (ddH_20) for 5 mins. Membranes were air-dried at room temperature. Blocking was performed with 5% non-fat dried milk diluted in TBS-T for 1 hour. Primary antibodies were diluted in 5% non-fat dried milk and incubated overnight at 4°C on a rotating plate. Blots were washed in TBS-T 3x 10 min and incubated with HRP secondary antibody at 1:5000 dilution in 5% non-fat dried milk for 1h at room temperature. Blots were washed in TBS-T 3x 10 min and imaged with high-sensitivity streptavidin-HRP (Thermo Fisher, catalog number 21134) on a chemiluminescent BioRad ChemiDoc Imaging System. Blots were converted to grayscale and densitometric analysis was performed using ImageJ (64-bit Java 8).

A table of the primary and secondary antibodies and dilutions used for WB can be found in **Table 4.**

2.10 Tau seeding assays

In vitro tau seeding activity was assessed as previously described (404,405,565) with minor modifications. HEK293 cells stably expressing the repeat domain of tau with the P301S mutation (Tau-RDP301S) fused with CFP and YFP were plated in poly-D-lysine treated 96-well clear bottom plates (Corning) at 20'000 cells/well. The next day cells were transduced with 4 µg/well total protein plus 1% lipofectamine 2000 (Invitrogen) diluted in OptiMEM (Thermo Fisher). Each lysate was applied in triplicate. Cells were exposed to lysate for 24 hs. At the time of collection, cells were trypsinized and transferred to 96-well U-bottom plates (Corning) using DMEM + 10% fetal bovine serum (FBS) to inhibit the activity of the trypsin. Cells were pelleted at 1000 x g, resuspended in freshly made 2% paraformaldehyde (PFA) (Electron Microscopy Services) for 10 min at room temperature in the dark, and pelleted at 1500 rpm. Cells were resuspended in PBS 1X and run on the MACSQuant VYB (Miltenyi) flow cytometer.

FRET was measured by exciting the cells using the 405 nm laser and reading fluorescence emission at the 530/30 nm filter. To quantify the FRET signal, a bivariate plot of FRET vs the CFP donor was generated and cells that received lipofectamine alone were used to identify the FRET-negative population. Using this gate, the `tau seeding' value was calculated by multiplying the percent of FRET-positive cells times the median fluorescence intensity of that FRET-positive population. Immediately prior to collection, representative images of HEK293 cells with aggregates were taken with the ZOE Fluorescent Cell Imager (BioRad) using the green fluorescent protein (GFP) channel.

2.11 Statistical analyses

D'Agostino-Pearson normality test was applied to test for Gaussian distribution. Multiple group analyses were performed using one-way ANOVA for parametric variables, and Kruskall-Wallis for non-parametric variables. Posthoc analyses to assess between group differences were evaluated with Holm-Šídák's test. Correlation analyses were performed with Pearson test when both variables were normally distributed, and with Spearman test when at least one variable was not normally distributed. Significance level was set at $p < 0.05$. All statistical analyses and graphs were generated using Graphpad Prism version 9.4.1 (Graphpad Software Inc, La Jolla, CA). Data are presented as mean ± standard deviation (SD), unless otherwise indicated.

3. Results

3.1 Regional amyloid-β plaque burden and number of neurofibrillary tangles is similar in resilient and demented brains at Braak III-IV stages

Recent studies have stressed that the regional burden of amyloid-β plaques and NFTs may better predict cognition than the only presence or absence of these lesions (27). It is well known that the amyloid-β burden increases in a linear fashion over a period of up to 15-20 years in advance of clinical symptoms and before reaching a plateau (544). NFTs, however, continue to accumulate linearly as tau pathology progresses along the well-defined tau stages (from Braak I-II stages affecting the transentorhinal/entorhinal cortex, to Braak VI stage involving the primary visual cortex) and they correlate with the severity of cognitive decline and the amount of neuronal loss in symptomatic individuals (544,566–568). To assess the potential involvement of AD neuropathologic lesion burdens on cognitive statuses in demented and resilient brains, a detailed quantitative assessment of ADNC lesion burden was performed.

Demented and resilient brains were well matched for Thal phases, Braak stages, and CERAD scores. Using the Aiforia-based quantification method, the burden of amyloid-β plaques and NFTs was evaluated. The amyloid-β plaque burden (defined as the percentage of cortex in the ROIs occupied by deposits immunolabeled with 4G8 antibody) did not show significant differences between resilient and demented brains in the temporal pole or visual cortex, suggesting that neither the amyloid-β plaque scores nor the regional amyloid-β plaque loads are predictive of the different cognitive statuses of these individuals. The total burden of amyloid-β plaque deposits was higher in the temporal compared with the visual cortex in each case (**Figure 10**). Quantification of the number of NFTs (as visualized by immunolabeling with AT8 antibody) in the temporal pole did not show significant differences between resilient and demented brains (p=0.33), although a trend towards higher NFT counts was observed in the demented group. As expected at tangle Braak III-IV stages, no NFTs were detected in the visual cortex of demented or resilient brains (see **Figure 2** and **Figure 3)**.

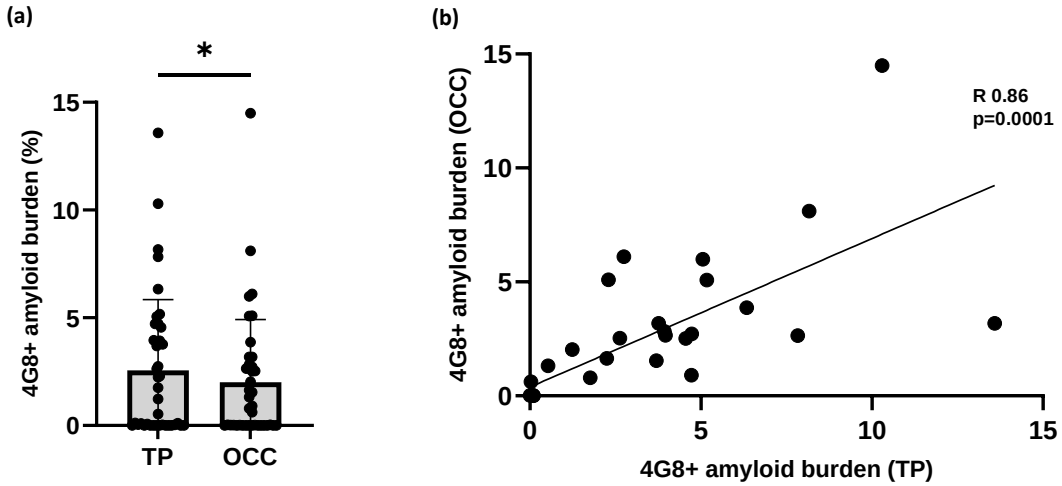

Figure 10: Amyloid-β burden in the temporal and visual cortex

4G8+ amyloid-β burden was significantly higher in the temporal pole (TP) compared with the visual cortex (OCC) of the studied brains (**a**); there was a strong correlation between temporal and occipital 4G8+ amyloid-β burdens across the studied cases (**b**). Data are presented as mean ± standard deviation.

3.2 Total number of astrocytes, microglial cells, and oligodendrocytes in cortical and subcortical brain regions does not differ between control, resilient, and demented brains at Braak III-IV stages

The quantitative immunohistochemical analyses of baseline glial cell markers (ALDH1L1, IBA1, Olig2) in the cortex and subcortical WM showed comparable total numbers and densities of astrocytes (ALDH1L1), microglial cells (IBA1), and oligodendrocytes (Olig2) in control, resilient, and demented brains in the two studied brain regions (temporal pole, visual cortex) (**Figure 11**)

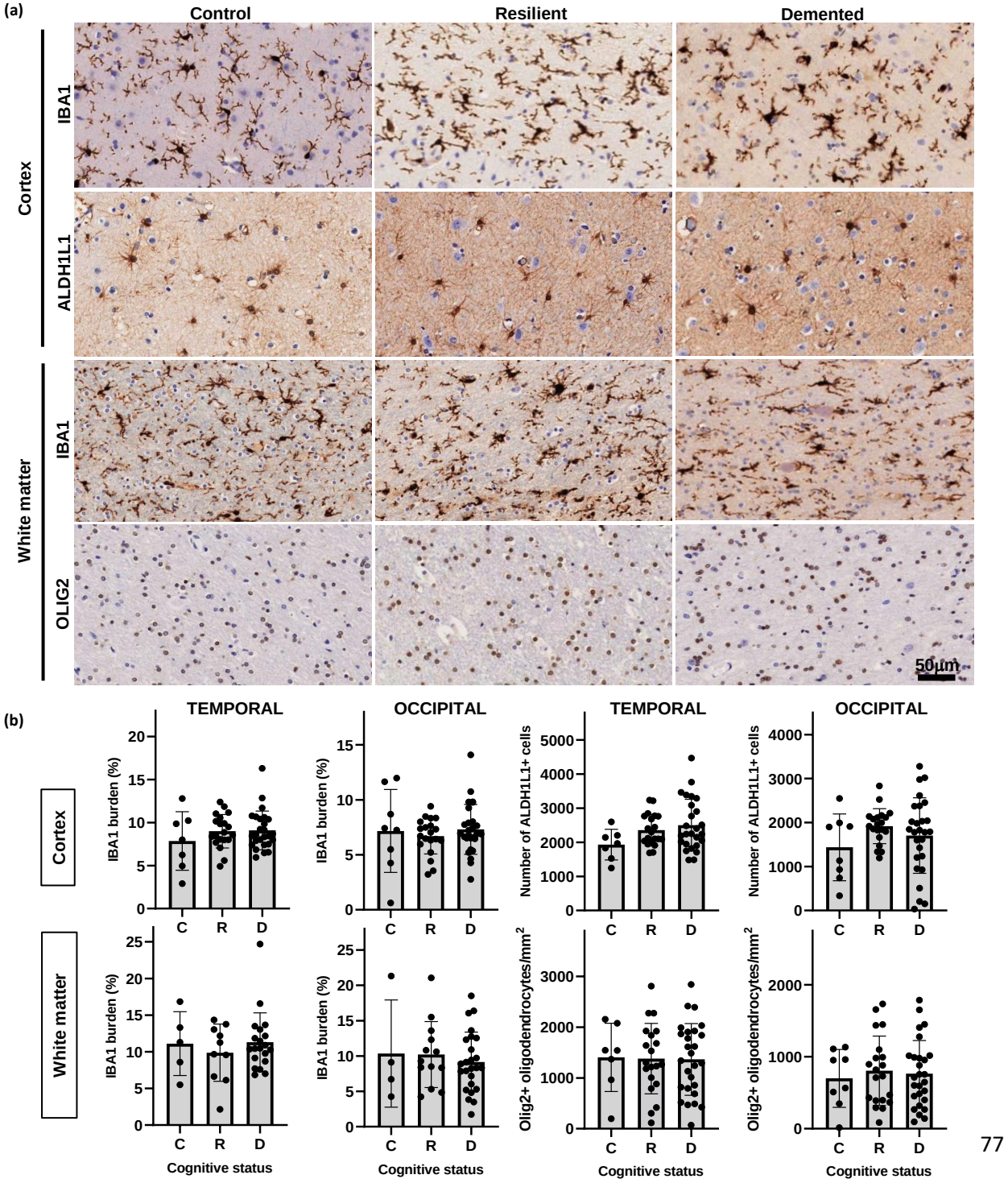

Figure 11: Baseline glial cell markers for microglia, astrocytes, and oligodendrocytes in the studied brains
Quantifications of IBA1 burden (percentage of cortex or white matter covered by IBA1+ microglia), total number of astrocytes (ALDH1L1), and number of oligodendrocytes (Olig2) in temporal and visual cortices (microglia and astrocytes) and white matter (microglia and oligodendrocytes) (**b**) did not show significant differences between demented, resilient, and control brains. Representative photomicrographs of IBA1+ microglia, ALDH1L1+ astrocytes and OLIG2+ oligodendrocytes on sections from control, resilient, and demented cases derived from the temporal cortex (**a**). C Control (Braak 0-II); R Resilient (Braak III/IV); D Demented (Braak III/IV). Scale bar 50 µm. Data are presented as mean ± standard deviation.

These data are in agreement with previous reports (569) and suggest that the total amount of glial cells remain unchanged in a healthy compared with a diseased AD brain, and that glial cell phenotypic changes rather than glial cell proliferation or death may underlie the glial cell signatures observed in AD brains.

3.3 Phenotypic glial cell changes distinguish demented from resilient/control brains, and they precede tau tangle pathology in brains at Braak III-IV stages

The quantitative immunohistochemical analyses of inflammatory (CD68, HLA-DR, GFAP) and homeostatic (P2RY12, TMEM119) glial cell markers showed phenotypic glial cell changes with higher expression of inflammatory microglial (CD68, HLA-DR) (**Figure 12**) and astrocytic (GFAP) markers (**Figure 13**) and reduced expression of homeostatic microglial markers (P2RY12, HLA-DR) in the temporal pole and visual cortex of demented compared with resilient and control brains (**Figure 14**).

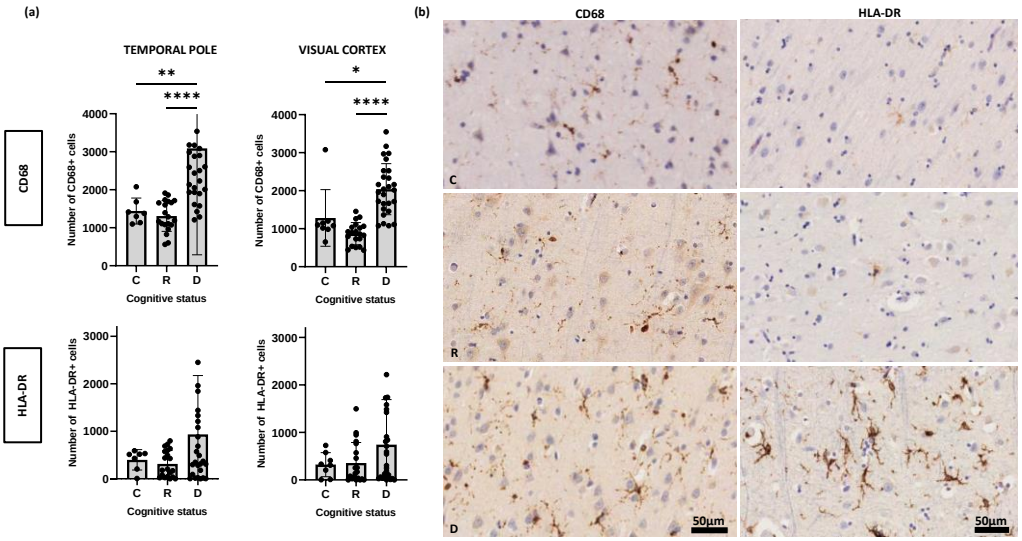

Figure 12: Inflammatory microglial changes (CD68 and HLA-DR) in the temporal and visual cortices
Number of CD68+ microglia was significantly higher in the temporal pole and visual cortex of demented compared with resilient and controls (**a**). A similar trend that did not reach statistical significance was observed in the number of HLA-DR+ microglia (**a**). Representative photomicrographs of CD68+ and HLD-DR+ microglia in sections from control, resilient, and demented cases derived from the temporal pole (**b**). C Control (Braak 0-II); R Resilient (Braak III/IV); D Demented (Braak III/IV); ***p** < 0.05; ****p** < 0.01; *****p** < 0.0001. Scale bars 50 µm. Data are presented as mean ± standard deviation.

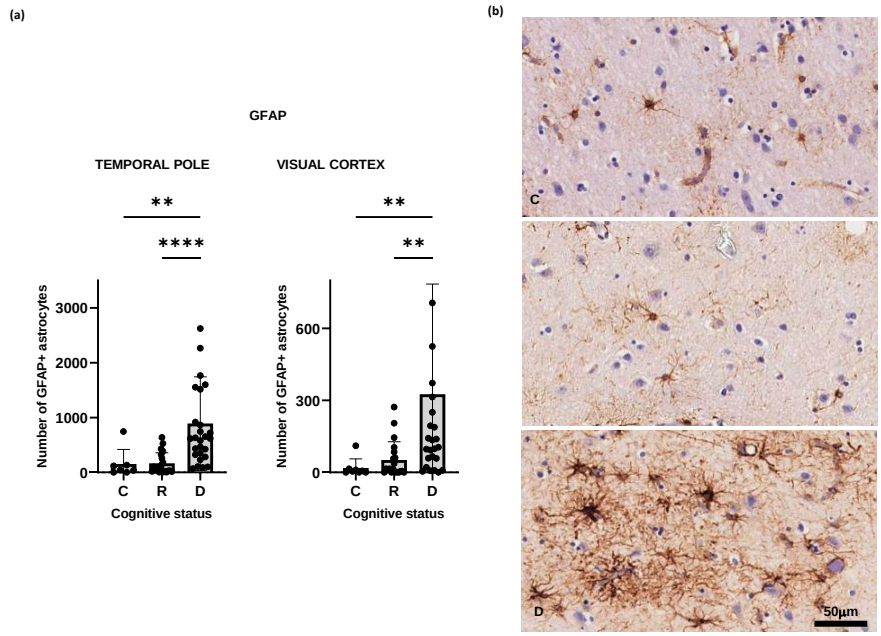

Figure 13: Inflammatory astrocytic changes (GFAP) in the temporal and visual cortices
Number of GFAP+ astrocytes were significantly higher in the temporal pole and visual cortex of demented compared with resilient and controls (**a**). Representative photomicrographs of GFAP + astrocytes in sections from control, resilient, and demented cases derived from the temporal pole (**b**). C Control (Braak 0-II); R Resilient (Braak III/IV); D Demented (Braak III/IV); ****p** < 0.01; *****p** < 0.0001. Scale bar 50 µm. Data are presented as mean ± standard deviation.

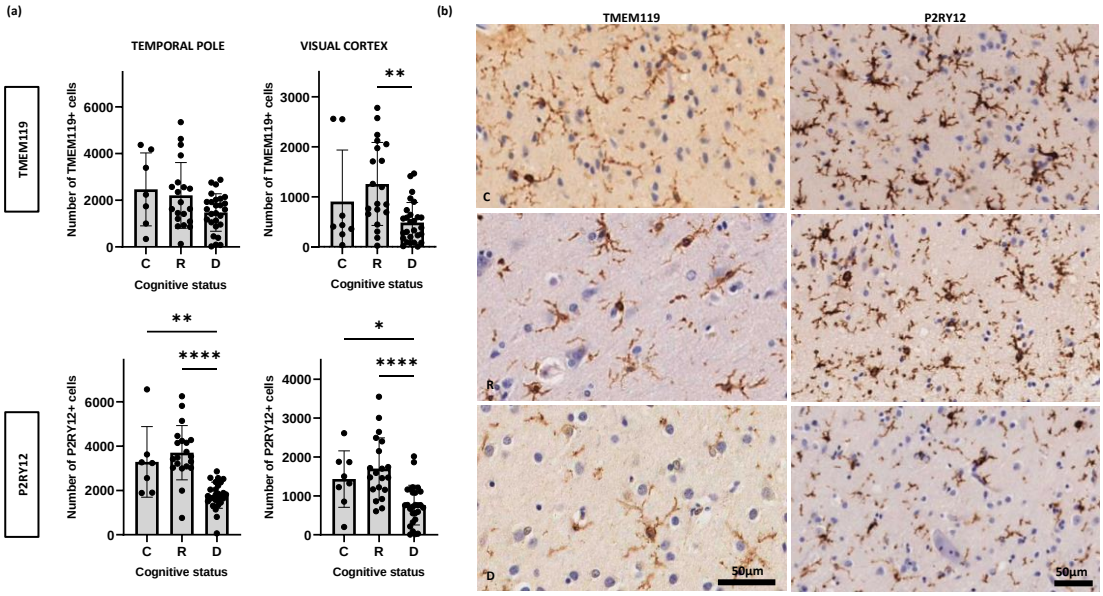

Figure 14: Homeostatic microglial changes (TMEM119 and P2RY12) in the temporal and visual cortices
Homeostatic microglia stained with TMEM119 and P2RY12 antibodies was significantly decreased in the temporal pole and visual cortex of demented compared with resilient and controls (**a**). Representative photomicrographs of TMEM119+ and P2RY12+ microglia in sections from control, resilient, and demented cases derived from the visual cortex (**b**). C Control (Braak 0-II); R Resilient (Braak III/IV); D Demented (Braak III/IV); ***p** < 0.05; ****p** < 0.01; *****p** < 0.0001. Scale bars 50 µm. Data are presented as mean ± standard deviation.

Interestingly, these glial cell signatures were observed in both, the temporal pole and the visual cortex of demented individuals, suggesting that glial cell phenotypic changes not only increase in parallel to NFTs in regions already affected by tau aggregates (temporal pole) but that they also

occur in advance of tau deposition in brain regions that are not yet impacted by tau pathology (visual cortex).

These data suggest that early glial phenotypic changes occur ahead of tau deposition in demented AD brains and that the absence of these aberrant glial cell responses in resilient brains may be contributing to the maintenance of neuronal cell and synaptic integrity and cognitive function in these individuals.

3.4 An early marker of cellular DNA damage (γH2AX) precedes tau tangle pathology and correlates with phenotypic glial cell changes of demented individuals at Braak III-IV stages

Gamma H2AX (γH2AX) is a well-established marker of early cellular damage. Previous studies have found that DNA damage resulting in double stranded DNA breakages initiates the phosphorylation of histone variant H2A at the Serine 139 site to generate γH2AX (570). Importantly, γH2AX is a marker of cellular dysfunction and cell cycle impairment that is fully reversible upon elimination of the damage inducing factor(s) (571). Using quantitative immunohistochemical analyses, the number of γH2AX-positive cells in the neocortex of the studied cases showed significantly higher γH2AX-positive cells in demented compared with resilient and control brains in the temporal pole and visual cortex (**Figure 15**). Interestingly, a significant correlation between γH2AX and cortical inflammatory glia (CD68, HLA-DR, GFAP) was observed (correlation analyses between cortical GFAP, CD68, HLA-DR, and γH2AX in temporal/visual regions, respectively: GFAP: R=0.57/0.45 and p=0.0006/<0.0001; CD68: R=0.44/0.46 and p=0.0009/0.0005; HLA-DR: R=0.32/0.07 and p=0.02/0.6).

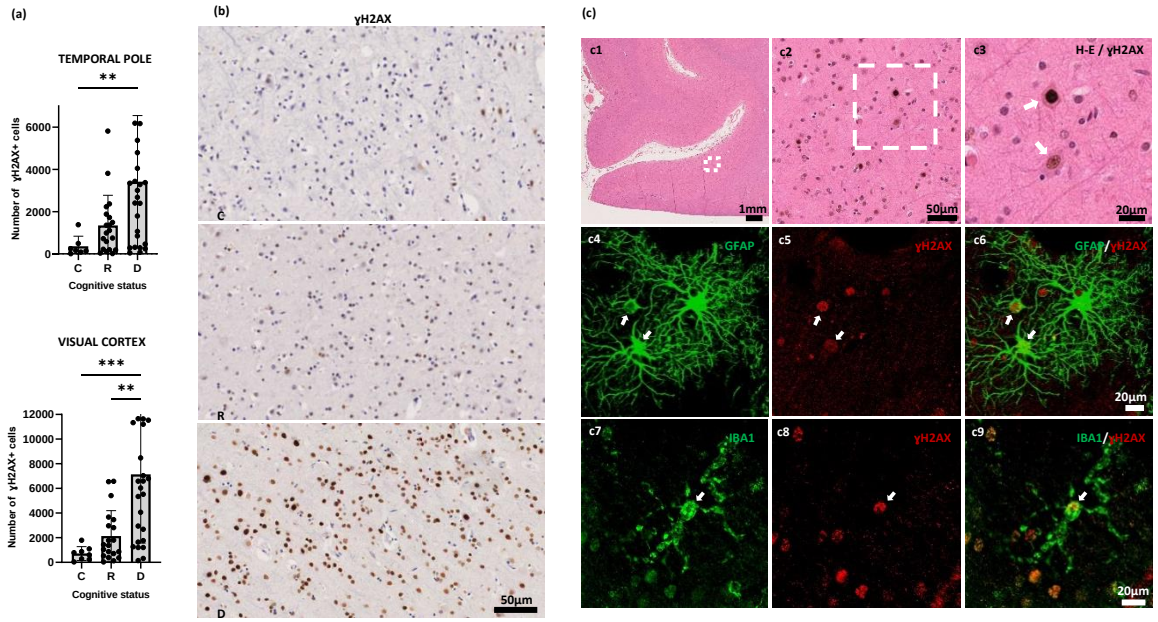

Figure 15: Early cellular damage marker (γH2AX) and cell-type positivity of γH2AX in the temporal and visual cortices

Number of γH2AX + cells was significantly higher in temporal pole and visual cortex of demented compared with resilient and controls (**a**). Representative photomicrographs of γH2AX+ cells in sections from control, resilient, and demented cases derived from the visual cortex (**b**). Representative immunofluorescence images showing colocalization of γH2AX+ cells (DAB, brown) with neurons (red) (**c1-3**, showing a progressively zoomed-in brain region), GFAP+ astrocytes (green) (**c4-6**, showing GFAP alone in **c4**, γH2AX alone in **c5**, both GFAP-γH2AX in **c6**), and IBA1 + microglia (green) (**c7-9**, showing IBA1 alone in **c7**, γH2AX alone in **c8**, both IBA1-γH2AX in **c9**). C Control (Braak 0-II); R Resilient (Braak III/IV); D Demented (Braak III/IV); **p < 0.01;

***p < 0.001. Scale bars 1 mm, 50 µm, and 20 µm. White arrows indicate colocalization between γH2AX+ cells and neurons, astrocytes, and microglia, respectively. Data are presented as mean ± standard deviation.

The differences in the number of γH2AX+ cells between demented and resilient brains were more pronounced in the visual cortex than in the temporal pole, suggesting that cellular damage responses precede NFT deposits, and indicating that the readily observed aberrant glial cell changes in the visual cortex of demented subjects could be pivotal to the early cellular vulnerability and brain dysfunction in these individuals. Using double immunohistochemical stainings for γH2AX and neurons (hematoxylin-eosin) and glial cell markers (IBA1, GFAP), γH2AX was observed predominantly in neurons, but also in a subset of glial cells in demented brains (**Figure 15**) suggesting that both, neuronal and glial cell damage may be part of the early brain injury responses in AD that ultimately result in functional changes and impaired cognition.

Importantly, no significant correlations were found between the number of γH2AX+ cells and 4G8+ amyloid-β burden in temporal and visual cortex (for temporal cortex: R=0.2, p=0.3; for visual cortex: R=0.23, p=0.26) and between γH2AX+ cells and AT8+ burden NFT or neuropil burden in temporal and visual cortex respectively (for temporal pole: R=0.1, p=0.43; for visual cortex: R=0.3, p=0.13). Importantly, the number of γH2AX+ cells showed no association with PMI (p=0.26 and p=0.09 in temporal pole and visual cortex respectively).

3.5. Glial cell changes in subcortical white matter precede tau tangle pathology and they correlate with early cortical cellular damage (γH2AX) in demented brains at Braak III-IV stages

The quantitative immunohistochemical analyses of glial cell phenotypes in juxtacortical WM immediately adjacent to the studied cortical regions showed significantly higher inflammatory (CD68, HLA-DR) **(Figure 16**) and lower homeostatic microglia (P2RY12, TMEM119) in demented compared with resilient and control brains (**Figure 17**). These WM changes were not only present in brain regions with cortical NFTs (temporal pole), but also in brain areas without detectable tau burden (visual cortex) suggesting that glial cell changes in WM occur early and that they precede tau deposition in the overlying brain cortices. In line with the previous results from the cortex of these brains, the total number of oligodendrocytes (Olig2) and total burden of microglial cells (IBA1) in WM were unchanged across groups irrespectively of presence or absence of NFT deposits in the overlying cortex, further reinforcing that qualitative rather than quantitative glial cell changes are the early glial cell signature of demented AD brains.

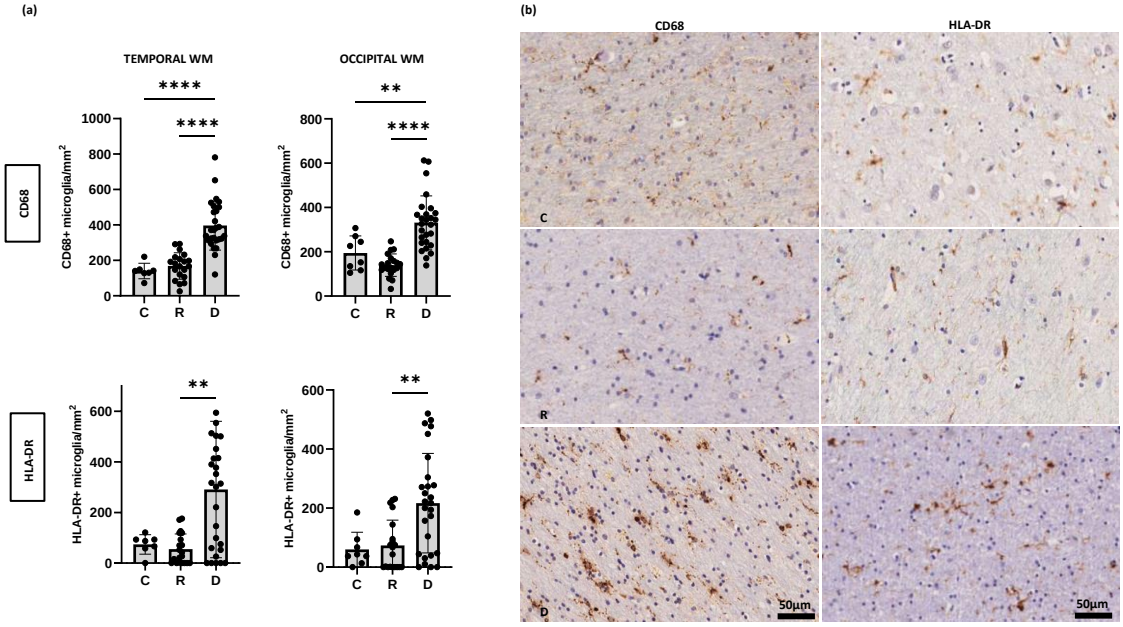

Figure 16: Inflammatory microglial changes (CD68 and HLA-DR) in the subcortical white matter of the temporal and visual cortices

Density of inflammatory microglia (CD68+, HLA-DR+) in the temporal and occipital white matter (WM) was significantly higher in demented compared with resilient and controls (**a**). Representative photomicrographs of CD68+ and HLA-DR+ microglia in sections from control, resilient, and demented cases derived from the temporal WM (**b**). C Control (Braak 0-II); R Resilient (Braak III/IV); D Demented (Braak III/IV); ****p** < 0.01; ******p** < 0.0001. Scale bars 50 µm. Data are presented as mean ± standard deviation.

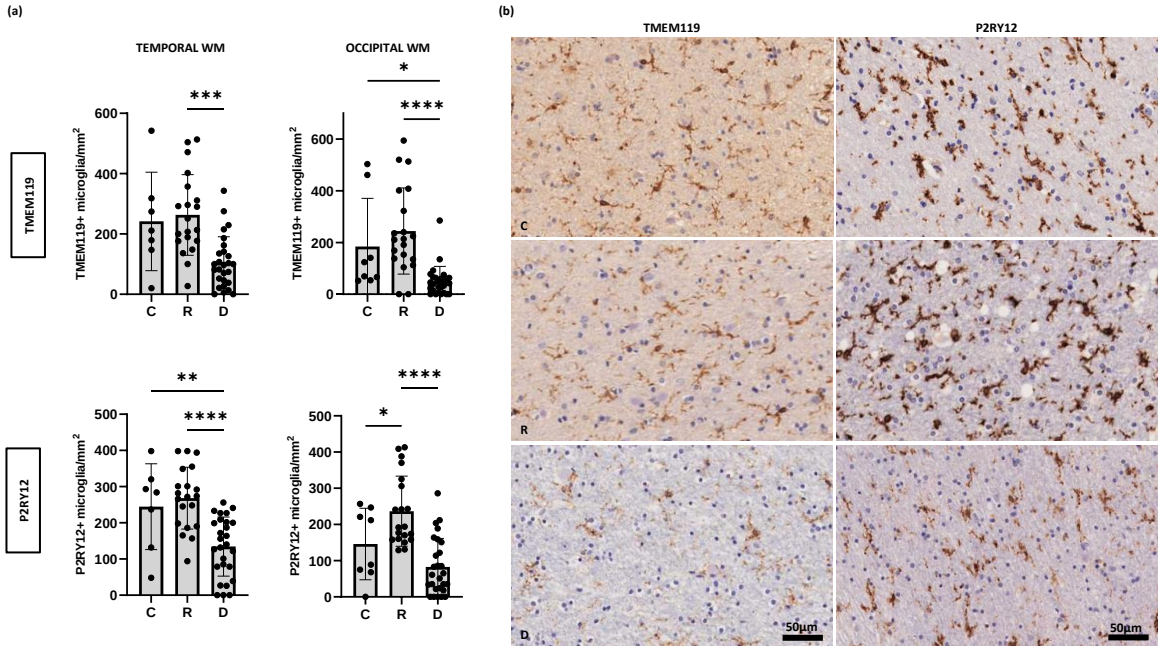

Figure 17: Homeostatic microglial changes (TMEM119 and P2RY12) in the subcortical white matter of the temporal and visual cortices

Density of homeostatic microglia (TMEM119+, P2RY12+) in the temporal and occipital white matter (WM) was significantly decreased in demented compared with resilient and controls (**a**). Representative photomicrographs of TMEM119+ and P2RY12+ microglia in sections from control, resilient, and demented cases derived from the temporal WM (**b**). C Control (Braak 0-II); R Resilient (Braak III/IV); D Demented (Braak III/IV); **p* < 0.05; ****p** < 0.01; *****p** < 0.001; ******p** < 0.0001. Scale bars 50 µm. Data are presented as mean ± standard deviation.

Interestingly, correlation analyses between subcortical WM glial cell changes and overlying 4G8+ amyloid-β burden were significant for inflammatory glia in occipital WM (for CD68 R=0.32, p=0.02; for HLA-DR R=0.29, R= 0.03) and for homeostatic glia in temporal WM (for TMEM119 R=-0.27, p=0.05, for P2RY12 R=-0.28, p=0.04) while only inflammatory glial cell changes in temporal WM showed significant association with overlying AT8+ NFTs (for CD68 R=0.36, p=0.007, for HLA-DR R=0.34, p=0.01). This suggests that subcortical WM glial cell changes involving higher inflammatory and lower homeostatic glial cell markers may be associated with amyloid-β and NFT burden in overlying cortices, and that WM glia could represent an early site of interaction and response to peripheral stimuli entering the brain through WM vasculature and hold relevance to the accumulation of ADNC in the overlying cortex.

Because the clinical symptoms characterizing the dementing disorder of AD are predominantly cortical rather than subcortical in nature, the correlation between WM glial cell changes and overlying cortical cellular vulnerability (γH2AX) were evaluated. The results showed significant associations between all inflammatory and homeostatic glial markers in temporal WM and cortical

γH2AX (for CD68 R=0.34, p=0.01, for HLA-DR R=0.27, p=0.05, for TMEM119 R=-0.36, p=0.007, for P2RY12 R=-0.31, p=0.02) and visual WM (for CD68 R=0.43, p=0.001, for TMEM119 R=-0.29, p=0.03, for P2RY12 R=-0.28, p=0.04) except for the inflammatory glial marker HLA-DR in occipital WM (R=0.19, p=0.17). Although the association between cortical glial cell changes and cortical γH2AX was also observed for some of the inflammatory and homeostatic glial cell markers in temporal cortex (for CD68 R=0.44, p=0.0009, for HLA-DR R=0.32, p=0.02, for P2RY12 R=-0.31, p=0.02) and visual cortex (for CD68 R=0.32, p=0.009, for P2RY12 R=-0.31, p=0.01), some of the glial cell signatures of the WM such as TMEM119 showed stronger association with overlying cellular damage than the same glial cell marker in the cortex suggesting that an early loss of homeostatic glial cell phenotype may be present in subcortical brain areas and may be contributing to the cellular damage observed in adjacent cortical structures. Of note, identical changes in cortical and subcortical/WM glial phenotypes were observed when analyses were limited to the subset of individuals with PART (not shown).

This suggests that loss of homeostatic microglia in the WM is an early brain change that may potentially contribute to cortical cell damage and loss of brain function in demented brains, which could potentially be targeted in the early dementia stages. It cannot be excluded that the higher burden of cerebrovascular disease present in cortical and subcortical regions of demented brains (see **Table 3**) might be contributing to some of the glial cell derangements observed in the WM of these individuals. However, vascular scores did not show significant associations with synapse densities or with MMSE score (correlation analyses between vascular score and synapse density in visual cortex: R=-0.18, p=0.38; MMSE: R=0.25, p=0.36; WAIS: R=-0.35, p=0.14), but a significant association with γH2AX+ cells in visual cortex (R=0.56, p=0.004), CDR-global (R=0.56, p=0.008) and CDR-SoB (R=0.54, p=0.01). This suggests that vascular damage could be partly contributing to some of the structural and functional changes observed in the early phases of AD dementia.

3.6. Synapse densities are significantly reduced in the visual cortex of demented compared with resilient brains at Braak III-IV stages

Recent evidence has suggested that synapse plasticity changes and synapse density loss are among the earliest and strongest determinants of cognitive dysfunction in AD (572). Biomarker studies have shown that the association between the loss of synaptic markers and the severity of cognitive dysfunction is stronger than the one of amyloid-β and tau biomarkers combined (292). This suggests that synapse loss may be the best neuropathologic correlate of dementia, surpassing the strength of association with amyloid-β/tau deposits, and serve as a reliable measure of earliest neuropathologic changes in a demented AD brain. Recent studies have proposed that inflammatory glial cells may be contributing to the engulfment and subsequent loss of synapses in the brains of AD mouse models and in two recent post-mortem human brain studies (61,422,430). Yet, the potential contribution of glia to enhanced synapse elimination in human brains at early disease stages of AD has so far not been studied. To assess whether synapse densities would be altered in demented brains in the early phases of ADNC and evaluate the contribution of (inflammatory) glial cells to synapse loss ahead of NFT deposits, synapses were quantified in the visual cortices of N=28 brains using ExM.

The results showed that synapsin1 (presynapses), PSD95 (excitatory postsynapses), and colocalized `mature' synapsin1-PSD95 puncta were significantly reduced in the visual cortex of demented compared with resilient and control brains (mean density of synapsin1+ puncta in demented $5.1x10^7$ $\pm0.25x10^7$ vs. $10.2x10^7\pm0.54x10^7$ in resilient vs. $8.9x10^7\pm0.61x10^7$ in controls, p=0.0001; mean density of PSD95+ puncta in demented $5.4x10^7\pm0.21$ $x10^7$vs. 9.5x107±0.54 $x10^7$ in resilient vs. $8.1x10^7\pm0.47$ $x10^7$ in controls, p=0.0001; mean density of double-labelled synapsin1+/PSD95+ puncta in demented 3.4 $x10^7\pm0.15$ $x10^7$ vs. 5.8 $x10^7\pm0.28$ $x10^7$ in resilient vs.5.5 $x10^7\pm0.31$ $x10^7$ in controls, p=0.0001) **(Figure 18).** Importantly, resilient brains did not show a difference in densities in any of

the three synaptic measures compared with control brains, suggesting that the mechanism by which resilient subjects may remain cognitively unimpaired is likely due to a better preservation of healthy and functioning synapses, rather than to a higher synaptic reserve at baseline. The percentage of colocalized mature synapsin1-PSD95 synapses observed across brains was of 65.2% (SEM 4.4%) which is in line with previous studies suggesting that at any given time only around 2/3 of synapses are properly arranged and functional (234,573). Interestingly, there was a strong association between loss of synapse densities and severity of memory impairment measured with CDR-SoB (R= -0.62 [p=0.003]), MMSE (R=-0.76 [p=0.001]), WAIS-R scores (R=-0.85, [p=0.0001]), and between synapse densities and early cellular damage measured with γH2AX-positive cells (R=-0.5 [p=0.009]) in the cortices of these brains **Figure 18).** Of note, the strong association observed between synapse densities and WAIS-R subscore assessing the digit symbol test (which specifically assesses visual memory tasks) reinforces the relevance of clinical-functional correlates of synapse changes observed here.

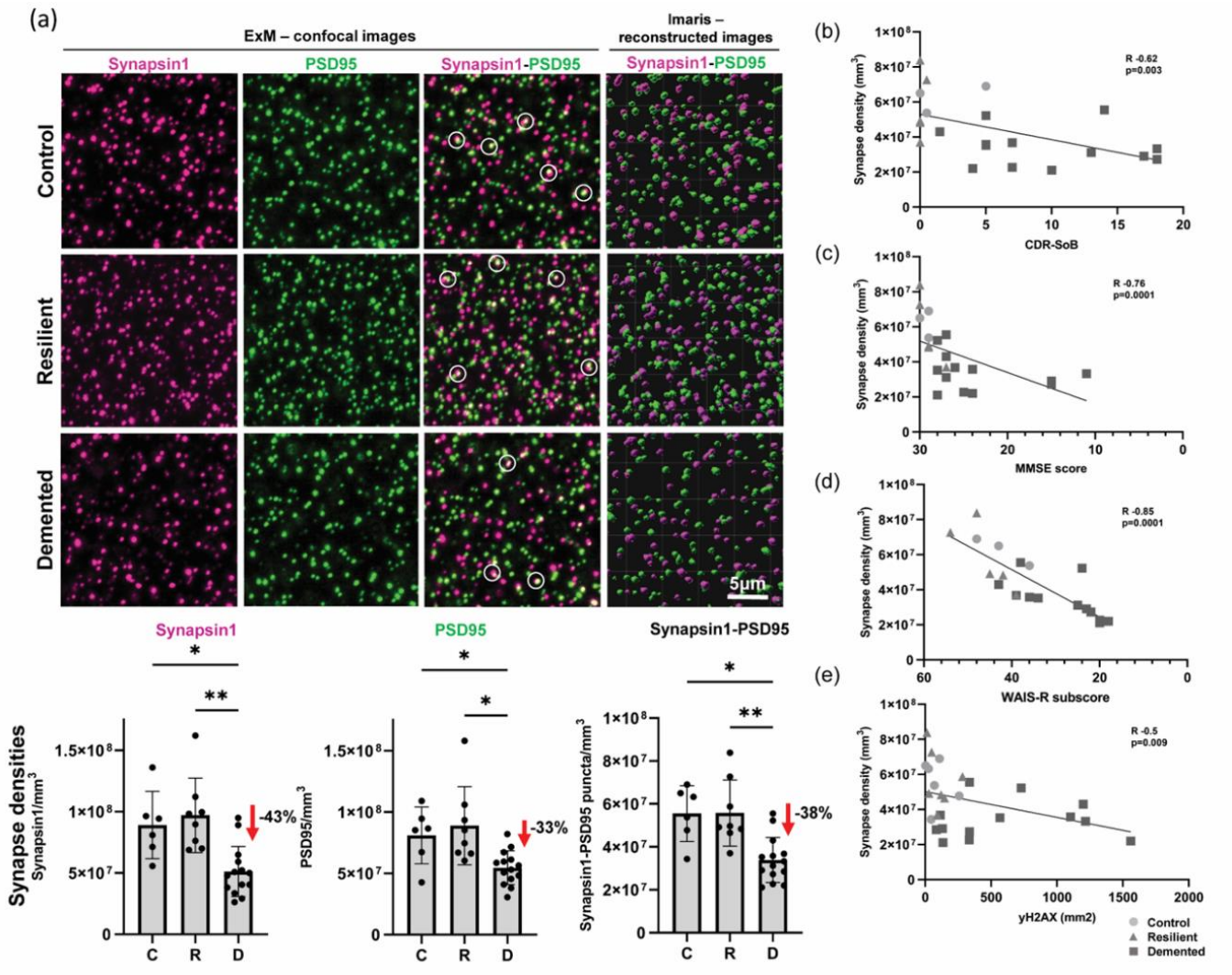

Figure 18: Synapse densities and correlation analyses between synapse densities and cognitive and neuropathological measures in the visual cortex

Synapse densities assessed using expansion microscopy (ExM) and confocal imaging were significantly reduced in the visual cortex of demented compared with resilient and controls when assessing synapsin1+ presynapses, PSD95+ postsynapses, and colocalized mature synapsin1+/PSD95+ synapses (**a**); representative images showing synapsin1+ presynapses in magenta, PSD95+ postsynapses in green, and colocalized `mature'

synapsin1+/PSD95+ synapses (**a**, first three columns) and Imaris 3D reconstructed images (**a**, fourth column); loss of mature synapses was significantly correlated with antemortem CDR-SoB (**b**), MMSE score (**c**), WAIS-R subscore (`digit symbol substitution test') (**d**), and with early cellular damage marker (γH2AX) (**e**). Analyses were performed on N=28 of the studied cases (6-8 FOV per case). Synapse densities represented in the graphs correspond to the values obtained from expanded tissue and must be multiplied by a factor of ~100 (=4.6^3) to account for the 4.6x volume expansion to extrapolate these results to pre-expanded tissue material. Light-grey circles = controls, medium-grey triangles = resilient, dark-grey squares = demented. C Control, N=6; R Resilient, N=8; D Demented, N=14; FOV: field of view. *$\mathbf{p} < 0.05$; **$\mathbf{p} < 0.01$. Scale bar 5 µm. Data are presented as mean ± standard deviation.

Importantly, correlation analyses between cognitive scores and 4G8+ amyloid-β burden and between cognitive scores and AT8+ neuropil thread in the visual cortex did not show significant associations (correlation analyses for 4G8: MMSE (R=-0.2, p=0.49), CDR-SoB (R=0.05, p=0.8), CDR-G (R=0.1, p=0.67), CDR-SoB subscores (including memory (R=0.06, p=0.8), orientation (R=0.05, p=0.8), judgement/executive function (R=-0.03, p=0.9), community affairs (R=0.03, p=0.9), home and hobbies (R=0.2, p=0.43), and personal care (R=0, p=0.99)), and the WAIS-R score (R=0, p=0.99); correlation analyses for AT8+ neuropil thread: MMSE (R=-0.11, p=0.6), CDR-SoB (R=0, p=0.98), CDR-G (R=0.03, p=0.88), CDR-SoB subscores (including memory (R=0.01, p=0.95), orientation (R=0.01, p=0.97), judgement/executive function (R=-0.03, p=0.9), community affairs (R=0, p=0.99), home and hobbies (R=0.2, p=0.4), and personal care (R=-0.03, p=0.89)), and the WAIS-R score (R=-0.03, p=0.9)).

These findings reinforce the presence of a close association between synapse density loss and memory dysfunction, which more reliably predicts cognitive decline than amyloid-β and tau deposits, suggesting that earliest neuropathogenic changes in AD may initiate at the synapse. Importantly, the changes observed here were present from the prodromal stages of dementia (MCI and mild AD dementia stages) indicating that interventions as early as at the MCI stage would be most effective to halt the readily substantial and progressive synapse loss leading to functional memory decline and development of formal dementia.

3.7. Astrocytes and microglial cells engulf higher amounts of synapses in the visual cortex of demented compared with resilient brains at Braak III-IV stages

Several *in vitro* and *in vivo* studies have found evidence of an increased internalization of synaptic elements by glial cells (422), and two recent human brain studies have shown that demented AD brains harbour higher amounts of microglia-internalized (pre-)synapses compared with control brains (96, 120). The excessive internalization of synapses by microglial cells has also been found in other neurological conditions, and it has been suggested to be a common mechanism underlying different neurodegenerative disorders (427,574,575). To evaluate the potential contribution of phenotypically changed glial cells in the visual cortex to the early synapse loss observed in this brain region, the internalization of synaptic elements by both, GFAP+ astrocytes and IBA1+ microglia, was quantified.

For the microglial cells, and as IBA1 labels all the phenotypes of this glial cell, a morphology-based ameboid microglial subtype was selected, which has been shown to harbour increased neurotoxic proprieties including release of neuroinflammatory cytokines and phagocytic behaviour (507). The results showed that IBA1+ ameboid-shaped microglial cells and interestingly also GFAP+ astrocytes contained a significantly higher proportion of presynapses, postsynapses, and colocalized synaptic puncta inside the cell body in demented compared with resilient and control brains (**Figure 19**)**.** Importantly, the engulfment of synapses did not only affect presynapses and postsynapses individually, but also colocalized synaptic puncta which are considered mature and functional. The significant proportion of internalized mature synapses by IBA1+ cells (% of mature synapses internalized by IBA1+ microglia in demented vs resilient vs control brains: 13.3%±1% vs. 2.6%±0.7%

vs. 0.9%±0.2%) and by GFAP+ cells (% of mature synapses internalized by GFAP+ astrocytes in demented vs resilient vs control brains: 17.2%±2.9% vs. 3.7%±1.4% vs. 2.7%±0.7%) indicates that a substantial amount of still potentially functional synapses could be actively eliminated by glia. Alternatively, the higher number of synapses within these glial cells could be the reflection of a primary dysfunction of astrocytic and microglial lysosomal/degradation pathways leading to an increased accumulation of engulfed elements.

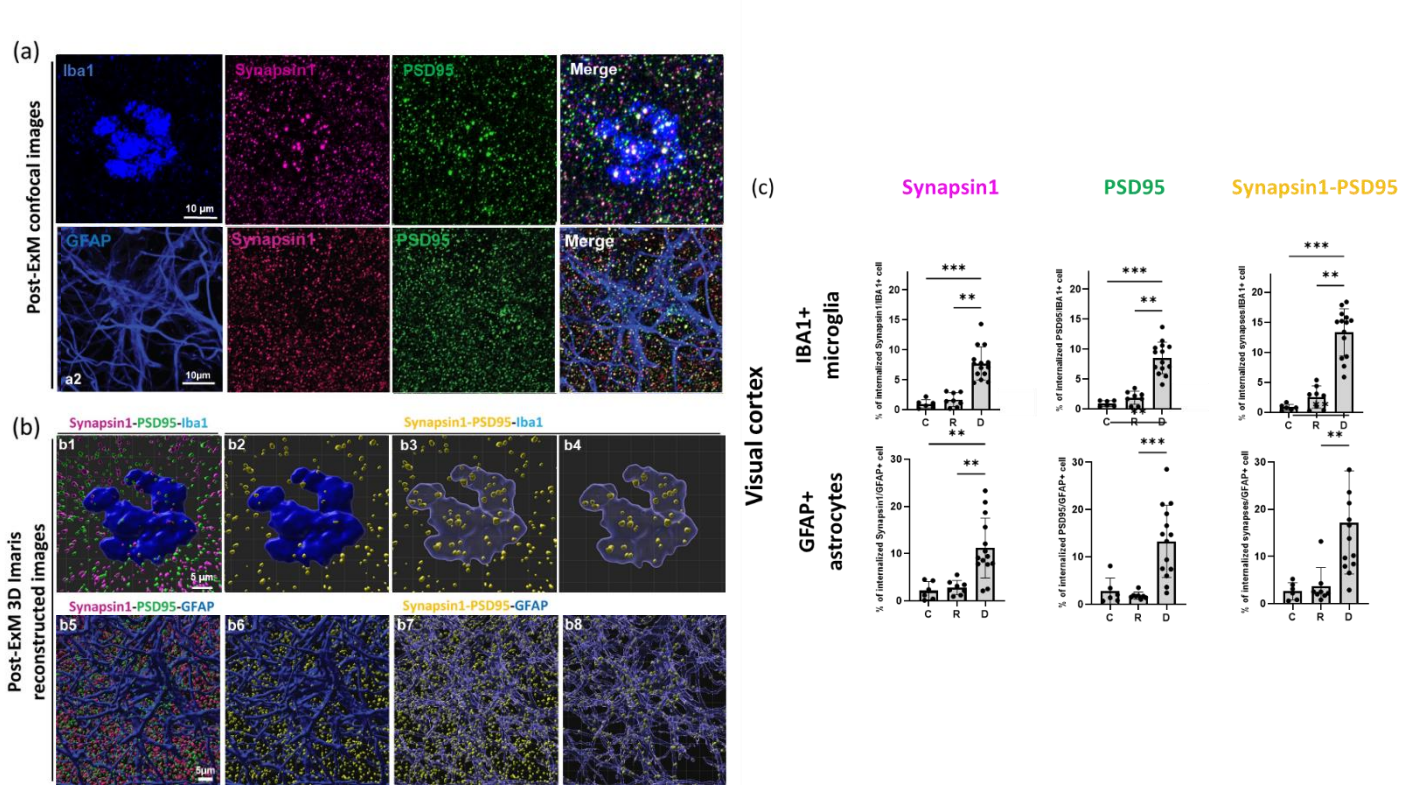

Figure 19: Quantitative analyses of internalized synaptic elements by microglia and astrocytes in the visual cortex

Analyses of internalized synaptic elements by glial cells were assessed using expansion microscopy (ExM) and confocal imaging. Microglia and astrocytes engulfed significantly more synapsin1+ presynapses, PSD95+ postsynapses and synapsin1+/PSD95+ colocalized synapses in demented compared with resilient and controls. Example of post-ExM with confocal imaging (**a**) and Imaris 3D image reconstructions (**b**) showing internalized synaptic elements inside an IBA1+ ameboid microglial cell and inside a GFAP+ astrocyte, and quantifications of engulfed synaptic elements inside IBA1+ microglia and GFAP+ astrocytes, respectively (**c**). Post-ExM with confocal imaging (**a**) of an IBA1+ ameboid microglia (**a1**) and a GFAP+ astrocyte (**a2**) in blue co-labelled with synapsin1 in magenta and PSD95 in green showing each channel individually and the merged image. Reconstructed 3D Imaris images (**b**) showing glial cells in blue, synapsin1+ presynapses in magenta (**b1, b5**), PSD95+ postsynapses in green (**b1, b5**), and colocalized synapsin1+/PSD95+ puncta in yellow (**b2-b4, b6-b8**), displaying colocalized synapses inside and outside of a microglial cell (**b3**) and an astrocyte (**b7**), and colocalized synapses only inside the microglia (**b4**) and astrocyte (**b8**). C: Control (Braak 0-II); R: Resilient (Braak III/IV); D: Demented (Braak III/IV); ****p** < 0.01; *****p** < 0.001. Scale bars 10 µm (**a1, a2**) and 5 µm (**b1-b8**). Data are presented as mean ± standard deviation.

These results are novel and indicate that not only microglia but also astrocytes are capable of engulfing synapses in the human brain, and that glia-mediated excessive internalization of synapses precedes overt NFT deposition likely contributing to early synaptic loss and loss of brain function in individuals with clinically manifest AD. Importantly, these findings propose a potentially primary role

of glia in early synapse loss but they also imply that there need to be additional determinants at play to explain the difference in internalized synapses in demented compared with resilient brains despite both presumably displaying phenotypically similar glial cells and synaptic receptors.

3.8 TOC1+ tau oligomers are higher in visual cortex-derived synaptosomes of demented compared with resilient brains at Braak III-IV stages

Oligomers of tau are viewed as the most neurotoxic species of tau protein, and recent evidence has suggested that tau oligomers are increased in the synapses of demented compared with resilient and control brains (272,520). Although several studies have shown that tau oligomers are synaptotoxic in cell culture and in *in vivo* models of AD (13,341,342,344,362–366) their potential role in the early dementia stages and their potential contribution to an enhanced synapse engulfment by glia has not been so far explored.

To evaluate oligomeric species of tau, tau oligomeric complex 1 (TOC1) antibody, a well-established marker of oligomeric conformational tau was used (576). The validation of this antibody with native western blotting showed its specificity for oligomeric over monomeric forms of tau (**Figure 20**) and its conformation-dependent binding epitope as this antibody was not detectable under non-native western blot conditions. TOC1 was assessed in the whole brain homogenates and in synaptosome-enriched fractions derived from the visual cortex of demented, resilient, and control brains. The results showed that while the total amount of TOC1+ tau oligomers in the PBS soluble fractions of total brain tissue homogenates did not significantly differ across groups, demented brains contained significantly higher amounts of TOC1+ tau oligomers in their synaptosomes compared with resilient and control brains (**Figure 20**). Importantly, the total amount of tau (measured with Tau5) did not differ across groups. Interestingly, correlation analyses between TOC1 and cellular damage (γH2AX) and between TOC1 and cognitive dysfunction (MMSE) showed significant associations ($R=0.73$, $p=0.003$ for TOC1-H2AX and $R=-0.58$, $p=0.03$ for γH2AX-MMSE) while this correlation was not significant when assessing AT8+ neuropil thread burden and structural damage (γH2AX, $p=0.1$) or functional memory loss (MMSE, $p=0.6$), supporting that oligomeric tau may be a better correlate of structural and functional damage in AD than fibrillar tau in the form of NFTs.

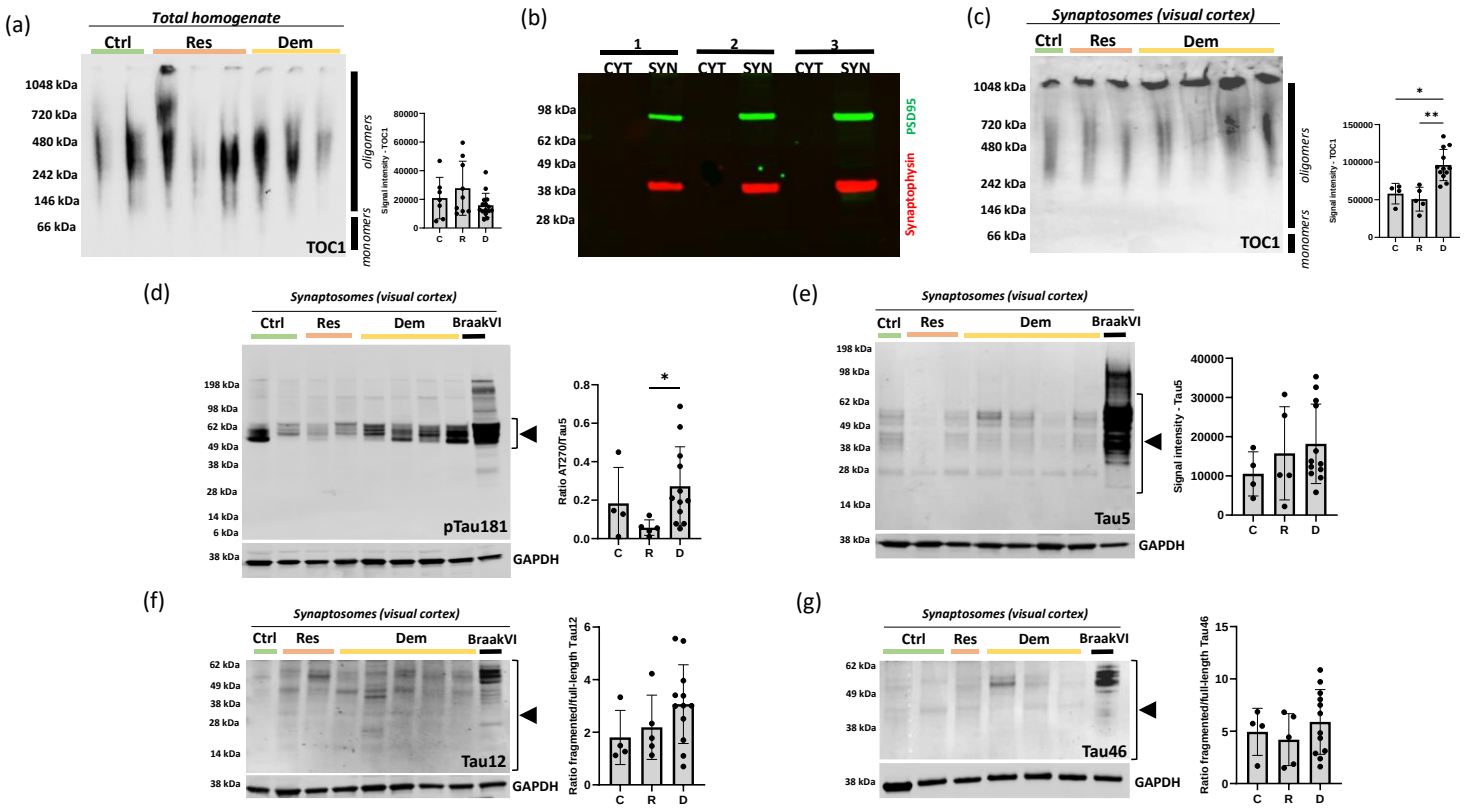

Figure 20: Assessment of oligomeric, hyperphosphorylated, and truncated tau species in total brain homogenates and synaptosomes extracted from the visual cortex

Western blot (WB) analyses of total brain homogenates showed no difference in TOC1 signal in demented compared with resilient and controls (**a**); synaptosome extractions and WB validation of three representative cytosolic (CYT) and synaptosome (SYN) samples (1-3) using the presynaptic marker synaptophysin (red) and the postsynaptic marker PSD95 (green) (**b**); WB analyses of synaptosome fractions (**c-g**) showed a significantly higher TOC1 signal in demented compared with resilient and controls (**c**) and significantly higher hyperphosphorylated AT270 (pThr 181)+ tau in demented compared with resilient and controls (**d**), while there was no difference in Tau217 (pThr 217) and/or AT180 (pThr 231)+ tau (not shown). Tau truncation, as measured with mid-domain total tau antibody (Tau5) (**e**), N-terminal tau (Tau12) (**f**), and C-terminal tau (Tau46) (**g**), did not differ across demented, resilient, and controls (**e-g**). Analyses were performed on N=31 total homogenates (6 controls, 10 resilient, 15 demented) and N=21 synaptosome extractions (4 controls, 5 resilient, 12 demented), respectively. Arrowheads indicate the quantified bands for each WB; C/Ctrl Control (Braak 0-II); R/Res Resilient (Braak III/IV); D/Dem Demented (Braak III/IV); WB: Western blot. *$\mathbf{p} < 0.05$; **$\mathbf{p} < 0.01$. Data are presented as mean ± standard deviation.

In line with previous studies (272), these data suggest that an early aberrant mistargeting and accumulation of tau oligomers in synaptic compartments may play a key role in the development of early dementia and that tau oligomers may be a better predictor of structural and functional change than burden of AT8+ fibrillar tau deposits. The underlying mechanisms of such translocation could involve an increased production or a reduced degradation of oligomers in the synapses of demented subjects or be the result of dysfunctional glia which could be contributing to the transport and/or translocation of extracellular tau oligomers into synapses.

3.9. Hyperphosphorylated pTau181 is higher in visual cortex-derived synaptosomes of demented compared with resilient and control brains at Braak III-IV stages

Hyperphosphorylation of tau is one of the most prevalent post-translational tau modifications that has been associated with the propensity of tau to aggregate and propagate (383,577). Different sites

of tau get hyperphosphorylated at different stages of AD development (380) and overall the brains of demented individuals show significantly higher amounts of phospho-tau compared with healthy controls. Three novel tau phospho-epitopes (pTau217, AT270 (pTau181), and AT180 (pTau231)) have been recently found to show close association with early dementia development and progression, and to be measurable in CSF and plasma (578).

The present brain cohort had no AT8+ NFT deposits in the visual cortex when assessed with immunohistochemical and/or western blotting. AT8 (pSer 202, pThr 205, pSer 208) is one of the earliest phospho-epitopes that becomes hyperphosphorylated at the pretangle stage of NFT development (385). The absence of NFTs thus enabled the unprecedented possibility to evaluate other early and possibly pathogenic modifications of tau protein that could be associated with incipient dementia stages and occur prior to NFT development. The commercially available antibodies against pTau217, AT270 (pTau181), and AT180 (pTau231) were used to measure earliest hyperphosphorylation signatures of demented and resilient brains using western blotting. The results showed that the synaptosomes of demented brains had a significantly higher AT270 (pThr 181) burden compared with resilient and controls (**Figure 20**), and absence of Tau217 (pThr 217) and/or no difference of AT180 (pThr 231) across groups (not shown). These findings suggest that specific tau hyperphosphorylation may occur early in the synapses of demented brains which could be potentially relevant to early synaptotoxicity and memory dysfunction.

Studies have shown that another prominent modification of tau is its truncation by proteases (387,392,393) which confers tau with pathogenic properties including self-aggregation and propagation (392,393). In particular, truncation of its C-terminus has been associated with increased hyper-phosphorylation and seeding activity (392,395,396). Controversy remains on the toxicity of the truncated proteins and/or the cleaved fragments, and on whether truncation precedes or follows hyperphosphorylation and NFT formation (387). Recent studies have found an independent association between pathologic tau truncation and neurotoxicity (398) and dementia severity (387).

In the present study N-/C-terminal fragments were assessed in the synaptosomes of demented, resilient, and control brains using western blotting. Antibodies against mid-domain `total' Tau (Tau5), N-terminal Tau (Tau12) and C-terminal Tau (Tau46) were used. Tau12 binds to the N-terminus and detects fragments that have been cleaved at the C-terminus, and Tau46 binds the C-terminus and detects fragments that have been cleaved at the N-terminus (579) with tau fragments <65kDA recognized by Tau12 corresponding to C-terminal cleaved tau and tau fragments <65kDA recognized by Tau46 corresponding to N-terminal cleaved tau (579). The results showed that neither the total amount of tau measured with Tau5, nor the quantity of N-/C-terminal cleaved tau fragments differed across groups, although a trend towards higher Tau12+ C-terminal cleaved tau was observed in the demented compared with resilient and control-derived synaptosomes **(Figure 20).**

Overall, these results suggest that not only tau oligomeric/conformational changes (TOC1) but also site-specific tau hyper-phosphorylation (pThr 181) may be among the earliest post-translational modifications of tau which occur in synapses of demented but not resilient AD brains prior to NFT development and could confer tau with potential pathogenicity. In contrast, tau truncation seems to be a later phenomenon or one that does not preferentially occur at the synapse in the early disease stages.

3.10 Tau seeding activity is not detectable in visual cortex synaptosomes of demented, resilient, or control brains at Braak III-IV stages

Pathologic propensity of tau to seed trans-synaptically may be among the earliest and main hallmarks of toxic tau conversion, which could determine incipient clinical change and severity of disease progression (580). Recent studies have found that tau seeding activity in synaptosomes of demented brains precedes NFT deposition by at least one Braak stage (404).

To evaluate presence of toxic tau seeds and evaluate the trans-synaptic spread of toxic tau seeds in the early phases of dementia and ahead of NFT deposition, tau seeding activity was assessed in the total brain homogenates and in synaptosome-enriched fractions derived from the visual cortex of demented, resilient, and control brains using the Diamond laboratory biosensor cell assay (405). The results showed absence of any detectable tau seeding activity across groups, in both the total brain homogenates of the cortex and WM, and the synaptosome-enriched fractions (**Figure 21**).

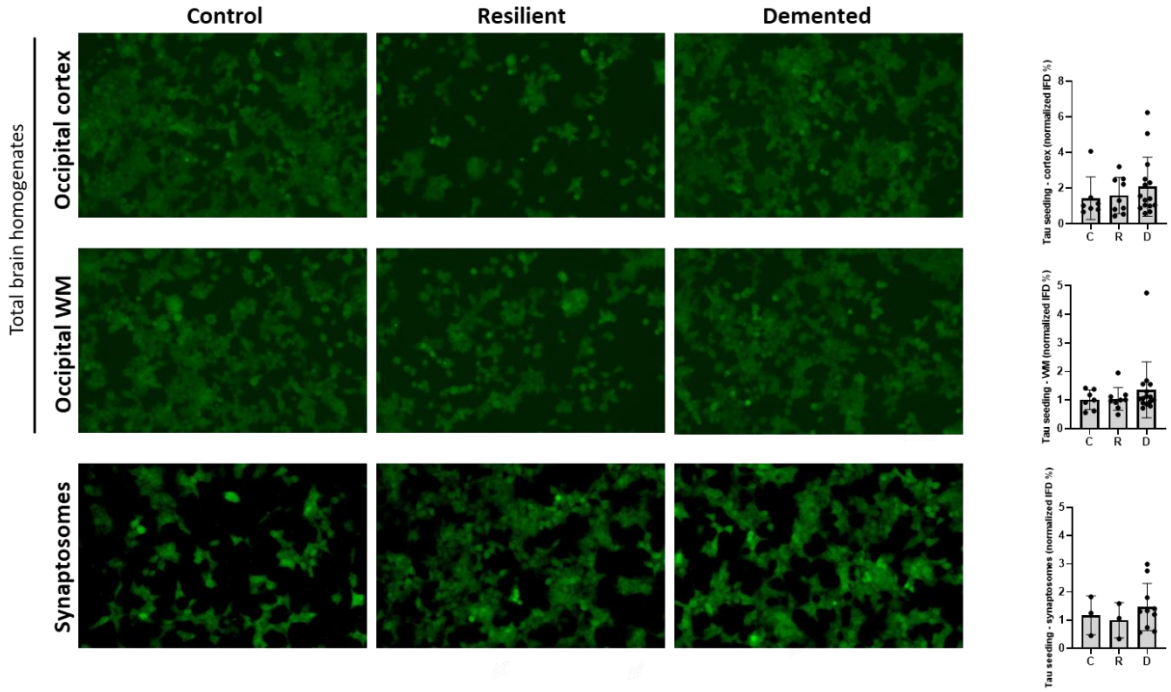

Figure 21: Tau seeding assays in cortical and WM derived brain homogenates and in synaptosomes extracted from the visual cortex
Tau seeding assays using total brain homogenates (cortex and WM) in N=31 cases showed minimal to no detectable seeding activity across groups; tau seeding assays performed using synaptosomes of N=15 cases showed minimal to no detectable seeding activity. Each assay was done in triplicate and tau seeding experiments were repeated three times and averaged for each case. C: Control (Braak 0-II); R: Resilient (Braak III/IV); D: Demented (Braak III/IV). Scale bar 100 µm. Data are presented as mean ± standard deviation.

The presently studied brain region lies one to two Braak stages ahead of tau deposition, thus these results suggest that toxic tau seeds may form during a temporally and spatially restrained period which may not exceed more than one Braak stage and thus be closely associated with presence of NFTs (404). Moreover, tau seeds may not be needed for synapse loss to occur and their effect on early synapse derangement may be negligible. In addition, the readily present increases in TOC1+ tau and pTau181+ tau in the synaptosomes of demented brains suggests that those early pathogenic

tau changes may primarily initiate locally at the synapse, and not depend on a pathogenic tau conversion derived from tau seeds. Recent studies have suggested that C-terminal truncated tau is more prone to seed (395), and the demented brains did not show higher C-truncated tau in the synaptosomes which may be a later phenomenon possibly yielding tau with additional toxic properties including seeding activity. While it remains possible that toxic tau conversion and seeding activity was not yet present in the early disease phases studied here, it cannot be excluded that seeding of early seed-competent tau moieties may not be adequately detected by the conventional Diamond laboratory biosensor cell constructs used here. Of note, the samples were also tested on a second and newly developed biosensor cell construct (581) but, once again, no tau seeding activity was detected (not shown).

3.11 TOC1+ tau oligomers are higher in the pre- and postsynapses of demented compared with resilient and control brains at Braak III-IV stages

To assess the in situ association of TOC1+ tau oligomers with synaptic elements, and evaluate the predilection of TOC1+ tau for presynaptic and postsynaptic elements individually, the association of TOC1+ puncta with Bassoon+ presynapses and PSD95+ postsynapses was assessed. Importantly, a subset of N=10 cases (4 demented, 4 resilient, and 2 controls) that were matched for age, gender, amyloid-β burden, neuropil thread, and composite vascular score, excluding any PART cases, were selected for this analysis (**Table 5**). The results showed significantly higher TOC1+ tau colocalized to presynapses and postsynapses in demented compared with resilient and controls (colocalized TOC1-Bassoon 49.9%±5.5% for demented, 28.2%±6.6% for resilient, and 18.7%± 2.3% for control brains; colocalized TOC1-PSD95 32.5%±6.7% for demented, 17.3±2.8% for resilient, and 14.5%±3.1% for control brains) (**Figure 22**) with a higher proportion of TOC1+ oligomers contained in presynapses when compared with postsynapses. These findings are in line with the previous western blot evaluation of TOC1 in synaptosomes of these same cases (**Figure 20**)**.**

Cognitive status	**Control**	**Resilient**	**Demented**
Number of subjects, total N=10	2	4	4
Cognitive scores			
MMSE (mean, SD)	30 (0)	29.5 (0.6)	26 (1.6)*
Age (years)			
Mean (SD)	83 (9.9)	80.8 (3.6)	85.2 (8.8)
Sex			
Female N (%)	1 (50%)	3 (75%)	3 (75%)
Male N (%)	1 (50%)	1 (25%)	1 (25%)
Neuropathology ('ABC' score)			
A-Thal phase, median (range)	0 (0)	2.5 (2)	4 (3)
B-Braak stage, median (range)	1.5 (1)	3 (1)	3.5 (1)
C-CERAD score, median (range)	0 (0)	1.5 (2)	1 (1)
Vascular score			
Composite score, mean (SD)	5 (1.4)	2.8 (3)	2.7 (1.3)
PMI (hours)			
Mean (SD)	24 (0)	25.5 (21.4)	22.7 (8.5)

Table 5: Baseline demographic and neuropathologic characteristics of the subset of N=10 cases used for assessments of oligomeric tau-driven synapse elimination by glia

Demographic and neuropathologic features of the total N=10 subjects included in the analyses of TOC1+ pre- and postsynapses, and microglial and astrocytic engulfment of TOC1-containing synapses (data are shown in Figure 22). Thal phase: No amyloid-β deposition (A0), amyloid-β in neocortex (A1), amyloid-β in allocortex/limbic regions (A2), amyloid-β in diencephalon/basal ganglia (A3), amyloid-β in brainstem/midbrain (A4), amyloid-β in cerebellum (A5); CERAD score: No neuritic plaques (C0), sparse plaques (C1), moderate plaques (C2), frequent plaques (C3); Cerebrovascular composite score includes subscores for: hypertensive cerebrovascular, atherosclerosis, cerebral atherosclerosis, occlusive atherosclerosis and cerebral amyloid angiopathy score; MMSE: Mini-Mental State Examination score; PMI: Post-mortem interval; N: number; SD: Standard deviation. C: Control (Braak 0-II); R: Resilient (Braak III/IV); D: Demented (Braak III/IV). Significance levels (*) indicate differences between demented and resilient brains with their respective p-value. ***p** < 0.05.

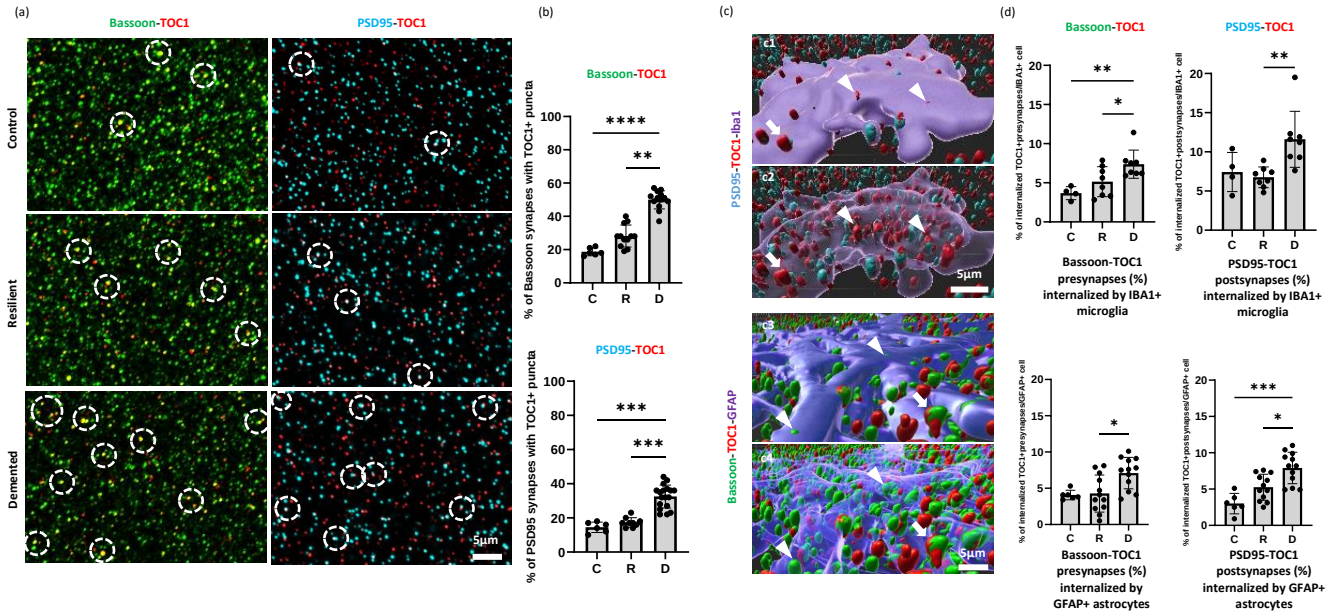

Figure 22: Quantitative assessments of TOC1-positive pre-/postsynapses and TOC1-driven synapse elimination by microglia and astrocytes

Analyses of TOC1-positive synaptic elements and TOC1-driven internalization of synaptic elements by glial cells were assessed using expansion microscopy (ExM) and confocal imaging. TOC1+ tau oligomers were higher in Bassoon+ presynapses and PSD95+ postsynapses of demented compared with resilient and controls (**a, b**); TOC1+ pre-/postsynapses were higher inside IBA1+ ameboid microglia and GFAP+ astrocytes in demented compared with resilient and controls (**c, d**). Representative images showing colocalized Bassoon+/TOC1+ puncta (white circles) in control, resilient, and demented brains (**a**); representative images showing TOC1+ puncta colocalized with Bassoon+ presynapses and PSD95+ postsynapses in demented, resilient, and control brains (**b**); representative Imaris 3D reconstructed images with white arrowheads indicating engulfed, and white arrows indicating non-engulfed PSD95+/TOC1+ synapses inside an IBA1+ ameboid microglia before (**c1**) and after (**c2**) making the cell body transparent, and Bassoon+/TOC1+ synapses inside an GFAP+ astrocyte before (**c3**) and after (**c4**) making the cell body transparent; quantitative assessments of the proportion of internalized TOC1+ presynapses and TOC1+ postsynapses inside IBA1+ ameboid microglia and GFAP+ astrocytes, respectively (**d**). Analyses were performed on N=20 IBA1+ and N=30 GFAP+ cells from N=10 brains (2 controls, 4 resilient, 4 demented); C Control (Braak 0-II); R Resilient (Braak III/IV); D Demented (Braak III/IV). ***p** < 0.05; ****p** < 0.01; *****p** < 0.001; ******p** < 0.0001. Scale bar 5 µm. Data are presented as mean ± standard deviation.

These results reinforce that an enhanced mistargeting and accumulation of tau oligomers in synapses is an early hallmark of demented compared with resilient brains, and that tau oligomers may selectively target both, presynapses and postsynapses in the early disease stages, potentially

involving different pathways in the process. Importantly, the increase in oligomeric tau in synapses occurred despite matched total tau (Tau5) and phospho-tau (AT8) burdens in the same brain region. This suggests that the mechanisms involved in the (pathologic) increase of oligomeric tau in synapses of demented brains may underlie a locally We developed tau FRET probes based on a single DNA construct using the T2A self-cleaving peptide - Lathuliere, 2023enhanced generation and/or an inefficient removal of tau oligomers from synapses, rather than a secondary effect derived from an increased total amount of tau in these brains.

3.12 TOC1+ synaptic elements are higher inside GFAP+ astrocytes and IBA1+ microglia in demented compared with resilient and control brains at Braak III-IV stages

Tau oligomers are known to be directly synaptotoxic, however the toxic effects of tau oligomers occur within hours, and they do not as such plausibly explain the slowly progressive dementia disorder characterizing AD. To evaluate the alternative possibility that accumulation of TOC1+ tau oligomers in synapses of demented brains could serve as a signal for glial cells to increase the engulfment of synapses, the proportion of internalized TOC1-tagged presynapses (Bassoon+) and TOC1-tagged postsynapses (PSD95+) by IBA1+ microglia and GFAP+ astrocytes were evaluated. For these analyses, the same subset of N=10 cases (4 demented, 4 resilient, and 2 controls) used previously and matched for age, gender, amyloid-β burden, neuropil thread, and composite vascular score, excluding any PART cases, was used (**Table 5**). The results showed that IBA1+ ameboid-shaped microglia and also GFAP+ astrocytes contained higher proportions of TOC1-labelled pre- and postsynapses in demented compared with resilient and control brains (demented vs. resilient vs. controls, TOC1+ synapses in microglia: 7.4%±0.6% vs. 5.1%±0.7% vs. 3.7%±0.4% internalized TOC1+/Bassoon+ puncta [p=0.006]; 11.6%±1.3% vs. 6.8%±0.5% vs. 7.4%±1.3% internalized TOC1+/PSD95+ puncta [p=0.001]); TOC1+ synapses in astrocytes: 7%±0.6% vs. 4.3%±0.7% vs. 4%±0.3% internalized TOC1+/Bassoon+ puncta [p=0.001]; 7.9%±0.6% vs. 5.3%±0.5% vs. 3%±0.6% internalized TOC1+/PSD95+ puncta [p=0.0006]) (**Figure 22**). Importantly, the internalized tau oligomer-containing synaptic puncta represented a large proportion of the total puncta engulfed by microglia and astrocytes in demented brains (91% of presynaptic and 93% of postsynaptic puncta in IBA1+ ameboid microglia, and 63% of presynaptic and 60% of postsynaptic puncta in GFAP+ astrocytes, respectively) suggesting that the mechanisms involved in the engulfment of tau oligomer-containing synaptic elements may be key in the early phases of dementia. Of note, if taking into account the previously shown total increase in inflammatory glial cells in demented brains (**Figure 12** and **Figure 13**), the total burden of internalized synapses by these glial cells would be of even higher magnitude, and account for an important proportion of synapse loss in these brains.

These findings suggest that an alternative and novel explanation of the early and increased elimination of synapses by glia in a demented human brain may be the presence of tau oligomers mistargeted to synapses. These findings however also suggest that additional determinants may be involved to explain the different internalization propensities of presumably phenotypically indistinguishable glial cells in a demented and a resilient/control brain in the presence of synaptic tau oligomers. It cannot be excluded that tau oligomer-tagged synapses were dysfunctional prior to their glial cell engulfment, and that glial cells were internalizing them to try to effectively remove them. However, and as previously shown in *in vivo* studies, the temporal disconnect between the relatively acute synaptotoxic effects of tau oligomers (in the range of hours) in contrast to the very slowly progressing dementia disorder characterizing AD (over the course of years), would argue against a primarily direct synaptotoxic role of tau oligomers on synapses. Of note, cases selected for this analysis were matched for vascular score burden which largely eliminates the potential involvement of vascular injury signals and/or the peripheral influx of elements that may alter the intimate interaction sites between oligomeric tau in synapses and inflammatory glial cell responses.

Importantly, no significant associations were found between PMI and synapse densities (R=0.19 (95% CI -0.23-0.55) [p=0.36]), 4G8 burden (R=0.1 (95% CI -0.32-0.5) [p=0.63]), AT8+ neuropil (R=0.04 (95% CI -0.37-0.44) [p=0.84]), p-tau181 (R=0.32 (95% CI -0.3-0.75) [p=0.28]), TOC1 (R=-0.1 (95% CI -0.64-0.47) [p=0.69]), and GFAP (R=-0.16 (95%CI -0.55-0.3) [p=0.48]), largely excluding the possibility that changes in the expression levels of these proteins would be due to PMI.

4. Discussion

4.1 Summary

The present work proposes that early glial cell changes involving an increase in pro-inflammatory and a decrease in homeostatic glial responses are present in the neocortex and WM of demented but not resilient and control brains in advance of NFT formation, and that glial cell changes show a close association with cortical cell damage and cognitive decline. Moreover, synapse loss is present in NFT-free brain regions of demented brains, and this neuropathologic change is an earlier and stronger determinant of dementia presence and severity than amyloid-β and/or tau deposits. In addition, presynapses, postsynapses, and mature colocalized synapses are excessively internalized by pro-inflammatory microglia and astrocytes in demented compared with resilient and control brains, and an early increase of tau oligomers in the synapses of demented brains is associated with a significant enhancement of synapse elimination by glial cells in these brains. These results are novel and indicate that early glial phenotypic changes precede tau tangle pathology in the brains of mildly demented individuals, that early synapse loss in these brains could be primarily driven by microglia and astrocytes, and that tau oligomers mistargeted to synapses could be driving and perpetuating the aberrant glial cell responses observed in demented brains in the early phases of AD dementia. This is the first study to report evidence of astrocyte and microglia engulfment of synapses in early AD dementia, and to suggest that tau oligomers in synapses may be detrimental through increasing the glia-mediated synapse elimination in demented brains.

4.2 General discussion

Even though the distribution and abundance of amyloid-β plaques and NFTs at post-mortem is a good predictor of the likelihood of cognitive impairment prior to death, in some instances there is a mismatch between lesions and symptoms, and these cases are referred to as `resilient' brains to ADNC (1,57,582–584). Cognitively normal individuals who harbor a high burden of ADNC (Braak V-VI stages) at autopsy are rare and represent a very small subset of outliers estimated at around 5-7%, but cognitively normal individuals with intermediate stages of ADNC (Braak III-IV stages) at post-mortem seem to represent a substantial proportion of around 45% of all elderly individuals whose brains show ADNC at autopsy (9). Previous studies of resilient brains at advanced Braak V-VI stages have found that inflammatory glial cell responses and accumulation of oligomeric tau in synapses are higher in demented but remain low in resilient brains (57,58,272,520,585). Although the study of these advanced AD stages allows to assess brain changes that would confer resilience to the effects of full-blown and ubiquitous amyloid-β plaque and NFT pathologies, these brains are less well suited to address the significance of other neuropathologic features including neuroinflammatory changes that could be developing at or even before classical AD neuropathologic lesions and be relevant for early dementia development. In the present study a cohort of 60 human brains with intermediate stages of tau pathology (Braak III-IV) was selected, which included a group of demented (N=29) and a group of non-demented `resilient' (N=21) age-matched subjects. To assess whether resilient subjects would harbour brain signatures unique to them and distinct from healthy cognitive ageing that would be key to overcome the effects of ADNC and enable an advantageous cognitive trajectory

in these individuals, a group of age-matched controls (N=10) was included. The control group comprised brains of non-demented subjects with negligible neocortical tau (Braak stage 0-II), absence of neuritic plaque burden (CERAD 0), and lack of other major neuropathologic lesions. Importantly, the age of the resilient and demented subjects was matched (mean age of 87.9 years for resilient and mean age of 88 years for demented subjects) suggesting that age, which is one of the strongest risk factors for dementia, did not have a major impact on the presence or absence of dementia in this brain cohort. Equally, the apoE4 allele status, one of the strongest genetic risk factors for AD dementia, was matched between groups.

Amyloid-β and tau deposits in early-stage AD brains

NFTs are known to start to form in the transentorhinal/entorhinal cortex (Braak stage I-II), they then affect the mesiolimbic and neocortical lobe structures (Braak stages III-IV), and ultimately culminate in the visual cortex (Braak stages V-VI), resulting in overt tau pathology along the same pathways (2). Importantly, in the Braak III stages NFTs are restricted to the medial temporal lobe and in Braak IV stages NFTs reach the temporal neocortex, but most neocortical regions still remain unaffected (586). Thus, brains at Braak III-IV stages provide a unique temporal window of opportunity to assess early changes occurring in neocortical regions in advance of the accumulation of NFTs. In the present study, human brains of demented and resilient subjects at Braak III-IV stages were included, and the temporal pole (a late Braak III region) and visual cortex (a Braak V-VI region) were assessed. The temporal pole (Brodmann area 38) is located at the most rostral part of the temporal lobe and it has been associated with a wide range of cognitive functions (119). Importantly, amyloid-β pathology typically accumulates in this brain region in the early Thal 2 stage, while NFTs reach this brain region in the late Braak III stage (545). This makes this brain area of particular interest since it represents an early interaction site between readily present amyloid-β plaques and newly developed tau tangles. In the present study, brains in the Braak III and/or IV stages were pooled together for further analyses. To ensure that none of the brains were ahead of NFT development in this brain region (e.g., at an early Braak III stage), all temporal poles were stained with AT8 antibody, and cases were included only when NFTs were present in this brain region (**Figure 2**). The visual cortex (Brodmann areas 17 and 18) is located at the most posterior part of the occipital lobe and it receives and integrates visual stimuli and is involved in visual and working memory tasks (121,122). The visual cortex typically gets affected by amyloid-β pathology in the late Thal 2 stage, and by NFTs in the late Braak V-VI stage (545), making this brain region ideally suited to evaluate how glial cells (and other potential neuropathologic changes) would behave ahead of NFT development in a brain region with relatively low amyloid-β burden. In line with this, quantitative analyses of the burden of 4G8 in temporal and visual cortex showed a significantly lower amount of 4G8 deposits in the visual cortex (mean area covered by 4G8 deposits: 1.8%) compared with the temporal pole (mean area covered by 4G8 deposits: 2.6%) (**Figure 10**). All visual cortices were stained for AT8 antibody and showed absence of NFT deposits, however minimal amounts of AT8+ neuropil threads were observed and quantitative analyses of the total burden of AT8+ neuropil threads did not significantly differ between resilient and demented brains (**Figure 3**). This suggests that neither the presence of fibrillar tau in the form of NFTs nor phospho-tau accumulation in the neuropil (dendrites and neurites) seem to distinguish demented from resilient subjects, and/or to have a major impact on functional and cognitive changes in an individual. Nonetheless, the overall very low burden of AT8+ neuropil threads with an average density of 0.0035/μm^2 across groups could be a potential explanation for the lack of effect of those tau deposits on cognitive function at these very low levels of tau accumulation. Maybe a higher burden of AT8+ tau in the neuropil would have had deleterious effects on structural and cognitive measures. Of note, the basic anatomic characteristics of temporal and visual cortices are similar and they display the typical six-layered structure characteristic of the human neocortex (587,588), allowing an optimal comparative analysis of neuropathologic changes across these two brain regions.

Clinicopathologic discrepancies in AD

Initial clinical symptoms in AD typically develop at Braak III-IV stages of tau pathology manifesting as prodromal MCI or mild dementia syndrome (20,586). Understanding the brain changes that beyond amyloid-β plaques and NFTs may result in the early clinical manifestations of the disease may be relevant for early preventative interventions to effectively halt neurodegeneration and clinical expression of ADNC and/or other neuropathologic changes that may be contributing to the memory loss in AD. In the present study, the demented subjects had an antemortem diagnosis of MCI or mild AD dementia in most except for two cases who had moderate dementia prior to death (mean MMSE of 24/30 points), and the age-matched resilient and control subjects showed no antemortem dementia (mean MMSE of 29.5/30 points for the resilient, mean MMSE of 29/30 for the control subjects) (**Table 3**). Of note, last clinical assessments prior to death took place within < 2 years (except for one control case). Demented and resilient brains showed similar burdens of 4G8+ amyloid-β plaques and AT8+ NFTs in the temporal cortex, and similar burdens of 4G8+ amyloid-β plaques and absence of NFTs in the visual cortex, as shown in the quantitative histopathologic assessments of these brains (**Figure 2**). Previous studies have suggested that cellular damage in a demented AD brain does not closely associate with the presence of amyloid-β plaques or NFTs (390). Although NFTs correlate better with the burden of neuronal loss and with the severity and duration of clinical symptoms than amyloid-β plaques (358,589), some neuronal populations in demented brains seem particularly vulnerable to cell loss even in the absence of NFT formation (390), and a substantial proportion of neurons containing NFTs can remain functional over several decades (21). In fact, the amount of neuronal loss in demented brains, even in areas with abundant NFTs, cannot be explained by the number of NFTs present at autopsy, and the burden of neuronal death in a demented brain exceeds by at least 7x the number of NFTs measured in the same brain region (19,358,590). Moreover, the majority of dead neurons in a demented brain are free of NFTs, with estimates suggesting that 9 out of 10 neurons that die do not contain a NFT (390). In addition, ghost tangles, which are the ultimate reflection of cellular death of tangle-bearing neurons, are exceedingly rare in demented brains, and are estimated at only around 1% of total neurons containing NFTs (391). Previous studies of resilient and demented human brains have reinforced the lack of association between the burden of AD neuropathologic lesions and symptoms (57) however, in some studies of resilient brains at advanced Braak V/VI stages of tau deposition, lower burdens of NFTs were present in select cortical brain regions of resilient when compared with demented subjects, and NFT burden was proposed to partly account for the lack of cognitive symptoms observed in these subjects (27,591). Contrary to this idea but in line with other previous studies of resilient brains, in the present study the detailed quantitative neuropathologic assessments of the burden of 4G8+ amyloid-β plaques and AT8+ NFTs and AT8+ neuropil threads showed no difference between resilient and demented brains (**Figure 2** and **Figure 3**). This suggests that neither the deposition stage of ADNC nor the burden of amyloid-β plaques and number of NFTs in these intermediate stages of AD neuropathology plausibly explains the opposite cognitive outcomes observed in these individuals. It remains possible that the previously reported effects of NFTs and neuropil thread burden on cognition may arise in more advanced stages of AD, in which the overall burden of NFTs and neuropil thread is higher. Importantly, the matching for amyloid-β and NFT burdens at baseline between resilient and demented set an important prerequisite for the subsequent assessment of other additional neuropathologic variables such as neuroinflammatory changes in these brains, ensuring a comparable AD neuropathologic burden at baseline and thus eliminating the need to correct for the potential effects that varying burdens of ADNC may possibly have.

Demographic and epidemiologic features of resilient and demented individuals with ADNC

Dementia incidence and prevalence notably increases with age and recent studies have estimated that the prevalence of dementia is of around 10% in individuals aged 65 years and it increases to up to 50% in individuals aged 85 years and above. Dementia is also higher in female compared with male and it is influenced by racial and ethnic differences. Highest incidence and prevalence of MCI and AD dementia is reported in Black and Hispanic populations (182,183). Disease severity and concomitant neuropsychiatric comorbidity are also significantly more common in Black and Hispanic subpopulations when compared with White individuals (592,593), overall contributing to a more deleterious trajectory of the dementia syndrome in these subpopulations. Several risk factors, including cardiovascular comorbidity and years of education, have been regarded as potentially modifiable contributors to the development and trajectory of dementia in these individuals and they are also viewed as important risk factors in the general population. Emerging studies have proposed that specific genetic risk loci of Hispanic and/or Black subpopulations may differ and possibly contribute to the increased dementia risk observed, although the AD etiology is ultimately considered to be the same across different ethnic and racial groups (594). The present brain cohort included a high proportion of White individuals (representing 96% of the cohort) and significantly underrepresented other ethnic and racial subpopulations including African-American (2%) and Asian (2%) subjects (**Table 3**). While the heavy bias towards an exclusively single-race population ensures consistency and comparability of results and removes potential differences in genetic and mechanistic hallmarks that may be associated with different racial entities, it also limits the generalizability of the obtained results to a subpopulation of White individuals only. The number of years of education have been proposed to represent an important protective factor against dementia development (595) and high educational attainment is viewed as a hallmark of resilience. Estimates have proposed that only sustained exposure to continuous education and cognitive stimulation for >10 years leads to a significant risk reduction in dementia development and to a milder disease trajectory (186). This has been attributed to the formation of higher cognitive reserve in individuals with higher cognitive attainment during lifetime, which promotes a higher ability of those brains to maintain cognitive function in the face of AD and/or other neuropathologic lesions (185,186). In line with this, higher years of education are considered a hallmark of resilient compared with demented individuals. In the present work, average years of education were >10 years for all included groups however, and contrary to previous reports, the mean years of education significantly differed between resilient and demented subjects with resilient showing significantly lower total years of education compared with demented (mean years of education of 14.4 (0.7) years for resilient and mean years of education of 17.4 (0.5) years for demented) (**Table 3**). These findings are interesting and propose that in a highly educated cohort such as the one assessed here (average of >14 years of education across groups), the relationship between cognitive attainment and functional decline may lose significance, maybe due to both demented and resilient equally reaching the top of the cognitive reserve potential where the effects of additional years of education would not substantially influence the cognitive functional compensation anymore, and instead other factors associated with demographic and/or neuropathologic features would become essential in determining the risk to ultimately develop or not develop AD dementia. Importantly, no significant differences in years of education were observed between control and resilient subjects (mean years of education of 17.5 (0.9) years for controls and mean years of education of 14.4 (0.7) years for resilient), indicating that the preservation of cognitive function in resilient brains, where amyloid-β and tau pathologies are significantly higher than in healthy control brains, does not necessitate of a significantly higher amount of cognitive reserve to counteract the detrimental effects of ADNC. On the other hand, it also denotes that an equal number of years of education does not seem to neuropathologically alter the trajectory of an individual and that some individuals will still develop ADNC in the brain while others with similar years of education will not. The positive effects of education on cognition are most evident in the early disease phases and they decrease

with increasing dementia severity, however the role of education attainment on ADNC burden is overall small and has shown great variability within different dementia stages (596). This reinforces that while the positive effects of cognitive attainment may directly alter dementia development and severity, its effect on ADNC is less straightforward and may not be directly mediated through changes in ADNC burdens in these brains. Interestingly, recent studies on bilingualism/ multilingualism have shown that people who habitually use two languages, which serves as a proxy measure of repeated activation of neural network connections, show a delay of dementia symptom onset by up to 5 years compared with monolingual subjects (597), suggesting that not only remote years of education in childhood/adulthood but also sustained cognitive stimulation in later adulthood/ageing may be beneficial to maintain a better brain reserve in an individual (598). Despite evidence of brain structural and functional benefits of multilingualism, the potential association between multilingualism and ADNC burden remains largely unknown (597). Ultimately, it is possible that the higher years of education of the presently studied demented cohort may have positively influenced the onset and trajectory of cognitive decline in these subjects as this group showed an overall average age of disease onset (mean 73.3 years) but a rather mild disease trajectory with a relatively long disease duration of 14.7 years, in which most of the subjects, except for three, had only progressed to a mild stage of AD dementia (mean MMSE 24/30 points). The overall duration of the MCI stage has been previously estimated at around 7 years and that of mild dementia at around 1-2 years, and as such the present population showed a particularly mild and slow overall progression of cognitive decline over a relatively long period of time compared with the general trajectory of AD dementia. It therefore remains possible that the overall high educational and cognitive attainment of the presently studied subjects may have enabled them to maintain a substantial amount of cognitive function over a relatively long period of time, maybe mediated through developing an overall lower burden of ADNC and/or additional mechanisms to better cope with ADNC in the brain.

It is well-known that the association between cognition and amyloid-β plaques or NFT deposits in AD is largely imperfect and that an important amount of cognitive decline is not explained by the presence of positive AD biomarkers and/or post-mortem ADNC alone (99). For the assessment of AD associated brain changes in living individuals, PET-imaging is the only biomarker that allows an estimate of the topographic distribution and the quantitative burden of amyloid-β and tau pathologies in the brain of subjects with AD dementia. In line with neuropathologic assessments obtained from brain autopsies, the association between amyloid-PET and tau-PET with cognition is not always present. In fact, between 12-31% of subjects diagnosed with AD dementia show amyloid-PET negativity (599,600) and around 28-34% of individuals show tau-PET negativity (600,601). The high variability observed in the false negative PET-imaging rates is dependent on the clinical stage at which the PET scans were performed. Of note, currently used tau-PET tracers are particularly insensitive to detect tau deposits at and below Braak IV stages of tau deposition, and as such tau-PET has a limited use for early stages of AD dementia. Interestingly, individuals without cognitive impairment show amyloid-PET positivity in around 10-30% of cases (111), and tau-PET positivity in around 5-10% of cases (112). This suggests that a subset of subjects diagnosed with AD dementia may not show AD biomarker positivity, and that a subset of healthy individuals may show AD biomarker positivity despite absence of symptoms. This is in line with post-mortem assessments of resilient human brains and reinforces the idea that neither amyloid-β nor tau deposits in the brain accurately predict the cognitive status and/or disease severity in an individual. The presently studied brains showed amyloid-β and tau pathologies deposited in a similar distribution and in a comparable burden in the brains of demented and resilient individuals, not allowing to accurately distinguish between these two groups when using amyloid-β and tau deposits as the only neuropathologic measure (**Figure 2**). In addition, the severity of cognitive dysfunction assessed with MMSE, CDR-global, CDR-SoB, CDR-SoB subscores (including orientation, executive function, community affairs, home and hobbies, and personal care), and WAIS-R score did not show significant association with

amyloid-β plaque burden and/or with AT8+ neuropil threads in these subjects (**see data in the results section**). This suggests that the presence of amyloid-β and tau deposits in the brain does not invariably impact cognitive function, and that the detrimental cognitive effects present in the demented cohort may rather derive from other neuropathologic changes distinct from ADNC.

Expansion microscopy for the study of synapses in human AD brains

Synapse loss is viewed as the closest and most reliable neuropathologic signature of cognitive decline in dementia of various etiologies including AD and, in contrast to amyloid-β and tau pathologies, synapse loss shows a strong association with the onset and progression of cognitive dysfunction (255). Moreover, synapses are lost before neurons become dysfunctional and die, and synaptic markers may serve as an earlier and more reliable measure of incipient cognitive change and subsequent dementia conversion and progression. There are around 10'000 synapses per neuron (602) and a total amount of around 60 trillion synapses in the adult human brain (603). Importantly, synaptic transmission is the major energy consuming process in the adult human brain, accounting for an estimated 43% of the total energy demands of the grey matter (604). Synapses are closely associated with glial cells and they form a tripartite functional unit together with astrocytic end-feet (605), or a tetrapartite functional unit when microglia are added to this intricate association (454). Synapses are also closely associated with oligodendrocytes which are predominantly found at the postsynapse (529). This places synaptic elements in a particularly central position when it comes to understanding early structural and functional/cognitive changes associated with AD, but it also challenges the study of this subcellular compartment in view of the high abundance of densely packed synaptic elements and the intimate crosstalks between synapses and glial cells in the brain. Synaptic sizes are in the nanoscale range and this poses a limiting factor for their adequate individual and global assessment, which is reinforced by major challenges in the evaluation of synapse densities in past histopathological studies (275,276). To overcome the important limitations set by the small size of synapses and by the optical resolution limits of conventional imaging techniques, in the present study, synapses were assessed with the novel technique of ExM, which allows overcoming the optical limitations of conventional microscopes in visualizing synaptic elements by physically magnifying the size of the tissue and the synapses contained within it, increasing nanoscale structures to the micrometre range (245,246,555). With the use of a slightly modified ExM protocol (245,249,560) an average expansion factor of 4.6x was obtained which enabled an effective resolution of 25-30 nm, optimal for the assessment of synapses and other structures such as oligomers (**Figure 6**). This also enabled an unprecedented in situ spatial assessment of synapses and oligomers with glial cells with the use of conventional confocal microscope imaging. Recent studies have suggested that ExM with postexpansion antibody labelling benefits from a `decrowding' phenomenon, in which the physical expansion process exposes additional epitope binding sites that can be better and more effectively targeted by conventional antibodies (249). This added benefit of ExM may allow a more accurate estimate of the true numbers of small nanoscale structures in the human brain such as synapses and oligomers. In addition, ExM protocol involves a partial tissue clearing in the homogenization step, in which elements other than proteins that are covalently bound to the gel matrix are removed through a heat-detergent treatment (555). This enables an improved resolution of small structures, and a better visualization of single synaptic or oligomeric structures, when compared with non-cleared tissue imaged with high-resolution microscopes. Several protocol amendments of the basic ExM protocol have been developed, among which one of the most interesting ones has been the possibility of re-expanding the readily expanded tissue with the use of an iterative ExM (iExM) protocol to achieve an expansion factor of 16-22x after one round, and 53x after two rounds of re-expansion (254). Although this approach seems ideally suited to study small structures such as synapses, and it has been shown to enable the visualization of receptors within the synaptic cleft at high resolution (606), the significantly higher expansion factor achieved by iExM causes an important distortion of the epitopes that makes them undetectable by

conventional antibodies, making the use of nanoantibodies necessary, which may substantially limit the possible targets that can be assessed and visualized. In the present brain cohort, the conventional ExM protocol was used together with postexpansion antibody labelling in order to benefit from a moderate expansion factor (4-5x) sufficient to visualize synaptic elements, a concomitant tissue clearing, and a decrowding of structures at the nanoscale. Conventional ExM has been previously applied to various human tissue specimens and it has been validated for its isotropic expansion in the 3-dimensions, and its lack of significant distortion of target elements which is estimated at the range of at most 1-2 nm (248,606,607). The rapidness of image acquisition and 3-D reconstruction of ExM tissue volumes using optical microscopes also provides more quantitative data compared with alternative high-resolution imaging methods such as EM (608).

The conventional ExM protocol was used with minor modifications (**see methods section**) and a validation of the ExM technique was performed. The validation showed that the density of presynapses and postsynapses and the percentage of colocalized mature synapses was comparable between expanded and non-expanded tissue albeit by a magnitude of ~10x higher in the expanded compared with the non-expanded samples (which may be due to the thicker sectioning of tissue for ExM, the decrowding phenomenon, and the increased resolution achieved by the tissue clearing process). The colocalization between synapses and glial cells and the proportion of internalized elements were comparable between the expanded and the non-expanded tissue of the same case (**Figure 7 and Figure 8**). Moreover, double immunolabeling of glial cells with different epitope targets showed an overlap of labelling signal, indicating specific binding and absence of evident glial cell distortion in the expansion process (**Figure 8)**. Co-staining of lysososmal marker LAMP2 with glial cells showed colocalization of LAMP2 with synapses inside the glial cell body supporting a biological underpinning rather than an artefactual effect in the finding of engulfed synaptic elements inside glial cells (**Figure 9**). In line with previous studies, the conventional ExM protocol used here allows an isotropic expansion of tissue specimens introducing at most minimal distortions that do not significantly alter the nanoscale arrangements of synapses and/or the spatial association of synapses with glial cells and other elements.

Synapse densities in early-stage AD brains

Previous studies have suggested that synapse loss occurs closely associated with the early stages of dementia and that it increases in parallel with increasing dementia severity (255). Estimates of synapse densities in the brains of healthy elderly and demented subjects vary widely and no study has so far performed a systematic and large-scale histopathologic assessment of synapse densities across brain regions in a single brain. Moreover, the use of different methods for synapse quantification (e.g., EM, superresolution microscopy, conventional microscopy with high magnification objectives) further limits the estimation of the values and ranges of normal vs. altered synapse densities in the human brain. Among some of the most recent and methodologically robust studies, synapse densities in the temporal human cortex have been estimated at around $1x10^9/mm^3$ (609) with ranges between $5x10^8/mm^3$ to $1.3x10^9/mm^3$ indicating that the variability of synapse densities obtained within one same study may be of around 3x. When considering synapse densities published by other groups in human neocortex, synapse densities have been estimated at $7.3x10e^8/mm^3$ (275) and $1.4x10e^8/mm^3$ (276) among others, increasing the overall variability of published synapse densities to up to 16x. In the present work, synapse densities were assessed with the use of ExM and confocal imaging in layer II of the visual cortex (V1 and V2). In the entorhinal cortex, the cortical layer II represents the most vulnerable layer to early neuronal loss in AD (19,610), which could also be a site of early vulnerability in other neocortical structures including the visual cortex, although this has not been systematically explored. Layer II was chosen based on its close association with cognitively relevant higher order functions including complex visual information processing, and due to its close anatomical and functional association with other cortical

brain regions (e.g., temporal lobe) through connections provided by the ILF, which is a WM tract that shows early vulnerability in AD. Synapses were labelled using synapsin1, a protein that is ubiquitously present on the surface of pre-synaptic vesicles (611), and PSD95 a protein that is found in the postsynaptic density of excitatory neurons and is involved in regulating the coordinated interaction between synaptic proteins (612). The use of this excitatory synapse combination allowed to visualize 80-90% of total synapses of the human brain (231,232). Inhibitory synapses have recently shown similar vulnerability to early dysfunction and loss in AD brains as excitatory synapses, and although this evidence derives from studies limited to transenthorinal/enthorinal regions (264), it remains possible that selective vulnerability of excitatory and inhibitory synapses is present in other brain regions, including the visual cortex, as well. Interestingly, despite previous evidence of an early loss of both, excitatory and inhibitory synapses in demented brains at post-mortem using the markers PSD95 (excitatory) and gephryn (inhibitory), there is a reported excitatory-inhibitory imbalance in AD with an overall increase in electrophysiological excitatory-inhibitory ratio that is suggested to contribute to increased activation of default mode networks which are directly associated with reduced performance in cognitive tasks (274). This suggests that despite a presumably equal vulnerability and quantitative change in excitatory and inhibitory synapse loss in demented brains, the functionality of synapses may be differentially affected in these subjects. Interestingly, glial cells have been involved in the excitatory-inhibitory synapse imbalance, in that microglial cells have been shown to selectively engulf excitatory (but so far no inhibitory) synapses in AD mouse models, and in that astrocytes have been found to produce and secrete the inhibitory neurotransmitter GABA whose levels are altered in early AD (258). In the present work, excitatory synapses were assessed with the combined use of synapsin1-PSD95 which enabled to evaluate a substantial proportion of the total synapse population (80-90%) of the visual cortex and to study subtle differences in synapse densities in the early disease stages. Moreover, excitatory synapse assessment also allowed a better understanding of the role of microglia and astrocytes on early synapse elimination, given previous evidence of an early interaction between excitatory synapses and (micro-)glia in animal models and in two human AD studies (258,327,430). The results of the quantitative synapse assessments in the studied brains showed that, in line with previous histopathologic and biomarker evidence, demented brains had a significant loss of synapses in the early dementia phases, and that synapse loss preceded NFT development in the visual cortex of these subjects (**Figure 18**). Importantly, after correcting for the absolute synapse densities taking into account the tissue expansion factor in 3-D by multiplying the synapse densities obtained from expanded tissue by a factor of ~100 (= times the obtained linear expansion factor^3 or x 4.6^3), the synapse densities obtained in healthy controls showed an average density of $5.4x10^9$ synapses/mm^3 which is largely consistent with the ranges of previously published work (232,270,613,614), although trending towards the upper limits of previously estimated synapse densities in human neocortex. The overall slightly higher synapse density in the order of magnitude of around 5x when compared with synapse densities obtained using EM (609) is likely due to the increased accessibility of antibodies to the post-expanded `decrowded' brain sections, and may also be due to an enhanced resolution of individual synapses obtained in the tissue clearing process of ExM. Importantly, the overall % of colocalized synapses of around 65% and the overall burden of synapse density loss of around 30-40% in the demented subjects is in line with previous studies comparing demented and healthy control brains at post-mortem (615) and with recent biomarker evidence of synapse marker reductions in CSF of subjects in the early dementia stages (89,297). Of note, a minimum of 6 ROIs were sampled in each brain to account for interindividual variability and to control for the possibility of increased synapse loss in the vicinity of amyloid-β plaques in these brains (334). Interestingly, when synapse densities were assessed in a subset of PART subjects (3 resilient and 5 demented) who showed no amyloid-β plaque deposits in the visual cortex, the results were not different in the average density of synapses when compared with amyloid-β plaque containing brains. This reinforces the idea that amyloid-β plaques and tau deposits are not the primary cause of the

synapse loss leading to dementia development in AD, and that synapse densities may be a robust and closer predictor of cognitive change in an individual.

Neuroinflammatory changes in early-stage AD brains

Neuroinflammatory changes are common in the brains of demented individuals with AD (616) and evidence from previous studies has shown that pro-inflammatory glial cell changes are higher in demented but remain low in resilient brains despite both harbouring comparable burdens of amyloid-β and tau pathologies (57,58). This suggests that neuroinflammatory changes in AD may represent an additional neuropathologic signature of demented brains with potential neurobiological significance, rather than a reactive or secondary response to the presence of AD neuropathology. Alternatively, the possibility exists that the important burden of cellular damage accompanying the neurodegenerative process of AD could be leading to this neuroinflammatory response. Several studies have shown that the burden of inflammatory glia and the number of synapses are closely associated, and recent evidence has found that microglia and astrocytes engulf synapses in animal models of AD and in *in vitro* assays (422,425,426,482,617), overall proposing that neuroinflammatory changes may be an independent phenomenon with neurobiological significance in driving the early synapse loss of AD. This is in line with the results obtained in the present work, where pro-inflammatory glial cell markers showed an association with cellular damage, synapse loss, and memory scores (**Figures 12** and **Figure 13**), and glial cells in demented brains showed an increase in engulfed synaptic elements inside their cellular boundaries (**Figure 19**).

Microglia and astrocytes are the two principal glial cell subtypes of the brain and they show close interactions with amyloid-β and tau pathologies (267). A series of genetic signatures and morphologic hallmarks of astrocytes and microglia allow to distinguish different glial cell subtypes, both under physiologic and pathologic conditions. While a series of antigenic markers, such as CD68, HLA-DR, and GFAP, are associated with an activated pro-inflammatory phenotype of glia, some makers, such as TMEM119 and P2RY12, have been linked to a homeostatic or surveying subtype of microglia. In addition, recent studies have proposed that the acquisition of a particular morphologic phenotype of glia is more commonly associated with a particular function of that cell (examples of morphologic microglial subtypes are shown in **Figure 1**). Interestingly, the morphologic hallmarks seem to temporally precede the respective antigenic expression profile of a particular glial cell state, and to confer them with different neurobiological behaviours ahead of the respective antigenic marker expression (507). However, with the emergence of large datasets using whole-genome transcriptomic and proteomic analyses, the phenotypic characterization of glial cells has been recently challenged (618,619). In fact, the categorization of glia into `pro-inflammatory' (termed M1 phenotype or disease associated microglia `DAM' for microglia and A1 phenotype for astrocytes, respectively) and `anti-inflammatory' or `homeostatic' (termed M2 phenotype for microglia and A2 phenotype for astrocytes, respectively) with the use of classical phenotypic markers has been claimed insufficient to understand the true pathophysiological significance of glia, and distinct glial cell subtypes may co-exist within these broadly defined phenotypes. Although the rapid change in phenotypic features of glia occurs within minutes and may provide a more accurate reflection of the functional state of a glial cell in a particular moment (438), this may also reflect a response to acute changes in the brain microenvironment and hence hinder the evaluation of chronic changes occurring in these brains. The phenotypic and morphologic glial cell signatures that are currently used to characterize glial cells may be overall poor and insufficient to understand the biological significance of glial cell subtypes. In the present brain cohort, a combined phenotypic and morphologic approach was used. Glial cells were primarily characterized from an antigenic point of view, and morphologic characteristics were added to identify a microglial subtype characterized by a pro-inflammatory and pro-phagocytic behaviour, also called ameboid-shaped microglia (620,621). The analyses of engulfed synapses by GFAP+ astrocytes and IBA1+ ameboid-shaped microglia

showed that demented brains contained significantly higher amounts of synaptic elements inside glial cells compared with resilient and controls (**Figure 19**). Interestingly, preliminary analyses unrestricted to microglial cell morphology including ramified and ameboid-shaped IBA1+ microglia combined did not show significant differences in glial-mediated synapse engulfment by demented and resilient brains, however this interaction reached significance when ameboid-shaped IBA1+ microglia were assessed alone. This reinforces the idea that despite similar phenotypic and morphologic glial hallmarks, glial cells may display different neurobiological behaviours including their propensity to engulf synapses in demented compared with resilient brains, and that additional molecular signatures, that are currently poorly defined, may likely account for this variability observed in the glial cell responses to synapse elimination. As recently suggested (469), disentangling the glial cell signatures that may have pathobiological relevance may require a more detailed molecular and functional characterization of these cells, and this could be key to better understanding their functional and dysfunctional effects in a demented AD brain.

Total glial cell changes in early-stage AD brains

Previous studies have suggested that the total amount of glial cells does not change in a healthy compared with a demented AD brain (569), however this does not preclude from the known temporospatial rearrangement of glial cells, local clustering of glia, acquisition of a dystrophic appearance, and selective increase in a subset of inflammatory glial markers observed in demented AD brains (61,622). In line with this, the quantitative analyses of total amount of microglia measured with IBA1, total amount of astrocytes measured with ALDH1L1, and total amount of oligodendrocytes assessed with Olig2 showed no significant differences in the temporal and/or visual cortex or WM of demented, resilient, or control brains (**Figure 11**). In addition, the average brain weights and cortical thicknesses of temporal and visual cortices of these brains showed no significant differences across groups (**Figure 5**), indicating that in the early AD dementia stages there is a relative preservation of macroscopic brain structure despite readily present functional cognitive changes, and that overt neuronal loss, which is the main contributor to brain atrophy (623), likely occurs in the more advanced stages of the condition. In contrast to neuronal cells, which are particularly vulnerable to cellular insults in AD, glial cells may be capable of remaining relatively functional and sustaining an important burden of potentially toxic neuropathologic changes including the ones driven by amyloid-β and tau pathologies in AD (624). Glial cell proliferation remains ongoing in an adult human brain in a subset of select locations which are called germinal zones and include the subependymal zone of the lateral ventricles and the dentate gyrus of the hippocampus (625). Proliferative capacity of glial cells is known to be restrained in adulthood and is estimated at 1-2% for astrocytes (626) and 0.5-2% for microglia (627). Despite the presence of machinery for glial cell proliferation in the adult human brain, an excessive glial cell proliferation does not seem to occur as part of the neuropathologic process in AD even in the presence of sustained brain injury and described dysfunction of glial cells in the disease process (628). It cannot be excluded that a dysfunction of a subset of glial cells may go along with their death and be compensated for by a mild increase in glial cell proliferation that is not evident in histopathological assessments unless performed within specific topographic niches and/or with more sensitive measures than immunohistochemical approaches (629). In fact, some studies have pointed to a local proliferation of microglia in the hippocampal zone of AD brains that later accumulate around amyloid-β plaques and retain a marker of proliferation in this location (630). This could suggest that microglia, which may be particularly closely associated with ADNC, may more quickly become dysfunctional and possibly die upon the AD pathogenic process, and therefore show higher regenerative and proliferative propensity in demented AD brains. In contrast, no evidence of an increased compensatory astrocytic or neuronal proliferation has been observed in AD brains (629,630). In line with previous evidence, the glial cell population studied here did not show a significantly higher or lower number of total glia in demented compared with resilient and control

brains (**Figure 11**). Although a marker of cellular proliferation was not used, the similar amount of total glial cell numbers across groups could be interpreted as a lack of substantial turnover of glial cells in demented brains. Interestingly, when using the marker of cellular senescence yH2AX, not only neuronal cells but also a subset of microglia and astrocytes showed positivity for this marker of cellular dysfunction in demented brains (**Figure 15**), which could point to the involvement and functional disruption of a subset of glial cells in the early AD disease phases irrespectively and ahead of amyloid-β and tau deposits. However, this marker is indicative of a dysfunctional state of the cell which is potentially reversible, and it can as such retain positivity for other cellular and glial cell markers such as GFAP and IBA1.

Phenotypic glial cell changes in early-stage AD brains

In contrast to the largely preserved total number of glial cells in demented AD brains, previous studies have observed qualitative changes in phenotypic glial markers in demented brains, and pro-inflammatory glial cell markers are regarded as a robust neuropathologic hallmark of demented brains, which remain much lower in neuropathology-matched resilient brains at advanced disease stages (57,58). In addition to the higher burden of pro-inflammatory markers, also a loss of homeostatic glial markers have been observed in demented AD brains (345,631). Yet, it remains unclear whether these glial cell signatures are a truly primary phenomenon of demented brains that could be associated with structural and functional brain changes, or whether those glial cell changes are just a reactive response to the presence of ADNC and neuronal damage in those brains. To overcome the limitations posed by the study of advanced disease stages of ADNC where amyloid-β, tau, and neurodegenerative changes are ubiquitous and advanced, the present study included a cohort of brains at early stages of ADNC and in the mild phases of dementia. By assessing this informative subset of brains, neuroinflammation could be studied ahead of ADNC development in a particularly relevant phase of the clinical disease where cognitive changes are just emerging and developing and where interventional therapies could be most effective. In line with prior studies, the results showed that demented brains had significantly higher pro-inflammatory microglial and astrocytic markers and lower homeostatic microglial numbers (**Figures 12-14, Figure 16,** and **Figure 17**). These changes were observed in the temporal pole proposing that despite equal burdens of amyloid-β and tau pathologies in this brain region glial cells already display a primary dysfunction that occurs independently of these two neuropathologic hallmarks, and that this phenotypic glial cell hallmark may be closely associated with the presence or absence of dementia in an individual. Interestingly, similar changes in astrocytic and microglial phenotypic changes were observed in the visual cortex of demented brains, further suggesting that the glial cell changes in demented individuals at Braak III-IV stages occur not only in the presence of amyloid-β plaques and NFTs but also ahead of NFT deposition. Importantly, a subset of cases who showed no amyloid-β plaque deposits in neither of the two neocortical brain regions, a neuropathologic feature termed PART, were also evaluated and, the analyses of glial cell changes in the subset of PART brains did not differ from the ones observed in amyloid-β plaque containing brains. This suggests that, similarly to the lack of effect observed for NFT deposits, the presence or absence of amyloid-β plaques seems to have minimal effect on the early glial cell changes observed in demented brains, which may possibly derive from an intrinsic and primary dysfunction of these glial cells instead. Alternatively, the relatively low number of PART cases included in the present study could account for the lack of difference observed. Although these findings are in line with previous evidence of altered glial cell responses in demented AD brains at advanced disease stages (632), they expand on these findings and propose that glial phenotypic changes are also present in the earlier disease phases, and importantly, ahead of amyloid-β plaque and/or NFT deposition. Glial changes may hence be a key phenomenon of demented AD brains that occur ahead of AD neuropathology development, and they may possibly contribute to the structural and functional changes observed in these brains, potentially facilitating the later development of fibrillar amyloid-β and/or tau conversion, deposition,

and spread. Alternatively, the observed glial cell responses could also be reactive to the presence of other proteins in these brains that are not fibrillar in their structure, such as soluble tau oligomers that may be present in the brain prior to overt NFT pathology; this has been recently suggested by studies indicating that tau seeds are measurable in brain regions that lie up to one Braak stage ahead of NFT formation (402). It is also possible that the glial cell changes of demented brains represent a response to a sustained and relevant burden of cellular damage in these brains, which is likely occurring from the early disease stages and ahead of evident brain atrophy, as shown by the presence of higher burdens of early cellular damage (γH2AX+ cells) in demented brains (**Figure 15**). Ultimately, the absence of aberrant glial cell responses in resilient brains may be contributing to the maintenance of a homeostatic regulation of neuroinflammation and account for the preservation of neuronal integrity and brain function in these individuals. Importantly, to rule out the possibility of artefactual inflammatory glial changes due to varying post-mortem intervals associated with different metabolic and/or homeostatic alterations of glia during the perimortem period, associations between PMI and glial cell phenotypes were conducted but no significant associations were found (**see data in the results section**). This makes the potential contribution of PMI to the observed glial cell changes rather unlikely.

Markers of incipient cellular damage in early-stage AD brains

The early clinical (MCI and mild dementia) and neuropathological AD stages (intermediate ADNC/Braak III-IV stages) of the subjects included in this work allowed the study of brains that were relatively free of altered brain structure, advanced burden of neuropathologies, or overt cortical atrophy, despite readily present functional loss in the demented subjects. To evaluate an early neuropathologic indicator of cellular dysfunction that could serve as a proxy measure of the functional loss of demented individuals, the antibody γH2AX was used. γH2AX labels the hyperphosphorylated histone variant H2A in the cellular nucleus which gets hyperphosphorylated at Ser139 upon presence of double-stranded DNA breakages (570). The mechanism of cellular damage associated with γH2AX is closely related to pathways of cellular apoptosis and, notably, other neuronal cell injury mechanisms, including necroptosis, autophagy, and pyroptosis, have been described in AD brains, and these were not assessed with the use of γH2AX (633). Importantly, γH2AX is rapidly induced upon cellular injury, and it is a reversible marker of cellular senescence/damage. Upon removal of the pathogenic stimulus, a previously γH2AX+ cell can revert to a γH2AX- cell and continue to function normally (634). The reversibility of γH2AX positivity reinforces its potential to immunohistochemically detect brain regions with incipient functional impairment ahead of evident anatomic disruption of tissue structure. Notably, the direct association of this marker with DNA damage allows to infer on one potential early mechanism of cellular damage in these brains, associated with specific gene expression profiles, chromatin stability, and cellular dysfunction (570). Previous studies in AD have identified an early and increased expression of γH2AX in neurons (570) and astrocytes (635), while the expression of γH2AX in dystrophic microglia has been detected in some reports but has not been widely assessed (628). In the present study, brain weights and cortical thicknesses were similar across the three groups, suggesting that macrostructural brain changes were not yet present in the early disease stages (**Figure 5**). γH2AX was used to assess if in the absence of evident neuronal loss in these brains, incipient changes of the neurodegenerative process would already be occurring and be reflected by the presence of early cellular damage relevant enough to disrupt cellular function without yet causing overt cellular death. A significantly higher number of γH2AX-positive cells was detected in the temporal pole and visual cortex of demented brains, which was much lower in resilient and was almost absent in controls. Interestingly, there was a more marked increase in γH2AX+ cells in the visual compared with the temporal cortex of the same demented brains (**Figure 15**), suggesting that cellular senescence occurs independently of NFT presence, and that possibly, the readily observed aberrant glial responses could be the ones contributing to the early cellular damage and brain dysfunction present in these

brains. In fact, the presence of amyloid-β and/or tau deposits in these brains insufficiently explained cognitive dysfunction in these individuals, and it also showed no association with cellular damage, suggested by higher γH2AX signal in brain regions without AD-typical deposits (visual cortex) compared with areas with typical ADNC (temporal pole). This reinforces the idea that amyloid-β and tau deposits are likely non-toxic and that NFTs may even be protective and isolate toxic tau species preventing them from causing further damage to the brain (150). Likewise, amyloid-β aggregates may be the protective response to cellular toxicity caused by amyloid-β oligomers and protofibrils (636). In fact, the burden of γH2AX+ cells showed significant association with synapse density, inflammatory glial cell markers, including GFAP and CD68, and cognitive scores, including MMSE, CDR-global, CDR-SoB, and WAIS scores, in the visual cortex, but the association between γH2AX and amyloid-β plaques and/or AT8+ neuropil threads was not significant (**see data in the results section**). This suggests that early cellular damage involving DNA disruption is happening in demented brains ahead of overt neuronal loss and brain atrophy, and that it closely associates with incipient synaptic and cognitive dysfunction in the early dementia stages, irrespectively of the presence or absence of amyloid-β and tau deposits. This marker was also found in similar amounts in the subset of PART cases, indicating that the contribution of amyloid-β plaques to cellular damage may be minimal. ɣH2AX can label every cellular subtype that has DNA damage to its nucleus and, as such, it does not allow to conclude on the specific cellular subtype when assessed alone. Thus, a co-labelling of ɣH2AX with GFAP, IBA1, or hematoxylin-eosin was performed to phenotypically and morphologically distinguish glial subtypes and neurons labelled with this marker (**Figure 15**). While the majority of cells that were positive for ɣH2AX+ were neuronal, also a subset of glial cells showed positive immunolabelling for this marker. This suggests that, although the early tissue injury responses in AD preferentially and primarily target neurons, also a subpopulation of glial cells suffers from early cellular damage in these brains, and a better characterization of this glial cell subpopulation could be particularly relevant to understanding the changes occurring in the early AD disease process. Given that demented brains showed a lower expression of homeostatic glial markers compared with resilient brains, one possibility may be that homeostatic glial cells could be particularly vulnerable to the early AD disease process and become dysfunctional and thus γH2AX-positive in the early AD stages leading to subsequent loss of brain function. While the possibility of γH2AX-positive nuclei observed inside glial cells could alternatively be interpreted as engulfed nuclei of other cells such as neurons, γH2AX is a marker of vulnerability that largely disappears in dead cells, and as such this possibility seems less likely. Importantly, and to rule out the possibility of perimortem agonal state causing differences in γH2AX positivity, associations between PMI and γH2AX were evaluated and no significant associations were found (**see data in the results section**), making it unlikely that premortem agonal state may have influenced the presence and burden of early cellular damage in these brains.

Cortical and subcortical damage in AD brains

The clinical and neuropathologic process of AD is reflective of a primary dysfunction of cerebral cortex, with hippocampal formation being altered first and temporoparietal neocortical structures becoming affected later in the disease course. The disruption of these anatomical structures also shows close functional association with the clinical syndrome characterizing AD dementia. Recent evidence has found that the subcortical WM of AD brains shows early structural changes, and that the early disease process may also affect subcortical tracts and connected pathways in the early dementia phases (159). Yet, the clinical syndrome characterizing AD is thought to originate from cortical damage, which is reflected by the presence of typical signs and symptoms related to specific cortical brain structures such as episodic memory dysfunction (hippocampus), aphasia (temporal cortex), and agnosia/apraxia (parietal cortex) (164). In some instances, cortical dysfunction in AD typical locations leads to the development of specific clinical syndromes such as the Gerstman tetrad (637,638). In contrast, subcortical cognitive dysfunction is more typically encountered in disease

processes affecting myelin, such as infectious diseases (HIV encephalopathy), autoimmune disorders (multiple sclerosis), or vascular damage (vascular dementia) (639). The characteristic clinical phenotype of subcortical damage is reflected by an overall slowing of mental processing, apathy, and other concomitant neuropsychiatric features. With the use of cognitive testing scales, the cortical vs subcortical dysfunction profile can be accurately distinguished. While late-stage AD dementia can clinically show combined clinical syndromes with high phenotypic variability which may not resemble the initial predominant symptoms anymore, the early disease stages are more succinct and restrained to a better-defined cognitive dysfunction profile, which also best allows to infer on the most likely origin and etiology of the underlying dementia syndrome. The present brain cohort was assessed clinically at antemortem, and the dysfunction profile was recorded as `AD etiology' suggesting the presence of typical clinical signs of hippocampal and/or parietotemporal dysfunction and largely absent atypical features of alternative dementia syndromes. Importantly, macrovascular injury was an exclusion criterion for the selection of subjects, although vascular comorbidity in the form of post-mortem histopathologic evidence of microvascular lesions were permitted, and they showed an overall higher burden of vascular injury in the demented compared with resilient and control brains.

Vascular damage in AD brains

Vascular pathology is very commonly observed in the brains of healthy elderly and in demented subjects at post-mortem, and is overall estimated at around 80% (133–135). The presence of vascular pathology in demented subjects can be detrimental to cognitive function, in particular in the early disease stages where AD neuropathology is not yet full-blown and may not account for a significant impact on cortical damage and cognitive dysfunction yet (153). Due to anatomical characteristics of blood vessels with increased tortuosity and lower tissue oxygen tension in WM, subcortical regions are particularly vulnerable to the effects of vascular disease (156,157). WM vascular lesions can be caused by primary cerebrovascular disease (hypoperfusion) and/or be secondary to AD neuropathology (retrograde degeneration) (160) potentially linking the cortical ADNC with the subcortical WM abnormalities. The present cohort was assessed for a composite vascular score composed of five microvascular subscores obtained from evaluations of tissue blocks derived from neocortex, WM, and basal ganglia. This enabled an informative and reliable measure of vascular damage in these brains on an individual basis, although the pooled score did not allow to infer on subregional differences that may have been relevant to the earliest vascular changes in these brains. The brains of demented subjects showed a significantly higher burden of microvascular lesions compared with resilient and healthy controls (**Table 3**), which is in line with previous reports and suggests that AD neuropathology, vascular lesion burden, and cognitive dysfunction are intimately linked. Moreover, it suggests that resilience may be partly attributed to fewer comorbid neuropathologic abnormalities including microvascular lesions in the brain, as previously proposed (640). In fact, recent large scale studies of resilient and demented brains have shown that lower microvascular burden is a hallmark of resilient brains, and that the effects of one additional comorbid neuropathology in demented AD brains has an exponential rather than additive effect on cognitive dysfunction and severity (640). Although the brains studied here were well matched for neuropathologic comorbidities including amyloid-β and tau deposits, and the absence of TDP43 and alpha-synuclein in the cortices was a prerequisite for case inclusion, the composite vascular score burden could not be matched across groups. The overall significantly higher burden of microvascular damage in demented brains must thus be considered when interpreting some of the results obtained here. While the primary vs secondary role of vascular disease and the interaction with glial cell phenotypic changes remains largely unknown, the clinical syndrome characterizing AD favours a cortical dysfunction profile, which would expectedly derive from lesions to the cortex rather than the subcortical WM. Microvascular lesions are predominantly found in the subcortical WM but they can also present in the cortex in the form of lacunar infarcts (641). Importantly, composite cortical

and subcortical vascular scores showed a significant association with the cellular damage marker γH2AX in the cortex and with some of the memory scores, but vascular scores did not reach significance with synapse densities and with two of the main cognitive scores, including MMSE and WAIS-R (**see data in the results section**). This suggests that vascular damage may have some pathobiological significance in AD, but that its effect alone may not be sufficient to explain the memory decline in an individual. Microvascular damage could alternatively mediate and enhance the toxic effects of glia, and/or amyloid-β and tau pathologies, but remain clinically less expressive when assessed in isolation, at least in the early disease stages studied here. The overall rather neutral effect of vascular disease on cognitive function is further supported by its very frequent occurrence of around 85% in the brains of healthy elderly without dementia. While WM abnormalities were an early description that date back to the first observational seminal paper of Alois Alzheimer of 1906, the understanding of the mechanisms linking WM changes, AD neuropathology and brain damage remain largely unknown. Vascular damage, glial cell changes, and associated neuropathological effects remain a particularly complex system to study at post-mortem and future studies aimed at creating models and/or improving imaging techniques that would allow to evaluate earliest vascular dysfunctional signatures and their temporal association with AD neuropathology, brain injury, and cognition in living individuals, would be highly informative. Although a more in-depth assessment of vascular co-pathology markers and/or endothelial cell phenotypes would have been interesting to address the potential derangement of vascular system in the early demented brains studied here, this assessment remained out of the scope of the present work and could be an important future avenue.

Glial cell changes in the subcortical WM of early-stage AD brains

Early vascular damage in demented AD brains may facilitate the crosstalk between the otherwise well isolated brain microenvironment and peripheral signals, facilitating the detrimental influx and effects of e.g., peripheral inflammatory or infectious responses on brain tissue injury. In fact, AD brains show an increase in blood-brain barrier leakage (642), which has been associated with infiltration of neurotoxic peripheral pathogens, immune cells, and toxic substances that would not normally be present in brain tissue and could negatively impact the brain microenvironment contributing to initiating and perpetuating neurodegenerative pathways in AD (642). To evaluate the possibility that early glial changes may occur in WM of demented AD brains as a possible first response to peripheral stimuli on WM, where cerebral vessels are known to be particularly vulnerable and leaky, phenotypic glial cell markers were assessed in the juxtacortical WM of the studied brains. The results showed that WM glial cells of demented brains displayed a significant increase in activated pro-inflammatory microglia (CD68, HLA-DR) accompanied by a loss of homeostatic microglia (TMEM119, P2RY12) compared with resilient and controls, and that these WM changes were not only present in brain regions with cortical NFTs (temporal pole), but also in areas without detectable NFT burden (occipital cortex) in the overlying cortices (**Figure 16** and **Figure 17**). This suggests that primary dysfunctional glial cell changes in the WM are present early and ahead of NFT deposition in the overlying brain cortex, and that these changes may be relevant to the incipient dementia stages. While the glial cell changes in WM showed significant associations with burden of overlying amyloid-β deposits in temporal and occipital cortices and with NFT deposits in temporal pole, the association of subcortical WM glial cell changes and overlying early cellular damage marker γH2AX were even higher in magnitude, indicating that subcortical glial cell changes may, to some extent, independently affect cellular and brain function in AD (**see data in the results section**). Interestingly, some of the subcortical homeostatic glial cell signatures, such as TMEM119, showed higher association with cortical cellular damage than the same homeostatic glial cell marker in the cortex, suggesting that glial cell changes in WM may be an early signature of demented brains that may be contributing to earliest cortical neuropathologic and functional changes in these individuals (**see data in the results section**). The overall lower magnitude of association observed

between homeostatic glial cell signatures in the cortex and γH2AX in the same brain region could reflect a secondary response of those glial cell signatures to an adverse brain microenvironment (e.g., amyloid-β and/or tau deposits) but not be a major contributor to the early cellular damage in these brains. Of note, identical changes in cortical and WM glial cell phenotypes and their correlation with γH2AX were present when analyses were limited to the subset of PART cases, suggesting that the possible effects of amyloid-β pathology on early glial cell responses may be minimal and that the association between glial cell changes and cellular damage may be independent of the presence or absence of amyloid-β deposits. In agreement with previous studies and with previous assessments of these brains, the total number of oligodendrocytes (Olig2) and microglia (IBA1) in WM was similar across groups (**Figure 11**) reinforcing the idea that qualitative rather than quantitative glial cell changes characterize the glial cell signature of demented AD brains. These results propose that a subset of glial cells in the WM could be contributing to vascular damage and/or be the first ones to respond to the detrimental effects of a peripheral influx of signals through diseased vessels in the WM of demented brains, and that they may be involved in the early anatomical and functional disruption of demented brains. Likewise, it remains unknown what potential effect(s) the influx of peripheral elements through damaged vessels in demented brains could have, and whether they could possibly contribute to the primary glial cell dysfunction observed in these brains.

Synapse densities in early-stage AD brains

Synapse loss is the strongest predictor of cognitive decline and dementia severity (255,258,259) and several studies have shown that synapse loss is a robust phenomenon in the brains of AD demented individuals. This has led to the recent idea that AD should be termed a `synaptopathy', rather than a disease characterized by amyloid-β and tau deposits in the brain (13,264,643). Contrary to the wide discrepancies found when evaluating classical amyloid-β and tau lesions in demented brains at post-mortem, synapse loss is to date a universal histopathologic finding present in every demented human brain (643). This suggests that synapse loss may be the best neuropathological signature of AD dementia. In line with this, synapse densities correlate better with cognitive dysfunction than any other neuropathological substrate present in an AD brain (255,644) setting a strong precedent for the turn in the focus of AD research towards understanding processes occurring at and around synapses, rather than phenomena occurring along the spectrum of amyloid-β and/or tau deposition alone. Synapse loss is known to precede neuronal loss, and therefore synapses may already be suffering from neuropathologic effects long time before demented brains display an evident loss of neurons and brain atrophy. The fact that synaptic elements are in the nanoscale range and hence difficult to visualize in the human brain contributes to the relatively late and still widely unexplored field of synapse pathology in dementia, and in fact, initial studies measuring synapse densities in human AD brains even failed to detect differences in synapse densities in demented compared with control brains, which was later attributed to inadequate technical measurements (276). In the present work, synapse densities were assessed in the visual cortex, a brain region with very early ADNC, and a significant loss of presynapses, postsynapses, and colocalized synapses was observed in demented compared with resilient and controls (**Figure 18**). Importantly, resilient and control brains showed largely similar synapse densities, suggesting that a higher `brain reserve' may not be the main cause of the better maintenance of synaptic health in resilient brains. It remains possible that a higher density of synapses was present in resilient brains many years prior to the present histopathologic assessment and that a higher brain reserve may have partly contributed to resilient subjects sustaining cognitive function over time. Importantly, a relevant proportion of around 65% of synapses were properly arranged forming colocalized `mature' synapses across the three groups. This is in line with previous studies that have proposed that at any given time not all but only around 2/3 of synaptic elements are forming active and functional synapses (645). Importantly, the present study shows that the loss of synaptic elements in demented AD brains equally affects single pre- and

postsynapses (whose functional and biological significance remains incompletely understood), as well as the presumably still functional colocalized synapses. These findings are important since they suggest that there is a loss in the burden of all synaptic elements in demented brains, and that there is no accumulation of single synaptic proteins (e.g., presynapses or postsynapses) in demented brains that may suggest a primary dysfunction in synapse elimination by glia, as previously proposed by some groups (646,647). Rather, an excessive loss of all synaptic proteins is likely occurring in these brains. It remains possible that a defective removal and an increased accumulation of synaptic elements by glia would become evident in more advanced disease stages where the chronic effects on glial dysfunction would become manifest, similar to the ones previously described for the dysfunctional processing of amyloid-β proteins by glia at advanced disease stages (648). Importantly, the present study also shows that presynapses are equally affected as postsynapses in the early stages of dementia, and this could be relevant to address potential underlying mechanisms and pathways involved in the disease process which may be distinct for elimination of presynapses and postsynapses. Of note, the synapse densities obtained in the present study were derived from expanded tissue material, and to correct for the tissue expansion factor in 3D, the synapse densities obtained from expanded material need to be multiplied by a factor of ~100 (= times the linear expansion factor^3 or x4.6^3) to be comparable with non-expanded synapse densities. After correcting for the expansion factor, average synapse densities observed here were similar to previously published work (282), albeit by a factor of ~5x higher when compared with the results obtained in previous EM studies (249) which is likely due to the decrowding phenomenon of ExM and to the improved resolution of cleared tissue, enabling a more accurate estimate of the true number of synapses in the human brain.

Synapse elimination by microglia and astrocytes in early-stage AD brains

Excessive elimination of synapses by glia has been suggested to underlie several neurodegenerative diseases including AD (422,649,650) and recent human studies have supported a key role of microglia in the excessive elimination of synapses in AD brains (327,430). These studies were, however, limited to the assessment of presynaptic elements (synaptophysin and synapsin1) and microglial cells only, and they evaluated a cohort of late-stage AD cases. Astrocytes are known to participate in synapse elimination during brain development (425,617) and they are also involved in synapse homeostasis throughout adulthood (651). Astrocytes have also been recently shown to eliminate synapses in adulthood and they have been involved in synapse loss in neurodegenerative conditions (650,651). Mouse models of AD have found evidence of astrocytic phagocytosis of excitatory pre- and postsynapses and plaque-associated reactive astrocytes have shown increased elimination of presynapses, overall proposing that synapse engulfment by astrocytes may be another potential contributor to synapse loss in AD (652). Yet, the potential excessive elimination of synapses by astrocytes in the human brain has so far not been explored. Given that many synapses are in close contact with astrocytes forming a `tripartite system', astrocytes may be the first ones to respond to synaptic changes and, given their privileged anatomic location in close association with synaptic proteins, they could be among the first to engulf and lead to the loss of synapses in demented AD brains (617). Astrocytes are significantly more abundant than microglial cells in the human cerebral cortex, accounting for 20-40% compared with around 10% of total glial cells respectively, and their potential cumulative effect on synapse elimination could be of important magnitude (536,653). Two previous papers showed first-ever evidence of a higher microglial-driven engulfment of pre-synapses in demented AD brains when assessing microglial cells in combination with the presynaptic markers synapsin1 and synaptophysin respectively (327,430). While the functional significance of non-colocalizing `single' presynapses and postsynapses remains unclear, growing evidence suggests that neuronal signal transmission in the CNS requires the presence of `functional synapses' with properly arranged pre- and postsynaptic elements (262). Thus, although the reported increase in engulfed presynaptic elements by microglial cells may be informative to

understand potentially deleterious behaviours of glia in the brains of demented compared with control subjects, the significance of these findings and their structural and functional relevance remains unclear. Importantly, the synapse arrangement into `mature' colocalized synapses is an active process that requires bidirectional signalling of cell-adhesion molecules that enable the presynapse to interact with the postsynapse and form a functional unit (654). Thus, the active process that this synaptic arrangement involves, theoretically eliminates the possibility that the readily engulfed synaptic elements would rearrange and form synaptic contacts by simple apposition of presynapses to postsynapses once inside the respective glial cell. In the present study, engulfment of presynapses, postsynapses, and colocalized synapses inside microglia and astrocytes were assessed separately, and presynaptic marker synapsin1 and postsynaptic excitatory marker PSD95 were evaluated in association with GFAP+ astrocytes and IBA1+ ameboid-shaped microglia (**Figure 19**). In line with previous studies, the results showed that microglia and astrocytes of demented subjects at early disease stages contained significantly higher amounts of synapses inside their cell boundaries compared with resilient and control brains, including the functionally most relevant colocalized synaptic elements. This is in line with previous work (327,430) but it adds novel evidence of an enhanced astrocyte-mediated engulfment of synapses in early AD, and a higher internalization of, not only pre- and postsynapses alone, but also colocalized `mature' synaptic elements. This suggests that early glial changes may be driving the primary loss of synapses in demented brains ahead of NFT deposition, and lead to the excessive elimination of mature and, presumably still functioning, synaptic elements. Interestingly, no significant difference in the proportion or type of engulfed material was observed in the subset of demented and resilient PART cases. This suggests that synapse elimination by glia occurs independently of amyloid-β and NFTs, and ahead of NFT development. Hence, glial cell propensity to eliminate synapses may be a primary dysfunction, and not the response to AD neuropathology in these brains. Alternatively, it remains possible that other non-fibrillar soluble forms of amyloid-β and/or tau (e.g., oligomers) are present in these brains and that they may be driving some of the dysfunctional glial-synapse interactions observed. Of note, the dysfunctional effect of glial cells on synapse loss was not associated with ApoE status in these subjects where glial engulfment of synapses did not differ in ApoE4+ compared with ApoE2+ or ApoE3+ carriers. This is interesting since ApoE4 allele is considered the strongest genetic risk factor for sporadic AD (655,656) and its presence has been associated with increased synapse elimination by glia (485,617). Although ApoE is preferentially expressed in astrocytes, also neurons and microglia express this protein albeit in lower amounts. Recent studies have found an association between apoE4+ astrocytes and synapse loss, however the exact mechanisms linking astrocytes and synapse loss remain to date unknown (617). The presence of ApoE4 in astrocytes has been associated with extensive morphological changes of astrocytes and with early loss of physiologic functions (657), and the detrimental effects of ApoE4+ astrocytes on synapse loss have been proposed to occur directly through dysfunctional synapse pruning, and indirectly through interactions with amyloid-β and tau pathologies in these brains (617). Importantly, internalized synapses were assessed for each GFAP+ glial cell and its surrounding processes individually, but only fully internalized synaptic elements were considered as engulfed synapses to exclude the possibility of including the physiologic contacts between astrocytes and synapses as engulfed elements. Astrocytic fine processes show the closest association with synapses, and they are highly dynamic sensing synapse homeostasis on a continuous basis, and responding to changes in the synapse microenvironment within minutes (653,658). Therefore, the main phagocytic ability of astrocytes may be localized to astrocytic processes. In contrast, microglia are highly motile cells that typically migrate to the respective target for its engulfment and, thus, phagocytosed elements are predominantly observed inside the microglial cell body. To account for interindividual and intraindividual variability in ramification density of astrocytes and in size of microglial cell body, the proportion of engulfed material was corrected for the respective volume of the glial cell. Although the higher number of synaptic elements inside astrocytes and microglia could be interpreted as the result of a primary dysfunction of these glial cells in AD (617,646,647), the present results did not show an overall higher density of

presynapses and postsynapses in demented compared with resilient or control brains, but rather a loss of all synaptic elements, supporting that the primary role of glia in the early disease phases of dementia may involve an active and excessive elimination of all synaptic elements leading to the subsequent loss of synapses.

Oligomeric tau in synapses of early-stage AD brains

Growing evidence suggests that NFTs are likely non-toxic forms of tau that may even play a neuroprotective role by sequestering toxic tau species in the brain. NFTs could therefore reflect a bystander phenomenon to the presence of toxic tau in the brain and have little or no detrimental effect on brain function by themselves (659). In line with this, animal models of AD have shown that selectively turning off tau expression after NFT formation ameliorates neurodegeneration and reverses memory deficits, despite still ongoing NFT formation in these brains. Moreover, NFT-bearing neurons do not show functional impairment in *in vivo* models of AD (389), and ghost tangles which are the ultimate reflection of neuronal cell death of NFT-bearing neurons, are exceedingly rare in the human AD brain representing only around 1% of total NFT population (391) suggesting that the majority of neurons with NFTs do not die. Despite NFTs being composed of toxic tau (150) they are thus likely not directly pathogenic in AD. In line with this, resilient and demented subjects in the present study showed similar burdens of AT8+ NFTs and of AT8+ neuropil threads in the temporal and visual cortices (**Figure 2** and **Figure 3**), suggesting that the presence and/or burden of tau deposits may not be the primary cause of the neuronal and functional derangement in these individuals. Of note, AT8 labels the phospho-epitopes pSer 202, pThr 205, and pSer 208 which are hyperphosphorylated in the early stages of tangle development, and previous studies have proposed that the higher the cumulative burden of hyperphosphorylated tau sites, the higher the toxicity associated with NFTs (387). Thus, it cannot be excluded that more advanced stages of tau hyperphosphorylation may confer those more mature NFTs with toxic properties and potentially lead to significant differences in the total burden of NFTs in resilient and demented brains. In contrast to fibrillar forms of tau, evidence has proposed that soluble oligomeric species of tau are most neurotoxic (150,361,370,660) and recent studies have found that tau oligomers are increased in the synapses of demented but remain low in resilient brains with similar burdens of ADNC (57,272,282). Tau oligomers are small and soluble proteins that are thought to mislocalize to synaptodendritic compartments to cause toxic effects (661). In fact, tau oligomers cause direct synaptic derangement and neuronal death when injected into the brains of AD mouse models (660,662), and they are closer and better predictors of memory decline than NFTs (663). Importantly, tau oligomers form from the early stages of neurodegeneration and they are increased before the formation of NFTs (660). The present study cohort was matched for AT8+ NFT deposits in the temporal cortex and showed absence of NFTs in the visual cortex (**Figure 2**). This enabled the unprecedented possibility to evaluate tau oligomers in a region not yet impacted by NFTs (visual cortex). With the use of tau oligomeric complex 1 (TOC1) antibody, a selective antibody for oligomeric over monomeric and fibrillar tau that binds to a conformation-dependent epitope of oligomeric tau (576), synaptosome fractions were extracted and assessed with western blotting. The results showed that demented brains had a significantly higher burden of TOC1+ oligomers in synapses compared with resilient and controls (**Figure 20**), proposing that tau oligomers could be better predictors of cognitive status than fibrillar tau deposits, and that tau oligomers could be associated with structural and functional changes in the early dementia phases. In line with this, correlation analyses between TOC1 and cellular damage (γH2AX) and cognitive dysfunction (MMSE) were significant, while the association between fibrillar AT8+ tau and structural damage (γH2AX) or memory loss (MMSE) did not reach significance (**see data in the results section**). This reinforces the idea that synaptic oligomeric tau may be a key contributor to the early synaptic and cognitive changes in AD and be a better predictor of structural and functional changes than NFTs. Interestingly, TOC1 burden measured in total brain homogenates did not show significant

differences across groups (**Figure 20**), suggesting that the presence of oligomers in extracellular space may be less relevant to disease status, and that the truly pathogenic significance associated with tau oligomers may be their selective mistargeting to synaptic compartments in demented brains. The mechanisms involved in the mistargeting and accumulation of TOC1 in synapses remain largely unknown, and they could involve an increased local production of toxic tau oligomers through dysfunctional enzymes in synapses, and/or be the result of a pathogenic translocation of tau oligomers to synapses from extracellular space or other intracellular compartments. Both these mechanisms could be facilitated by glial cells through microvesicular transport of oligomeric tau species and/or enzymes involved in tau conformational changes across the brain (664). Uncovering the underlying pathways involved in the translocation and accumulation of tau oligomers in synapses would be key to developing novel targets for early therapeutic interventions. These assessments were beyond the scope of the present work, and they could be a promising avenue for future studies.

Tau hyperphosphorylation and tau truncation in the synapses of early-stage AD brains

To assess other early posttranslational modifications of tau protein that could be relevant to the early development of dementia, tau hyperphosphorylation and tau truncation were evaluated. Tau hyperphosphorylation follows a sequential pattern of phospho-epitopes that progresses along with increasing tau tangle maturity until around 55 hyperphosphorylation sites are reached in advanced AD stages (385,577). Interestingly, tau hyperphosphorylation can occur in normal ageing and under physiological conditions such as hibernation, where phospho-tau shows no apparent association with neuronal damage. Still, some of the hyperphosphorylation sites found in hibernating animals are the same as the ones observed in seed-competent tau fractions isolated from demented AD brains (386,665). Thus, even in the presence of presumably pathogenic tau hyperphosphorylation, the potential toxicity of tau may be determined by other additional factors. Inversely, primarily non-pathogenic phospho-tau could, under certain pathological influences, have toxic effects on surrounding neurons. There is widespread overlap in the phospho-epitopes of tau under physiological and pathological conditions, which hinders the identification of a unique signature(s) of phospho-tau that could be reliably associated with dementia (577). Supported by recent biomarker studies in the CSF and plasma of early demented individuals, significant increases in hyperphosphorylated tau181, tau217, and tau231 have been shown (578,666,667). However, these three hyperphosphorylation sites can also be found in normal ageing, although at lower levels (577). To evaluate the potential accumulation of these newly described phospho-epitopes in synapses and assess their potential association with early synapse loss and cognitive dysfunction, synaptosomes were isolated and evaluated for presence of ptau181, ptau217, and ptau231. The results showed that levels of ptau181 were significantly higher in the synapses of demented compared with resilient brains, but that ptau217 and ptau231 remained unchanged and/or undetectable across groups (**Figure 20**). This is in contrast to recent biomarker studies where these two tau epitopes show significant increases in the early stages of dementia (578). These results suggest that ptau181 may be a relevant and early change of demented brains, that may directly affect synapse health and/or contribute to the detrimental interactions of glial cells with synapses. Importantly, low but not undetectable levels of ptau181 were also present in the synapses of control and resilient subjects, suggesting that synapses may remain functional below a certain threshold of synaptic ptau181 accumulation and that a certain level of ptau181 may even be beneficial for synapse homeostasis. In line with previous studies of ptau181 in CSF (668), demented brains showed a ~1-2x increase in ptau181 compared with controls and a ~2-3x increase in ptau181 levels compared with resilient brains. While the absolute amount of change in ptau181 is of relatively modest magnitude, it is likely that this phospho-epitope may interact with other pathogenic tau species or other elements in these brains and contribute to synapse and functional changes. Interestingly, there was no detectable ptau217 in the studied brains, despite previous evidence proposing an even higher relative increase

of ptau217 by around 6x in CSF of demented compared with healthy controls (104). Almost undetectable signal was also observed for ptau231 antibody. It is interesting to note that none of these two phospho-epitopes were elevated in any of the studied groups despite them representing phosphorylation sites that can be present in healthy brains (577). It is possible that a specific mistargeting of these two phospho-epitopes to synapses would be a truly synaptotoxic phenomenon unique to demented brains, and that this effect may occur in the later stages of the neuropathologic process once AD neuropathology and/or glial cell changes are more advanced. The absence of an increase in hyperphosphorylation of tau217 and tau231 in demented brains could therefore suggest that these epitopes may be downstream of other tau post-translational modifications and may be contributing to disease in the later stages of dementia. Alternatively, these two phospho-epitopes may already be present in demented brains but accumulate in other compartments different than synapses (e.g., in neuronal cell bodies or glial cells) that were not evaluated in the present study. In line with this, the discrepancies observed between the absence of synaptosome-enriched ptau217 and ptau231 fractions in this study and the previously suggested increase in ptau217 and ptau231 in CSF of early-stage demented individuals (306,668) could be due to a different anatomical location of these phospho-epitopes other than the synapse, or be due to technical artifacts given that, at least for ptau217, this antibody has just been commercialized and may not be of high specificity/sensitivity for its detection in brain-derived homogenates yet. Of note, recent evaluation of concordance of premortem CSF AD biomarkers and post-mortem brain findings in the same case have shown 100% accuracy in confirming CSF+ AD markers at autopsy, suggesting that AD biomarker positivity in CSF virtually always correlates with brain histopathologic findings (669). Interestingly, the main kinase involved in the hyperphosphorylation of tau181, tau217, and tau231 is presumably the same and is mediated by GSK3 (670,671), and the present results therefore suggest that alterations in GSK3 alone may not be the main reason for the different hyperphosphorylation seen in these three epitopes. Another important posttranslational modification of tau involves tau truncation which depends on the activity of proteases and caspases that generate tau fragments cleaved at the N- or C-terminal domain of tau (392). Tau truncation can occur under physiological conditions in the brains of young and elderly individuals, but C-terminal cleaved tau species are predominantly increased in demented AD brains and *in vitro* studies have shown that C-terminal cleaved tau has toxic properties contributing to mitochondrial dysfunction, synapse loss, and seeding activity (579,672). In the present study, tau truncation was assessed in the synaptosomes using a mid-domain total tau (Tau5), N-terminal tau (Tau 12), and a C-terminal tau (Tau46) antibody (**Figure 20**). No differences were observed in the total amount of tau protein (Tau5) nor in the amounts of N-terminal cleaved tau (Tau46+) or C-terminal cleaved tau (Tau12+), although a non-significant trend towards higher amounts of C-terminal cleaved tau in demented compared to resilient and controls was noted. This non-significant trend could be partly due to the relatively low number of samples included. These results align with previous reports and indicate that an early enzymatic activity increasing the production of C-terminal cleaved tau may be associated with some of the toxic properties of tau protein (397). Yet, the presence of readily significant changes in synapse densities in these brains despite the absence of a substantial accumulation of C-terminal cleaved tau in the synapses, indicates that the early synapse loss may rather underlie other causes than pathologic tau truncation alone, at least in the early dementia stages. Nonetheless, the potential contribution of C-terminal cleaved tau to other neuropathologic tau changes or to the detrimental interactions between synapses and glial cells in the demented brains may still be of potential relevance.

<u>Tau seeding activity in the synapses of early-stage AD brains</u>

Tau seeding activity is regarded as a biological/functional property of tau that confers it with a prion-like nature. Tau seeding is characterized by the ability of some tau species to propagate from one cell to another (673), and induce conformational changes and aggregation of monomeric tau in the invaded cell (674). Specific hallmarks of tau post-translational modifications have been associated

with seed-competent tau strains, but the underlying signatures of seed-competent tau are not yet fully understood (675,676). In particular, oligomeric forms of tau and high-molecular weight tau have shown high seeding activity and propagation propensity (410,677). Seeding activity has been found ahead of NFT development in the brains of demented individuals, and tau seeds are particularly enriched at the synapses, where tau seeds are thought to propagate between neurons (404). Recent evidence has shown that astrocytes and microglia engulf tau-containing neurons in AD, and that they become dysfunctional upon internalizing tau (509,512). Interestingly, astrocytes and microglia secrete seed-competent tau and induce tau pathology in healthy neurons in *in vitro* assays (512) and the tau proteoforms secreted by glial cells have shown exceptional seeding capacity when compared with the engulfed original tau species (509,678). Oligodendrocytes are the most abundant glial cell subtype in the neocortex and WM, and they have been shown to take up and seed tau pathology in the WM in several tauopathy models, including AD (539), proposing that tau seeding in AD may not be limited to the neocortex and that tau spread across brain regions may be driven by oligodendrocytes. This suggests that tau toxicity may not only derive from a primary property of tau, but also be substantially enhanced by glial cell processing and spreading of tau. Among the potential mechanisms involved in the transsynaptic spread of seed-competent tau, synaptic vesicles, secreted exosomes, and tunnelling nanotubes have been proposed (417,679), and various uptake mechanisms through various endocytosis pathways have been suggested (259). To evaluate whether seed-competent, and hence biologically active and `toxic' tau, could be increased in the synapses of demented brains, seeding activity was measured in the synaptosomes of the visual cortex, a brain region without evidence of NFT deposits. The results showed that tau seeding activity was not detectable across groups in this subcellular location. Moreover, seeding activity in total brain tissue homogenates derived from the cortex and WM of the same cases was also absent across groups (**Figure 21**). These findings suggest that, contrary to previous reports (404), there is no detectable seeding activity in brain regions that lie one to two Braak stages ahead of tau tangle pathology. Interestingly, the absence of tau seeding activity in the synaptosomes was observed despite the readily present loss of synapses in demented brains. Although likely toxic in nature, the presence of tau seeds in synapses may hence not be necessary for the early synapse loss to occur in a demented brain. Moreover, other tau modifications observed in the synaptosomes of these brains (e.g., oligomeric TOC1+ tau and hyperphosphorylated tau181) may not be primarily due to a priming of tau induced by toxic tau seeds from extracellular space and/or connected brain regions, but rather represent a local pathogenic process occurring at or around the synapses. Hence, seed-competent tau may be linked to other posttranslational modifications than tau conformational changes and/or ptau181, and it may arise in the later stages of the disease. Conversely, the toxic tau modifications readily present in these synapses may not be directly associated with seeding activity, and this could represent a promising window of opportunity for early interventions targeting tau to prevent its potential development into seed-competent tau in the later stages. It cannot be excluded that the lack of seeding activity observed here may underlie a low detection sensitivity of the biosensor cell constructs used, which may be useful for the detection of tau seeds in brain regions with presence of NFTs and/or more mature species of tau but may not be suitable for the detection of tau seeds at earlier stages of tau maturity. Altogether, selective tau pathogenic processes occur at the synapse of demented brains before the onset of tau tangle deposits, and this select and cumulative acquisition of tau changes may play different roles in the increasing disease stages. The likely later development of seed-competent tau in synapses, suggests that the other tau posttranslational modifications could be most effectively targeted in the early disease phases, and ahead of their conversion into seed-competent tau.

<u>In situ visualization of synaptic oligomeric tau in early-stage AD brains</u>

To visually assess the in situ interaction of TOC1+ tau oligomers with synaptic elements and evaluate the potential association of tau oligomers with different synaptic locations, TOC1 was evaluated in

expanded tissue sections of the visual cortex (**Figure 22**). In line with the previous biochemical analyses of TOC1, the in situ assessments showed a higher number of TOC1 in Bassoon+ presynapses and in PSD95+ postsynapses of demented compared with resilient and control brains, with a slightly higher burden of synaptic TOC1 colocalized with the presynapses (**Figure 22**). This is aligned with recent studies suggesting that tau oligomers preferentially accumulate in the presynapses when compared with the postsynapses of demented brains. This pre- to postsynaptic tau gradient has been proposed to reflect the likely transsynaptic spread of tau (282). Interestingly, recent evidence has proposed that the presynaptic scaffolding protein Bassoon may harbour neurobiological significance in itself by acting as a target for toxic tau species enhancing tau seeding and propagation propensity (680). Thus, it cannot be excluded that, in the early dementia phases studied here, a particularly prone interaction between oligomeric tau and Bassoon may be due to its potential pathobiological significance in AD, and that the assessment of other presynaptic proteins may have shown a lower burden of association between presynapses and oligomeric tau species (680). On the other hand, the present observation of a particularly prominent and early interaction site between oligomeric tau and Bassoon may suggest novel pathways and treatment avenues with potential relevance in the early stages of dementia. Alternatively, it remains possible that the exclusively excitatory postsynaptic marker (PSD95) used here may be underestimating a possibly additional burden of oligomeric tau accumulation in inhibitory postsynapses, that are emerging as a particularly vulnerable synaptic subpopulation in AD (681), and which may have lead to an overall more balanced pre- to postsynaptic ratio. Interestingly, the burden of synapse loss was higher for presynaptic elements compared with postsynaptic elements in the studied brains, and this could point to a primary role of TOC1+ oligomeric tau in inducing synapse toxicity and loss. This is in line with previous reports showing a direct synaptotoxic effect of tau oligomers (57,272). For technical reasons with antibody host incompatibility, colocalized synapses and TOC1 oligomers could not be assessed together, and only single synaptic elements in combination with TOC1 could be evaluated at the time. Hence, the assessment of single synaptic elements in combination with TOC1 may not allow to determine the functionality of those synaptic elements, thus limiting the biological and functional relevance of TOC1 accumulating in those synapses. It could be argued that TOC1 would preferentially target the silent and non-functional synapses and not affect the mature and functional ones. However, knowing that around 65% of total synaptic elements were forming `mature' colocalized synapses in the studied brains, a significant proportion of single synaptic targets would still be expected to form part of mature and functional synapses, suggesting that the increased accumulation of TOC1 in the synapses of demented brains may possibly play an important and primary role in the early synapse derangement in the demented brains. Future *in vitro* and *in vivo* studies aimed at evaluating the association and mechanisms of early synapse dysfunction driven by tau oligomers will be needed. TOC1 could also be evaluated as a potential early biomarker of AD dementia to more accurately detect tau neuropathologic substrates indicative of early cognitive change, and this could be important for the development of better tau targets for diagnostic purposes and for therapeutic use.

<u>Tau oligomer-driven synapse elimination by glial cells in early-stage AD brains</u>

Glial cells have been recently found to contribute to synapse loss in AD by excessively engulfing synapses in demented brains (327,430). Studies have found that glia erroneously target and excessively eliminate synapses in animal models of AD (682) and two human brain studies have found evidence of an excessive synapse elimination by microglial cells in post-mortem AD brains (327,430). While the underlying drivers of the excessive synapse elimination by glial cells remain largely unknown, recent evidence has proposed an involvement of inflammatory signalling pathways including complement C1q and C3 and phosphatidylserine/osteopontin (421,422,475,683). Tau oligomers accumulate in the synapses of demented subjects from the early phases of dementia and their toxicity has been attributed to direct synaptotoxic effects (282). Moreover, tau oligomers and

glial cells are intimately linked, in that tau oligomers induce inflammatory responses in microglia and astrocytes (514,678) which in turn engulf, process, and release seed-competent tau that is further propagated across the brain (259,509,512,678). In the present study, TOC1 antibody was used to label tau oligomers and, in line with a recent study using oligomeric tau antibody T22 (282), a mistargeting and increase of tau oligomers in synapses was found in demented compared with resilient and control brains (**Figures 20** and **Figure 22**). Tau oligomers have shown toxicity *in vivo* and *in vitro* and they have been involved in synapse dysfunction and neuronal loss (360,413). In fact, synapse dysfunction has been detected as early as <60 mins after incubation of neurons with oligomeric tau (684) and recent evidence from chronic traumatic encephalopathy (CTE), a tauopathy characterized by similar 3R and 4R tau than the one observed in AD (685), has shown that oligomeric tau is detectable after 4 hs of traumatic brain injury (TBI) and that neuronal loss in these animal models initiates at a similar timepoint of around 4 hs after TBI (686), overall suggesting a temporally close association between oligomeric tau burden and neuronal dysfunction. However, the relatively slowly progressive dementing disorder characterizing AD with a clinical disease progression that spans over a timeframe of several years, would argue against a major involvement of direct oligomer-driven synaptotoxicity, if the synapse and neuronal loss induced by tau oligomers is so immediate as suggested by these models. Alternatively, synaptotoxicity of tau oligomers could be driven indirectly, through dysfunctional interactions between tau oligomers and glial cells that would induce glial cells to eliminate tau oligomer-containing synapses, hereby leading to the slowly progressive loss of synapses and the typical dementia syndrome of AD. It is possible that the acute effects of toxic tau oligomers in the AD brain may be partly attenuated by the presence of other concomitant factors that would limit tau oligomers from being the primary mechanism driving synaptotoxicity and dementia in AD. To evaluate the alternative possibility that toxic tau oligomers accumulating in the synapses could be a driver for surrounding glia to target and eliminate those synapses, TOC1+ presynapses and TOC1+ postsynapses were assessed together with IBA1+ ameboid-shaped microglia and GFAP+ astrocytes. The results showed that tau oligomer-tagged presynapses and postsynapses were excessively internalized by microglia and astrocytes in demented compared with resilient and control brains (**Figure 22**), suggesting that the mistargeting of tau oligomers to synapses could lead to a selective and excessive elimination of synapses by glia. Despite the technical limitations of only assessing one synaptic marker together with TOC1 at the time, a significant proportion of TOC1-tagged synapses would still be expected to be colocalized with another synaptic element forming an active synapse, suggesting that a substantial proportion of internalized TOC1+ synapses were likely functional prior to their engulfment. The internalization of TOC1-tagged synapses by glia may temporally better resemble the slowly progressive dementia syndrome of AD and may serve as a more plausible biological explanation of the underlying pathogenic processes occurring at the synapses in AD dementia. Given that tau oligomers are per se synaptotoxic (57,272) it remains possible that a proportion of the internalized oligomer-tagged synapses by glial cells were already dysfunctional prior to their engulfment, and that glial cells were trying to effectively remove them. However, given the rather acute toxic effects of tau oligomers on synapses, this explanation may only account for a small proportion of tau oligomer-driven toxicity in AD dementia, which could instead be studied as a potential underlying mechanism in more rapidly progressive forms of dementia, such as prion disease, and autoimmune/paraneoplastic dementia syndromes. Additionally, dysfunctional synaptic elements disrupted by oligomeric tau would likely lose their synaptic antibody positivity and not be visualizable with conventional antibodies anymore. Thus, the present observation of synaptic proteins and oligomeric tau contained inside glial cells with relatively preserved anatomical structure, likely reflects an early stage of structural and functional damage ahead of a later and more profound structural change in those target elements, which would render them dysfunctional and undetectable by conventional antibodies. It is likely that the preservation of synaptic antibody signal inside glial cells may be due to their still early association within phagosomes that would later fuse with lysosomes where degradation of internalized synaptic elements would commence (687). This is further reinforced by the observation

of LAMP2+ phagolysosomes in a subset of the internalized synaptic elements by glial cells (**Figure 9**). It is possible that the observed synaptic elements inside glial cells may represent only a small proportion of the total amount of synaptic elements contained inside these cells, and that those undetectable synaptic elements may have lost the antibody positivity due to a more advanced digestion stage with significant distortion of epitope binding sites. Future mechanistic studies will be key to evaluating the underlying pathways of the dysfunctional interactions between synaptic oligomers and glial cells in demented brains, which could help discover the mechanisms and develop novel and effective treatment targets to halt the elimination of synapses by glia in the early phases of AD dementia.

4.3 Conclusions

In sum, this work suggests that a subset of glial cells show early phenotypic changes in the cortex and WM of demented compared with resilient and control subjects, and that these glial cell signatures occur independently of ADNC and ahead of NFT deposits. Moreover, it shows that synapse loss is a key signature of demented brains in the early phases of cognitive dysfunction and a strong determinant of dementia severity. It also provides novel evidence of a subset of microglia and astrocytes that excessively internalize synaptic elements in demented brains, and it suggests a potential novel mechanism of oligomeric tau-driven synapse elimination by glia in demented brains. Notably, the neuropathologic changes shown here occurred irrespectively of amyloid-β and tau deposits, and ahead of NFT development, reinforcing that ADNC alone may not be the main driver of dementia development in AD. Importantly, the present study included a select subset of human subjects who were in the early stages of dementia, and the novel mechanistic insights gained from this work may enable the discovery of better diagnostic biomarkers and effective therapeutic targets to prevent synapse loss in the early and most preventable phases of the disease.

Overall, this work proposes a novel model of AD in which a primary dysfunction in a subset of glial cells could drive the early and excessive loss of synapses through an increased internalization of synaptic elements, which could determine clinical expression of dementia. This neuropathologic effect could be substantially induced and self-perpetuated by the presence of tau oligomers in synapses. These novel insights could lead to the discovery of much needed `proximity markers' to detect early synapse loss and glial cell dysfunction, defined by glia with the propensity to excessively eliminate oligomer-containing synapses, which could serve as robust biomarkers in the era of disease modifying therapies to detect imminent dementia onset and track dementia progression. Future studies aimed at exploring the pathways involved in the interaction between glia and tau oligomer-tagged synapses in early AD dementia could unravel novel and targetable pathways to effectively halt dementia development and progression in its earliest phases.

The present results can be interpreted in various ways. In my personal view, the obtained findings indicate that glial cells play a key role in early AD pathogenesis that could indicate a primary glial cell dysfunction, but also reflect the effects on glial cells of other local (e.g. oligomeric proteins) and/or distant contributors (e.g. the peripheral influx of pathogens/substances facilitated by vascular damage). The novel findings of pathogenic tau (e.g. oligomeric, hyperphosphorylated) mislocalized to synapses in the early dementia stages, could be one such driver of glial dysfunction, and the key to eliciting and perpetuating the chronic synapse loss driven by glial cells in AD. Although direct toxicity of tau oligomers on synapses has been shown *in vivo* and *in vitro*, the acute effects of such mechanisms do not associate closely with the clinical disease course of AD, and the presence of largely preserved synapse proteins containing tau oligomers observed in this work would rather suggest that the oligomeric proteins attached to the engulfed synapse proteins by glial cells had low direct pathogenic effects on those glia-engulfed synapses. While the mechanisms underlying the translocation and accumulation of oligomeric proteins in synapses and their direct effects on

synapse function in demented brains remain a matter of ongoing study, this work raises the novel possibility that the presence of oligomers in synapses may drive the chronic elimination of healthy synapses in AD. The signals elicited by the tau oligomer-containing synapses, that may signal to glia to target and engulf those synapses, remain unexplored and will be an important future direction. Equally, additional studies addressing the degradation efficiency of synaptic elements by glial cells in the presence and/or absence of oligomeric proteins, will be key to assess the possibility of a dysfunctional degradation of engulfed synapses, and hence, a secondary accumulation of these proteins inside glial cells. Yet, recent evidence has proposed that the glia-driven internalization of tau remains efficacious until the glial cell is overburdened and unable to adequately degrade tau protein (514); the present study addressed a brain region with exquisitely low burdens of pathologic tau and absence of NFTs, thus likely supporting a still efficient degradation ability of glia and a likely accumulation of synapses inside glia due to an active mistargeting and an excessive elimination of healthy and still functional synapses. Overall, this work raises many new and unanswered questions for future studies, and it allows to propose and alternative disease model of AD, where the early synapse loss in demented AD brains would be due to the combined effects of increased oligomeric tau in synapses and phenotypically altered microglia and astrocytes, that would elicit the mistargeting of oligomeric-tau tagged synapses by glial cells, leading to an excessive elimination of still functional synapses, and the development of AD dementia.

4.4 Limitations

A caveat of the present study is that the cross-sectional nature of post-mortem assessment of human brains only offers a snapshot of the neuropathological processes occurring in these brains at the time of death of an individual and therefore the conclusions derived from the present work do not allow to infer on the possible mechanisms involved. Although the in situ visualization of synapses, oligomers, and glia are novel and can substantially aid in the understanding of the set of processes occurring in these brains, the ultimate evaluation of dynamic processes underlying synapse loss using *in vivo* and *in vitro* evaluations will be needed to complement the observational approaches used here.

Secondly, the lack of consensus definition of human brain resilience can pose difficulties in the study design and interpretation of results when evaluating resilient brains with the aim to better characterize human traits of resilience. In the present study, an operational definition of resilience was created based on histopathological hallmarks and cognitive scores obtained from detailed antemortem clinical and post-mortem histopathologic evaluations to ensure consistency in case selection and standardized categorization of subjects into the respective cognitive categories, including not only the differentiation between demented and resilient, but also between resilient and controls. However, the operational definition used here is not formally validated or used in large scale settings, and the conclusions derived from this work may be limited to the predefined case selection used here.

Another potential drawback in the study of resilient human brains is that close clinical evaluations prior to death may be particularly important to ensure that the cognitive status of a subject did not change and convert into the demented category just prior to death. While previous studies have suggested that a close interval of <2 years is desired and sufficient to ensure adequate clinical categorization, this time interval has been defined by consensus and formal studies comparing the reliability of such time measure is limited. In the present cohort, a particularly short time interval (<1 year) was present between the last clinical assessment and the time of death, and this adds robustness and validity to the correct clinical categorization of cases into their respective groups and to the results derived from their assessments. Although rather unlikely, it cannot be fully excluded

that some subjects may have suffered from a change in cognitive status within the short time period between last clinical assessment and time of death.

Detailed neurocognitive testing was performed in a subset of cases and the testing scores were correlated with local synapse densities and with various immunohistochemical quantitative measures. Although significant correlations were observed and some of the cognitive testing scores (e.g. DSST included in the WAIS-R score) were functionally closely related to the anatomical brain region studied here (visual cortex), most of the cognitive scales evaluated broad functional networks, and they did not allow to sensitively associate local brain anatomical changes with a similarly sensitive clinical measure of cognitive dysfunction. The development of more sensitive cognitive testing measures to detect select and anatomically restrained brain changes will be key to assessing the clinical relevance of locoregional brain changes. Moreover, the possibility should be considered that some of the locoregional anatomic changes (e.g. synapse density loss) may have anatomical and functional effects in connected and remote brain areas, and that some of the cognitive dysfunction profiles observed here may derive from disruptions in those distant anatomic brain regions.

The present study included subjects of relatively old age at death (>85 years) and previous studies have highlighted differences in clinicopathological hallmarks and in potential mechanisms of resilience to AD in resilient so-called `super-agers' (>85 years old) compared with younger resilient individuals (<85 years old) (688,689). Thus, it cannot be excluded that the potential mechanisms proposed here may be linked to the particularly favourable cognitive trajectory observed in the cohort of super-agers and that the results derived from this study may have relevance to mechanisms linked to not only to sustaining effects of ADNC in the brain (`resilience'), but also to maintaining cognitive function over a longer time span (`super-ageing'). It remains possible that both phenomena may be ultimately linked and that the benefits derived from them together would account for the most favourable cognitive trajectory of individuals across different lifespans.

While the subjects included in the present work were matched for concomitant neuropathologies including amyloid-β, tau, alpha-synuclein, and TDP-43 deposits, the demented brains showed a higher vascular composite score compared with the resilient and control subjects, and it cannot be excluded that some of the observed effects of vascular pathology on synapse function and/or glial-driven synapse elimination may be partly due to vascular comorbidity. While vascular pathology in the form of WM lesions is a common finding of healthy elderly brains, presenting in up to 85% of unselected autopsies, it is also very commonly found in AD brains, presenting in around 75% of demented brains (133–135). Yet, despite the presence of vascular lesions in most of the brains, the burden of those changes significantly differed between demented and resilient/controls, and it could theoretically be possible that this could have contributed to some of the other neuropathologic changes observed (e.g., synapse loss, glial dysfunction). However, the association between vascular burden and some of the used memory scales and synapse densities was not significant, supporting a rather low direct effect of vascular burden on the main neuropathologic outcomes studied here. However, the calculated vascular score burden derived from tissue blocks of the neocortex, WM, and basal ganglia, and it did not specifically address the burden of vascular lesions in the studied brain areas, nor the potential locoregional effects of CAA on glial cell phenotypic changes. A more detailed in situ evaluation of vascular changes and their interactions with glial cells could have rendered significant associations that were not observed with the global score used here. Of note, the study of synaptic TOC1 in association with glial cells was performed on a select subset of N=10 brains that were matched for vascular score burden to eliminate the potential effects of vascular comorbidity on this intricate interaction(s). The total of N=60 brains included did not allow to match them for vascular score burden unless eliminating an important number of cases.

The assessment of synaptic elements was limited to excitatory (post)synapses (PSD95) only. While this provides an understanding of a relevant proportion of the total synapses of the human brain (80-90% of synapses are excitatory), there is a small proportion of inhibitory synapses (10-20%) that was not assessed in this study. Recent evidence has proposed that excitatory and inhibitory synapses may be equally affected in the early stages of AD dementia and therefore, it cannot be excluded that some of the changes observed in the present study, such as the presynaptic over postsynaptic predominance of oligomeric tau accumulation and/or the increased presynaptic over postsynaptic elimination by glial cells, could be due to a lack of assessment of an inhibitory (post)synapse subpopulation.

ExM is a highly innovative technique that offers the unprecedented possibility of separating densely packed biomolecules in tissue sections to study their locoregional interactions. Several groups have previously validated ExM in different tissue types (FFPE, frozen) and origins (human, mouse) showing the isotropic expansion with minimal tissue distortion of expansion. The validation performed in the present study comparing unexpanded frozen with expanded FFPE sections and using various epitope targets for one same biological substrate, showed overlap of signal, and the assessment of internalized synaptic elements using lyososmal co-labeling showed co-localization of engulfed synapses with lysosomes, undepinning their biological relevance. Despite robust validation of ExM in the past and present study, it cannot be fully excluded that minimal tissue distortions and under-/overestimations of engulfed material occurred.

Long PMIs can alter protein expression at post-mortem and although recent studies have suggested that most proteins retain stable expression levels even with PMIs of >24hs (690), the present study included subjects who had relatively long PMIs (mean 21.9±15.8 hours). Although the three groups were matched for PMIs, we cannot exclude that PMI could have influenced the expression levels of some of the proteins measured here. Nonetheless, there were no significant associations between PMI and synapse densities, glial cell changes, and AD neuropathologic measures suggesting that, at an individual level, the PMI did not directly alter the neuropathologic expression of the proteins assessed here, and that it would be rather unlikely that the differences observed in the present study would be attributable to PMI.

4.5 Future directions

The present study assessed resilient brains at intermediate stages of ADNC (Braak III-IV stages) that harboured low burdens of cortical amyloid-β plaques and had brain areas with (temporal cortex) and without (visual cortex) NFT deposits. While the potential determinants of resilience to these intermediate ADNC stages could be relevant to address mechanisms that may help sustain cognitive function in the face of ADNC, a future avenue to assess the larger-scale implications of resilience factors in preventing dementia could involve the study of resilience factors in brains with even lower or absent ADNC burdens comparing cognitively normal with so-called frail brains (demented subjects with low/negligible ADNC at post-mortem) (55). This could help determine whether the absence of resilience in these subjects would be sufficient to explain cognitive decline, or alternatively, if resilience hallmarks would only be beneficial to preserve memory in subjects with ADNC. The implications of such findings could be relevant for guidance of future preventative treatments aimed at preserving cognition in a subset of ADNC+ and maybe also of ADNC- human subjects ahead of the development of cognitive decline. Ultimately, the study of these interesting frail brains with virtually absent ADNC at post-mortem but presence of dementia prior to death, which has been described in around 5% of autopsies of demented individuals, would further help understand the true significance of ADNC in the brain and the relevance of other factors for the development of dementia in an individual.

The amyloid cascade hypothesis is the most widely accepted explanation of AD pathogenesis, and it posits that the deposition of amyloid-β is the causative agent of AD, and that NFTs, neuronal loss, vascular damage, and dementia development follow as a direct result of this deposition (691). Based on recent evidence of tau being a better and closer predictor of synaptic and cognitive dysfunction in AD than amyloid, the present study was centered on the study of tau protein, and it largely obliterated the assessment of the role of amyloid-β deposits. Given that oligomeric forms of amyloid-β have shown direct synaptotoxic and neuroinflammatory effects, it is likely that the presence and interaction between amyloid-β and tau oligomers may additionally contribute to the toxic effects on synapses observed here. Understanding the effects of the single and combined oligomeric proteins on synapse dysfunction in AD, including amyloid, tau, and also alpha-synuclein, will be an interesting future direction that may aid in the more accurate definition and development of synapse-protective strategies for AD dementia.

Resilience to ADNC is not exclusive or unique to the presence of AD lesions in the brain. In fact, recent evidence has shown that resilience to other neuropathologies, including TDP-43 and alpha-synuclein, exists. In fact, cognitively unimpaired elderly with TDP43 aggregates in the brain have been observed in 24%, and with alpha-synuclein aggregates in 21% of autopsies (72,73). While studies on resilience to ADNC are rapidly evolving, the study of resilience to these other two key neuropathologic signatures remain largely unexplored. Future work addressing these interesting subsets of outliers could help understand the protective mechanisms associated with these individuals, and unravel individual and combined mechanisms of resilience, which could ultimately efficaciously address the pathways most relevant to maintaining cognitive function in dementia of various etiologies.

The comorbid presence of ADNC with other neuropathologies, including TDP43 and alpha-synuclein, is a very common finding in the brains of demented individuals, and *in vitro* and *in vivo* studies have shown an exponential rather than additive effect of these combined proteins on synapse and cognitive dysfunction. Some of these proteins are particularly increased in the synapses, where they likely exert detrimental effects on synapse function. Yet, the interactions between amyloid-β, tau, TDP43 and alpha-synuclein oligomers at the synapse remain largely unexplored, and future studies addressing the single and combined effects of these proteins on synapse and cognitive function may be crucial to understanding the mechanisms and developing potential synapto-protective treatments for AD and other neurodegenerative dementia syndromes.

Synapse subpopulations are highly diverse, and they include not only excitatory and inhibitory synapses, but also specific receptors in the presynapse and postsynapse. As part of the `synaptopathy' characterizing AD very little is known about the specific synapse subpopulations and receptors that get affected at different disease stages and in the emerging clinical subtypes of AD and other dementia syndromes, and the study of those subpopulations could be relevant to understanding the underlying pathways and mechanisms involved. Given that synapse subpopulations and clinical presentations are widely heterogenous, it is likely that mechanisms affecting each synaptic subpopulation will be distinct for each dementia subtype, and that targeting the adequate pathway at the right time for each specific dementia syndrome will lead to most effective preservation of synaptic health and cognitive outcome in an individual. Limited means to assess synapses in living individuals with biomarkers and/or at post-mortem with staining and imaging techniques currently hinder the detailed evaluation of synaptic changes in the spectrum of AD and other dementias. Future work aimed at improving clinico-biomarker associations with the use of high-sensitivity proteomic analyses in biofluids and brain tissue combined with improved high-resolution nanoscale in situ assessments of synapses in the brain, may help reliably determine the vulnerability of specific synapse subpopulations in different dementing disorders and study their interactome to discover the initiating and driving pathways of synapse derangement and dementia

development. This could enable the discovery and development of novel biomarkers and treatment targets aimed at preserving specific synapse subpopulations in AD dementia subtypes and other dementia syndromes.

Vascular pathology is highly prevalent in the brains of healthy and demented individuals, and it may interact and affect other neuropathologic elements in the brain. Given the limitations of the study of vascular changes in post-mortem brains, future studies aimed at creating *in vivo* or *in vitro* models and improved imaging techniques to evaluate the effect(s) of early vascular changes on the development and progression of ADNC and other neuropathologic signatures (e.g., synapse loss, glial dysfunction) would be highly informative. This could enable addressing the possibility of detrimental peripheral effects on the AD brain through an influx of peripheral elements which could be inducing or perpetuating glial dysfunction and subsequent synapse loss. This would allow to identify potential pathways driving the interaction between vascular/peripheral elements and glial cells in AD brains, with the potential to develop treatments to help reduce the primary glial dysfunction and preserve cognition ahead of cognitive decline in at-risk populations with known vascular comorbidity.

While the present work proposes that the presence of oligomers in synapses and increased engulfment of oligomer-tagged synapses by glia is due to an oligomer-driven synapse elimination in demented brains, alternative explanations exist such as a physiological elimination of readily dysfunctional synapses containing tau oligomers by glia, and an increased accumulation of synaptic elements inside dysfunctional glial cells. To address these important alternative possibilities and identify potential underlying mechanisms, *in vivo* and *in vitro* models are needed to show the engulfment of synapses by glia in cell culture, and to address the potential effects of oligomeric proteins on the degradation efficiency of internalized debris by glia. Moreover, it will be interesting to assess the effects of cellular co-culture models including astrocytes, microglia, and potentially oligodendroglia, in eliminating synapses derived from demented and resilient brains, and to assess potential changes on synapse elimination when associating glial cell subtypes, and when adding oligomeric proteins beyond tau (e.g., amyloid and alpha-synuclein) to those co-cultures. This could help understand the intricate processes leading to synapse loss in AD and help identify mechanisms and pathways that may be targetable to prevent the progression of synapse loss in these brains.

The drivers of increased oligomeric tau production and pathologic tau spread across the brain remain widely unknown. Future studies addressing the potential mechanisms involved in the pathologic tethering of tau to synaptic membranes of demented brains, the transsynaptic spread of tau, and the recently suggested glia-induced pathologic tau conversion and seeding propensity may help find pathways that could be effectively targeted to halt synapse loss in the early dementia stages. With the presently proposed novel data of an astrocytic (in addition to microglial) involvement in early synapse elimination of oligomer-containing synapses in AD, future studies aimed at addressing the interactions between oligomeric proteins and synaptic membranes, as well as between synapses (with and without oligomers) and glial cells may be key to identify the underlying altered pathways that may lead to the excessive synapse elimination in demented brains.

Recent studies have identified a subset of receptors involved in excessive synaptic pruning in mouse models of AD, including C1q and C3 complement, and phosphatidylserine/osteopontin. In the present study the involvement of underlying pathways in excessive synapse elimination by glia was not addressed partly due to technical difficulties with complement protein staining in expanded brain tissue. Future studies directed at evaluating the interactome between synapses and glial cells would help identify potentially druggable treatment targets that could be tested *in vitro* and *in vivo* and which may effectively interfere with the excessive synapse elimination by glia in those brains.

Although presently available AD biomarkers show high sensitivity to diagnose AD, they are not always closely associated with the presence of dementia in an individual. The here presented findings of higher burdens of tau oligomers and hyperphosphorylated tau in synapses of demented brains in the early disease stages could help in the development of better biomarkers to track the development and progression of dementia, and help guide earliest interventions and therapeutic trials in AD. Moreover, oligomeric tau and/or other tau species could be incorporated into future neuropathologic frameworks and ultimately replace fibrillar forms of tau to more accurately define AD histopathologically.

Newly revised biomarker definition of AD using the ATN framework has recently proposed incorporation of inflammatory (I), vascular (V), and alpha-synuclein (S) measures to the presently used biomarker definition of AD creating an updated ATN-IVS framework. Moreover, some of the A, T, and N measures have been amended with the addition of oligomeric species of amyloid-β (A), other posttranslational modifications of tau (T), and the inclusion of synaptic biomarkers to measure neurodegeneration (N) into the present definition. Although the present work addressed one potential pathologic mechanism leading to early synapse loss by studying the association of glia with oligomeric tau, future studies expanding on this and most importantly assessing the combined effects of various oligomeric proteins on synapse loss including oligomeric amyloid-β and alpha-synuclein may help better understand the mechanisms of early synapse derangement and help discover better biomarkers and more effective treatment targets for AD and other dementia syndromes.

The challenges posed by clinico-pathologic discrepancies in the diagnosis of AD could be addressed in the future by combining better clinical definitions of AD subtypes (e.g., frontal, language, PCA subtypes of AD) with more detailed neuropathologic characterizations of each of those clinical subtypes. The more accurate definition of clinical syndromes of AD in association with characteristic neuropathologic signatures may enable to improve diagnostic accuracy and reduce the gap between the pre-mortem and post-mortem discrepancies currently observed in AD, which may ultimately shift the at present only neuropathologic definition of AD to a combined clinico-pathologic entity. It is likely that the presently combined assessment of distinct clinical AD phenotypes as one single entity termed `AD dementia' may underestimate individual neurobiological and pathological differences of those clinically distinct presentations, and that this may be hindering the development of effective treatments for AD. An individualized approach based on clinical AD subtype presentations combined with corresponding underlying AD biomarker statuses may ultimately define distinct AD entities and help develop effective and individualized treatment strategies for each AD subtype. The better clinical and neuropathologic definition of AD may enable overcoming the important limitations in the clinico-pathologic discrepancies and the lack of disease-modifying treatments available to date and allow targeting the adequate pathways at the right time for each AD dementia subtype to prevent the development and progression of the disease at an individual level.

5. References

1. Hyman BT, Phelps CH, Beach TG, Bigio EH, Cairns NJ, Carrillo MC, et al. National Institute on Aging-Alzheimer's Association guidelines for the neuropathologic assessment of Alzheimer's disease. Alzheimers Dement J Alzheimers Assoc. 2012 Jan;8(1):1–13.

2. Jack CR Jr, Bennett DA, Blennow K, Carrillo MC, Dunn B, Haeberlein SB, et al. NIA-AA Research Framework: Toward a biological definition of Alzheimer's disease. Alzheimers Dement J Alzheimers Assoc. 2018 Apr;14(4):535–62.

3. DeTure MA, Dickson DW. The neuropathological diagnosis of Alzheimer's disease. Mol Neurodegener. 2019 Aug 2;14(1):32.

4. Malek-Ahmadi M, Perez SE, Chen K, Mufson EJ. Neuritic and Diffuse Plaque Associations with Memory in Non-Cognitively Impaired Elderly. J Alzheimers Dis JAD. 2016 Jul 14;53(4):1641–52.

5. Pensalfini A, Albay R 3rd, Rasool S, Wu JW, Hatami A, Arai H, et al. Intracellular amyloid and the neuronal origin of Alzheimer neuritic plaques. Neurobiol Dis. 2014/08/01 ed. 2014 Nov;71:53–61.

6. Dietmar R. Thal, Udo Rüb, Mario Orantes, Heiko Braak. Phases of Aβ-deposition in the human brain and its relevance for the development of AD. Neurology. 2002 Jun 25;58(12):1791.

7. Davidson YS, Robinson A, Prasher VP, Mann DMA. The age of onset and evolution of Braak tangle stage and Thal amyloid pathology of Alzheimer's disease in individuals with Down syndrome. Acta Neuropathol Commun. 2018 Jul 4;6(1):56.

8. Boluda S, Toledo JB, Irwin DJ, Raible KM, Byrne MD, Lee EB, et al. A comparison of Aβ amyloid pathology staging systems and correlation with clinical diagnosis. Acta Neuropathol (Berl). 2014 Oct 1;128(4):543–50.

9. Serrano-Pozo A, Frosch MP, Masliah E, Hyman BT. Neuropathological alterations in Alzheimer disease. Cold Spring Harb Perspect Med. 2011 Sep;1(1):a006189–a006189.

10. Vonsattel JPG, Myers RH, Tessa Hedley-Whyte E, Ropper AH, Bird ED, Richardson Jr EP. Cerebral amyloid angiopathy without and with cerebral hemorrhages: A comparative histological study. Ann Neurol. 1991 Nov 1;30(5):637–49.

11. Braak H, Braak E. Neuropathological stageing of Alzheimer-related changes. Acta Neuropathol (Berl). 1991 Sep 1;82(4):239–59.

12. Braak H, Alafuzoff I, Arzberger T, Kretzschmar H, Del Tredici K. Staging of Alzheimer disease-associated neurofibrillary pathology using paraffin sections and immunocytochemistry. Acta Neuropathol (Berl). 2006/08/12 ed. 2006 Oct;112(4):389–404.

13. Jackson J, Jambrina E, Li J, Marston H, Menzies F, Phillips K, et al. Targeting the Synapse in Alzheimer's Disease. Front Neurosci [Internet]. 2019;13. Available from: https://www.frontiersin.org/article/10.3389/fnins.2019.00735

14. Busche MA, Hyman BT. Synergy between amyloid-β and tau in Alzheimer's disease. Nat Neurosci. 2020 Oct 1;23(10):1183–93.

15. Nicoll JAR, Buckland GR, Harrison CH, Page A, Harris S, Love S, et al. Persistent neuropathological effects 14 years following amyloid-β immunization in Alzheimer's disease. Brain J Neurol. 2019 Jul 1;142(7):2113–26.

16. Bennett DA, Schneider JA, Arvanitakis Z, Kelly JF, Aggarwal NT, Shah RC, et al. Neuropathology of older persons without cognitive impairment from two community-based studies. Neurology. 2006 Jun 27;66(12):1837.

17. O'Brien RJ, Resnick SM, Zonderman AB, Ferrucci L, Crain BJ, Pletnikova O, et al. Neuropathologic Studies of the Baltimore Longitudinal Study of Aging (BLSA). J Alzheimers Dis. 2009;18(3):665–75.

18. Arnold SE, Louneva N, Cao K, Wang LS, Han LY, Wolk DA, et al. Cellular, synaptic, and biochemical features of resilient cognition in Alzheimer's disease. Neurobiol Aging. 2012/05/02 ed. 2013 Jan;34(1):157–68.

19. Gómez-Isla T, Price JL, McKeel Jr. DW, Morris JC, Growdon JH, Hyman BT. Profound Loss of Layer II Entorhinal Cortex Neurons Occurs in Very Mild Alzheimer's Disease. J Neurosci. 1996 Jul 15;16(14):4491.

20. Guillozet AL, Weintraub S, Mash DC, Mesulam MM. Neurofibrillary Tangles, Amyloid, and Memory in Aging and Mild Cognitive Impairment. Arch Neurol. 2003 May 1;60(5):729–36.

21. Bondareff W, Mountjoy CQ, Roth M, Hauser DL. Neurofibrillary degeneration and neuronal loss in alzheimer's disease. Neurobiol Aging. 1989 Nov 1;10(6):709–15.

22. Bobinski M, Wegiel J, Wisniewski HM, Tarnawski M, Bobinski M, Reisberg B, et al. Neurofibrillary pathology — correlation with hippocampal formation atrophy in Alzheimer disease. Neurobiol Aging. 1996 Nov 1;17(6):909–19.

23. Novak P, Schmidt R, Kontsekova E, Zilka N, Kovacech B, Skrabana R, et al. Safety and immunogenicity of the tau vaccine AADvac1 in patients with Alzheimer's disease: a randomised, double-blind, placebo-controlled, phase 1 trial. Lancet Neurol. 2017 Feb 1;16(2):123–34.

24. Imbimbo BP, Balducci C, Ippati S, Watling M. Initial failures of anti-tau antibodies in Alzheimer's disease are reminiscent of the amyloid-β story. Neural Regen Res [Internet]. 2023;18(1). Available from: https://journals.lww.com/nrronline/fulltext/2023/01000/initial_failures_of_anti_tau_antibodies_in.21.aspx

25. Wolk D, Salloway S, Dickerson B. Putting the New Alzheimer Disease Amyloid, Tau, Neurodegeneration (AT[N]) Diagnostic System to the Test. JAMA. 2019 Jun 18;321(23):2289–91.

26. Bishop NA, Lu T, Yankner BA. Neural mechanisms of ageing and cognitive decline. Nature. 2010 Mar 25;464(7288):529–35.

27. Latimer CS, Burke BT, Liachko NF, Currey HN, Kilgore MD, Gibbons LE, et al. Resistance and resilience to Alzheimer's disease pathology are associated with reduced cortical pTau and absence of limbic-predominant age-related TDP-43 encephalopathy in a community-based cohort. Acta Neuropathol Commun. 2019 Jun 7;7(1):91.

28. Latimer CS, Keene CD, Flanagan ME, Hemmy LS, Lim KO, White LR, et al. Resistance to Alzheimer Disease Neuropathologic Changes and Apparent Cognitive Resilience in the Nun and Honolulu-Asia Aging Studies. J Neuropathol Exp Neurol. 2017 Jun 1;76(6):458–66.

29. Neuner SM, Telpoukhovskaia M, Menon V, O'Connell KMS, Hohman TJ, Kaczorowski CC. Translational approaches to understanding resilience to Alzheimer's disease. Trends Neurosci. 2022 May 1;45(5):369–83.

30. Yaakov S. Collaboratory on Research Definitions for Reserve and Resilience in Cognitive Aging and Dementia.

31. Yao T, Sweeney E, Nagorski J, Shulman JM, Allen GI. Quantifying cognitive resilience in Alzheimer's Disease: The Alzheimer's Disease Cognitive Resilience Score. PLOS ONE. 2020 Nov 5;15(11):e0241707.

32. Serra L, Musicco M, Cercignani M, Torso M, Spanò B, Mastropasqua C, et al. Cognitive reserve and the risk for Alzheimer's disease: a longitudinal study. Neurobiol Aging. 2015 Feb 1;36(2):592–600.

33. Jones RN, Manly J, Glymour MM, Rentz DM, Jefferson AL, Stern Y. Conceptual and Measurement Challenges in Research on Cognitive Reserve. J Int Neuropsychol Soc. 2011/03/17 ed. 2011;17(4):593–601.

34. Lesuis SL, Hoeijmakers L, Korosi A, de Rooij SR, Swaab DF, Kessels HW, et al. Vulnerability and resilience to Alzheimer's disease: early life conditions modulate neuropathology and determine cognitive reserve. Alzheimers Res Ther. 2018 Sep 19;10(1):95.

35. Ossenkoppele R, Lyoo CH, Jester-Broms J, Sudre CH, Cho H, Ryu YH, et al. Assessment of Demographic, Genetic, and Imaging Variables Associated With Brain Resilience and Cognitive Resilience to Pathological Tau in Patients With Alzheimer Disease. JAMA Neurol. 2020 May 1;77(5):632–42.

36. Lee DH, Seo SW, Roh JH, Oh M, Oh JS, Oh SJ, et al. Effects of Cognitive Reserve in Alzheimer's Disease and Cognitively Unimpaired Individuals. Front Aging Neurosci [Internet]. 2022;13. Available from: https://www.frontiersin.org/articles/10.3389/fnagi.2021.784054

37. Crystal H, Dickson D, Fuld P, Masur D, Scott R, Mehler M, et al. Clinico-pathologic studies in dementia. Neurology. 1988 Nov 1;38(11):1682.

38. Katzman R, Terry R, DeTeresa R, Brown T, Davies P, Fuld P, et al. Clinical, pathological, and neurochemical changes in dementia: A subgroup with preserved mental status and numerous neocortical plaques. Ann Neurol. 1988 Feb 1;23(2):138–44.

39. Blessed G, Tomlinson BE, Roth M. The Association Between Quantitative Measures of Dementia and of Senile Change in the Cerebral Grey Matter of Elderly Subjects. Br J Psychiatry. 2018/01/29 ed. 1968;114(512):797–811.

40. Prokopis C. Prokopiou, Nina Engels-Domínguez, Aaron P. Schultz, Jorge Sepulcre, Elouise A. Koops, Kathryn V. Papp, et al. Association of Novelty-Related Locus Coeruleus Function With Entorhinal Tau Deposition and Memory Decline in Preclinical Alzheimer Disease. Neurology. 2023 Sep 19;101(12):e1206.

41. Zhang Q, Fan C, Wang L, Li T, Wang M, Han Y, et al. Glucose metabolism in posterior cingulate cortex has supplementary value to predict the progression of cognitively unimpaired to dementia due to Alzheimer's disease: an exploratory study of 18F-FDG-PET. GeroScience [Internet]. 2023 Aug 23; Available from: https://doi.org/10.1007/s11357-023-00897-0

42. P. Gelber R, J. Launer L, R. White L. The Honolulu-Asia Aging Study: Epidemiologic and Neuropathologic Research on Cognitive Impairment. Curr Alzheimer Res. 2012;9(6):664–72.

43. Snowdon, David A. Healthy Aging and Dementia: Findings from the Nun Study. Annals of Internal Medicine 139 (2003): 450-454.

44. Stern Y, Barnes CA, Grady C, Jones RN, Raz N. Brain reserve, cognitive reserve, compensation, and maintenance: operationalization, validity, and mechanisms of cognitive resilience. Neurobiol Aging. 2019 Nov 1;83:124–9.

45. Thomas J. Montine, Maria M. Corrada, Claudia Kawas, Syed A. Bukhari, Lon R. White, Lu Tian, et al. Association of Cognition and Dementia With Neuropathologic Changes of Alzheimer Disease and Other Conditions in the Oldest Old. Neurology. 2022 Sep 6;99(10):e1067.

46. Stern Y. Cognitive reserve. Neuropsychologia. 2009/03/13 ed. 2009 Aug;47(10):2015–28.

47. Robert Katzman. Education and the prevalence of dementia and Alzheimer's disease. Neurology. 1993 Jan 1;43(1 Part 1):13.

48. Mortimer JA, Graves AB. Education and other socioeconomic determinants of dementia and Alzheimer's disease. Neurology. 1993;43:S39–44.

49. Aiello Bowles EJ, Crane PK, Walker RL, Chubak J, LaCroix AZ, Anderson ML, et al. Cognitive Resilience to Alzheimer's Disease Pathology in the Human Brain. J Alzheimers Dis JAD. 2019;68(3):1071–83.

50. Mohamed H, Gurrola T, Berman R, Collins M, Sariyer IK, Nonnemacher MR, et al. Targeting CCR5 as a Component of an HIV-1 Therapeutic Strategy. Front Immunol [Internet]. 2022;12. Available from: https://www.frontiersin.org/articles/10.3389/fimmu.2021.816515

51. White NJ. Anaemia and malaria. Malar J. 2018 Oct 19;17(1):371.

52. Arenaza-Urquijo EM, Vemuri P. Resistance vs resilience to Alzheimer disease: Clarifying terminology for preclinical studies. Neurology. 2018/03/28 ed. 2018 Apr 10;90(15):695–703.

53. Diana I. Bocancea, Anna C. van Loenhoud, Colin Groot, Frederik Barkhof, Wiesje M. van der Flier, Rik Ossenkoppele. Measuring Resilience and Resistance in Aging and Alzheimer Disease Using Residual Methods. Neurology. 2021 Sep 7;97(10):474.

54. Brenowitz WD, Keene CD, Hawes SE, Hubbard RA, Longstreth WT, Woltjer RL, et al. Alzheimer's disease neuropathologic change, Lewy body disease, and vascular brain injury in clinic- and community-based samples. Neurobiol Aging. 2017 May 1;53:83–92.

55. Carlyle BC, Kandigian SE, Kreuzer J, Das S, Trombetta BA, Kuo Y, et al. Synaptic proteins associated with cognitive performance and neuropathology in older humans revealed by multiplexed fractionated proteomics. Neurobiol Aging. 2021 Sep 1;105:99–114.

56. Anna Catharina van Loenhoud, Wiesje Maria van der Flier, Alle Meije Wink, Ellen Dicks, Colin Groot, Jos Twisk, et al. Cognitive reserve and clinical progression in Alzheimer disease. Neurology. 2019 Jul 23;93(4):e334.

57. Perez-Nievas BG, Stein TD, Tai HC, Dols-Icardo O, Scotton TC, Barroeta-Espar I, et al. Dissecting phenotypic traits linked to human resilience to Alzheimer's pathology. Brain J Neurol. 2013/07/03 ed. 2013 Aug;136(Pt 8):2510–26.

58. Barroeta-Espar I, Weinstock LD, Perez-Nievas BG, Meltzer AC, Siao Tick Chong M, Amaral AC, et al. Distinct cytokine profiles in human brains resilient to Alzheimer's pathology. Neurobiol Dis. 2018/10/15 ed. 2019 Jan;121:327–37.

59. Boros BD, Greathouse KM, Gentry EG, Curtis KA, Birchall EL, Gearing M, et al. Dendritic spines provide cognitive resilience against Alzheimer's disease. Ann Neurol. 2017/10/22 ed. 2017 Oct;82(4):602–14.

60. Bennett DA, Buchman AS, Boyle PA, Barnes LL, Wilson RS, Schneider JA. Religious Orders Study and Rush Memory and Aging Project. J Alzheimers Dis. 2018;64(s1):S161–89.

61. Paasila PJ, Davies DS, Sutherland GT, Goldsbury C. Clustering of activated microglia occurs before the formation of dystrophic neurites in the evolution of Aβ plaques in Alzheimer's disease. Free Neuropathol. 2020 Aug 4;1(0):20.

62. Galiano-Landeira J, Torra A, Vila M, Bové J. CD8 T cell nigral infiltration precedes synucleinopathy in early stages of Parkinson's disease. Brain. 2020 Dec 1;143(12):3717–33.

63. Ahangari N, Fischer CE, Schweizer TA, Munoz DG. Cognitive resilience and severe Alzheimer's disease neuropathology. Aging Brain. 2023 Jan 1;3:100065.

64. Dumitrescu L, Mahoney ER, Mukherjee S, Lee ML, Bush WS, Engelman CD, et al. Genetic variants and functional pathways associated with resilience to Alzheimer's disease. Brain. 2020 Aug 1;143(8):2561–75.

65. Barker SJ, Raju RM, Milman NEP, Wang J, Davila-Velderrain J, Gunter-Rahman F, et al. MEF2 is a key regulator of cognitive potential and confers resilience to neurodegeneration. Sci Transl Med. 13(618):eabd7695.

66. Lopera F, Marino C, Chandrahas AS, O'Hare M, Villalba-Moreno ND, Aguillon D, et al. Resilience to autosomal dominant Alzheimer's disease in a Reelin-COLBOS heterozygous man. Nat Med. 2023 May 1;29(5):1243–52.

67. Arboleda-Velasquez JF, Lopera F, O'Hare M, Delgado-Tirado S, Marino C, Chmielewska N, et al. Resistance to autosomal dominant Alzheimer's disease in an APOE3 Christchurch homozygote: a case report. Nat Med. 2019 Nov 1;25(11):1680–3.

68. Hou J, Hess JL, Armstrong N, Bis JC, Grenier-Boley B, Karlsson IK, et al. Polygenic resilience scores capture protective genetic effects for Alzheimer's disease. Transl Psychiatry. 2022 Jul 25;12(1):296.

69. Mathys H, Peng Z, Boix CA, Victor MB, Leary N, Babu S, et al. Single-cell atlas reveals correlates of high cognitive function, dementia, and resilience to Alzheimer's disease pathology. Cell. 2023 Sep 28;186(20):4365-4385.e27.

70. Buciuc M, Whitwell JL, Tosakulwong N, Weigand SD, Murray ME, Boeve BF, et al. Association between transactive response DNA-binding protein of 43 kDa type and cognitive resilience to Alzheimer's disease: a case-control study. Neurobiol Aging. 2020 Aug 1;92:92–7.

71. Melikyan ZA, Corrada MM, Leiby AM, Sajjadi SA, Bukhari S, Montine TJ, et al. Cognitive resilience to three dementia-related neuropathologies in an oldest-old man: A case report from The 90+ Study. Neurobiol Aging. 2022 Aug 1;116:12–5.

72. Nascimento C, Di Lorenzo Alho AT, Bazan Conceição Amaral C, Leite REP, Nitrini R, Jacob-Filho W, et al. Prevalence of transactive response DNA-binding protein 43 (TDP-43) proteinopathy in cognitively normal older adults: systematic review and meta-analysis. Neuropathol Appl Neurobiol. 2018 Apr 1;44(3):286–97.

73. Parkkinen L, Soininen H, Alafuzoff I. Regional Distribution of α-Synuclein Pathology in Unimpaired Aging and Alzheimer Disease. J Neuropathol Exp Neurol. 2003 Apr 1;62(4):363–7.

74. Palmqvist S, Rossi M, Hall S, Quadalti C, Mattsson-Carlgren N, Dellavalle S, et al. Cognitive effects of Lewy body pathology in clinically unimpaired individuals. Nat Med. 2023 Aug 1;29(8):1971–8.

75. Zhang Y, Wu KM, Yang L, Dong Q, Yu JT. Tauopathies: new perspectives and challenges. Mol Neurodegener. 2022 Apr 7;17(1):28.

76. Biel D, Brendel M, Rubinski A, Buerger K, Janowitz D, Dichgans M, et al. Tau-PET and in vivo Braak-staging as prognostic markers of future cognitive decline in cognitively normal to demented individuals. Alzheimers Res Ther. 2021 Aug 12;13(1):137.

77. Wang D, Chen F, Han Z, Yin Z, Ge X, Lei P. Relationship Between Amyloid-β Deposition and Blood–Brain Barrier Dysfunction in Alzheimer's Disease. Front Cell Neurosci [Internet]. 2021;15. Available from: https://www.frontiersin.org/articles/10.3389/fncel.2021.695479

78. Serrano-Pozo A, Qian J, Muzikansky A, Monsell SE, Montine TJ, Frosch MP, et al. Thal Amyloid Stages Do Not Significantly Impact the Correlation Between Neuropathological Change and Cognition in the Alzheimer Disease Continuum. J Neuropathol Exp Neurol. 2016 Jun 1;75(6):516–26.

79. Maura Malpetti, Renaud La Joie, Gil D. Rabinovici. Tau Beats Amyloid in Predicting Brain Atrophy in Alzheimer Disease: Implications for Prognosis and Clinical Trials. J Nucl Med. 2022 Jun 1;63(6):830.

80. Brier MR, Gordon B, Friedrichsen K, McCarthy J, Stern A, Christensen J, et al. Tau and Aβ imaging, CSF measures, and cognition in Alzheimer's disease. Sci Transl Med. 2016 May 11;8(338):338ra66-338ra66.

81. K.M. Rodrigue, K.M. Kennedy, M.D. Devous Sr, J.R. Rieck, A.C. Hebrank, R. Diaz-Arrastia, et al. β-Amyloid burden in healthy aging. Neurology. 2012 Feb 7;78(6):387.

82. Aizenstein HJ, Nebes RD, Saxton JA, Price JC, Mathis CA, Tsopelas ND, et al. Frequent amyloid deposition without significant cognitive impairment among the elderly. Arch Neurol. 2008 Nov;65(11):1509–17.

83. Nasrabady SE, Rizvi B, Goldman JE, Brickman AM. White matter changes in Alzheimer's disease: a focus on myelin and oligodendrocytes. Acta Neuropathol Commun. 2018 Mar 2;6(1):22.

84. Planche V, Manjon JV, Mansencal B, Lanuza E, Tourdias T, Catheline G, et al. Structural progression of Alzheimer's disease over decades: the MRI staging scheme. Brain Commun. 2022 Jun 1;4(3):fcac109.

85. Logue MW, Posner H, Green RC, Moline M, Cupples LA, Lunetta KL, et al. Magnetic resonance imaging-measured atrophy and its relationship to cognitive functioning in vascular dementia and Alzheimer's disease patients. Alzheimers Dement. 2011 Sep 1;7(5):493–500.

86. Keret O, Staffaroni AM, Ringman JM, Cobigo Y, Goh SYM, Wolf A, et al. Pattern and degree of individual brain atrophy predicts dementia onset in dominantly inherited Alzheimer's disease. Alzheimers Dement Diagn Assess Dis Monit. 2021 Jan 1;13(1):e12197.

87. Serrano ME, Kim E, Petrinovic MM, Turkheimer F, Cash D. Imaging Synaptic Density: The Next Holy Grail of Neuroscience? Front Neurosci [Internet]. 2022;16. Available from: https://www.frontiersin.org/articles/10.3389/fnins.2022.796129

88. Chen MK, Mecca AP, Naganawa M, Finnema SJ, Toyonaga T, Lin S fei, et al. Assessing Synaptic Density in Alzheimer Disease With Synaptic Vesicle Glycoprotein 2A Positron Emission Tomographic Imaging. JAMA Neurol. 2018 Oct 1;75(10):1215–24.

89. Mecca AP, Chen MK, O'Dell RS, Naganawa M, Toyonaga T, Godek TA, et al. In vivo measurement of widespread synaptic loss in Alzheimer's disease with SV2A PET. Alzheimers Dement J Alzheimers Assoc. 2020/05/13 ed. 2020 Jul;16(7):974–82.

90. Guilarte TR, Rodichkin AN, McGlothan JL, Acanda De La Rocha AM, Azzam DJ. Imaging neuroinflammation with TSPO: A new perspective on the cellular sources and subcellular localization. Pharmacol Ther. 2022 Jun 1;234:108048.

91. Zhou R, Ji B, Kong Y, Qin L, Ren W, Guan Y, et al. PET Imaging of Neuroinflammation in Alzheimer's Disease. Front Immunol [Internet]. 2021;12. Available from: https://www.frontiersin.org/articles/10.3389/fimmu.2021.739130

92. Garland EF, Dennett O, Lau LC, Chatelet DS, Bottlaender M, Nicoll JAR, et al. The mitochondrial protein TSPO in Alzheimer's disease: relation to the severity of AD pathology and the neuroinflammatory environment. J Neuroinflammation. 2023 Aug 14;20(1):186.

93. Villemagne VL, Lopresti BJ, Doré V, Tudorascu D, Ikonomovic MD, Burnham S, et al. What Is T+? A Gordian Knot of Tracers, Thresholds, and Topographies. J Nucl Med. 2021 May;62(5):614–9.

94. Lowe VJ, Lundt ES, Albertson SM, Przybelski SA, Senjem ML, Parisi JE, et al. Neuroimaging correlates with neuropathologic schemes in neurodegenerative disease. Alzheimers Dement. 2019 Jul 1;15(7):927–39.

95. Frisoni GB, Boccardi M, Barkhof F, Blennow K, Cappa S, Chiotis K, et al. Strategic roadmap for an early diagnosis of Alzheimer's disease based on biomarkers. Lancet Neurol. 2017 Aug 1;16(8):661–76.

96. Mouton PR, Martin LJ, Calhoun ME, Dal Forno G, Price DL. Cognitive decline strongly correlates with cortical atrophy in Alzheimer's dementia. Neurobiol Aging. 1998 Sep 1;19(5):371–7.

97. Skillbäck T, Farahmand BY, Rosén C, Mattsson N, Nägga K, Kilander L, et al. Cerebrospinal fluid tau and amyloid-β1-42 in patients with dementia. Brain. 2015 Sep 1;138(9):2716–31.

98. Radanovic M, Oshiro CA, Freitas TQ, Talib LL, Forlenza OV. Correlation between CSF biomarkers of Alzheimer's disease and global cognition in a psychogeriatric clinic cohort. Rev Bras Psiquiatr Sao Paulo Braz 1999. 2019;41(6):479–84.

99. Pena Pardo FJ, García Vicente AM, Amo-Salas M, Mondéjar Marín B, Navarro Muñoz S, García Hortelano P, et al. Correlation of Global and Regional Amyloid Burden by 18F-Florbetaben PET/CT With Cognitive Impairment Profile and Severity. Clin Nucl Med [Internet]. 2022;47(11). Available from: https://journals.lww.com/nuclearmed/Fulltext/2022/11000/Correlation_of_Global_and_Regional_Amyloid_Burden.1.aspx

100. Val J. Lowe, Tyler J. Bruinsma, Heather J. Wiste, Hoon-Ki Min, Stephen D. Weigand, Ping Fang, et al. Cross-sectional associations of tau-PET signal with cognition in cognitively unimpaired adults. Neurology. 2019 Jul 2;93(1):e29.

101. Weise D, Tiepolt S, Awissus C, Hoffmann KT, Lobsien D, Kaiser T, et al. Critical Comparison of Different Biomarkers for Alzheimer's Disease in a Clinical Setting. J Alzheimers Dis. 2015;48(2):425–32.

102. Sengupta U, Portelius E, Hansson O, Farmer K, Castillo-Carranza D, Woltjer R, et al. Tau oligomers in cerebrospinal fluid in Alzheimer's disease. Ann Clin Transl Neurol. 2017 Mar 1;4(4):226–35.

103. An SSA, Hulme JP. Plasma amyloid-beta oligomer and phosphorylated tau: diagnostic tools for progressive Alzheimer's disease. Neural Regen Res [Internet]. 2023;18(11). Available from: https://journals.lww.com/nrronline/fulltext/2023/11000/plasma_amyloid_beta_oligomer_and_phosphorylated.15.aspx

104. Janelidze S, Stomrud E, Smith R, Palmqvist S, Mattsson N, Airey DC, et al. Cerebrospinal fluid p-tau217 performs better than p-tau181 as a biomarker of Alzheimer's disease. Nat Commun. 2020 Apr 3;11(1):1683.

105. Tomiyama T, Shimada H. APP Osaka Mutation in Familial Alzheimer's Disease—Its Discovery, Phenotypes, and Mechanism of Recessive Inheritance. Int J Mol Sci. 2020;21(4).

106. Basun H, Bogdanovic N, Ingelsson M, Almkvist O, Näslund J, Axelman K, et al. Clinical and Neuropathological Features of the Arctic APP Gene Mutation Causing Early-Onset Alzheimer Disease. Arch Neurol. 2008 Apr 1;65(4):499–505.

107. Kalimo H, Lalowski M, Bogdanovic N, Philipson O, Bird TD, Nochlin D, et al. The Arctic AβPP mutation leads to Alzheimer's disease pathology with highly variable topographic deposition of differentially truncated Aβ. Acta Neuropathol Commun. 2013 Sep 10;1(1):60.

108. Meng X, Li T, Wang X, Lv X, Sun Z, Zhang J, et al. Association between increased levels of amyloid-β oligomers in plasma and episodic memory loss in Alzheimer's disease. Alzheimers Res Ther. 2019 Oct 25;11(1):89.

109. Lewczuk P, Łukaszewicz-Zając M, Mroczko P, Kornhuber J. Clinical significance of fluid biomarkers in Alzheimer's Disease. Pharmacol Rep. 2020 Jun 1;72(3):528–42.

110. Ferreira D, Perestelo-Perez L, Westman E, Wahlund L olof, Sarria A, Serrano-Aguilar P. Meta-Review of CSF Core Biomarkers in Alzheimer's Disease: The State-of-the-Art after the New

Revised Diagnostic Criteria. Front Aging Neurosci [Internet]. 2014;6. Available from: https://www.frontiersin.org/articles/10.3389/fnagi.2014.00047

111. Marianne Chapleau, Leonardo Iaccarino, David Soleimani-Meigooni, Gil D. Rabinovici. The Role of Amyloid PET in Imaging Neurodegenerative Disorders: A Review. J Nucl Med. 2022 Jun 1;63(Supplement 1):13S.

112. Ossenkoppele R, Pichet Binette A, Groot C, Smith R, Strandberg O, Palmqvist S, et al. Amyloid and tau PET-positive cognitively unimpaired individuals are at high risk for future cognitive decline. Nat Med. 2022 Nov 1;28(11):2381–7.

113. Lowe VJ, Lundt ES, Albertson SM, Min HK, Fang P, Przybelski SA, et al. Tau-positron emission tomography correlates with neuropathology findings. Alzheimers Dement. 2020 Mar 1;16(3):561–71.

114. Ossenkoppele R, Reimand J, Smith R, Leuzy A, Strandberg O, Palmqvist S, et al. Tau PET correlates with different Alzheimer's disease-related features compared to CSF and plasma p-tau biomarkers. EMBO Mol Med. 2021 Aug 9;13(8):e14398.

115. Sebastian Palmqvist, Henrik Zetterberg, Niklas Mattsson, Per Johansson, For the Alzheimer's Disease Neuroimaging Initiative, Lennart Minthon, et al. Detailed comparison of amyloid PET and CSF biomarkers for identifying early Alzheimer disease. Neurology. 2015 Oct 6;85(14):1240.

116. Bischof GN, Dodich A, Boccardi M, van Eimeren T, Festari C, Barthel H, et al. Clinical validity of second-generation tau PET tracers as biomarkers for Alzheimer's disease in the context of a structured 5-phase development framework. Eur J Nucl Med Mol Imaging. 2021 Jul 1;48(7):2110–20.

117. Iaccarino L, Chiotis K, Alongi P, Almkvist O, Wall A, Cerami C, et al. A Cross-Validation of FDG- and Amyloid-PET Biomarkers in Mild Cognitive Impairment for the Risk Prediction to Dementia due to Alzheimer's Disease in a Clinical Setting. J Alzheimers Dis. 2017;59(2):603–14.

118. Han X, Guo S, Ji N, Li T, Liu J, Ye X, et al. Whole human-brain mapping of single cortical neurons for profiling morphological diversity and stereotypy. Sci Adv. 9(41):eadf3771.

119. Herlin B, Navarro V, Dupont S. The temporal pole: From anatomy to function—A literature appraisal. J Chem Neuroanat. 2021 Apr 1;113:101925.

120. Tomadesso C, Perrotin A, Mutlu J, Mézenge F, Landeau B, Egret S, et al. Brain structural, functional, and cognitive correlates of recent versus remote autobiographical memories in amnestic Mild Cognitive Impairment. NeuroImage Clin. 2015 Jan 1;8:473–82.

121. Supèr H. Working Memory in the Primary Visual Cortex. Arch Neurol. 2003 Jun 1;60(6):809–12.

122. Brewer A, Barton B. Visual cortex in aging and Alzheimer's disease: changes in visual field maps and population receptive fields. Front Psychol [Internet]. 2014;5. Available from: https://www.frontiersin.org/article/10.3389/fpsyg.2014.00074

123. Liao C, Xu J, Chen Y, Ip NY. Retinal Dysfunction in Alzheimer's Disease and Implications for Biomarkers. Biomolecules. 2021;11(8).

124. López-Cuenca I, Nebreda A, García-Colomo A, Salobrar-García E, de Frutos-Lucas J, Bruña R, et al. Early visual alterations in individuals at-risk of Alzheimer's disease: a multidisciplinary approach. Alzheimers Res Ther. 2023 Jan 24;15(1):19.

125. Plaza-Rosales I, Brunetti E, Montefusco-Siegmund R, Madariaga S, Hafelin R, Ponce DP, et al. Visual-spatial processing impairment in the occipital-frontal connectivity network at early stages of Alzheimer's disease. Front Aging Neurosci [Internet]. 2023;15. Available from: https://www.frontiersin.org/articles/10.3389/fnagi.2023.1097577

126. Alyssa A. Brewer, Brian Barton. Changes in Visual Cortex in Healthy Aging and Dementia. In: Davide Vito Moretti, editor. Update on Dementia [Internet]. Rijeka: IntechOpen; 2016 [cited 2023 May 30]. p. Ch. 12. Available from: https://doi.org/10.5772/64562

127. Schott JM, Crutch SJ. Posterior Cortical Atrophy. Contin Lifelong Learn Neurol [Internet]. 2019;25(1). Available from: https://journals.lww.com/continuum/Fulltext/2019/02000/Posterior_Cortical_Atrophy.6.aspx

128. Herbet G, Zemmoura I, Duffau H. Functional Anatomy of the Inferior Longitudinal Fasciculus: From Historical Reports to Current Hypotheses. Front Neuroanat [Internet]. 2018;12. Available from: https://www.frontiersin.org/articles/10.3389/fnana.2018.00077

129. Yu X, Shao K, Wan K, Li T, Li Y, Zhu X, et al. Progress in blood biomarkers of subjective cognitive decline in preclinical Alzheimer's disease. Chin Med J (Engl) [Internet]. 2023;136(5). Available from: https://journals.lww.com/cmj/Fulltext/2023/03050/Progress_in_blood_biomarkers_of_subjective.1.aspx

130. Brookmeyer R, Corrada MM, Curriero FC, Kawas C. Survival Following a Diagnosis of Alzheimer Disease. Arch Neurol. 2002 Nov 1;59(11):1764–7.

131. Plassman BL, Langa KM, Fisher GG, Heeringa SG, Weir DR, Ofstedal MB, et al. Prevalence of Dementia in the United States: The Aging, Demographics, and Memory Study. Neuroepidemiology. 2007;29(1–2):125–32.

132. Schneider JA, Arvanitakis Z, Bang W, Bennett DA. Mixed brain pathologies account for most dementia cases in community-dwelling older persons. Neurology. 2007 Dec 11;69(24):2197.

133. Fernando MS, Ince PG. Vascular pathologies and cognition in a population-based cohort of elderly people. Proc First Congr Int Soc Vasc Behav Cogn Disord VAS-COG 2003. 2004 Nov 15;226(1):13–7.

134. Pathological correlates of late-onset dementia in a multicentre, community-based population in England and Wales. The Lancet. 2001 Jan 20;357(9251):169–75.

135. Jellinger KA, Attems J. Challenges of multimorbidity of the aging brain: a critical update. J Neural Transm. 2015 Apr 1;122(4):505–21.

136. Twohig D, Nielsen HM. α-synuclein in the pathophysiology of Alzheimer's disease. Mol Neurodegener. 2019 Jun 11;14(1):23.

137. Leverenz JB, Fishel MA, Peskind ER, Montine TJ, Nochlin D, Steinbart E, et al. Lewy body pathology in familial Alzheimer disease: evidence for disease- and mutation-specific pathologic phenotype. Arch Neurol. 2006 Mar;63(3):370–6.

138. Beach TG, Malek-Ahmadi M. Alzheimer's Disease Neuropathological Comorbidities are Common in the Younger-Old. J Alzheimers Dis JAD. 2021;79(1):389–400.

139. Nelson PT, Dickson DW, Trojanowski JQ, Jack CR, Boyle PA, Arfanakis K, et al. Limbic-predominant age-related TDP-43 encephalopathy (LATE): consensus working group report. Brain. 2019 Jun 1;142(6):1503–27.

140. Tomé SO, Tsaka G, Ronisz A, Ospitalieri S, Gawor K, Gomes LA, et al. TDP-43 pathology is associated with increased tau burdens and seeding. Mol Neurodegener. 2023 Sep 30;18(1):71.

141. Kawas CH, Kim RC, Sonnen JA, Bullain SS, Trieu T, Corrada MM. Multiple pathologies are common and related to dementia in the oldest-old: The 90+ Study. Neurology. 2015/07/15 ed. 2015 Aug 11;85(6):535–42.

142. Sengupta U, Kayed R. Amyloid β, Tau, and α-Synuclein aggregates in the pathogenesis, prognosis, and therapeutics for neurodegenerative diseases. Prog Neurobiol. 2022 Jul 1;214:102270.

143. McAleese KE, Colloby SJ, Thomas AJ, Al-Sarraj S, Ansorge O, Neal J, et al. Concomitant neurodegenerative pathologies contribute to the transition from mild cognitive impairment to dementia. Alzheimers Dement. 2021 Jul 1;17(7):1121–33.

144. Badiola N, de Oliveira RM, Herrera F, Guardia-Laguarta C, Gonçalves SA, Pera M, et al. Tau enhances α-synuclein aggregation and toxicity in cellular models of synucleinopathy. PloS One. 2011/10/24 ed. 2011;6(10):e26609–e26609.

145. Moszczynski AJ, Harvey M, Fulcher N, de Oliveira C, McCunn P, Donison N, et al. Synergistic toxicity in an in vivo model of neurodegeneration through the co-expression of human TDP-43M337V and tauT175D protein. Acta Neuropathol Commun. 2019 Nov 8;7(1):170.

146. Jo M, Lee S, Jeon YM, Kim S, Kwon Y, Kim HJ. The role of TDP-43 propagation in neurodegenerative diseases: integrating insights from clinical and experimental studies. Exp Mol Med. 2020 Oct 1;52(10):1652–62.

147. Twohig D, Nielsen HM. α-synuclein in the pathophysiology of Alzheimer's disease. Mol Neurodegener. 2019 Jun 11;14(1):23.

148. Ebenau JL, Timmers T, Wesselman LMP, Verberk IMW, Verfaillie SCJ, Slot RER, et al. ATN classification and clinical progression in subjective cognitive decline: The SCIENCe project. Neurology. 2020/06/10 ed. 2020 Jul 7;95(1):e46–58.

149. Colom-Cadena M, Pegueroles J, Herrmann AG, Henstridge CM, Muñoz L, Querol-Vilaseca M, et al. Synaptic phosphorylated α-synuclein in dementia with Lewy bodies. Brain J Neurol. 2017 Dec 1;140(12):3204–14.

150. Niewiadomska G, Niewiadomski W, Steczkowska M, Gasiorowska A. Tau Oligomers Neurotoxicity. Life Basel Switz. 2021 Jan 6;11(1):28.

151. de Heus RAA, Olde Rikkert MGM, Tully PJ, Lawlor BA, Claassen JAHR, null null. Blood Pressure Variability and Progression of Clinical Alzheimer Disease. Hypertension. 2019 Nov 1;74(5):1172–80.

152. Mahinrad S, Bennett DA, Sorond FA, Gorelick PB. Blood pressure variability, dementia, and role of antihypertensive medications in older adults. Alzheimers Dement [Internet]. 2023 Jan 19 [cited 2023 Jul 4];n/a(n/a). Available from: https://doi.org/10.1002/alz.12935

153. Attems J, Jellinger KA. The overlap between vascular disease and Alzheimer's disease - lessons from pathology. BMC Med. 2014 Nov 11;12(1):206.

154. Rocco J. Cannistraro, Mohammed Badi, Benjamin H. Eidelman, Dennis W. Dickson, Erik H. Middlebrooks, James F. Meschia. CNS small vessel disease. Neurology. 2019 Jun 11;92(24):1146.

155. Dewenter A, Jacob MA, Cai M, Gesierich B, Hager P, Kopczak A, et al. Disentangling the effects of Alzheimer's and small vessel disease on white matter fibre tracts. Brain. 2023 Feb 1;146(2):678–89.

156. Hase Y, Ding R, Harrison G, Hawthorne E, King A, Gettings S, et al. White matter capillaries in vascular and neurodegenerative dementias. Acta Neuropathol Commun. 2019 Feb 7;7(1):16.

157. Kalaria RN, Sepulveda-Falla D. Cerebral Small Vessel Disease in Sporadic and Familial Alzheimer Disease. Am J Pathol. 2021 Nov 1;191(11):1888–905.

158. Matthews FE, Brayne C, Lowe J, McKeith I, Wharton SB, Ince P. Epidemiological Pathology of Dementia: Attributable-Risks at Death in the Medical Research Council Cognitive Function and Ageing Study. PLOS Med. 2009 Nov 10;6(11):e1000180.

159. Burns JM, Church JA, Johnson DK, Xiong C, Marcus D, Fotenos AF, et al. White Matter Lesions Are Prevalent but Differentially Related With Cognition in Aging and Early Alzheimer Disease. Arch Neurol. 2005 Dec 1;62(12):1870–6.

160. S Artero, H Tiemeier, N D Prins, R Sabatier, M M B Breteler, K Ritchie. Neuroanatomical localisation and clinical correlates of white matter lesions in the elderly. J Neurol Neurosurg Amp Psychiatry. 2004 Sep 1;75(9):1304.

161. Charles D. Smith, David A. Snowdon, Hao Wang, William R. Markesbery. White matter volumes and periventricular white matter hyperintensities in aging and dementia. Neurology. 2000 Feb 22;54(4):838.

162. A A Capizzano, L Ación, T Bekinschtein, M Furman, H Gomila, A Martínez, et al. White matter hyperintensities are significantly associated with cortical atrophy in Alzheimer's disease. J Neurol Neurosurg Amp Psychiatry. 2004 Jun 1;75(6):822.

163. M. Tullberg, E. Fletcher, C. DeCarli, D. Mungas, B. R. Reed, D. J. Harvey, et al. White matter lesions impair frontal lobe function regardless of their location. Neurology. 2004 Jul 27;63(2):246.

164. Assal F. History of Dementia. In: Frontiers of Neurology and Neuroscience [Internet]. 2019. p. 118–26. Available from: https://www.karger.com/DOI/10.1159/000494959

165. Sachdev PS, Blacker D, Blazer DG, Ganguli M, Jeste DV, Paulsen JS, et al. Classifying neurocognitive disorders: the DSM-5 approach. Nat Rev Neurol. 2014 Nov 1;10(11):634–42.

166. Lethin C, Rahm Hallberg I, Renom Guiteras A, Verbeek H, Saks K, Stolt M, et al. Prevalence of dementia diagnoses not otherwise specified in eight European countries: a cross-sectional cohort study. BMC Geriatr. 2019 Jun 24;19(1):172.

167. Wingo TS, Lah JJ, Levey AI, Cutler DJ. Autosomal Recessive Causes Likely in Early-Onset Alzheimer Disease. Arch Neurol. 2012 Jan 1;69(1):59–64.

168. Christiane Reitz, Ekaterina Rogaeva, Gary W. Beecham. Late-onset vs nonmendelian early-onset Alzheimer disease. Neurol Genet. 2020 Oct 1;6(5):e512.

169. Kremen WS, Jak AJ, Panizzon MS, Spoon KM, Franz CE, Thompson WK, et al. Early identification and heritability of mild cognitive impairment. Int J Epidemiol. 2014 Apr 1;43(2):600–10.

170. Plassman BL, Langa KM, McCammon RJ, Fisher GG, Potter GG, Burke JR, et al. Incidence of dementia and cognitive impairment, not dementia in the united states. Ann Neurol. 2011 Sep 1;70(3):418–26.

171. Devi G. A how-to guide for a precision medicine approach to the diagnosis and treatment of Alzheimer's disease. Front Aging Neurosci [Internet]. 2023;15. Available from: https://www.frontiersin.org/articles/10.3389/fnagi.2023.1213968

172. Beam CR, Kaneshiro C, Jang JY, Reynolds CA, Pedersen NL, Gatz M. Differences Between Women and Men in Incidence Rates of Dementia and Alzheimer's Disease. J Alzheimers Dis. 2018;64(4):1077–83.

173. Hale JM, Schneider DC, Mehta NK, Myrskylä M. Cognitive impairment in the U.S.: Lifetime risk, age at onset, and years impaired. SSM - Popul Health. 2020 Aug 1;11:100577.

174. Anderson ND. State of the science on mild cognitive impairment (MCI). CNS Spectr. 2019/01/17 ed. 2019;24(1):78–87.

175. Gillis C, Mirzaei F, Potashman M, Ikram MA, Maserejian N. The incidence of mild cognitive impairment: A systematic review and data synthesis. Alzheimers Dement Diagn Assess Dis Monit. 2019 Dec 1;11(1):248–56.

176. Shigemizu D, Akiyama S, Higaki S, Sugimoto T, Sakurai T, Boroevich KA, et al. Prognosis prediction model for conversion from mild cognitive impairment to Alzheimer's disease created by integrative analysis of multi-omics data. Alzheimers Res Ther. 2020 Nov 10;12(1):145.

177. Chen Y, Qian X, Zhang Y, Su W, Huang Y, Wang X, et al. Prediction Models for Conversion From Mild Cognitive Impairment to Alzheimer's Disease: A Systematic Review and Meta-Analysis. Front Aging Neurosci [Internet]. 2022;14. Available from: https://www.frontiersin.org/articles/10.3389/fnagi.2022.840386

178. Matthews KA, Xu W, Gaglioti AH, Holt JB, Croft JB, Mack D, et al. Racial and ethnic estimates of Alzheimer's disease and related dementias in the United States (2015–2060) in adults aged ≥65 years. Alzheimers Dement. 2019 Jan 1;15(1):17–24.

179. Hebert LE, Scherr PA, Bienias JL, Bennett DA, Evans DA. Alzheimer Disease in the US Population: Prevalence Estimates Using the 2000 Census. Arch Neurol. 2003 Aug 1;60(8):1119–22.

180. Amjad H, Roth DL, Sheehan OC, Lyketsos CG, Wolff JL, Samus QM. Underdiagnosis of Dementia: an Observational Study of Patterns in Diagnosis and Awareness in US Older Adults. J Gen Intern Med. 2018 Jul 1;33(7):1131–8.

181. Gamble LD, Matthews FE, Jones IR, Hillman AE, Woods B, Macleod CA, et al. Characteristics of people living with undiagnosed dementia: findings from the CFAS Wales study. BMC Geriatr. 2022 May 10;22(1):409.

182. Wright CB, DeRosa JT, Moon MP, Strobino K, DeCarli C, Cheung YK, et al. Race/Ethnic Disparities in Mild Cognitive Impairment and Dementia: The Northern Manhattan Study. J Alzheimers Dis. 2021;80(3):1129–38.

183. Kornblith E, Bahorik A, Boscardin WJ, Xia F, Barnes DE, Yaffe K. Association of Race and Ethnicity With Incidence of Dementia Among Older Adults. JAMA. 2022 Apr 19;327(15):1488–95.

184. M.-X. Tang, P. Cross, H. Andrews, D. M. Jacobs, S. Small, K. Bell, et al. Incidence of AD in African-Americans, Caribbean Hispanics, and Caucasians in northern Manhattan. Neurology. 2001 Jan 9;56(1):49.

185. Sharp ES, Gatz M. Relationship Between Education and Dementia: An Updated Systematic Review. Alzheimer Dis Assoc Disord [Internet]. 2011;25(4). Available from: https://journals.lww.com/alzheimerjournal/Fulltext/2011/10000/Relationship_Between_Education_and_Dementia__An.2.aspx

186. Then FS, Luck T, Angermeyer MC, Riedel-Heller SG. Education as protector against dementia, but what exactly do we mean by education? Age Ageing. 2016 Jul 1;45(4):523–8.

187. Dekhtyar S, Wang HX, Scott K, Goodman A, Koupil I, Herlitz A. A Life-Course Study of Cognitive Reserve in Dementia—From Childhood to Old Age. Longitud Stud. 2015 Sep 1;23(9):885–96.

188. Reisberg B, Ferris SH, Leon MJ de, Franssen ESE, Kluger A, Mir P, et al. Stage-specific behavioral, cognitive, and in vivo changes in community residing subjects with age-associated memory impairment and primary degenerative dementia of the Alzheimer type. Drug Dev Res. 1988;15.

189. Oscar L. Lopez. Mild Cognitive Impairment. Contin Minneap Minn 2013 Apr 192 Dement 411–424.

190. Caffò AO, Spano G, Tinella L, Lopez A, Ricciardi E, Stasolla F, et al. The Prevalence of Amnestic and Non-Amnestic Mild Cognitive Impairment and Its Association with Different Lifestyle Factors in a South Italian Elderly Population. Int J Environ Res Public Health. 2022;19(5).

191. Csukly G, Sirály E, Fodor Z, Horváth A, Salacz P, Hidasi Z, et al. The Differentiation of Amnestic Type MCI from the Non-Amnestic Types by Structural MRI. Front Aging Neurosci [Internet]. 2016;8. Available from: https://www.frontiersin.org/articles/10.3389/fnagi.2016.00052

192. Rosenberg A, Solomon A, Jelic V, Hagman G, Bogdanovic N, Kivipelto M. Progression to dementia in memory clinic patients with mild cognitive impairment and normal β-amyloid. Alzheimers Res Ther. 2019 Dec 5;11(1):99.

193. Thaipisuttikul P, Jaikla K, Satthong S, Wisajun P. Rate of conversion from mild cognitive impairment to dementia in a Thai hospital-based population: A retrospective cohort. Alzheimers Dement Transl Res Clin Interv. 2022 Jan 1;8(1):e12272.

194. Rosebud O. Roberts, David S. Knopman, Michelle M. Mielke, Ruth H. Cha, V. Shane Pankratz, Teresa J.H. Christianson, et al. Higher risk of progression to dementia in mild cognitive impairment cases who revert to normal. Neurology. 2014 Jan 28;82(4):317.

195. Jia X, Wang Z, Huang F, Su C, Du W, Jiang H, et al. A comparison of the Mini-Mental State Examination (MMSE) with the Montreal Cognitive Assessment (MoCA) for mild cognitive impairment screening in Chinese middle-aged and older population: a cross-sectional study. BMC Psychiatry. 2021 Oct 4;21(1):485.

196. Sanford AM. Mild Cognitive Impairment. Clin Geriatr Med. 2017 Aug 1;33(3):325–37.

197. Thomas KR, Edmonds EC, Eppig JS, Wong CG, Weigand AJ, Bangen KJ, et al. MCI-to-normal reversion using neuropsychological criteria in the Alzheimer's Disease Neuroimaging Initiative. Alzheimers Dement. 2019 Oct 1;15(10):1322–32.

198. Canevelli M, Bruno G, Remiddi F, Vico C, Lacorte E, Vanacore N, et al. Spontaneous Reversion of Clinical Conditions Measuring the Risk Profile of the Individual: From Frailty to Mild Cognitive Impairment. Front Med [Internet]. 2017;4. Available from: https://www.frontiersin.org/articles/10.3389/fmed.2017.00184

199. Malek-Ahmadi M. Reversion From Mild Cognitive Impairment to Normal Cognition: A Meta-Analysis. Alzheimer Dis Assoc Disord [Internet]. 2016;30(4). Available from: https://journals.lww.com/alzheimerjournal/Fulltext/2016/10000/Reversion_From_Mild_Cognitive_Impairment_to_Normal.6.aspx

200. Mooldijk SS, Yaqub A, Wolters FJ, Licher S, Koudstaal PJ, Ikram MK, et al. Life expectancy with and without dementia in persons with mild cognitive impairment in the community. J Am Geriatr Soc. 2022 Feb 1;70(2):481–9.

201. Kukull WA, Brenner DE, Speck CE, Nochlin D, Bowen J, McCormick W, et al. Causes of Death Associated with Alzheimer Disease: Variation by Level of Cognitive Impairment Before Death. J Am Geriatr Soc. 1994 Jul 1;42(7):723–6.

202. Henrik Zetterberg, Jonathan M. Schott. Objectifying Subjective Cognitive Decline. Neurology. 2022 Oct 25;99(17):735.

203. Jessen F, Amariglio RE, van Boxtel M, Breteler M, Ceccaldi M, Chételat G, et al. A conceptual framework for research on subjective cognitive decline in preclinical Alzheimer's disease. Alzheimers Dement. 2014 Nov 1;10(6):844–52.

204. Jessen F, Amariglio RE, Buckley RF, van der Flier WM, Han Y, Molinuevo JL, et al. The characterisation of subjective cognitive decline. Lancet Neurol. 2020 Mar 1;19(3):271–8.

205. Parfenov VA, Zakharov VV, Kabaeva AR, Vakhnina NV. Subjective cognitive decline as a predictor of future cognitive decline: a systematic review. Dement Neuropsychol. 2020;14.

206. Ahn Sangwoo, Mathiason Michelle A., Salisbury Dereck, Yu Fang. Factors Predicting the Onset of Amnestic Mild Cognitive Impairment or Alzheimer's Dementia in Persons With Subjective Cognitive Decline. J Gerontol Nurs. 2020 Aug 1;46(8):28–36.

207. Hong YJ, Lee JH. Subjective Cognitive Decline and Alzheimer's Disease Spectrum Disorder. Dement Neurocogn Disord. 2017 Jun;16(2):40–7.

208. Wolfsgruber S, Molinuevo JL, Wagner M, Teunissen CE, Rami L, Coll-Padrós N, et al. Prevalence of abnormal Alzheimer's disease biomarkers in patients with subjective cognitive decline: cross-sectional comparison of three European memory clinic samples. Alzheimers Res Ther. 2019 Jan 17;11(1):8.

209. Catherine Randall LG Lisa Mosconi, Mony de Leon. Cerebrospinal fluid biomarkers of Alzheimer's disease in healthy elderly. FBL. 2013;18(3):1150–73.

210. Verde F, Aiello EN, Milone I, Giacopuzzi Grigoli E, Dubini A, Ratti A, et al. A + T ± status across MCI and dementia due to AD: a clinic-based, retrospective study. Neurol Sci. 2022 Nov 1;43(11):6547–50.

211. Tsoi KKF, Chan JYC, Hirai HW, Wong SYS, Kwok TCY. Cognitive Tests to Detect Dementia: A Systematic Review and Meta-analysis. JAMA Intern Med. 2015 Sep 1;175(9):1450–8.

212. Folstein MF, Folstein SE, McHugh PR. "Mini-mental state": A practical method for grading the cognitive state of patients for the clinician. J Psychiatr Res. 1975 Nov 1;12(3):189–98.

213. Ciolek CH, Lee SY. Chapter 19 - Cognitive Issues in the Older Adult. In: Avers D, Wong RA, editors. Guccione's Geriatric Physical Therapy (Fourth Edition) [Internet]. St. Louis (MO): Mosby; 2020. p. 425–52. Available from: https://www.sciencedirect.com/science/article/pii/B9780323609128000191

214. Kukull WA, Larson EB, Teri L, Bowen J, McCormick W, Pfanschmidt ML. The mini-mental state examination score and the clinical diagnosis of dementia. J Clin Epidemiol. 1994 Sep 1;47(9):1061–7.

215. Zhang S, Qiu Q, Qian S, Lin X, Yan F, Sun L, et al. Determining Appropriate Screening Tools and Cutoffs for Cognitive Impairment in the Chinese Elderly. Front Psychiatry [Internet]. 2021;12. Available from: https://www.frontiersin.org/articles/10.3389/fpsyt.2021.773281

216. Salis F, Costaggiu D, Mandas A. Mini-Mental State Examination: Optimal Cut-Off Levels for Mild and Severe Cognitive Impairment. Geriatrics. 2023;8(1).

217. Kaufman DM, Milstein MJ. Chapter 7 - Dementia. In: Kaufman DM, Milstein MJ, editors. Kaufman's Clinical Neurology for Psychiatrists (Seventh Edition) [Internet]. Philadelphia: W.B. Saunders; 2013. p. 109–54. Available from: https://www.sciencedirect.com/science/article/pii/B9780723437482000074

218. Siqueira GSA, Hagemann P de MS, Coelho D de S, Santos FHD, Bertolucci PHF. Can MoCA and MMSE Be Interchangeable Cognitive Screening Tools? A Systematic Review. The Gerontologist. 2019 Nov 16;59(6):e743–63.

219. Nasreddine ZS, Phillips NA, Bédirian V, Charbonneau S, Whitehead V, Collin I, et al. The Montreal Cognitive Assessment, MoCA: A Brief Screening Tool For Mild Cognitive Impairment. J Am Geriatr Soc. 2005 Apr 1;53(4):695–9.

220. Fasnacht JS, Wueest AS, Berres M, Thomann AE, Krumm S, Gutbrod K, et al. Conversion between the Montreal Cognitive Assessment and the Mini-Mental Status Examination. J Am Geriatr Soc. 2023 Mar 1;71(3):869–79.

221. Pasternak E, Smith G. Chapter 6 - Cognitive and neuropsychological examination of the elderly. In: Dekosky ST, Asthana S, editors. Handbook of Clinical Neurology [Internet]. Elsevier; 2019. p. 89–104. Available from: https://www.sciencedirect.com/science/article/pii/B9780128047668000066

222. O'Bryant SE, Waring SC, Cullum CM, Hall J, Lacritz L, Massman PJ, et al. Staging Dementia Using Clinical Dementia Rating Scale Sum of Boxes Scores: A Texas Alzheimer's Research Consortium Study. Arch Neurol. 2008 Aug 1;65(8):1091–5.

223. Woolf C, Slavin MJ, Draper B, Thomassen F, Kochan NA, Reppermund S, et al. Can the Clinical Dementia Rating Scale Identify Mild Cognitive Impairment and Predict Cognitive and Functional Decline? Dement Geriatr Cogn Disord. 2016 Aug;41(5–6):292+.

224. Tulsky DS, Zhu J, Prifitera A. Chapter 5 - Assessment of Adult Intelligence with the WAIS-III. In: Goldstein G, Hersen M, editors. Handbook of Psychological Assessment (Third Edition) [Internet]. Amsterdam: Pergamon; 2000. p. 97–129. Available from: https://www.sciencedirect.com/science/article/pii/B9780080436456500835

225. Jaeger J. Digit Symbol Substitution Test: The Case for Sensitivity Over Specificity in Neuropsychological Testing. J Clin Psychopharmacol [Internet]. 2018;38(5). Available from: https://journals.lww.com/psychopharmacology/Fulltext/2018/10000/Digit_Symbol_Substitution_Test__The_Case_for.19.aspx

226. Rosano C, Perera S, Inzitari M, Newman AB, Longstreth WT, Studenski S. Digit Symbol Substitution test and future clinical and subclinical disorders of cognition, mobility and mood in older adults. Age Ageing. 2016 Sep 1;45(5):688–95.

227. Williamson M, Maruff P, Schembri A, Cummins H, Bird L, Rosenich E, et al. Validation of a digit symbol substitution test for use in supervised and unsupervised assessment in mild Alzheimer's disease. J Clin Exp Neuropsychol. 2022 Nov 26;44(10):768–79.

228. Tsatali M, Poptsi E, Moraitou D, Agogiatou C, Bakoglidou E, Gialaouzidis M, et al. Discriminant Validity of the WAIS-R Digit Symbol Substitution Test in Subjective Cognitive Decline, Mild Cognitive Impairment (Amnestic Subtype) and Alzheimer's Disease Dementia (ADD) in Greece. Brain Sci. 2021;11(7).

229. Schnaider Beeri M, Silverman JM, Schmeidler J, Wysocki M, Grossman HZ, Purohit DP, et al. Clinical Dementia Rating Performed Several Years prior to Death Predicts Regional Alzheimer's Neuropathology. Dement Geriatr Cogn Disord. 2008 Mar 27;25(5):392–8.

230. Constance Hammond, Monique Esclapez,. The chemical synapses in Cellular and Molecular Neurophysiology (Fourth Edition), 2015.

231. Kubota Y, Karube F, Nomura M, Kawaguchi Y. The Diversity of Cortical Inhibitory Synapses. Front Neural Circuits [Internet]. 2016;10. Available from: https://www.frontiersin.org/article/10.3389/fncir.2016.00027

232. Sherwood CC, Miller SB, Karl M, Stimpson CD, Phillips KA, Jacobs B, et al. Invariant Synapse Density and Neuronal Connectivity Scaling in Primate Neocortical Evolution. Cereb Cortex. 2020 Sep 3;30(10):5604–15.

233. Sneve MA, Piatkevich KD. Towards a Comprehensive Optical Connectome at Single Synapse Resolution via Expansion Microscopy. Front Synaptic Neurosci [Internet]. 2022;13. Available from: https://www.frontiersin.org/articles/10.3389/fnsyn.2021.754814

234. Südhof TC. The cell biology of synapse formation. J Cell Biol. 2021 Jun 4;220(7):e202103052.

235. Xu T, Yu X, Perlik AJ, Tobin WF, Zweig JA, Tennant K, et al. Rapid formation and selective stabilization of synapses for enduring motor memories. Nature. 2009 Dec 1;462(7275):915–9.

236. Yang G, Pan F, Gan WB. Stably maintained dendritic spines are associated with lifelong memories. Nature. 2009 Dec 1;462(7275):920–4.

237. Berry KP, Nedivi E. Spine Dynamics: Are They All the Same? Neuron. 2017 Sep 27;96(1):43–55.

238. Attardo A, Fitzgerald JE, Schnitzer MJ. Impermanence of dendritic spines in live adult CA1 hippocampus. Nature. 2015 Jul 1;523(7562):592–6.

239. Holtmaat AJGD, Trachtenberg JT, Wilbrecht L, Shepherd GM, Zhang X, Knott GW, et al. Transient and Persistent Dendritic Spines in the Neocortex In Vivo. Neuron. 2005 Jan 20;45(2):279–91.

240. Vardalaki D, Chung K, Harnett MT. Filopodia are a structural substrate for silent synapses in adult neocortex. Nat 30 Nov 2022 6127939323-327 DOI 101038s41586-022-05483-6.

241. Nosov G, Kahms M, Klingauf J. The Decade of Super-Resolution Microscopy of the Presynapse. Front Synaptic Neurosci. 2020 Aug 11;12:32–32.

242. Sheng M, Kim E. The Postsynaptic Organization of Synapses. Cold Spring Harb Perspect Biol [Internet]. 2011 Nov 1; Available from: http://cshperspectives.cshlp.org/content/early/2011/11/01/cshperspect.a005678.abstract

243. Kay KR, Smith C, Wright AK, Serrano-Pozo A, Pooler AM, Koffie R, et al. Studying synapses in human brain with array tomography and electron microscopy. Nat Protoc. 2013 Jul 1;8(7):1366–80.

244. Smith SJ. Q&A: Array tomography. BMC Biol. 2018 Sep 6;16(1):98.

245. Chen F, Tillberg PW, Boyden ES. Optical imaging. Expansion microscopy. Science. 2015/01/15 ed. 2015 Jan 30;347(6221):543–8.

246. Tillberg PW, Chen F, Piatkevich KD, Zhao Y, Yu CC (Jay), English BP, et al. Protein-retention expansion microscopy of cells and tissues labeled using standard fluorescent proteins and antibodies. Nat Biotechnol. 2016 Sep 1;34(9):987–92.

247. Wassie AT, Zhao Y, Boyden ES. Expansion microscopy: principles and uses in biological research. Nat Methods. 2018/12/20 ed. 2019 Jan;16(1):33–41.

248. Zhao Y, Bucur O, Irshad H, Chen F, Weins A, Stancu AL, et al. Nanoscale imaging of clinical specimens using pathology-optimized expansion microscopy. Nat Biotechnol. 2017 Aug 1;35(8):757–64.

249. Sarkar D, Kang J, Wassie AT, Schroeder ME, Peng Z, Tarr TB, et al. Expansion Revealing: Decrowding Proteins to Unmask Invisible Brain Nanostructures. bioRxiv. 2020 Jan 1;2020.08.29.273540.

250. Ku T, Swaney J, Park JY, Albanese A, Murray E, Cho JH, et al. Multiplexed and scalable super-resolution imaging of three-dimensional protein localization in size-adjustable tissues. Nat Biotechnol. 2016 Sep 1;34(9):973–81.

251. Gao R, Asano SM, Upadhyayula S, Pisarev I, Milkie DE, Liu TL, et al. Cortical column and whole-brain imaging with molecular contrast and nanoscale resolution. Science. 2019 Jan 18;363(6424):eaau8302.

252. Gallagher BR, Zhao Y. Expansion microscopy: A powerful nanoscale imaging tool for neuroscientists. Neurobiol Dis. 2021 Jul 1;154:105362.

253. Li R, Chen X, Lin Z, Wang Y, Sun Y. Expansion enhanced nanoscopy. Nanoscale. 2018;10(37):17552–6.

254. Chang JB, Chen F, Yoon YG, Jung EE, Babcock H, Kang JS, et al. Iterative expansion microscopy. Nat Methods. 2017/04/17 ed. 2017 Jun;14(6):593–9.

255. DeKosky ST, Scheff SW. Synapse loss in frontal cortex biopsies in Alzheimer's disease: Correlation with cognitive severity. Ann Neurol. 1990 May 1;27(5):457–64.

256. Koffie RM, Hyman BT, Spires-Jones TL. Alzheimer's disease: synapses gone cold. Mol Neurodegener. 2011 Aug 26;6(1):63.

257. Terry RD, Masliah E, Salmon DP, Butters N, DeTeresa R, Hill R, et al. Physical basis of cognitive alterations in alzheimer's disease: Synapse loss is the major correlate of cognitive impairment. Ann Neurol. 1991 Oct 1;30(4):572–80.

258. Henstridge CM, Tzioras M, Paolicelli RC. Glial Contribution to Excitatory and Inhibitory Synapse Loss in Neurodegeneration. Front Cell Neurosci. 2019;13:63.

259. Vogels T, Murgoci AN, Hromádka T. Intersection of pathological tau and microglia at the synapse. Acta Neuropathol Commun. 2019 Jul 5;7(1):109.

260. Peter R. H. Synaptic density in human frontal cortex — Developmental changes and effects of aging. Brain Res. 1979 Mar 16;163(2):195–205.

261. Masliah E, Mallory M, Hansen L, DeTeresa R, Terry RD. Quantitative synaptic alterations in the human neocortex during normal aging. Neurology. 1993 Jan 1;43(1 Part 1):192.

262. Camporesi E, Nilsson J, Brinkmalm A, Becker B, Ashton NJ, Blennow K, et al. Fluid Biomarkers for Synaptic Dysfunction and Loss. Biomark Insights. 2020 Jan 1;15:1177271920950319.

263. Masliah E, Mallory M, Hansen L, Richard D, Alford M, Terry R. Synaptic and neuritic alterations during the progression of Alzheimer's disease. Neurosci Lett. 1994 Jun 6;174(1):67–72.

264. Martínez-Serra R, Alonso-Nanclares L, Cho K, Giese KP. Emerging insights into synapse dysregulation in Alzheimer's disease. Brain Commun. 2022 Apr 1;4(2):fcac083.

265. Qiang Q, Skudder-Hill L, Toyota T, Wei W, Adachi H. CSF GAP-43 as a biomarker of synaptic dysfunction is associated with tau pathology in Alzheimer's disease. Sci Rep. 2022 Oct 17;12(1):17392.

266. Sangyun Jeong. Molecular and Cellular Basis of Neurodegeneration in Alzheimer's Disease. Mol Cells. 2017/09/30 ed. 2017 Sep;40(9):613–20.

267. Griffiths J, Grant SGN. Synapse pathology in Alzheimer's disease. Spec Issue Alzheimer's Dis Eff Brain Circuits Synap. 2023 Apr 1;139:13–23.

268. Scheff SW, Price DA, Schmitt FA, Scheff MA, Mufson EJ. Synaptic loss in the inferior temporal gyrus in mild cognitive impairment and Alzheimer's disease. J Alzheimers Dis JAD. 2011;24(3):547–57.

269. Duits FH, Brinkmalm G, Teunissen CE, Brinkmalm A, Scheltens P, Van der Flier WM, et al. Synaptic proteins in CSF as potential novel biomarkers for prognosis in prodromal Alzheimer's disease. Alzheimers Res Ther. 2018 Jan 15;10(1):5.

270. Domínguez-Álvaro M, Montero-Crespo M, Blazquez-Llorca L, Insausti R, DeFelipe J, Alonso-Nanclares L. Three-dimensional analysis of synapses in the transentorhinal cortex of Alzheimer's disease patients. Acta Neuropathol Commun. 2018 Mar 2;6(1):20–20.

271. Montero-Crespo M, Domínguez-Álvaro M, Alonso-Nanclares L, DeFelipe J, Blazquez-Llorca L. Three-dimensional analysis of synaptic organization in the hippocampal CA1 field in Alzheimer's disease. Brain J Neurol. 2021 Mar 3;144(2):553–73.

272. Singh A, Allen D, Fracassi A, Tumurbaatar B, Natarajan C, Scaduto P, et al. Functional Integrity of Synapses in the Central Nervous System of Cognitively Intact Individuals with High Alzheimer's Disease Neuropathology Is Associated with Absence of Synaptic Tau Oligomers. J Alzheimers Dis. 2020;78(4):1661–78.

273. Mecca AP, O'Dell RS, Sharp ES, Banks ER, Bartlett HH, Zhao W, et al. Synaptic density and cognitive performance in Alzheimer's disease: A PET imaging study with [11C]UCB-J. Alzheimers Dement. 2022 Dec 1;18(12):2527–36.

274. Lauterborn JC, Scaduto P, Cox CD, Schulmann A, Lynch G, Gall CM, et al. Increased excitatory to inhibitory synaptic ratio in parietal cortex samples from individuals with Alzheimer's disease. Nat Commun. 2021 May 10;12(1):2603.

275. Davies CA, Mann DMA, Sumpter PQ, Yates PO. A quantitative morphometric analysis of the neuronal and synaptic content of the frontal and temporal cortex in patients with Alzheimer's disease. J Neurol Sci. 1987 Apr 1;78(2):151–64.

276. Gibson PH. EM study of the numbers of cortical synapses in the brains of ageing people and people with Alzheimer-type dementia. Acta Neuropathol (Berl). 1983 Mar 1;62(1):127–33.

277. Davidsson P, Blennow K. Neurochemical Dissection of Synaptic Pathology in Alzheimer's Disease. Int Psychogeriatr. 2005/01/10 ed. 1998;10(1):11–23.

278. Sze CI, Troncoso JC, Kawas C, Mouton P, Price DL, Martin LJ. Loss of the Presynaptic Vesicle Protein Synaptophysin in Hippocampus Correlates with Cognitive Decline in Alzheimer Disease. J Neuropathol Exp Neurol. 1997 Aug 1;56(8):933–44.

279. McMillan DB, Harris RJ. Chapter F - Nervous Tissue. In: McMillan DB, Harris RJ, editors. An Atlas of Comparative Vertebrate Histology [Internet]. San Diego: Academic Press; 2018. p. 141–70. Available from: https://www.sciencedirect.com/science/article/pii/B9780124104242000068

280. Kozikowski P. Extracting Three-dimensional Information from SEM Images by Means of Photogrammetry. Micron. 2020 Jul 1;134:102873.

281. Xu CS, Hayworth KJ, Lu Z, Grob P, Hassan AM, García-Cerdán JG, et al. Enhanced FIB-SEM systems for large-volume 3D imaging. Nathans J, editor. eLife. 2017 May 13;6:e25916.

282. Colom-Cadena M, Davies C, Sirisi S, Lee JE, Simzer EM, Tzioras M, et al. Synaptic oligomeric tau in Alzheimer's disease — A potential culprit in the spread of tau pathology through the brain. Neuron [Internet]. [cited 2023 May 26]; Available from: https://doi.org/10.1016/j.neuron.2023.04.020

283. Davidsson P, Jahn R, Bergquist J, Ekman R, Blennow K. Synaptotagmin, a synaptic vesicle protein, is present in human cerebrospinal fluid. Mol Chem Neuropathol. 1996 Feb 1;27(2):195–210.

284. Kvartsberg H, Portelius E, Andreasson U, Brinkmalm G, Hellwig K, Lelental N, et al. Characterization of the postsynaptic protein neurogranin in paired cerebrospinal fluid and plasma samples from Alzheimer's disease patients and healthy controls. Alzheimers Res Ther. 2015 Jul 1;7(1):40.

285. Das S, Goossens J, Jacobs D, Dewit N, Pijnenburg YAL, In 't Veld SGJG, et al. Synaptic biomarkers in the cerebrospinal fluid associate differentially with classical neuronal biomarkers in patients with Alzheimer's disease and frontotemporal dementia. Alzheimers Res Ther. 2023 Mar 24;15(1):62.

286. Bereczki E, Branca RM, Francis PT, Pereira JB, Baek JH, Hortobágyi T, et al. Synaptic markers of cognitive decline in neurodegenerative diseases: a proteomic approach. Brain. 2018 Feb 1;141(2):582–95.

287. Colom-Cadena M, Spires-Jones T, Zetterberg H, Blennow K, Caggiano A, DeKosky ST, et al. The clinical promise of biomarkers of synapse damage or loss in Alzheimer's disease. Alzheimers Res Ther. 2020 Mar 2;12(1):21.

288. Milà-Alomà M, Brinkmalm A, Ashton NJ, Kvartsberg H, Shekari M, Operto G, et al. CSF Synaptic Biomarkers in the Preclinical Stage of Alzheimer Disease and Their Association With MRI and PET. Neurology. 2021 Nov 23;97(21):e2065.

289. Nilsson J, Gobom J, Sjödin S, Brinkmalm G, Ashton NJ, Svensson J, et al. Cerebrospinal fluid biomarker panel for synaptic dysfunction in Alzheimer's disease. Alzheimers Dement Diagn Assess Dis Monit. 2021 Jan 1;13(1):e12179.

290. Ma QL, Teng E, Zuo X, Jones M, Teter B, Zhao EY, et al. Neuronal pentraxin 1: A synaptic-derived plasma biomarker in Alzheimer's disease. Neurobiol Dis. 2018/03/06 ed. 2018 Jun;114:120–8.

291. Vrillon A, Mouton-Liger F, Martinet M, Cognat E, Hourregue C, Dumurgier J, et al. Plasma neuregulin 1 as a synaptic biomarker in Alzheimer's disease: a discovery cohort study. Alzheimers Res Ther. 2022 May 23;14(1):71.

292. Goetzl EJ, Abner EL, Jicha GA, Kapogiannis D, Schwartz JB. Declining levels of functionally specialized synaptic proteins in plasma neuronal exosomes with progression of Alzheimer's disease. FASEB J Off Publ Fed Am Soc Exp Biol. 2018/01/04 ed. 2018 Feb;32(2):888–93.

293. Kivisäkk P, Carlyle BC, Sweeney T, Quinn JP, Ramirez CE, Trombetta BA, et al. Increased levels of the synaptic proteins PSD-95, SNAP-25, and neurogranin in the cerebrospinal fluid of patients with Alzheimer's disease. Alzheimers Res Ther. 2022 Apr 23;14(1):58.

294. Clarke MTM, Brinkmalm A, Foiani MS, Woollacott IOC, Heller C, Heslegrave A, et al. CSF synaptic protein concentrations are raised in those with atypical Alzheimer's disease but not frontotemporal dementia. Alzheimers Res Ther. 2019 Dec 17;11(1):105.

295. Palmqvist S, Insel PS, Stomrud E, Janelidze S, Zetterberg H, Brix B, et al. Cerebrospinal fluid and plasma biomarker trajectories with increasing amyloid deposition in Alzheimer's disease. EMBO Mol Med. 2019 Dec 1;11(12):e11170.

296. Smailovic U, Kåreholt I, Koenig T, Ashton NJ, Winblad B, Höglund K, et al. Synaptic Molecular and Neurophysiological Markers Are Independent Predictors of Progression in Alzheimer's Disease. J Alzheimers Dis JAD. 2021;83(1):355–66.

297. Colom-Cadena M, Spires-Jones T, Zetterberg H, Blennow K, Caggiano A, DeKosky ST, et al. The clinical promise of biomarkers of synapse damage or loss in Alzheimer's disease. Alzheimers Res Ther. 2020 Mar 2;12(1):21.

298. Smailovic U, Koenig T, Savitcheva I, Chiotis K, Nordberg A, Blennow K, et al. Regional Disconnection in Alzheimer Dementia and Amyloid-Positive Mild Cognitive Impairment: Association Between EEG Functional Connectivity and Brain Glucose Metabolism. Brain Connect. 2020 Dec 1;10(10):555–65.

299. Galasko D, Xiao M, Xu D, Smirnov D, Salmon DP, Dewit N, et al. Synaptic biomarkers in CSF aid in diagnosis, correlate with cognition and predict progression in MCI and Alzheimer's disease. Alzheimers Dement N Y N. 2019 Dec 9;5:871–82.

300. Portelius E, Zetterberg H, Skillbäck T, Törnqvist U, Andreasson U, Trojanowski JQ, et al. Cerebrospinal fluid neurogranin: relation to cognition and neurodegeneration in Alzheimer's disease. Brain. 2015 Nov 1;138(11):3373–85.

301. Peters van Ton AM, Verbeek MM, Alkema W, Pickkers P, Abdo WF. Downregulation of synapse-associated protein expression and loss of homeostatic microglial control in cerebrospinal fluid of infectious patients with delirium and patients with Alzheimer's disease. Brain Behav Immun. 2020 Oct 1;89:656–67.

302. Lleó A, Núñez-Llaves R, Alcolea D, Chiva C, Balateu-Paños D, Colom-Cadena M, et al. Changes in Synaptic Proteins Precede Neurodegeneration Markers in Preclinical Alzheimer's Disease Cerebrospinal Fluid *. Mol Cell Proteomics. 2019 Mar 1;18(3):546–60.

303. Oeckl P, Janelidze S, Halbgebauer S, Stomrud E, Palmqvist S, Otto M, et al. Higher plasma β-synuclein indicates early synaptic degeneration in Alzheimer's disease. Alzheimers Dement [Internet]. 2023 Apr 27 [cited 2023 Oct 5];n/a(n/a). Available from: https://doi.org/10.1002/alz.13103

304. Fessel J. The potential for one drug, administered at the earliest preclinical stage, to prevent the subsequent decline of cognition that eventuates in dementia. Alzheimers Dement Transl Res Clin Interv. 2020 Jan 1;6(1):e12084.

305. Zhang H, Lyu D, Jia J, for the Alzheimer's Disease Neuroimaging Initiative. The Trajectory of Cerebrospinal Fluid Growth-Associated Protein 43 in the Alzheimer's Disease Continuum: A Longitudinal Study. J Alzheimers Dis. 2022;85(4):1441–52.

306. Utz J, Berner J, Muñoz LE, Oberstein TJ, Kornhuber J, Herrmann M, et al. Cerebrospinal Fluid of Patients With Alzheimer's Disease Contains Increased Percentages of Synaptophysin-Bearing Microvesicles. Front Aging Neurosci [Internet]. 2021;13. Available from: https://www.frontiersin.org/articles/10.3389/fnagi.2021.682115

307. Libiger O, Shaw LM, Watson MH, Nairn AC, Umaña KL, Biarnes MC, et al. Longitudinal CSF proteomics identifies NPTX2 as a prognostic biomarker of Alzheimer's disease. Alzheimers Dement. 2021 Dec 1;17(12):1976–87.

308. Guillaume Becker. The Rise of Synaptic Density PET Imaging. Mol 2020 2510 2303 Httpsdoiorg103390molecules25102303.

309. Bajjalieh SM, Peterson K, Linial M, Scheller RH. Brain contains two forms of synaptic vesicle protein 2. Proc Natl Acad Sci. 1993 Mar 15;90(6):2150–4.

310. Lynch BA, Lambeng N, Nocka K, Kensel-Hammes P, Bajjalieh SM, Matagne A, et al. The synaptic vesicle protein SV2A is the binding site for the antiepileptic drug levetiracetam. Proc Natl Acad Sci. 2004 Jun 29;101(26):9861–6.

311. Kelly Smart, Isabelle Boileau. Uncovering the link between synaptic density and mental illness through in vivo imaging. J Psychiatry Neurosci. 2023 Apr 25;48(2):E143.

312. Soares Martins T, Marçalo R, da Cruz e Silva CB, Trindade D, Catita J, Amado F, et al. Novel Exosome Biomarker Candidates for Alzheimer's Disease Unravelled Through Mass Spectrometry Analysis. Mol Neurobiol. 2022 May 1;59(5):2838–54.

313. Tkach M, Théry C. Communication by Extracellular Vesicles: Where We Are and Where We Need to Go. Cell. 2016 Mar 10;164(6):1226–32.

314. Di Bella MA. Overview and Update on Extracellular Vesicles: Considerations on Exosomes and Their Application in Modern Medicine. Biology. 2022;11(6).

315. Cano A, Ettcheto M, Bernuz M, Puerta R, Esteban de Antonio E, Sánchez-López E, et al. Extracellular vesicles, the emerging mirrors of brain physiopathology. Int J Biol Sci. 2023;19(3):721–43.

316. Goetzl EJ, Kapogiannis D, Schwartz JB, Lobach IV, Goetzl L, Abner EL, et al. Decreased synaptic proteins in neuronal exosomes of frontotemporal dementia and Alzheimer's disease. FASEB J. 2016 Dec 1;30(12):4141–8.

317. Goetzl EJ, Schwartz JB, Abner EL, Jicha GA, Kapogiannis D. High complement levels in astrocyte-derived exosomes of Alzheimer disease. Ann Neurol. 2018 Mar 1;83(3):544–52.

318. Winston CN, Goetzl EJ, Schwartz JB, Elahi FM, Rissman RA. Complement protein levels in plasma astrocyte-derived exosomes are abnormal in conversion from mild cognitive

impairment to Alzheimer's disease dementia. Alzheimers Dement Diagn Assess Dis Monit. 2019 Dec 1;11(1):61–6.

319. Venturini A, Passalacqua M, Pelassa S, Pastorino F, Tedesco M, Cortese K, et al. Exosomes From Astrocyte Processes: Signaling to Neurons. Front Pharmacol [Internet]. 2019;10. Available from: https://www.frontiersin.org/articles/10.3389/fphar.2019.01452

320. Huo L, Du X, Li X, Liu S, Xu Y. The Emerging Role of Neural Cell-Derived Exosomes in Intercellular Communication in Health and Neurodegenerative Diseases. Front Neurosci [Internet]. 2021;15. Available from: https://www.frontiersin.org/articles/10.3389/fnins.2021.738442

321. Delaby C, Hirtz C, Lehmann S. Overview of the blood biomarkers in Alzheimer's disease: Promises and challenges. Rev Neurol (Paris). 2023 Mar 1;179(3):161–72.

322. Tian C, Stewart T, Hong Z, Guo Z, Aro P, Soltys D, et al. Blood extracellular vesicles carrying synaptic function- and brain-related proteins as potential biomarkers for Alzheimer's disease. Alzheimers Dement. 2023 Mar 1;19(3):909–23.

323. Smailovic U, Koenig T, Kåreholt I, Andersson T, Kramberger MG, Winblad B, et al. Quantitative EEG power and synchronization correlate with Alzheimer's disease CSF biomarkers. Neurobiol Aging. 2018 Mar 1;63:88–95.

324. Maestú F, Cuesta P, Hasan O, Fernandéz A, Funke M, Schulz PE. The Importance of the Validation of M/EEG With Current Biomarkers in Alzheimer's Disease. Front Hum Neurosci [Internet]. 2019;13. Available from: https://www.frontiersin.org/articles/10.3389/fnhum.2019.00017

325. Henstridge CM, Pickett E, Spires-Jones TL. Synaptic pathology: A shared mechanism in neurological disease. Ageing Res Rev. 2016 Jul 1;28:72–84.

326. Spires-Jones TL, Hyman BT. The intersection of amyloid beta and tau at synapses in Alzheimer's disease. Neuron. 2014 May 21;82(4):756–71.

327. Paasila PJ, Fok SYY, Flores-Rodriguez N, Sajjan S, Svahn AJ, Dennis CV, et al. Ground state depletion microscopy as a tool for studying microglia-synapse interactions. J Neurosci Res. 2021/03/07 ed. 2021 Jun;99(6):1515–32.

328. Martínez-Serra R, Alonso-Nanclares L, Cho K, Giese KP. Emerging insights into synapse dysregulation in Alzheimer's disease. Brain Commun. 2022 Apr 1;4(2):fcac083.

329. Zhou L, McInnes J, Wierda K, Holt M, Herrmann AG, Jackson RJ, et al. Tau association with synaptic vesicles causes presynaptic dysfunction. Nat Commun. 2017 May 11;8(1):15295.

330. Buchanan H, Mackay M, Palmer K, Tothová K, Katsur M, Platt B, et al. Synaptic Loss, ER Stress and Neuro-Inflammation Emerge Late in the Lateral Temporal Cortex and Associate with Progressive Tau Pathology in Alzheimer's Disease. Mol Neurobiol. 2020/06/08 ed. 2020 Aug;57(8):3258–72.

331. Zhou L, McInnes J, Wierda K, Holt M, Herrmann AG, Jackson RJ, et al. Tau association with synaptic vesicles causes presynaptic dysfunction. Nat Commun. 2017 May 11;8(1):15295.

332. de Wilde MC, Overk CR, Sijben JW, Masliah E. Meta-analysis of synaptic pathology in Alzheimer's disease reveals selective molecular vesicular machinery vulnerability. Alzheimers Dement J Alzheimers Assoc. 2016/01/14 ed. 2016 Jun;12(6):633–44.

333. Gkanatsiou E, Nilsson J, Toomey CE, Vrillon A, Kvartsberg H, Portelius E, et al. Amyloid pathology and synaptic loss in pathological aging. J Neurochem. 2021 Oct 1;159(2):258–72.

334. Spires-Jones TL, Hyman BT. The intersection of amyloid beta and tau at synapses in Alzheimer's disease. Neuron. 2014 May 21;82(4):756–71.

335. Koffie RM, Meyer-Luehmann M, Hashimoto T, Adams KW, Mielke ML, Garcia-Alloza M, et al. Oligomeric amyloid beta associates with postsynaptic densities and correlates with excitatory synapse loss near senile plaques. Proc Natl Acad Sci U A. 2009 Mar;106(10):4012–7.

336. O'Dell RS, Mecca AP, Chen MK, Naganawa M, Toyonaga T, Lu Y, et al. Association of Aβ deposition and regional synaptic density in early Alzheimer's disease: a PET imaging study with [11C]UCB-J. Alzheimers Res Ther. 2021 Jan 5;13(1):11.

337. Walsh DM, Klyubin I, Fadeeva JV, Cullen WK, Anwyl R, Wolfe MS, et al. Naturally secreted oligomers of amyloid β protein potently inhibit hippocampal long-term potentiation in vivo. Nature. 2002 Apr 1;416(6880):535–9.

338. He Y, Wei M, Wu Y, Qin H, Li W, Ma X, et al. Amyloid β oligomers suppress excitatory transmitter release via presynaptic depletion of phosphatidylinositol-4,5-bisphosphate. Nat Commun. 2019 Mar 13;10(1):1193.

339. Stephen TL, Tamagnini F, Piegsa J, Sung K, Harvey J, Oliver-Evans A, et al. Imbalance in the response of pre- and post-synaptic components to amyloidopathy. Sci Rep. 2019 Oct 16;9(1):14837.

340. Subramanian J, Tremblay MÈ. Editorial: Synaptic Loss and Neurodegeneration. Front Cell Neurosci [Internet]. 2021;15. Available from: https://www.frontiersin.org/article/10.3389/fncel.2021.681029

341. Kilinc D, Vreulx AC, Mendes T, Flaig A, Marques-Coelho D, Verschoore M, et al. Pyk2 overexpression in postsynaptic neurons blocks amyloid β1–42-induced synaptotoxicity in microfluidic co-cultures. Brain Commun [Internet]. 2020 Jul 1 [cited 2021 Oct 14];2(2). Available from: https://doi.org/10.1093/braincomms/fcaa139

342. Koffie RM, Hashimoto T, Tai HC, Kay KR, Serrano-Pozo A, Joyner D, et al. Apolipoprotein E4 effects in Alzheimer's disease are mediated by synaptotoxic oligomeric amyloid-β. Brain J Neurol. 2012/05/26 ed. 2012 Jul;135(Pt 7):2155–68.

343. Bilousova T, Miller CA, Poon WW, Vinters HV, Corrada M, Kawas C, et al. Synaptic Amyloid-β Oligomers Precede p-Tau and Differentiate High Pathology Control Cases. Am J Pathol. 2016 Jan 1;186(1):185–98.

344. Bjorklund NL, Reese LC, Sadagoparamanujam VM, Ghirardi V, Woltjer RL, Taglialatela G. Absence of amyloid β oligomers at the postsynapse and regulated synaptic Zn2+ in cognitively intact aged individuals with Alzheimer's disease neuropathology. Mol Neurodegener. 2012 May 28;7(1):23.

345. Leng K, Li E, Eser R, Piergies A, Sit R, Tan M, et al. Molecular characterization of selectively vulnerable neurons in Alzheimer's disease. Nat Neurosci. 2021/01/11 ed. 2021 Feb;24(2):276–87.

346. Lee KY, Ratté S, Prescott SA. Excitatory neurons are more disinhibited than inhibitory neurons by chloride dysregulation in the spinal dorsal horn. Wyart C, Marder E, Ma Q, editors. eLife. 2019 Nov 19;8:e49753.

347. Tseng H an, Han X. Distinct Spiking Patterns of Excitatory and Inhibitory Neurons and LFP Oscillations in Prefrontal Cortex During Sensory Discrimination. Front Physiol [Internet]. 2021;12. Available from: https://www.frontiersin.org/article/10.3389/fphys.2021.618307

348. Koo EH. Mechanisms of Aβ induced synaptic toxicity. Mol Neurodegener. 2013 Sep 13;8(Suppl 1):O26–O26.

349. LaFerla FM, Green KN, Oddo S. Intracellular amyloid-β in Alzheimer's disease. Nat Rev Neurosci. 2007 Jul 1;8(7):499–509.

350. Lue LF, Kuo YM, Roher AE, Brachova L, Shen Y, Sue L, et al. Soluble amyloid beta peptide concentration as a predictor of synaptic change in Alzheimer's disease. Am J Pathol. 1999 Sep;155(3):853–62.

351. Bao F, Wicklund L, Lacor PN, Klein WL, Nordberg A, Marutle A. Different β-amyloid oligomer assemblies in Alzheimer brains correlate with age of disease onset and impaired cholinergic activity. Neurobiol Aging. 2012 Apr;33(4):825.e1-13.

352. O'Dell RS, Mecca AP, Chen MK, Naganawa M, Toyonaga T, Lu Y, et al. Association of Aβ deposition and regional synaptic density in early Alzheimer's disease: a PET imaging study with [11C]UCB-J. Alzheimers Res Ther. 2021 Jan 5;13(1):11.

353. Sengupta U, Nilson AN, Kayed R. The Role of Amyloid-β Oligomers in Toxicity, Propagation, and Immunotherapy. EBioMedicine. 2016/04/05 ed. 2016 Apr;6:42–9.

354. Markesbery WR, Schmitt FA, Kryscio RJ, Davis DG, Smith CD, Wekstein DR. Neuropathologic Substrate of Mild Cognitive Impairment. Arch Neurol. 2006 Jan 1;63(1):38–46.

355. Feuillette S, Miguel L, Frébourg T, Campion D, Lecourtois M. Drosophila models of human tauopathies indicate that Tau protein toxicity in vivo is mediated by soluble cytosolic phosphorylated forms of the protein. J Neurochem. 2010 May 1;113(4):895–903.

356. McAleese KE, Miah M, Graham S, Hadfield GM, Walker L, Johnson M, et al. Frontal white matter lesions in Alzheimer's disease are associated with both small vessel disease and AD-associated cortical pathology. Acta Neuropathol (Berl) [Internet]. 2021 Oct 4; Available from: https://doi.org/10.1007/s00401-021-02376-2

357. Li HL, Wang HH, Liu SJ, Deng YQ, Zhang YJ, Tian Q, et al. Phosphorylation of tau antagonizes apoptosis by stabilizing beta-catenin, a mechanism involved in Alzheimer's neurodegeneration. Proc Natl Acad Sci U S A. 2007/02/21 ed. 2007 Feb 27;104(9):3591–6.

358. Gómez-Isla T, Hollister R, West H, Mui S, Growdon JH, Petersen RC, et al. Neuronal loss correlates with but exceeds neurofibrillary tangles in Alzheimer's disease. Ann Neurol. 1997 Jan 1;41(1):17–24.

359. Rocher, A. B., Crimins, J. L., Amatrudo, J. M., Kinson, M. S., Todd-Brown, M. A., Lewis, J. Structural and functional changes in tau mutant mice neurons are not linked to the presence of NFTs. Exp Neurol 223 385–393 Doi 101016jexpneurol200907029.

360. Niewiadomska G, Niewiadomski W, Steczkowska M, Gasiorowska A. Tau Oligomers Neurotoxicity. Life Basel Switz. 2021 Jan 6;11(1):28.

361. Maeda S, Takashima A. Tau Oligomers. In: Takashima A, Wolozin B, Buee L, editors. Tau Biology [Internet]. Singapore: Springer Singapore; 2019. p. 373–80. Available from: https://doi.org/10.1007/978-981-32-9358-8_27

362. Wu M, Zhang M, Yin X, Chen K, Hu Z, Zhou Q, et al. The role of pathological tau in synaptic dysfunction in Alzheimer's diseases. Transl Neurodegener. 2021 Nov 10;10(1):45.

363. Tai HC, Serrano-Pozo A, Hashimoto T, Frosch MP, Spires-Jones TL, Hyman BT. The synaptic accumulation of hyperphosphorylated tau oligomers in Alzheimer disease is associated with dysfunction of the ubiquitin-proteasome system. Am J Pathol. 2012/08/04 ed. 2012 Oct;181(4):1426–35.

364. Tai HC, Wang BY, Serrano-Pozo A, Frosch MP, Spires-Jones TL, Hyman BT. Frequent and symmetric deposition of misfolded tau oligomers within presynaptic and postsynaptic terminals in Alzheimer's disease. Acta Neuropathol Commun. 2014 Oct 21;2:146–146.

365. Wysocka A, Palasz E, Steczkowska M, Niewiadomska G. Dangerous Liaisons: Tau Interaction with Muscarinic Receptors. Curr Alzheimer Res. 2020;17(3):224–37.

366. Pampuscenko K, Morkuniene R, Krasauskas L, Smirnovas V, Tomita T, Borutaite V. Distinct Neurotoxic Effects of Extracellular Tau Species in Primary Neuronal-Glial Cultures. Mol Neurobiol. 2021 Feb 1;58(2):658–67.

367. Regan P, Whitcomb DJ, Cho K. Physiological and Pathophysiological Implications of Synaptic Tau. The Neuroscientist. 2017 Apr 1;23(2):137–51.

368. Frandemiche ML, De Seranno S, Rush T, Borel E, Elie A, Arnal I, et al. Activity-dependent tau protein translocation to excitatory synapse is disrupted by exposure to amyloid-beta oligomers. J Neurosci Off J Soc Neurosci. 2014 Apr 23;34(17):6084–97.

369. Wu M, Zhang M, Yin X, Chen K, Hu Z, Zhou Q, et al. The role of pathological tau in synaptic dysfunction in Alzheimer's diseases. Transl Neurodegener. 2021 Nov 10;10(1):45.

370. Guerrero-Muñoz MJ, Gerson J, Castillo-Carranza DL. Tau Oligomers: The Toxic Player at Synapses in Alzheimer's Disease. Front Cell Neurosci. 2015;9:464.

371. Yin X, Zhao C, Qiu Y, Zhou Z, Bao J, Qian W. Dendritic/Post-synaptic Tau and Early Pathology of Alzheimer's Disease. Front Mol Neurosci [Internet]. 2021;14. Available from: https://www.frontiersin.org/articles/10.3389/fnmol.2021.671779

372. Robbins M, Clayton E, Kaminski Schierle GS. Synaptic tau: A pathological or physiological phenomenon? Acta Neuropathol Commun. 2021 Sep 9;9(1):149.

373. Tiernan CT, Mufson EJ, Kanaan NM, Counts SE. Tau Oligomer Pathology in Nucleus Basalis Neurons During the Progression of Alzheimer Disease. J Neuropathol Exp Neurol. 2018 Mar 1;77(3):246–59.

374. G Amadoro. Endogenous Aβ causes cell death via early tau hyperphosphorylation. Neurobiol Aging 2011 Jun326969-90 Doi 101016jneurobiolaging200906005 Epub 2009 Jul 22.

375. Qiu-Lan Ma, Fusheng Yang, Emily R. Rosario, Oliver J. Ubeda, Walter Beech, Dana J. Gant, et al. β-Amyloid Oligomers Induce Phosphorylation of Tau and Inactivation of Insulin Receptor Substrate via c-Jun N-Terminal Kinase Signaling: Suppression by Omega-3 Fatty Acids and Curcumin. J Neurosci. 2009 Jul 15;29(28):9078.

376. Amar F, Sherman MA, Rush T, Larson M, Boyle G, Chang L, et al. The amyloid-β oligomer Aβ*56 induces specific alterations in neuronal signaling that lead to tau phosphorylation and aggregation. Sci Signal. 2017 May 9;10(478):eaal2021.

377. Daniela Puzzo. Tau is not necessary for amyloid-β–induced synaptic and memory impairments. J Clin Invest 202013094831-4844 Httpsdoiorg101172JCI137040.

378. Marcatti M, Fracassi A, Montalbano M, Natarajan C, Krishnan B, Kayed R, et al. Aβ/tau oligomer interplay at human synapses supports shifting therapeutic targets for Alzheimer's disease. Cell Mol Life Sci. 2022 Apr 4;79(4):222.

379. Goedert M, Spillantini MG, Jakes R, Rutherford D, Crowther RA. Multiple isoforms of human microtubule-associated protein tau: sequences and localization in neurofibrillary tangles of Alzheimer's disease. Neuron. 1989 Oct 1;3(4):519–26.

380. Xia Y, Prokop S, Giasson BI. "Don't Phos Over Tau": recent developments in clinical biomarkers and therapies targeting tau phosphorylation in Alzheimer's disease and other tauopathies. Mol Neurodegener. 2021 Jun 5;16(1):37.

381. Gu J lan, Liu F. Tau in Alzheimer's Disease: Pathological Alterations and an Attractive Therapeutic Target. Curr Med Sci. 2020 Dec 1;40(6):1009–21.

382. Köpke E, Tung YC, Shaikh S, Alonso AC, Iqbal K, Grundke-Iqbal I. Microtubule-associated protein tau. Abnormal phosphorylation of a non-paired helical filament pool in Alzheimer disease. J Biol Chem. 1993 Nov 15;268(32):24374–84.

383. Alonso AD, Cohen LS, Corbo C, Morozova V, ElIdrissi A, Phillips G, et al. Hyperphosphorylation of Tau Associates With Changes in Its Function Beyond Microtubule Stability. Front Cell Neurosci [Internet]. 2018;12. Available from: https://www.frontiersin.org/articles/10.3389/fncel.2018.00338

384. Bancher C, Brunner C, Lassmann H, Budka H, Jellinger K, Wiche G, et al. Accumulation of abnormally phosphorylated τ precedes the formation of neurofibrillary tangles in Alzheimer's disease. Brain Res. 1989 Jan 16;477(1):90–9.

385. Moloney CM, Lowe VJ, Murray ME. Visualization of neurofibrillary tangle maturity in Alzheimer's disease: A clinicopathologic perspective for biomarker research. Alzheimers Dement. 2021 Sep 1;17(9):1554–74.

386. Duquette A, Pernègre C, Veilleux Carpentier A, Leclerc N. Similarities and Differences in the Pattern of Tau Hyperphosphorylation in Physiological and Pathological Conditions: Impacts on the Elaboration of Therapies to Prevent Tau Pathology. Front Neurol. 2021;11:1823.

387. Limorenko G, Lashuel HA. Revisiting the grammar of Tau aggregation and pathology formation: how new insights from brain pathology are shaping how we study and target Tauopathies. Chem Soc Rev. 2021;

388. Bierer LM, Hof PR, Purohit DP, Carlin L, Schmeidler J, Davis KL, et al. Neocortical Neurofibrillary Tangles Correlate With Dementia Severity in Alzheimer's Disease. Arch Neurol. 1995 Jan 1;52(1):81–8.

389. Kuchibhotla KV, Wegmann S, Kopeikina KJ, Hawkes J, Rudinskiy N, Andermann ML, et al. Neurofibrillary tangle-bearing neurons are functionally integrated in cortical circuits in vivo. Proc Natl Acad Sci U S A. 2013/12/24 ed. 2014 Jan 7;111(1):510–4.

390. Gómez-Isla T, Frosch MP. Lesions without symptoms: understanding resilience to Alzheimer disease neuropathological changes. Nat Rev Neurol. 2022 Jun 1;18(6):323–32.

391. Zwang TJ, Woost B, Bailey J, Hoglund Z, Richardson DS, Bennett RE, et al. Spatial characterization of tangle-bearing neurons and ghost tangles in the human inferior temporal gyrus with three-dimensional imaging. Brain Commun. 2023 Jun 1;5(3):fcad130.

392. Gu J, Xu W, Jin N, Li L, Zhou Y, Chu D, et al. Truncation of Tau selectively facilitates its pathological activities. J Biol Chem. 2020 Oct 2;295(40):13812–28.

393. Florenzano F, Veronica C, Ciasca G, Ciotti MT, Pittaluga A, Olivero G, et al. Extracellular truncated tau causes early presynaptic dysfunction associated with Alzheimer's disease and other tauopathies. Oncotarget. 2017 Apr 22;8(39):64745–78.

394. Jadhav S, Cubinkova V, Zimova I, Brezovakova V, Madari A, Cigankova V, et al. Tau-mediated synaptic damage in Alzheimer's disease. 2015;6(1):214–26.

395. Miyoshi E, Bilousova T, Melnik M, Fakhrutdinov D, Poon WW, Vinters HV, et al. Exosomal tau with seeding activity is released from Alzheimer's disease synapses, and seeding potential is associated with amyloid beta. Lab Invest. 2021 Dec 1;101(12):1605–17.

396. Guo T, Dakkak D, Rodriguez-Martin T, Noble W, Hanger DP. A pathogenic tau fragment compromises microtubules, disrupts insulin signaling and induces the unfolded protein response. Acta Neuropathol Commun. 2019 Jan 3;7(1):2.

397. Sokolow S, Henkins KM, Bilousova T, Gonzalez B, Vinters HV, Miller CA, et al. Pre-synaptic C-terminal truncated tau is released from cortical synapses in Alzheimer's disease. J Neurochem. 2015 May 1;133(3):368–79.

398. Ferreira A, Bigio EH. Calpain-Mediated Tau Cleavage: A Mechanism Leading to Neurodegeneration Shared by Multiple Tauopathies. Mol Med. 2011 Jul 1;17(7):676–85.

399. Tai HC, Wang BY, Serrano-Pozo A, Frosch MP, Spires-Jones TL, Hyman BT. Frequent and symmetric deposition of misfolded tau oligomers within presynaptic and postsynaptic terminals in Alzheimer's disease. Acta Neuropathol Commun. 2014 Oct 21;2(1):146.

400. de Calignon A, Polydoro M, Suárez-Calvet M, William C, Adamowicz DH, Kopeikina KJ, et al. Propagation of Tau Pathology in a Model of Early Alzheimer's Disease. Neuron. 2012 Feb 23;73(4):685–97.

401. Liu L, Drouet V, Wu JW, Witter MP, Small SA, Clelland C, et al. Trans-Synaptic Spread of Tau Pathology In Vivo. PLOS ONE. 2012 Feb 1;7(2):e31302.

402. DeVos SL, Corjuc BT, Oakley DH, Nobuhara CK, Bannon RN, Chase A, et al. Synaptic Tau Seeding Precedes Tau Pathology in Human Alzheimer's Disease Brain. Front Neurosci. 2018 Apr 24;12:267–267.

403. Maina KN, Smet-Nocca C, Bitan G. Using FRET-Based Biosensor Cells to Study the Seeding Activity of Tau and α-Synuclein. In: Cieplak AS, editor. Protein Aggregation: Methods and Protocols [Internet]. New York, NY: Springer US; 2023. p. 125–45. Available from: https://doi.org/10.1007/978-1-0716-2597-2_10

404. DeVos SL, Corjuc BT, Oakley DH, Nobuhara CK, Bannon RN, Chase A, et al. Synaptic Tau Seeding Precedes Tau Pathology in Human Alzheimer's Disease Brain. Front Neurosci. 2018;12:267.

405. Holmes BB, Furman JL, Mahan TE, Yamasaki TR, Mirbaha H, Eades WC, et al. Proteopathic tau seeding predicts tauopathy in vivo. Proc Natl Acad Sci. 2014 Oct 14;111(41):E4376–85.

406. AU - Furman JL, AU - Holmes BB, AU - Diamond MI. Sensitive Detection of Proteopathic Seeding Activity with FRET Flow Cytometry. J Vis Exp. 2015 Dec 8;(106):e53205.

407. Samuel J. Jackson, Caroline Kerridge, Jane Cooper, Annalisa Cavallini, Benjamin Falcon, Claire V. Cella, et al. Short Fibrils Constitute the Major Species of Seed-Competent Tau in the Brains of Mice Transgenic for Human P301S Tau. J Neurosci. 2016 Jan 20;36(3):762.

408. Tanaka Y, Yamada K, Satake K, Nishida I, Heuberger M, Kuwahara T, et al. Seeding Activity-Based Detection Uncovers the Different Release Mechanisms of Seed-Competent Tau Versus Inert Tau via Lysosomal Exocytosis. Front Neurosci [Internet]. 2019;13. Available from: https://www.frontiersin.org/articles/10.3389/fnins.2019.01258

409. Jiang L, Zhao J, Cheng JX, Wolozin B. Tau Oligomers and Fibrils Exhibit Differential Patterns of Seeding and Association With RNA Binding Proteins. Front Neurol [Internet]. 2020;11. Available from: https://www.frontiersin.org/articles/10.3389/fneur.2020.579434

410. Mate De Gerando A, Welikovitch LA, Khasnavis A, Commins C, Glynn C, Chun JE, et al. Tau seeding and spreading in vivo is supported by both AD-derived fibrillar and oligomeric tau. Acta Neuropathol (Berl). 2023 Aug 1;146(2):191–210.

411. Swanson E, Breckenridge L, McMahon L, Som S, McConnell I, Bloom GS. Extracellular Tau Oligomers Induce Invasion of Endogenous Tau into the Somatodendritic Compartment and Axonal Transport Dysfunction. J Alzheimers Dis JAD. 2017;58(3):803–20.

412. Gibbons GS, Lee VMY, Trojanowski JQ. Mechanisms of Cell-to-Cell Transmission of Pathological Tau: A Review. JAMA Neurol. 2019 Jan 1;76(1):101–8.

413. Manassero G, Guglielmotto M, Monteleone D, Vasciaveo V, Butenko O, Tamagno E, et al. Dual Mechanism of Toxicity for Extracellular Injection of Tau Oligomers versus Monomers in Human Tau Mice. J Alzheimers Dis JAD. 2017;59(2):743–51.

414. Zhang H, Cao Y, Ma L, Wei Y, Li H. Possible Mechanisms of Tau Spread and Toxicity in Alzheimer's Disease. Front Cell Dev Biol. 2021 Jul 28;9:707268–707268.

415. Hu W, Liu F, Gong CX, Iqbal K. Does proteopathic tau propagate trans-synaptically in the brain? Mol Neurodegener. 2022 Mar 16;17(1):21.

416. Braak H, Del Tredici K. From the Entorhinal Region via the Prosubiculum to the Dentate Fascia: Alzheimer Disease-Related Neurofibrillary Changes in the Temporal Allocortex. J Neuropathol Exp Neurol. 2020 Feb 1;79(2):163–75.

417. Wang Y, Balaji V, Kaniyappan S, Krüger L, Irsen S, Tepper K, et al. The release and trans-synaptic transmission of Tau via exosomes. Mol Neurodegener. 2017 Jan 13;12(1):5.

418. Frost B, Jacks RL, Diamond MI. Propagation of tau misfolding from the outside to the inside of a cell. J Biol Chem. 2009/03/11 ed. 2009 May 8;284(19):12845–52.

419. Fá M, Puzzo D, Piacentini R, Staniszewski A, Zhang H, Baltrons MA, et al. Extracellular Tau Oligomers Produce An Immediate Impairment of LTP and Memory. Sci Rep. 2016 Jan 20;6:19393–19393.

420. Bellenguez C, Küçükali F, Jansen I, Andrade V, Moreno-Grau S, Amin N, et al. New insights on the genetic etiology of Alzheimer's and related dementia. medRxiv. 2020 Jan 1;2020.10.01.20200659.

421. Stevens B, Allen NJ, Vazquez LE, Howell GR, Christopherson KS, Nouri N, et al. The Classical Complement Cascade Mediates CNS Synapse Elimination. Cell. 2007 Dec 14;131(6):1164–78.

422. Hong S, Beja-Glasser VF, Nfonoyim BM, Frouin A, Li S, Ramakrishnan S, et al. Complement and microglia mediate early synapse loss in Alzheimer mouse models. Science. 2016/03/31 ed. 2016 May 6;352(6286):712–6.

423. Weinhard L, di Bartolomei G, Bolasco G, Machado P, Schieber NL, Neniskyte U, et al. Microglia remodel synapses by presynaptic trogocytosis and spine head filopodia induction. Nat Commun. 2018 Mar 26;9(1):1228.

424. Perez-Nievas BG, Johnson L, Beltran-Lobo P, Hughes MM, Gammallieri L, Tarsitano F, et al. Astrocytic C-X-C motif chemokine ligand-1 mediates β-amyloid-induced synaptotoxicity. bioRxiv. 2021 Jan 1;2021.09.22.458716.

425. Chung WS, Clarke LE, Wang GX, Stafford BK, Sher A, Chakraborty C, et al. Astrocytes mediate synapse elimination through MEGF10 and MERTK pathways. Nature. 2013/11/24 ed. 2013 Dec 19;504(7480):394–400.

426. Lee SY, Chung WS. The roles of astrocytic phagocytosis in maintaining homeostasis of brains. J Pharmacol Sci. 2021 Mar 1;145(3):223–7.

427. Dejanovic B, Huntley MA, De Mazière A, Meilandt WJ, Wu T, Srinivasan K, et al. Changes in the Synaptic Proteome in Tauopathy and Rescue of Tau-Induced Synapse Loss by C1q Antibodies. Neuron. 2018 Dec 19;100(6):1322-1336.e7.

428. P. Kelly, M.V. Sanchez-Mico, SS. Hou, S. Whiteman, A. Russ, E. Hudry, et al. Neuronally-derived soluble Abeta evokes cell-wide astrocytic calcium dysregulation in absence of amyloid plaques in vivo. J Neurosci. 2023 May 26;JN-RM-1988-22.

429. McGonigle P, Ruggeri B. Animal models of human disease: Challenges in enabling translation. Spec Issue Pharmacol 21st Century Biomed Res. 2014 Jan 1;87(1):162–71.

430. Tzioras M, Daniels MJD, King D, Popovic K, Holloway RK, Stevenson AJ, et al. Altered synaptic ingestion by human microglia in Alzheimer's disease. bioRxiv. 2019 Jan 1;795930.

431. Chen X, Firulyova M, Manis M, Herz J, Smirnov I, Aladyeva E, et al. Microglia-mediated T cell infiltration drives neurodegeneration in tauopathy. Nature. 2023 Mar 1;615(7953):668–77.

432. Park KHJ, Barrett T. Gliosis Precedes Amyloid-β Deposition and Pathological Tau Accumulation in the Neuronal Cell Cycle Re-Entry Mouse Model of Alzheimer's Disease. J Alzheimers Dis Rep. 2020;4(1):243–53.

433. Ying C, Kang P, Binkley MM, Ford AL, Chen Y, Hassenstab J, et al. Neuroinflammation and amyloid deposition in the progression of mixed Alzheimer and vascular dementia. NeuroImage Clin. 2023 Jan 1;38:103373.

434. Qing Wang, Gengsheng Chen, Suzanne E. Schindler, Jon Christensen, Nicole S. McKay, Jingxia Liu, et al. Baseline Microglial Activation Correlates With Brain Amyloidosis and Longitudinal Cognitive Decline in Alzheimer Disease. Neurol - Neuroimmunol Neuroinflammation. 2022 May 1;9(3):e1152.

435. Ginhoux F, Lim S, Hoeffel G, Low D, Huber T. Origin and differentiation of microglia. Front Cell Neurosci [Internet]. 2013;7. Available from: https://www.frontiersin.org/articles/10.3389/fncel.2013.00045

436. Verkhratsky A, Zorec R, Parpura V. Stratification of astrocytes in healthy and diseased brain. Brain Pathol Zurich Switz. 2017 Sep;27(5):629–44.

437. Réu P, Khosravi A, Bernard S, Mold JE, Salehpour M, Alkass K, et al. The Lifespan and Turnover of Microglia in the Human Brain. Cell Rep. 2017 Jul 25;20(4):779–84.

438. Schwabenland M, Brück W, Priller J, Stadelmann C, Lassmann H, Prinz M. Analyzing microglial phenotypes across neuropathologies: a practical guide. Acta Neuropathol (Berl). 2021 Dec 1;142(6):923–36.

439. Das Sarma S, Chatterjee K, Dinda H, Chatterjee D, Das Sarma J. Cytomorphological and Cytochemical Identification of Microglia. Varga SM, El Ridi R, editors. ISRN Immunol. 2013 Aug 27;2013:205431.

440. Lier J, Streit WJ, Bechmann I. Beyond Activation: Characterizing Microglial Functional Phenotypes. Cells. 2021;10(9).

441. Taylor SE, Morganti-Kossmann C, Lifshitz J, Ziebell JM. Rod Microglia: A Morphological Definition. PLOS ONE. 2014 May 15;9(5):e97096.

442. Leyh J, Paeschke S, Mages B, Michalski D, Nowicki M, Bechmann I, et al. Classification of Microglial Morphological Phenotypes Using Machine Learning. Front Cell Neurosci [Internet]. 2021;15. Available from: https://www.frontiersin.org/articles/10.3389/fncel.2021.701673

443. Okajima T, Tsuruta F. Microglial dynamics during brain development. Neural Regen Res [Internet]. 2018;13(2). Available from: https://journals.lww.com/nrronline/Fulltext/2018/13020/Microglial_dynamics_during_brain_development.8.aspx

444. Laprell L, Schulze C, Brehme ML, Oertner TG. The role of microglia membrane potential in chemotaxis. J Neuroinflammation. 2021 Jan 10;18(1):21.

445. W. Shawn Carbonell, Shin-Ichi Murase, Alan F. Horwitz, James W. Mandell. Migration of Perilesional Microglia after Focal Brain Injury and Modulation by CC Chemokine Receptor 5: An In Situ Time-Lapse Confocal Imaging Study. J Neurosci. 2005 Jul 27;25(30):7040.

446. Holloway OG, Canty AJ, King AE, Ziebell JM. Rod microglia and their role in neurological diseases. SI Calcium Signal. 2019 Oct 1;94:96–103.

447. Davies DS, Ma J, Jegathees T, Goldsbury C. Microglia show altered morphology and reduced arborization in human brain during aging and Alzheimer's disease. Brain Pathol. 2017 Nov 1;27(6):795–808.

448. Keren-Shaul H, Spinrad A, Weiner A, Matcovitch-Natan O, Dvir-Szternfeld R, Ulland TK, et al. A Unique Microglia Type Associated with Restricting Development of Alzheimer's Disease. Cell. 2017 Jun 15;169(7):1276-1290.e17.

449. Izzy S, Liu Q, Fang Z, Lule S, Wu L, Chung JY, et al. Time-Dependent Changes in Microglia Transcriptional Networks Following Traumatic Brain Injury. Front Cell Neurosci [Internet]. 2019;13. Available from: https://www.frontiersin.org/articles/10.3389/fncel.2019.00307

450. Perego C, Fumagalli S, De Simoni MG. Temporal pattern of expression and colocalization of microglia/macrophage phenotype markers following brain ischemic injury in mice. J Neuroinflammation. 2011 Dec 10;8(1):174.

451. Siracusa R, Fusco R, Cuzzocrea S. Astrocytes: Role and Functions in Brain Pathologies. Front Pharmacol [Internet]. 2019;10. Available from: https://www.frontiersin.org/articles/10.3389/fphar.2019.01114

452. Cunningham C, Dunne A, Lopez-Rodriguez AB. Astrocytes: Heterogeneous and Dynamic Phenotypes in Neurodegeneration and Innate Immunity. The Neuroscientist. 2019 Oct 1;25(5):455–74.

453. Monterey MD, Wei H, Wu X, Wu JQ. The Many Faces of Astrocytes in Alzheimer's Disease. Front Neurol [Internet]. 2021;12. Available from: https://www.frontiersin.org/article/10.3389/fneur.2021.619626

454. Hindley N, Sanchez Avila A, Henstridge C. Bringing synapses into focus: Recent advances in synaptic imaging and mass-spectrometry for studying synaptopathy. Front Synaptic Neurosci [Internet]. 2023;15. Available from: https://www.frontiersin.org/articles/10.3389/fnsyn.2023.1130198

455. Margaux Saint-Martin. Astrocyte–synapse interactions and cell adhesion molecules. FEBS J 2023 Httpsdoiorg101111febs16540.

456. Jessen NA, Munk ASF, Lundgaard I, Nedergaard M. The Glymphatic System: A Beginner's Guide. Neurochem Res. 2015 Dec 1;40(12):2583–99.

457. Fleeman RM, Proctor EA. Astrocytic Propagation of Tau in the Context of Alzheimer's Disease. Front Cell Neurosci [Internet]. 2021;15. Available from: https://www.frontiersin.org/articles/10.3389/fncel.2021.645233

458. Konishi H, Koizumi S, Kiyama H. Phagocytic astrocytes: Emerging from the shadows of microglia. Glia. 2022 Jun 1;70(6):1009–26.

459. Zhan JS, Gao K, Chai RC, Jia XH, Luo DP, Ge G, et al. Astrocytes in Migration. Neurochem Res. 2017 Jan 1;42(1):272–82.

460. Elly M Hol. Glial fibrillary acidic protein (GFAP) and the astrocyte intermediate filament system in diseases of the central nervous system. Curr Opin Cell Biol 2015 Feb32121-30 Doi 101016jceb201502004 Epub 2015 Mar 2.

461. Carole Escartin. Reactive astrocyte nomenclature, definitions, and future directions. Nat Neurosci 2021 Mar 243 312–325 Doi 101038s41593-020-00783-4.

462. Jinte Middeldorp. Specific Human Astrocyte Subtype Revealed by Affinity Purified GFAP+1 Antibody; Unpurified Serum Cross-Reacts with Neurofilament-L in Alzheimer. PLOS ONE 2009 Httpsdoiorg101371journalpone0007663.

463. Chiareli RA, Carvalho GA, Marques BL, Mota LS, Oliveira-Lima OC, Gomes RM, et al. The Role of Astrocytes in the Neurorepair Process. Front Cell Dev Biol [Internet]. 2021;9. Available from: https://www.frontiersin.org/articles/10.3389/fcell.2021.665795

464. Ashley Sterpka. Diverged morphology changes of astrocytic and neuronal primary cilia under reactive insults. Mol Brain 13 28 2020 Httpsdoiorg101186s13041-020-00571-.

465. Lagos-Cabré R, Burgos-Bravo F, Avalos AM, Leyton L. Connexins in Astrocyte Migration. Front Pharmacol [Internet]. 2020;10. Available from: https://www.frontiersin.org/articles/10.3389/fphar.2019.01546

466. Raul Lagos-Cabre. Connexins in Astrocyte Migration.

467. Tony W. Hsiao. Astrocyte spreading and migration on aggrecan–laminin dot gradients. Biointerphases 2018 Feb 131 01A401.

468. Hsiao TW, Tresco PA, Hlady V. Astrocyte spreading and migration on aggrecan–laminin dot gradients. Biointerphases. 2017 Sep 11;13(1):01A401.

469. Escartin C, Galea E, Lakatos A, O'Callaghan JP, Petzold GC, Serrano-Pozo A, et al. Reactive astrocyte nomenclature, definitions, and future directions. Nat Neurosci. 2021 Mar 1;24(3):312–25.

470. Tabata H. Diverse subtypes of astrocytes and their development during corticogenesis. Front Neurosci [Internet]. 2015;9. Available from: https://www.frontiersin.org/articles/10.3389/fnins.2015.00114

471. Galloway DA, Phillips AEM, Owen DRJ, Moore CS. Phagocytosis in the Brain: Homeostasis and Disease. Front Immunol. 2019 Apr 16;10:790–790.

472. De Schepper S, Ge JZ, Crowley G, Ferreira LSS, Garceau D, Toomey CE, et al. Perivascular cells induce microglial phagocytic states and synaptic engulfment via SPP1 in mouse models of Alzheimer's disease. Nat Neurosci. 2023 Mar 1;26(3):406–15.

473. Korotzer AR, Watt J, Cribbs D, Tenner AJ, Burdick D, Glabe C, et al. Cultured Rat Microglia Express C1q and Receptor for C1q: Implications for Amyloid Effects on Microglia. Exp Neurol. 1995 Aug 1;134(2):214–21.

474. Zhao Y, Wu X, Li X, Jiang LL, Gui X, Liu Y, et al. TREM2 Is a Receptor for β-Amyloid that Mediates Microglial Function. Neuron. 2018 Mar 7;97(5):1023-1031.e7.

475. Rueda-Carrasco J, Sokolova D, Lee SE, Childs T, Jurčáková N, De Schepper S, et al. Microglia Detect Externalized Phosphatidylserine on Synapses for Elimination via TREM2 in Alzheimer's Disease Models. bioRxiv. 2022 Jan 1;2022.04.04.486424.

476. Guerreiro R, Wojtas A, Bras J, Carrasquillo M, Rogaeva E, Majounie E, et al. TREM2 Variants in Alzheimer's Disease. N Engl J Med. 2013 Jan 10;368(2):117–27.

477. Lee JH, Kim J young, Noh S, Lee H, Lee SY, Mun JY, et al. Astrocytes phagocytose adult hippocampal synapses for circuit homeostasis. Nature. 2021 Feb 1;590(7847):612–7.

478. Tal Iram, Zaida Ramirez-Ortiz, Michael H. Byrne, Uwanda A. Coleman, Nathan D. Kingery, Terry K. Means, et al. Megf10 Is a Receptor for C1Q That Mediates Clearance of Apoptotic Cells by Astrocytes. J Neurosci. 2016 May 11;36(19):5185.

479. Morizawa YM, Hirayama Y, Ohno N, Shibata S, Shigetomi E, Sui Y, et al. Reactive astrocytes function as phagocytes after brain ischemia via ABCA1-mediated pathway. Nat Commun. 2017 Jun 22;8(1):28.

480. Jon Iker Etchegaray, Emma J. Elguero, Jennifer A. Tran, Vincent Sinatra, Mel B. Feany, Kimberly McCall. Defective Phagocytic Corpse Processing Results in Neurodegeneration and Can Be Rescued by TORC1 Activation. J Neurosci. 2016 Mar 16;36(11):3170.

481. Ye Zhang, Kenian Chen, Steven A. Sloan, Mariko L. Bennett, Anja R. Scholze, Sean O'Keeffe, et al. An RNA-Sequencing Transcriptome and Splicing Database of Glia, Neurons, and Vascular Cells of the Cerebral Cortex. J Neurosci. 2014 Sep 3;34(36):11929.

482. Damisah EC, Hill RA, Rai A, Chen F, Rothlin CV, Ghosh S, et al. Astrocytes and microglia play orchestrated roles and respect phagocytic territories during neuronal corpse removal in vivo. Sci Adv. 2020 Jun 26;6(26):eaba3239–eaba3239.

483. Konishi H, Okamoto T, Hara Y, Komine O, Tamada H, Maeda M, et al. Astrocytic phagocytosis is a compensatory mechanism for microglial dysfunction. EMBO J. 2020 Nov 16;39(22):e104464.

484. Jackson RJ, Meltzer JC, Nguyen H, Commins C, Bennett RE, Hudry E, et al. APOE4 derived from astrocytes leads to blood–brain barrier impairment. Brain. 2022 Oct 3;145(10):3582–93.

485. Wang C, Xiong M, Gratuze M, Bao X, Shi Y, Andhey PS, et al. Selective removal of astrocytic APOE4 strongly protects against tau-mediated neurodegeneration and decreases synaptic phagocytosis by microglia. Neuron. 2021 May 19;109(10):1657-1674.e7.

486. Hiroaki Wake, Andrew J. Moorhouse, Shozo Jinno, Shinichi Kohsaka, Junichi Nabekura. Resting Microglia Directly Monitor the Functional State of Synapses In Vivo and Determine the Fate of Ischemic Terminals. J Neurosci. 2009 Apr 1;29(13):3974.

487. Davalos D, Grutzendler J, Yang G, Kim JV, Zuo Y, Jung S, et al. ATP mediates rapid microglial response to local brain injury in vivo. Nat Neurosci. 2005 Jun 1;8(6):752–8.

488. Liddelow SA, Guttenplan KA, Clarke LE, Bennett FC, Bohlen CJ, Schirmer L, et al. Neurotoxic reactive astrocytes are induced by activated microglia. Nature. 2017/01/18 ed. 2017 Jan 26;541(7638):481–7.

489. Kono R, Ikegaya Y, Koyama R. Phagocytic Glial Cells in Brain Homeostasis. Cells. 2021;10(6).

490. Lööv C, Hillered L, Ebendal T, Erlandsson A. Engulfing Astrocytes Protect Neurons from Contact-Induced Apoptosis following Injury. PLOS ONE. 2012 Mar 26;7(3):e33090.

491. Di Benedetto G, Burgaletto C, Bellanca CM, Munafò A, Bernardini R, Cantarella G. Role of Microglia and Astrocytes in Alzheimer's Disease: From Neuroinflammation to Ca2+ Homeostasis Dysregulation. Cells. 2022;11(17).

492. Kreher C, Favret J, Maulik M, Shin D. Lysosomal Functions in Glia Associated with Neurodegeneration. Biomolecules. 2021;11(3).

493. Hickman SE, Allison EK, El Khoury J. Microglial dysfunction and defective beta-amyloid clearance pathways in aging Alzheimer's disease mice. J Neurosci Off J Soc Neurosci. 2008 Aug 13;28(33):8354–60.

494. Söllvander S, Nikitidou E, Brolin R, Söderberg L, Sehlin D, Lannfelt L, et al. Accumulation of amyloid-β by astrocytes result in enlarged endosomes and microvesicle-induced apoptosis of neurons. Mol Neurodegener. 2016 May 12;11(1):38.

495. Sanchez-Mejias E, Navarro V, Jimenez S, Sanchez-Mico M, Sanchez-Varo R, Nuñez-Diaz C, et al. Soluble phospho-tau from Alzheimer's disease hippocampus drives microglial degeneration. Acta Neuropathol (Berl). 2016 Dec 1;132(6):897–916.

496. Perez-Nievas BG, Serrano-Pozo A. Deciphering the Astrocyte Reaction in Alzheimer's Disease. Front Aging Neurosci [Internet]. 2018;10. Available from: https://www.frontiersin.org/articles/10.3389/fnagi.2018.00114

497. Hansen DV, Hanson JE, Sheng M. Microglia in Alzheimer's disease. J Cell Biol. 2017/12/01 ed. 2018 Feb 5;217(2):459–72.

498. d'Errico P, Ziegler-Waldkirch S, Aires V, Hoffmann P, Mezö C, Erny D, et al. Microglia contribute to the propagation of Aβ into unaffected brain tissue. Nat Neurosci. 2022 Jan 1;25(1):20–5.

499. Sudeshna Das, Zhaozhi Li, Astrid Wachter, Srinija Alla, Ayush Noori, Aicha Abdourahman, et al. Distinct Transcriptomic Responses to Aβ plaques, Neurofibrillary Tangles, and APOE in Alzheimer's Disease. bioRxiv. 2023 Jan 1;2023.03.20.533303.

500. Sebastian Monasor L, Müller SA, Colombo AV, Tanrioever G, König J, Roth S, et al. Fibrillar Aβ triggers microglial proteome alterations and dysfunction in Alzheimer mouse models. Stevens B, Zoghbi HY, Stevens B, Blurton-Jones M, Spires-Jones TL, editors. eLife. 2020 Jun 8;9:e54083.

501. Joshi P, Turola E, Ruiz A, Bergami A, Libera DD, Benussi L, et al. Microglia convert aggregated amyloid-β into neurotoxic forms through the shedding of microvesicles. Cell Death Differ. 2014 Apr 1;21(4):582–93.

502. C Haass, AY Hung, DJ Selkoe. Processing of beta-amyloid precursor protein in microglia and astrocytes favors an internal localization over constitutive secretion. J Neurosci. 1991 Dec 1;11(12):3783.

503. Frost GR, Li YM. The role of astrocytes in amyloid production and Alzheimer's disease. Open Biol. 2017 Dec 13;7(12):170228.

504. Singh N, Das B, Zhou J, Hu X, Yan R. Targeted BACE-1 inhibition in microglia enhances amyloid clearance and improved cognitive performance. Sci Adv. 8(29):eabo3610.

505. Jha MK, Jo M, Kim JH, Suk K. Microglia-Astrocyte Crosstalk: An Intimate Molecular Conversation. The Neuroscientist. 2019;25:227–40.

506. Serrano-Pozo A, Mielke ML, Gómez-Isla T, Betensky RA, Growdon JH, Frosch MP, et al. Reactive glia not only associates with plaques but also parallels tangles in Alzheimer's disease. Am J Pathol. 2011/07/21 ed. 2011 Sep;179(3):1373–84.

507. Ohm DT, Fought AJ, Martersteck A, Coventry C, Sridhar J, Gefen T, et al. Accumulation of neurofibrillary tangles and activated microglia is associated with lower neuron densities in the aphasic variant of Alzheimer's disease. Brain Pathol. 2021 Jan 1;31(1):189–204.

508. Perea JR, Llorens-Martín M, Ávila J, Bolós M. The Role of Microglia in the Spread of Tau: Relevance for Tauopathies. Front Cell Neurosci [Internet]. 2018;12. Available from: https://www.frontiersin.org/articles/10.3389/fncel.2018.00172

509. Brelstaff JH, Mason M, Katsinelos T, McEwan WA, Ghetti B, Tolkovsky AM, et al. Microglia become hypofunctional and release metalloproteases and tau seeds when phagocytosing live neurons with P301S tau aggregates. Sci Adv. 7(43):eabg4980.

510. Kahlson MA, Colodner KJ. Glial Tau Pathology in Tauopathies: Functional Consequences. J Exp Neurosci. 2016 Feb 10;9(Suppl 2):43–50.

511. Allen NJ. Astrocyte Regulation of Synaptic Behavior. Annu Rev Cell Dev Biol. 2014 Oct 11;30(1):439–63.

512. Reid MJ, Beltran-Lobo P, Johnson L, Perez-Nievas BG, Noble W. Astrocytes in Tauopathies. Front Neurol [Internet]. 2020;11. Available from: https://www.frontiersin.org/article/10.3389/fneur.2020.572850

513. Chiarini A, Armato U, Gardenal E, Gui L, Dal Prà I. Amyloid β-Exposed Human Astrocytes Overproduce Phospho-Tau and Overrelease It within Exosomes, Effects Suppressed by Calcilytic NPS 2143—Further Implications for Alzheimer's Therapy. Front Neurosci [Internet]. 2017;11. Available from: https://www.frontiersin.org/articles/10.3389/fnins.2017.00217

514. Amro Z, Yool AJ, Collins-Praino LE. The potential role of glial cells in driving the prion-like transcellular propagation of tau in tauopathies. Brain Behav Immun - Health. 2021 Jul 1;14:100242.

515. Leclerc B, Abulrob A. Perspectives in Molecular Imaging Using Staging Biomarkers and Immunotherapies in Alzheimer's Disease. Thompson EJ, Kira JI, editors. Sci World J. 2013 Feb 5;2013:589308.

516. Milà-Alomà M, Salvadó G, Gispert JD, Vilor-Tejedor N, Grau-Rivera O, Sala-Vila A, et al. Amyloid beta, tau, synaptic, neurodegeneration, and glial biomarkers in the preclinical stage of the Alzheimer's continuum. Alzheimers Dement J Alzheimers Assoc. 2020/06/23 ed. 2020 Oct;16(10):1358–71.

517. Petersen RC. Alzheimer's disease: progress in prediction. Lancet Neurol. 2010 Jan 1;9(1):4–5.

518. Jack CR Jr, Knopman DS, Jagust WJ, Shaw LM, Aisen PS, Weiner MW, et al. Hypothetical model of dynamic biomarkers of the Alzheimer's pathological cascade. Lancet Neurol. 2010 Jan 1;9(1):119–28.

519. Fein JA, Sokolow S, Miller CA, Vinters HV, Yang F, Cole GM, et al. Co-localization of amyloid beta and tau pathology in Alzheimer's disease synaptosomes. Am J Pathol. 2008/05/08 ed. 2008 Jun;172(6):1683–92.

520. Bilousova T, Miller CA, Poon WW, Vinters HV, Corrada M, Kawas C, et al. Synaptic Amyloid-β Oligomers Precede p-Tau and Differentiate High Pathology Control Cases. Am J Pathol. 2016 Jan 1;186(1):185–98.

521. Wu HY, Kuo PC, Wang YT, Lin HT, Roe AD, Wang BY, et al. β-Amyloid Induces Pathology-Related Patterns of Tau Hyperphosphorylation at Synaptic Terminals. J Neuropathol Exp Neurol. 2018 Sep 1;77(9):814–26.

522. Otero-Garcia M, Xue YQ, Shakouri T, Deng Y, Morabito S, Allison T, et al. Single-soma transcriptomics of tangle-bearing neurons in Alzheimer's disease reveals the signatures of tau-associated synaptic dysfunction. bioRxiv. 2020 Jan 1;2020.05.11.088591.

523. Walker JM, Kazempour Dehkordi S, Fracassi A, Vanschoiack A, Pavenko A, Taglialatela G, et al. Differential protein expression in the hippocampi of resilient individuals identified by digital spatial profiling. Acta Neuropathol Commun. 2022 Feb 14;10(1):23.

524. Rodriguez GA, Barrett GM, Duff KE, Hussaini SA. Chemogenetic attenuation of neuronal activity in the entorhinal cortex reduces Aβ and tau pathology in the hippocampus. PLoS Biol. 2020 Aug 21;18(8):e3000851–e3000851.

525. Robbins M, Clayton E, Kaminski Schierle GS. Synaptic tau: A pathological or physiological phenomenon? Acta Neuropathol Commun. 2021 Sep 9;9(1):149.

526. Dai C ling, Tung YC, Liu F, Gong CX, Iqbal K. Tau passive immunization inhibits not only tau but also Aβ pathology. Alzheimers Res Ther. 2017 Jan 10;9(1):1.

527. Silvestro S, Valeri A, Mazzon E. Aducanumab and Its Effects on Tau Pathology: Is This the Turning Point of Amyloid Hypothesis? Int J Mol Sci. 2022;23(4).

528. Small SA, Duff K. Linking Aβ and Tau in Late-Onset Alzheimer's Disease: A Dual Pathway Hypothesis. Neuron. 2008 Nov 26;60(4):534–42.

529. Duncan GJ, Simkins TJ, Emery B. Neuron-Oligodendrocyte Interactions in the Structure and Integrity of Axons. Front Cell Dev Biol. 2021;9:460.

530. Salvadores N, Gerónimo-Olvera C, Court FA. Axonal Degeneration in AD: The Contribution of Aβ and Tau. Front Aging Neurosci. 2020;12:319.

531. Zhang Xinwen, Wang Rihua, Hu Di, Sun Xiaoyan, Fujioka Hisashi, Lundberg Kathleen, et al. Oligodendroglial glycolytic stress triggers inflammasome activation and neuropathology in Alzheimer's disease. Sci Adv. 6(49):eabb8680.

532. Kneynsberg A, Combs B, Christensen K, Morfini G, Kanaan NM. Axonal Degeneration in Tauopathies: Disease Relevance and Underlying Mechanisms. Front Neurosci. 2017 Oct 17;11:572–572.

533. Coelho A, Fernandes HM, Magalhães R, Moreira PS, Marques P, Soares JM, et al. Signatures of white-matter microstructure degradation during aging and its association with cognitive status. Sci Rep. 2021 Feb 25;11(1):4517.

534. Kim GW, Park SE, Park K, Jeong GW. White Matter Connectivity and Gray Matter Volume Changes Following Donepezil Treatment in Patients With Mild Cognitive Impairment: A Preliminary Study Using Probabilistic Tractography. Front Aging Neurosci. 2021;12:506.

535. Sedmak G, Judaš M. White Matter Interstitial Neurons in the Adult Human Brain: 3% of Cortical Neurons in Quest for Recognition. Cells. 2021;10(1).

536. von Bartheld CS, Bahney J, Herculano-Houzel S. The search for true numbers of neurons and glial cells in the human brain: A review of 150 years of cell counting. J Comp Neurol. 2016 Dec 15;524(18):3865–95.

537. Zhang P, Kishimoto Y, Grammatikakis I, Gottimukkala K, Cutler RG, Zhang S, et al. Senolytic therapy alleviates Aβ-associated oligodendrocyte progenitor cell senescence and cognitive deficits in an Alzheimer's disease model. Nat Neurosci. 2019/04/01 ed. 2019 May;22(5):719–28.

538. Collins-Praino LE, Francis YI, Griffith EY, Wiegman AF, Urbach J, Lawton A, et al. Soluble amyloid beta levels are elevated in the white matter of Alzheimer's patients, independent of cortical plaque severity. Acta Neuropathol Commun. 2014 Aug 17;2(1):83.

539. Ferrer I, Aguiló García M, Carmona M, Andrés-Benito P, Torrejón-Escribano B, Garcia-Esparcia P, et al. Involvement of Oligodendrocytes in Tau Seeding and Spreading in Tauopathies. Front Aging Neurosci [Internet]. 2019;11. Available from: https://www.frontiersin.org/articles/10.3389/fnagi.2019.00112

540. Thal D, Rüb U, Schultz C, Sassin I, Ghebremedhin E, Tredici K, et al. Sequence of A b-Protein Deposition in the Human Medial Temporal Lobe. In 2000.

541. Mirra SS, Heyman A, McKeel D, Sumi SM, Crain BJ, Brownlee LM, et al. The Consortium to Establish a Registry for Alzheimer's Disease (CERAD). Neurology. 1991 Apr 1;41(4):479.

542. Vonsattel JPG, Del Amaya MP, Keller CE. Twenty-first century brain banking. Processing brains for research: the Columbia University methods. Acta Neuropathol (Berl). 2007/11/06 ed. 2008 May;115(5):509–32.

543. Wharton SB, Minett T, Drew D, Forster G, Matthews F, Brayne C, et al. Epidemiological pathology of Tau in the ageing brain: application of staging for neuropil threads (BrainNet Europe protocol) to the MRC cognitive function and ageing brain study. Acta Neuropathol Commun. 2016 Feb 8;4(1):11.

544. Jack CR Jr, Wiste HJ, Lesnick TG, Weigand SD, Knopman DS, Vemuri P, et al. Brain β-amyloid load approaches a plateau. Neurology. 2013/02/27 ed. 2013 Mar 5;80(10):890–6.

545. Hyman BT, Trojanowski JQ. Editorial on Consensus Recommendations for the Postmortem Diagnosis of Alzheimer Disease from the National Institute on Aging and the Reagan Institute

Working Group on Diagnostic Criteria for the Neuropathological Assessment of Alzheimer Disease. J Neuropathol Exp Neurol. 1997 Oct 1;56(10):1095–7.

546. Nelson PT, Trojanowski JQ, Abner EL, Al-Janabi OM, Jicha GA, Schmitt FA, et al. "New Old Pathologies": AD, PART, and Cerebral Age-Related TDP-43 With Sclerosis (CARTS). J Neuropathol Exp Neurol. 2016/05/21 ed. 2016 Jun;75(6):482–98.

547. Hage TA, Bosma-Moody A, Baker CA, Kratz MB, Campagnola L, Jarsky T, et al. Synaptic connectivity to L2/3 of primary visual cortex measured by two-photon optogenetic stimulation. Mao T, Calabrese RL, editors. eLife. 2022 Jan 21;11:e71103.

548. Weintraub S, Salmon D, Mercaldo N, Ferris S, Graff-Radford NR, Chui H, et al. The Alzheimer's Disease Centers' Uniform Data Set (UDS): the neuropsychologic test battery. Alzheimer Dis Assoc Disord. 2009;23(2):91–101.

549. D'Andrea MR, Reiser PA, Polkovitch DA, Gumula NA, Branchide B, Hertzog BM, et al. The use of formic acid to embellish amyloid plaque detection in Alzheimer's disease tissues misguides key observations. Neurosci Lett. 2003 May 15;342(1):114–8.

550. Elmer BM, Swanson KA, Bangari DS, Piepenhagen PA, Roberts E, Taksir T, et al. Gene delivery of a modified antibody to Aβ reduces progression of murine Alzheimer's disease. PLOS ONE. 2020 Dec 30;14(12):e0226245.

551. Bankhead P, Loughrey MB, Fernández JA, Dombrowski Y, McArt DG, Dunne PD, et al. QuPath: Open source software for digital pathology image analysis. Sci Rep. 2017 Dec 4;7(1):16878.

552. Hama H, Kurokawa H, Kawano H, Ando R, Shimogori T, Noda H, et al. Scale: a chemical approach for fluorescence imaging and reconstruction of transparent mouse brain. Nat Neurosci. 2011 Nov 1;14(11):1481–8.

553. Tanaka T, Fillmore D, Sun ST, Nishio I, Swislow G, Shah A. Phase Transitions in Ionic Gels. Phys Rev Lett. 1980 Nov 17;45(20):1636–9.

554. Cohen Y, Ramon O, Kopelman IJ, Mizrahi S. Characterization of inhomogeneous polyacrylamide hydrogels. J Polym Sci Part B Polym Phys. 1992 Aug 1;30(9):1055–67.

555. Klimas A, Gallagher B, Zhao Y. Basics of Expansion Microscopy. Curr Protoc Cytom. 2019 Dec 1;91(1):e67.

556. Cho I, Chang JB. Simultaneous expansion microscopy imaging of proteins and mRNAs via dual-ExM. Sci Rep. 2022 Mar 1;12(1):3360.

557. Truckenbrodt S, Maidorn M, Crzan D, Wildhagen H, Kabatas S, Rizzoli SO. X10 expansion microscopy enables 25-nm resolution on conventional microscopes. EMBO Rep. 2018 Sep 1;19(9):e45836.

558. Shi X, Li Q, Dai Z, Tran AA, Feng S, Ramirez AD, et al. Label-retention expansion microscopy. J Cell Biol. 2021 Jul 6;220(9):e202105067.

559. Sherry DM, Stiles MA. Improved fluorescent signal in expansion microscopy using fluorescent Fab fragment secondary antibodies. MethodsX. 2022 Jan 1;9:101796.

560. Asano SM, Gao R, Wassie AT, Tillberg PW, Chen F, Boyden ES. Expansion Microscopy: Protocols for Imaging Proteins and RNA in Cells and Tissues. Curr Protoc Cell Biol. 2018/08/02 ed. 2018 Sep;80(1):e56–e56.

561. Kenkhuis B, Somarakis A, Kleindouwel LRT, van Roon-Mom WMC, Höllt T, van der Weerd L. Co-expression patterns of microglia markers Iba1, TMEM119 and P2RY12 in Alzheimer's disease. Neurobiol Dis. 2022 Jun 1;167:105684.

562. Yu CC (Jay), Barry NC, Wassie AT, Sinha A, Bhattacharya A, Asano S, et al. Expansion microscopy of C. elegans. Dernburg AF, Ron D, editors. eLife. 2020 May 1;9:e46249.

563. Fogarty MJ, Hammond LA, Kanjhan R, Bellingham MC, Noakes PG. A method for the three-dimensional reconstruction of Neurobiotin™-filled neurons and the location of their synaptic inputs. Front Neural Circuits. 2013 Oct 1;7:153–153.

564. Schmolesky M. The Primary Visual Cortex. Organ Retina Vis Syst Internet Salt Lake City UT Univ Utah Health Sci Cent 1995.

565. Dujardin S, Commins C, Lathuiliere A, Beerepoot P, Fernandes AR, Kamath TV, et al. Tau molecular diversity contributes to clinical heterogeneity in Alzheimer's disease. Nat Med. 2020/06/22 ed. 2020 Aug;26(8):1256–63.

566. Ishiki A, Okamura N, Furukawa K, Furumoto S, Harada R, Tomita N, et al. Longitudinal Assessment of Tau Pathology in Patients with Alzheimer's Disease Using [18F]THK-5117 Positron Emission Tomography. PloS One. 2015 Oct 13;10(10):e0140311–e0140311.

567. Harrison TM, La Joie R, Maass A, Baker SL, Swinnerton K, Fenton L, et al. Longitudinal tau accumulation and atrophy in aging and alzheimer disease. Ann Neurol. 2019/01/17 ed. 2019 Feb;85(2):229–40.

568. Uematsu M, Nakamura A, Ebashi M, Hirokawa K, Takahashi R, Uchihara T. Brainstem tau pathology in Alzheimer's disease is characterized by increase of three repeat tau and independent of amyloid β. Acta Neuropathol Commun. 2018 Jan 3;6(1):1.

569. Hopperton KE, Mohammad D, Trépanier MO, Giuliano V, Bazinet RP. Markers of microglia in post-mortem brain samples from patients with Alzheimer's disease: a systematic review. Mol Psychiatry. 2018 Feb 1;23(2):177–98.

570. Shanbhag NM, Evans MD, Mao W, Nana AL, Seeley WW, Adame A, et al. Early neuronal accumulation of DNA double strand breaks in Alzheimer's disease. Acta Neuropathol Commun. 2019 May 17;7(1):77.

571. Siddiqui MS, François M, Fenech MF, Leifert WR. Persistent γH2AX: A promising molecular marker of DNA damage and aging. Mutat Res Mutat Res. 2015 Oct 1;766:1–19.

572. Soria Lopez JA, González HM, Léger GC. Chapter 13 - Alzheimer's disease. In: Dekosky ST, Asthana S, editors. Handbook of Clinical Neurology [Internet]. Elsevier; 2019. p. 231–55. Available from: https://www.sciencedirect.com/science/article/pii/B9780128047668000133

573. Pfeiffer T, Poll S, Bancelin S, Angibaud J, Inavalli VK, Keppler K, et al. Chronic 2P-STED imaging reveals high turnover of dendritic spines in the hippocampus in vivo. Svoboda K, editor. eLife. 2018 Jun 22;7:e34700.

574. Janda E, Boi L, Carta AR. Microglial Phagocytosis and Its Regulation: A Therapeutic Target in Parkinson's Disease? Front Mol Neurosci [Internet]. 2018;11. Available from: https://www.frontiersin.org/articles/10.3389/fnmol.2018.00144

575. Morini R, Bizzotto M, Perrucci F, Filipello F, Matteoli M. Strategies and Tools for Studying Microglial-Mediated Synapse Elimination and Refinement. Front Immunol [Internet]. 2021;12. Available from: https://www.frontiersin.org/articles/10.3389/fimmu.2021.640937

576. Ward SM, Himmelstein DS, Lancia JK, Fu Y, Patterson KR, Binder LI. TOC1: Characterization of a Selective Oligomeric Tau Antibody. J Alzheimers Dis. 2013;37(3):593–602.

577. Wegmann S, Biernat J, Mandelkow E. A current view on Tau protein phosphorylation in Alzheimer's disease. Mol Neurosci. 2021 Aug 1;69:131–8.

578. Suárez-Calvet M, Karikari TK, Ashton NJ, Lantero Rodríguez J, Milà-Alomà M, Gispert JD, et al. Novel tau biomarkers phosphorylated at T181, T217 or T231 rise in the initial stages of the preclinical Alzheimer's continuum when only subtle changes in Aβ pathology are detected. EMBO Mol Med. 2020 Dec 7;12(12):e12921.

579. Friedrich MG, Skora A, Hancock SE, Mitchell TW, Else PL, Truscott RJW. Tau Is Truncated in Five Regions of the Normal Adult Human Brain. Int J Mol Sci. 2021;22(7).

580. Stopschinski BE, Del Tredici K, Estill-Terpack SJ, Ghebremdehin E, Yu FF, Braak H, et al. Anatomic survey of seeding in Alzheimer's disease brains reveals unexpected patterns. Acta Neuropathol Commun. 2021 Oct 11;9(1):164.

581. Lathuiliere A, Jo Y, Perbet R, Donahue C, Commins C, Quittot N, et al. Specific detection of tau seeding activity in Alzheimer's disease using rationally designed biosensor cells. Mol Neurodegener. 2023 Aug 8;18(1):53.

582. Corrada MM, Berlau DJ, Kawas CH. A population-based clinicopathological study in the oldest-old: the 90+ study. Curr Alzheimer Res. 2012 Jul;9(6):709–17.

583. Riley KP, Snowdon DA, Desrosiers MF, Markesbery WR. Early life linguistic ability, late life cognitive function, and neuropathology: findings from the Nun Study. Dev Orig Aging Brain Blood Vessels. 2005 Mar 1;26(3):341–7.

584. Schneider JA, Aggarwal NT, Barnes L, Boyle P, Bennett DA. The neuropathology of older persons with and without dementia from community versus clinic cohorts. J Alzheimers Dis JAD. 2009;18(3):691–701.

585. Lue LF, Brachova L, Civin WH, Rogers J. Inflammation, Aβ Deposition, and Neurofibrillary Tangle Formation as Correlates of Alzheimer's Disease Neurodegeneration. J Neuropathol Exp Neurol. 1996 Oct 1;55(10):1083–8.

586. Braak H, Del Tredici K. Evolutional Aspects of Alzheimer's Disease Pathogenesis. J Alzheimers Dis. 2013;33(s1):S155–61.

587. Yakoubi R, Rollenhagen A, von Lehe M, Miller D, Walkenfort B, Hasenberg M, et al. Ultrastructural heterogeneity of layer 4 excitatory synaptic boutons in the adult human temporal lobe neocortex. Marder E, Helmstaedter M, Rockland K, editors. eLife. 2019 Nov 20;8:e48373.

588. Trevor Huff. Neuroanatomy, Visual Cortex. StatPearls 2022.

589. Arriagada PV, Marzloff K, Hyman BT. Distribution of Alzheimer-type pathologic changes in nondemented elderly individuals matches the pattern in Alzheimer's disease. Neurology. 1992 Sep 1;42(9):1681.

590. Vogt L. Laminar distribution of neuron degeneration in posterior cingulate cortex in Alzheimer's disease. Acta neuropathologica vol. 80,6 (1990): 581-9. doi:10.1007/BF00307624.

591. SantaCruz KS, Sonnen JA, Pezhouh MK, Desrosiers MF, Nelson PT, Tyas SL. Alzheimer Disease Pathology in Subjects Without Dementia in 2 Studies of Aging: The Nun Study and the Adult Changes in Thought Study. J Neuropathol Exp Neurol. 2011 Oct 1;70(10):832–40.

592. Lennon JC, Aita SL, Bene VAD, Rhoads T, Resch ZJ, Eloi JM, et al. Black and White individuals differ in dementia prevalence, risk factors, and symptomatic presentation. Alzheimers Dement. 2022 Aug 1;18(8):1461–71.

593. Chin AL, Negash S, Hamilton R. Diversity and Disparity in Dementia: The Impact of Ethnoracial Differences in Alzheimer Disease. Alzheimer Dis Assoc Disord [Internet]. 2011;25(3). Available from: https://journals.lww.com/alzheimerjournal/Fulltext/2011/07000/Diversity_and_Disparity_in_Dementia__The_Impact_of.1.aspx

594. Kunkle BW, Schmidt M, Klein HU, Naj AC, Hamilton-Nelson KL, Larson EB, et al. Novel Alzheimer Disease Risk Loci and Pathways in African American Individuals Using the African Genome Resources Panel: A Meta-analysis. JAMA Neurol. 2021 Jan 1;78(1):102–13.

595. Livingston G, Huntley J, Sommerlad A, Ames D, Ballard C, Banerjee S, et al. Dementia prevention, intervention, and care: 2020 report of the Lancet Commission. The Lancet. 2020 Aug 8;396(10248):413–46.

596. Jansen MG, Geerligs L, Claassen JAHR, Overdorp EJ, Brazil IA, Kessels RPC, et al. Positive Effects of Education on Cognitive Functioning Depend on Clinical Status and Neuropathological Severity. Front Hum Neurosci [Internet]. 2021;15. Available from: https://www.frontiersin.org/articles/10.3389/fnhum.2021.723728

597. Kim S, Jeon SG, Nam Y, Kim H soo, Yoo DH, Moon M. Bilingualism for Dementia: Neurological Mechanisms Associated With Functional and Structural Changes in the Brain. Front Neurosci [Internet]. 2019;13. Available from: https://www.frontiersin.org/articles/10.3389/fnins.2019.01224

598. Rosselli M, Uribe IV, Ahne E, Shihadeh L. Culture, Ethnicity, and Level of Education in Alzheimer's Disease. Neurotherapeutics. 2022 Jan 1;19(1):26–54.

599. Susan M. Landau, Andy Horng, Allison Fero, William J. Jagust, For the Alzheimer's Disease Neuroimaging Initiative. Amyloid negativity in patients with clinically diagnosed Alzheimer disease and MCI. Neurology. 2016 Apr 12;86(15):1377.

600. Altomare D, Caprioglio C, Assal F, Allali G, Mendes A, Ribaldi F, et al. Diagnostic value of amyloid-PET and tau-PET: a head-to-head comparison. Eur J Nucl Med Mol Imaging. 2021 Jul 1;48(7):2200–11.

601. Jiao F, Wang M, Sun X, Ju Z, Lu J, Wang L, et al. Based on Tau PET Radiomics Analysis for the Classification of Alzheimer's Disease and Mild Cognitive Impairment. Brain Sci. 2023;13(2).

602. Jiawei Zhang. Basic Neural Units of the Brain: Neurons, Synapses and Action Potential. Arxiv 2019.

603. Gulati A. Understanding neurogenesis in the adult human brain. Indian J Pharmacol Ser Online 2015 Cited 2023 Jul 247583-4.

604. Faria-Pereira A, Morais VA. Synapses: The Brain's Energy-Demanding Sites. Int J Mol Sci. 2022;23(7).

605. Araque A, Parpura V, Sanzgiri RP, Haydon PG. Tripartite synapses: glia, the unacknowledged partner. Trends Neurosci. 1999 May 1;22(5):208–15.

606. Gallagher B, Zhao Y. Nanoscale Imaging of Synaptic Connections with Expansion Microscopy. Discov Craiova Rom. 2019 Sep 30;7(3):e101–e101.

607. Karagiannis ED, Boyden ES. Expansion microscopy: development and neuroscience applications. Neurotechnologies. 2018 Jun 1;50:56–63.

608. Gorilak P, Pružincová M, Vachova H, Olšinová M, Schmidt Cernohorska M, Varga V. Expansion microscopy facilitates quantitative super-resolution studies of cytoskeletal structures in kinetoplastid parasites. Open Biol. 11(9):210131.

609. Alonso-Nanclares L, Gonzalez-Soriano J, Rodriguez JR, DeFelipe J. Gender differences in human cortical synaptic density. Proc Natl Acad Sci. 2008 Sep 23;105(38):14615–9.

610. Stranahan AM, Mattson MP. Selective Vulnerability of Neurons in Layer II of the Entorhinal Cortex during Aging and Alzheimer's Disease. Dutia MB, editor. Neural Plast. 2010 Dec 1;2010:108190.

611. Mertens R, Melchert S, Gitler D, Schou MB, Saether SG, Vaaler A, et al. Epitope specificity of anti-synapsin autoantibodies: Differential targeting of synapsin I domains. PLOS ONE. 2018 Dec 13;13(12):e0208636.

612. Yoo KS, Lee K, Oh JY, Lee H, Park H, Park YS, et al. Postsynaptic density protein 95 (PSD-95) is transported by KIF5 to dendritic regions. Mol Brain. 2019 Nov 21;12(1):97.

613. CRAGG BG. THE DENSITY OF SYNAPSES AND NEURONS IN NORMAL, MENTALLY DEFECTIVE AND AGEING HUMAN BRAINS. Brain. 1975 Jan 1;98(1):81–90.

614. Shapson-Coe A, Januszewski M, Berger DR, Pope A, Wu Y, Blakely T, et al. A connectomic study of a petascale fragment of human cerebral cortex. bioRxiv. 2021 Jan 1;2021.05.29.446289.

615. Domínguez-Álvaro M, Montero-Crespo M, Blazquez-Llorca L, Plaza-Alonso S, Cano-Astorga N, DeFelipe J, et al. 3D Analysis of the Synaptic Organization in the Entorhinal Cortex in Alzheimer's Disease. eneuro. 2021 May 1;8(3):ENEURO.0504-20.2021.

616. Chai YL, Lee JH, Chong JR, Ballard C, Francis PT, Kennedy BK, et al. Inflammatory panel cytokines are elevated in the neocortex of late-stage Alzheimer's disease but not Lewy body dementias. J Neuroinflammation. 2023 May 8;20(1):111.

617. Hulshof LA, van Nuijs D, Hol EM, Middeldorp J. The Role of Astrocytes in Synapse Loss in Alzheimer's Disease: A Systematic Review. Front Cell Neurosci [Internet]. 2022;16. Available from: https://www.frontiersin.org/articles/10.3389/fncel.2022.899251

618. Ransohoff RM. A polarizing question: do M1 and M2 microglia exist? Nat Neurosci. 2016 Aug 1;19(8):987–91.

619. Lawrence JM, Schardien K, Wigdahl B, Nonnemacher MR. Roles of neuropathology-associated reactive astrocytes: a systematic review. Acta Neuropathol Commun. 2023 Mar 13;11(1):42.

620. Papageorgiou IE, Lewen A, Galow LV, Cesetti T, Scheffel J, Regen T, et al. TLR4-activated microglia require IFN-γ to induce severe neuronal dysfunction and death in situ. Proc Natl Acad Sci. 2016 Jan 5;113(1):212–7.

621. Au NPB, Ma CHE. Recent Advances in the Study of Bipolar/Rod-Shaped Microglia and their Roles in Neurodegeneration. Front Aging Neurosci [Internet]. 2017;9. Available from: https://www.frontiersin.org/articles/10.3389/fnagi.2017.00128

622. Streit WJ, Braak H, Del Tredici K, Leyh J, Lier J, Khoshbouei H, et al. Microglial activation occurs late during preclinical Alzheimer's disease. Glia. 2018 Dec 1;66(12):2550–62.

623. Neil SN Graham, David J Sharp. Understanding neurodegeneration after traumatic brain injury: from mechanisms to clinical trials in dementia. J Neurol Neurosurg Amp Psychiatry. 2019 Nov 1;90(11):1221.

624. Roussarie JP, Yao V, Rodriguez-Rodriguez P, Oughtred R, Rust J, Plautz Z, et al. Selective Neuronal Vulnerability in Alzheimer's Disease: A Network-Based Analysis. Neuron. 2020 Sep 9;107(5):821-835.e12.

625. Curtis MA, Low VF, Faull RLM. Neurogenesis and progenitor cells in the adult human brain: A comparison between hippocampal and subventricular progenitor proliferation. Dev Neurobiol. 2012 Jul 1;72(7):990–1005.

626. Colodner KJ, Montana RA, Anthony DC, Folkerth RD, De Girolami U, Feany MB. Proliferative Potential of Human Astrocytes. J Neuropathol Exp Neurol. 2005 Feb 1;64(2):163–9.

627. Askew K, Li K, Olmos-Alonso A, Garcia-Moreno F, Liang Y, Richardson P, et al. Coupled Proliferation and Apoptosis Maintain the Rapid Turnover of Microglia in the Adult Brain. Cell Rep. 2017 Jan 10;18(2):391–405.

628. Lau V, Ramer L, Tremblay MÈ. An aging, pathology burden, and glial senescence build-up hypothesis for late onset Alzheimer's disease. Nat Commun. 2023 Mar 25;14(1):1670.

629. Serrano-Pozo A, Gómez-Isla T, Growdon JH, Frosch MP, Hyman BT. A phenotypic change but not proliferation underlies glial responses in Alzheimer disease. Am J Pathol. 2013/04/18 ed. 2013 Jun;182(6):2332–44.

630. Marlatt MW, Bauer J, Aronica E, van Haastert ES, Hoozemans JJM, Joels M, et al. Proliferation in the Alzheimer Hippocampus Is due to Microglia, Not Astroglia, and Occurs at Sites of Amyloid Deposition. Korosi A, editor. Neural Plast. 2014 Aug 19;2014:693851.

631. Dai DL, Li M, Lee EB. Human Alzheimer's disease reactive astrocytes exhibit a loss of homeostastic gene expression. Acta Neuropathol Commun. 2023 Aug 2;11(1):127.

632. Leng F, Edison P. Neuroinflammation and microglial activation in Alzheimer disease: where do we go from here? Nat Rev Neurol. 2021 Mar 1;17(3):157–72.

633. Goel P, Chakrabarti S, Goel K, Bhutani K, Chopra T, Bali S. Neuronal cell death mechanisms in Alzheimer's disease: An insight. Front Mol Neurosci [Internet]. 2022;15. Available from: https://www.frontiersin.org/articles/10.3389/fnmol.2022.937133

634. Solier S, Pommier Y. The nuclear γ-H2AX apoptotic ring: implications for cancers and autoimmune diseases. Cell Mol Life Sci. 2014 Jun 1;71(12):2289–97.

635. Myung NH, Zhu X, Kruman II, Castellani RJ, Petersen RB, Siedlak SL, et al. Evidence of DNA damage in Alzheimer disease: phosphorylation of histone H2AX in astrocytes. AGE. 2008 Dec 1;30(4):209–15.

636. Castellani RJ, Lee H gon, Siedlak SL, Nunomura A, Hayashi T, Nakamura M, et al. Reexamining Alzheimer's Disease: Evidence for a Protective Role for Amyloid-β Protein Precursor and Amyloid-β. J Alzheimers Dis. 2009;18(2):447–52.

637. Allen P, Moore H, Corcoran CM, Gilleen J, Kozhuharova P, Reichenberg A, et al. Emerging Temporal Lobe Dysfunction in People at Clinical High Risk for Psychosis. Front Psychiatry [Internet]. 2019;10. Available from: https://www.frontiersin.org/articles/10.3389/fpsyt.2019.00298

638. Rubin RD, Watson PD, Duff MC, Cohen NJ. The role of the hippocampus in flexible cognition and social behavior. Front Hum Neurosci [Internet]. 2014;8. Available from: https://www.frontiersin.org/articles/10.3389/fnhum.2014.00742

639. Burke JR. Subcortical Dementia. In: Principles and Practice of Geriatric Psychiatry [Internet]. 2002 [cited 2023 Aug 3]. p. 269–71. Available from: https://doi.org/10.1002/0470846410.ch50b

640. Lon R. White, Steven D. Edland, Laura S. Hemmy, Kathleen S. Montine, Chris Zarow, Joshua A. Sonnen, et al. Neuropathologic comorbidity and cognitive impairment in the Nun and Honolulu-Asia Aging Studies. Neurology. 2016 Mar 15;86(11):1000.

641. van Norden AG, de Laat KF, Gons RA, van Uden IW, van Dijk EJ, van Oudheusden LJ, et al. Causes and consequences of cerebral small vessel disease. The RUN DMC study: a prospective cohort study. Study rationale and protocol. BMC Neurol. 2011 Feb 28;11(1):29.

642. Sweeney MD, Sagare AP, Zlokovic BV. Blood–brain barrier breakdown in Alzheimer disease and other neurodegenerative disorders. Nat Rev Neurol. 2018 Mar 1;14(3):133–50.

643. Meftah S, Gan J. Alzheimer's disease as a synaptopathy: Evidence for dysfunction of synapses during disease progression. Front Synaptic Neurosci [Internet]. 2023;15. Available from: https://www.frontiersin.org/articles/10.3389/fnsyn.2023.1129036

644. Selkoe DJ. Alzheimer's Disease Is a Synaptic Failure. Science. 2002 Oct 25;298(5594):789.

645. Verstraelen P, Garcia-Diaz Barriga G, Verschuuren M, Asselbergh B, Nuydens R, Larsen PH, et al. Systematic Quantification of Synapses in Primary Neuronal Culture. iScience [Internet]. 2020 Sep 25 [cited 2022 Nov 27];23(9). Available from: https://doi.org/10.1016/j.isci.2020.101542

646. Lawrence Rajendran, Rosa C. Paolicelli. Microglia-Mediated Synapse Loss in Alzheimer's Disease. J Neurosci. 2018 Mar 21;38(12):2911.

647. Zhan Y, Paolicelli RC, Sforazzini F, Weinhard L, Bolasco G, Pagani F, et al. Deficient neuron-microglia signaling results in impaired functional brain connectivity and social behavior. Nat Neurosci. 2014 Mar;17(3):400–6.

648. Navarro V, Sanchez-Mejias E, Jimenez S, Muñoz-Castro C, Sanchez-Varo R, Davila JC, et al. Microglia in Alzheimer's Disease: Activated, Dysfunctional or Degenerative. Front Aging Neurosci [Internet]. 2018;10. Available from: https://www.frontiersin.org/articles/10.3389/fnagi.2018.00140

649. Gelon PA, Dutchak PA, Sephton CF. Synaptic dysfunction in ALS and FTD: anatomical and molecular changes provide insights into mechanisms of disease. Front Mol Neurosci [Internet]. 2022;15. Available from: https://www.frontiersin.org/articles/10.3389/fnmol.2022.1000183

650. Chung WS, Welsh CA, Barres BA, Stevens B. Do glia drive synaptic and cognitive impairment in disease? Nat Neurosci. 2015 Nov 1;18(11):1539–45.

651. Lee E, Chung WS. Glial Control of Synapse Number in Healthy and Diseased Brain. Front Cell Neurosci [Internet]. 2019;13. Available from: https://www.frontiersin.org/articles/10.3389/fncel.2019.00042

652. Liu Y, Shen X, Zhang Y, Zheng X, Cepeda C, Wang Y, et al. Interactions of glial cells with neuronal synapses, from astrocytes to microglia and oligodendrocyte lineage cells. Glia. 2023 Jun 1;71(6):1383–401.

653. Perez-Catalan NA, Doe CQ, Ackerman SD. The role of astrocyte-mediated plasticity in neural circuit development and function. Neural Develop. 2021 Jan 7;16(1):1.

654. Südhof TC. Towards an Understanding of Synapse Formation. Neuron. 2018 Oct 24;100(2):276–93.

655. Bellenguez C, Küçükali F, Jansen IE, Kleineidam L, Moreno-Grau S, Amin N, et al. New insights into the genetic etiology of Alzheimer's disease and related dementias. Nat Genet. 2022 Apr 1;54(4):412–36.

656. Skene NG, Bryois J, Bakken TE, Breen G, Crowley JJ, Gaspar HA, et al. Genetic identification of brain cell types underlying schizophrenia. Nat Genet. 2018 Jun 1;50(6):825–33.

657. Xiong M, Wang C, Gratuze M, Saadi F, Bao X, Bosch ME, et al. Astrocytic APOE4 removal confers cerebrovascular protection despite increased cerebral amyloid angiopathy. Mol Neurodegener. 2023 Mar 16;18(1):17.

658. Jung YJ, Chung WS. Phagocytic Roles of Glial Cells in Healthy and Diseased Brains. Biomol Ther. 2018/07/01 ed. 2018 Jul;26(4):350–7.

659. Cathy Andorfer, Christopher M. Acker, Yvonne Kress, Patrick R. Hof, Karen Duff, Peter Davies. Cell-Cycle Reentry and Cell Death in Transgenic Mice Expressing Nonmutant Human Tau Isoforms. J Neurosci. 2005 Jun 1;25(22):5446.

660. Gutierrez BA, Limon A. Synaptic Disruption by Soluble Oligomers in Patients with Alzheimer's and Parkinson's Disease. Biomedicines. 2022;10(7).

661. Abounit S, Wu JW, Duff K, Victoria GS, Zurzolo C. Tunneling nanotubes: A possible highway in the spreading of tau and other prion-like proteins in neurodegenerative diseases. Prion. 2016 Sep 2;10(5):344–51.

662. Marija Usenovic, Shahriar Niroomand, Robert E. Drolet, Lihang Yao, Renee C. Gaspar, Nathan G. Hatcher, et al. Internalized Tau Oligomers Cause Neurodegeneration by Inducing Accumulation of Pathogenic Tau in Human Neurons Derived from Induced Pluripotent Stem Cells. J Neurosci. 2015 Oct 21;35(42):14234.

663. Kopeikina KJ, Hyman BT, Spires-Jones TL. Soluble forms of tau are toxic in Alzheimer's disease. Transl Neurosci. 2012 Sep;3(3):223–33.

664. Zhao Y, Gu Y, Zhang Q, Liu H, Liu Y. The Potential Roles of Exosomes Carrying APP and Tau Cleavage Products in Alzheimer's Disease. J Clin Med. 2023;12(5).

665. Wesseling H, Mair W, Kumar M, Schlaffner CN, Tang S, Beerepoot P, et al. Tau PTM Profiles Identify Patient Heterogeneity and Stages of Alzheimer's Disease. Cell. 2020 Dec 10;183(6):1699-1713.e13.

666. Thijssen EH, La Joie R, Strom A, Fonseca C, Iaccarino L, Wolf A, et al. Plasma phosphorylated tau 217 and phosphorylated tau 181 as biomarkers in Alzheimer's disease and frontotemporal lobar degeneration: a retrospective diagnostic performance study. Lancet Neurol. 2021 Sep 1;20(9):739–52.

667. Wang X, Liu Q, Li XG, Zhou QZ, Wu DQ, Li SH, et al. T217-Phosphorylation Exacerbates Tau Pathologies and Tau-Induced Cognitive Impairment. J Alzheimers Dis. 2021;81(4):1403–18.

668. Barthélemy NR, Bateman RJ, Hirtz C, Marin P, Becher F, Sato C, et al. Cerebrospinal fluid phospho-tau T217 outperforms T181 as a biomarker for the differential diagnosis of Alzheimer's disease and PET amyloid-positive patient identification. Alzheimers Res Ther. 2020 Mar 17;12(1):26.

669. Vromen EM, de Boer SCM, Teunissen CE, Rozemuller A, Sieben A, Bjerke M, et al. Biomarker A+T−: is this Alzheimer's disease or not? A combined CSF and pathology study. Brain. 2023 Mar 1;146(3):1166–74.

670. Dolan PJ, Johnson GVW. The role of tau kinases in Alzheimer's disease. Curr Opin Drug Discov Devel. 13(5):595–603.

671. Cavallini A, Brewerton S, Bell A, Sargent S, Glover S, Hardy C, et al. An Unbiased Approach to Identifying Tau Kinases That Phosphorylate Tau at Sites Associated with Alzheimer Disease. J Biol Chem. 2013 Aug 9;288(32):23331–47.

672. Bryan L, Awasthi S, Li Y, Nirmalraj PN, Balog S, Yang J, et al. Site-Specific C-Terminal Fluorescent Labeling of Tau Protein. ACS Omega. 2022 Dec 20;7(50):47009–14.

673. Falcon B, Noad J, McMahon H, Randow F, Goedert M. Galectin-8–mediated selective autophagy protects against seeded tau aggregation. J Biol Chem. 2018 Feb 16;293(7):2438–51.

674. Lathuiliere A, Hyman BT. Quantitative Methods for the Detection of Tau Seeding Activity in Human Biofluids. Front Neurosci [Internet]. 2021;15. Available from: https://www.frontiersin.org/articles/10.3389/fnins.2021.654176

675. Cohen TJ, Guo JL, Hurtado DE, Kwong LK, Mills IP, Trojanowski JQ, et al. The acetylation of tau inhibits its function and promotes pathological tau aggregation. Nat Commun. 2011 Mar 22;2(1):252.

676. Despres C, Byrne C, Qi H, Cantrelle FX, Huvent I, Chambraud B, et al. Identification of the Tau phosphorylation pattern that drives its aggregation. Proc Natl Acad Sci. 2017 Aug 22;114(34):9080–5.

677. Ghag G, Bhatt N, Cantu DV, Guerrero-Munoz MJ, Ellsworth A, Sengupta U, et al. Soluble tau aggregates, not large fibrils, are the toxic species that display seeding and cross-seeding behavior. Protein Sci Publ Protein Soc. 2018/10/19 ed. 2018 Nov;27(11):1901–9.

678. Mothes T, Portal B, Konstantinidis E, Eltom K, Libard S, Streubel-Gallasch L, et al. Astrocytic uptake of neuronal corpses promotes cell-to-cell spreading of tau pathology. Acta Neuropathol Commun. 2023 Jun 17;11(1):97.

679. Pooler AM, Phillips EC, Lau DHW, Noble W, Hanger DP. Physiological release of endogenous tau is stimulated by neuronal activity. EMBO Rep. 2013 Apr 1;14(4):389–94.

680. Martinez P, Patel H, You Y, Jury N, Perkins A, Lee-Gosselin A, et al. Bassoon contributes to tau-seed propagation and neurotoxicity. Nat Neurosci. 2022 Dec 1;25(12):1597–607.

681. Mariano Gabitto, Kyle Travaglini, Jeannelle Ariza et al. Integrated multimodal cell atlas of Alzheimer's disease. 23 May 2023 Prepr Version 1 Available Res Sq Httpsdoiorg1021203rs3rs-2921860v1.

682. Raiders S, Han T, Scott-Hewitt N, Kucenas S, Lew D, Logan MA, et al. Engulfed by Glia: Glial Pruning in Development, Function, and Injury across Species. J Neurosci. 2021 Feb 3;41(5):823.

683. De Schepper S, Ge JZ, Crowley G, Ferreira LS, Garceau D, Toomey CE, et al. Perivascular SPP1 Mediates Microglial Engulfment of Synapses in Alzheimer's Disease Models. bioRxiv. 2022 Jan 1;2022.04.04.486547.

684. Emily Hill, Thomas K. Karikari, Kevin G. Moffat, Magnus J. E. Richardson, Mark J. Wall. Introduction of Tau Oligomers into Cortical Neurons Alters Action Potential Dynamics and Disrupts Synaptic Transmission and Plasticity. eneuro. 2019 Sep 1;6(5):ENEURO.0166-19.2019.

685. Katsumoto A, Takeuchi H, Tanaka F. Tau Pathology in Chronic Traumatic Encephalopathy and Alzheimer's Disease: Similarities and Differences. Front Neurol [Internet]. 2019;10. Available from: https://www.frontiersin.org/articles/10.3389/fneur.2019.00980

686. Hawkins BE, Krishnamurthy S, Castillo-Carranza DL, Sengupta U, Prough DS, Jackson GR, et al. Rapid Accumulation of Endogenous Tau Oligomers in a Rat Model of Traumatic Brain Injury: POSSIBLE LINK BETWEEN TRAUMATIC BRAIN INJURY AND SPORADIC TAUOPATHIES*. J Biol Chem. 2013 Jun 7;288(23):17042–50.

687. Tremblay ME, Cookson MR, Civiero L. Glial phagocytic clearance in Parkinson's disease. Mol Neurodegener. 2019 Apr 5;14(1):16.

688. Kawas CH, Kim RC, Sonnen JA, Bullain SS, Trieu T, Corrada MM. Multiple pathologies are common and related to dementia in the oldest-old: The 90+ Study. Neurology. 2015/07/15 ed. 2015 Aug 11;85(6):535–42.

689. Rogalski EJ, Sridhar J, Martersteck A, Makowski-Woidan B, Engelmeyer J, Parrish T, et al. SuperAging: A model for studying mechanisms of resilience and resistance. Alzheimers Dement. 2020 Dec 1;16(S10):e037932.

690. Nagy C, Maheu M, Lopez JP, Vaillancourt K, Cruceanu C, Gross JA, et al. Effects of Postmortem Interval on Biomolecule Integrity in the Brain. J Neuropathol Exp Neurol. 2015 May 1;74(5):459–69.

691. Ricciarelli R, Fedele E. The Amyloid Cascade Hypothesis in Alzheimer's Disease: It's Time to Change Our Mind. Curr Neuropharmacol. 2017;15(6):926–35.

6. Appendix

6.1 Publications

Taddei RN, Sanchez-Mico MV, Bonnar O, Connors T, Gaona A, Denbow D, et al. Changes in glial cell phenotypes precede overt neurofibrillary tangle formation, correlate with markers of cortical cell damage, and predict cognitive status of individuals at Braak III-IV stages. Acta Neuropathologica Communications. 2022 May 9;10(1):72.

Taddei RN, Perbet R, Mate de Gerando A, Wiedmer AE, Sanchez-Mico M, Connors Stewart T, et al. Tau Oligomer–Containing Synapse Elimination by Microglia and Astrocytes in Alzheimer Disease. JAMA Neurology [Internet]. 2023 Oct 9 [cited 2023 Oct 11]; Available from: https://doi.org/10.1001/jamaneurol.2023.3530

6.2 Glossary of terms

2D	2-dimensional
3D	3-dimensional
4-HT	4-Hydroxy-TEMPO
AcX	Acryloyl-X
AD	Alzheimer disease
AD	Autosomal dominant
ADAD	Autosomal dominant Alzheimer disease
ADNC	Alzheimer disease neuropathologic changes
ALDH1L1	Aldehyde dehydrogenase 1 family member L1
APP	Amyloid precursor protein
APS	Ammonium persulfate
AT	Array tomography
AT100	Anti-Phospho-Tau 100
AT8	Anti-Phospho-Tau 8
ATP	Adenosine triphosphate (ATP)
AUC	Area under the ROC Curve
BACE1	Beta-site amyloid precursor protein cleaving enzyme-1
C	Control
C1q	Complement component 1q
C3	Complement component 3
C3R	Complement component 3 receptor

CAA	Cerebral amyloid angiopathy
CBS	Corticobasal syndrome
CD18	Cluster of differentiation 18
CD68	Cluster of differentiation 68
CD81	Cluster of differentiation 81
CDR	Clinical dementia rating scale
CDR-G	Clinical dementia rating - global
CDR-SoB	Clinical dementia rating - sum of boxes
CERAD	Consortium to Establish a Registry for Alzheimer's Disease
CFP	Cyan fluorescent protein
CNS	Central nervous system
CP13	Tau antibody
CSF	Cerebrospinal fluid
CTE	Chronic traumatic encephalopathy
D	Demented
DLB	Dementia with Lewy bodies
DNA	Deoxyribonucleic acid
DSM	Diagnostic and Statistical Manual of Mental Disorders
DSST	Digit Symbol Substitution Test
EDTA	Ethylenediaminetetraacetic Acid
EEG	Electroencephalogram
e.g.	exempli gratia
EM	Electron microscopy
EOAD	Early-Onset Alzheimer Disease
ExM	Expansion microscopy
FA	Formic acid
FDG	Fluorodeoxyglucose
FFPE	Formalin-Fixed Paraffin-Embedded
FIB-SEM	Focused ion beam-scanning electron microscope
FOV	Field of view
FRET	Fluorescence resonance energy transfer
GABA	Gamma-aminobutyric acid
GAP-43	Growth-associated Protein 43
GFAP	Glial fibrillary acidic protein
GT38	Tau antibody
HEK293	Human embryonic kidney 293 cells
HEXB	Hexosaminidase subunit beta
HLA-DR	Human Leukocyte Antigen - DR isotype
IBA1	Ionized calcium-binding adaptor molecule 1
IL1	Interleukin-1
IL33	Interleukin-33
IL6	Interleukin-6
LAMP2	Lysosome-associated membrane protein 2
LATE	Limbic-predominant age-related TDP-43 encephalopathy
LOAD	Late-Onset Alzheimer Disease
MCI	Mild cognitive impairment
mm	millimeter
MMSE	Mini-Mental State Examination
MN423	Tau antibody
MOCA	Montreal cognitive assessment scale
MRI	Magnetic resonance imaging

N	Number
NFT	Neurofibrillary tangle
NIA-AA	National Institute on Aging and Alzheimer's Association
nm	nanometer
N-N-Mb	N-N-Methylenebisacrylamide
NPTX	Neuronal pentraxin
NRG1	Neuregulin-1
OCC	Occipital cortex
p	Probability
P2RY12	Purinergic receptor P2Y G protein-coupled 12
PART	Primary age-related tauopathy
PBS	Phosphate buffered saline
PCA	Posterior cortical atrophy
PD	Parkinson’s disease
PET	Positron emission tomography
PHF1	Paired Helical Filaments
PMI	Postmortem interval
PS	Phosphatidylserine
PSD95	Postsynaptic density protein 95
PSEN1	Presenilin 1
PSP	Progressive supranuclear palsy
p-tau	Phosphorylated tau
pTDP-43	phosphorylated TAR DNA Binding Protein 43 kDa
R	Correlation coefficient
R	Resilient
ROI	Region of interest
SALL1	Sal-like 1
SCD	Subjective cognitive decline
SD	Standard deviation
SDS	Sodium dodecyl-sulfate
SIM	Structured Illumination Microscopy
SNAP-1	Alpha-Soluble NSF
SOB	Sum of boxes
SOFI	Super-resolution optical fluctuation imaging
STED	Stimulated emission depletion
STORM	Stochastic Optical Reconstruction Microscopy
SV2A	Synaptic vesicle glycoprotein 2A
TBI	Traumatic brain injury
TBS-T	Tris-buffered saline with 0.25% Tween
TDP43	TAR DNA Binding Protein 43 kDa
TEMED	Tetramethyl-ethylenediamine
TMEM119	Transmembrane protein 119
TOC1	Tau oligomeric complex 1
TP	Temporal pole
TSPO	Translocator protein
UK	United Kingdom
US	United States
USA	United States of America
WAIS	Wechsler adult intelligence scale
WB	Western blot
WM	White matter

WMH	White matter hyperintensity
YFP	Yellow fluorescent protein
γH2AX	H2A histone family member X
µm	micrometer